

Catalytic Steam Gasification of Biomass over Nickel Based Catalysts via Reactive Flash Volatilisation

By

Fan Liang Chan
M. Sc. (Chemical Eng.)

A thesis submitted in fulfilment of the requirements for the degree of

Doctor of Philosophy

Department of Chemical Engineering
Faculty of Engineering
Monash University
Australia



May 2015

Copyright Notice

© The author 2015. Except as provided in the Copyright Act 1968, this thesis may not be reproduced in any form without the written permission of the author.

Table of Contents

Chapter 1: Introduction	1
1.1 Background	3
1.2 Research Aims.....	4
1.3 Thesis Structure and Chapter Outline.....	5
1.4 References	7
Chapter 2: Literature Review- Review of recent developments in Ni-based catalysts for biomass gasification	11
2.1 Introduction	13
2.2 Tar	14
2.3 Biomass Gasification with Commercial Nickel Based Catalyst.....	18
2.3.1 Commercial Nickel Catalyst as Primary Catalyst.....	18
2.3.2 Commercial Nickel Catalyst as Secondary Catalyst	19
2.4 Recent Advancements in Nickel Based Catalyst for Biomass Gasification.....	24
2.4.1 Effect of Support on Nickel Based Catalysts	25
2.4.2 Promoted Nickel Based Catalyst	27
2.4.3 Nickel Nanoparticle Catalyst.....	31
2.5 Future Directions of Biomass Gasification	32
2.6 Conclusions	34
2.7 Acknowledgement.....	34
2.8 References	35
Chapter 3: Catalytic Steam Gasification of Cellulose Using Reactive Flash Volatilization	43
3.1 Introduction	45
3.2 Experimental Section.....	47
3.2.1 Catalyst Preparation.....	47
3.2.2 Catalyst Characterization.....	48
3.2.3 Catalytic Activity Evaluation	50
3.3 Results and Discussion.....	52
3.3.1 Catalyst Characterisation.....	52
3.3.2 Reactive Flash Volatilisation of Cellulose	58
3.4 Conclusions	77
3.5 Acknowledgements	77
3.6 References	77
Chapter 4: Kinetic Study of Catalytic Steam Gasification of Biomass by Reactive Flash Volatilisation	83

4.1 Introduction.....	85
4.2 Experimental Section.....	86
4.2.1 Materials	86
4.2.2 Experimental Methods.....	87
4.2.3 Pseudo First Order Kinetic Model	88
4.3 Results and Discussion	90
4.3.1 Effect of Gasification Agent on Cellulose Volatilisation Kinetics without a Catalyst .	90
4.3.2 Effect of Biomass Feedstock on Volatilisation Kinetics without a Catalyst.....	92
4.3.3 Effect of Catalysts on Cellulose Volatilisation Kinetics.....	98
4.3.4 Effect of Catalysts on Pinewood Sawdust Volatilisation Kinetics	102
4.4 Conclusions.....	104
4.5 Acknowledgements.....	105
4.6 References.....	105
Chapter 5: Catalytic Steam Gasification of Pinewood and Eucalyptus Sawdust Using Reactive Flash volatilization.....	109
5.1 Introduction.....	111
5.2 Experimental.....	112
5.2.1 Biomass.....	112
5.2.2 Biomass Characterization	112
5.2.3 Catalyst	112
5.2.4 Reactor Setup.....	113
5.2.5 Catalyst Characterisation	114
5.3 Results and Discussion	114
5.3.1 Biomass Characterisation.....	114
5.3.2 Effect of carbon-to-oxygen ratio in RFV of Pinewood Sawdust	115
5.3.3 Effect of carbon-to-steam ratio in RFV of Pinewood Sawdust.....	122
5.3.4 Effect of Feedstock and Alkali and Alkaline Earth Metallic in RFV of Biomass	125
5.3.5 Stability of catalyst.....	131
5.4 Conclusions.....	141
5.5 References.....	143
Chapter 6: Conclusions.....	149
6.1 Effects of Catalyst Promoters	151
6.2 Effects of Temperature	151
6.3 Effects of Carbon to Oxygen Ratio.....	152
6.4 Effects of Carbon to Steam Ratio	152
6.5 Effects of Biomass Feedstocks and Ash Content.....	153

6.6 Kinetics of Reactive Flash volatilisation	153
Chapter 7: Recommendations and Future Works	155
7.1 Catalyst Research	157
7.1.1 Catalyst Support	157
7.1.2 Active metal nanoparticles	157
7.1.3 Regeneration of the catalyst	157
7.1.4 Fundamental understanding of the effect of promoter on Ni based catalysts.....	158
7.2 Detailed Kinetic Study and Reactor Kinetic Modelling	158
7.3 Other Directions for Future Research in RFV	159
7.3.1 Alternative Reactor Setup.....	159
7.3.2 Alternative Gasifying Agent.....	159
7.3.3 Different Feedstock	159
Appendix	161
Appendix A- Theoretical Estimation of Sample Heating Rate	163
Appendix B- Published Journal Article Front Page	165
B1- Chapter 2- Literature Review: Review of Recent Developments in Ni-based Catalysts for Biomass Gasification	165
B2- Chapter 3- Catalytic Steam Gasification of Cellulose Using Reactive Flash Volatilization	166
B3- Chapter 4- Kinetic Study of Catalytic Steam Gasification of Biomass by Reactive Flash Volatilisation	167

List of Figures

Chapter 2

Figure 2. 1- Pathways for biomass pyrolysis.	14
Figure 2. 2- Comparison of the tar classification methods	16
Figure 2. 3- Simplified reactor setup used in Caballero et al. and Aznar et al.....	22
Figure 2. 4- Comparison of the space velocity, mass flow rate, amount of catalyst required and reactor size of various reactor setups. (Adapted from Colby et al.).....	32

Chapter 3

Figure 3. 1- Schematic diagram of the custom made TPR-TPD-TPO Instrument	49
Figure 3. 2- Schematic diagram of Reactive Flash Volatilization Reactor Setup.....	50
Figure 3. 3- Comparison of the TPR profile of promoted nickel supported on alumina catalysts: (▲) Ni, (●) Pt-Ni, (▼) Ru-Ni, (■) Re-Ni, (◆) Rh-Ni.	56
Figure 3. 4- (a) CO TPD profiles and (b) CO ₂ TPD profiles of promoted nickel based catalysts with alumina support. (▲) Ni, (●) Pt-Ni, (▼) Ru-Ni, (■) Re-Ni, (◆) Rh-Ni.	57
Figure 3. 5- Effect of reactive flash volatilisation temperature and catalyst promoters on the selectivity of Char (■), Tar (■) and Gas (■) based upon carbon balance. The numbers on the top of each bar represent gasification efficiency which is the percentage of carbon in the gas and tar combined. Reaction conditions: cellulose flow rate = 15 g/h, C/O = 0.5, C/S = 1.0 and residence time =50ms. Here Tar is defined as water soluble organics.....	60
Figure 3. 6- Effect of reactive flash volatilisation temperature and catalyst promoters on product gas composition. C ₂ compounds include ethane, ethylene and acetylene. Reaction conditions: cellulose flow rate = 15 g/h, C/O = 0.5, C/S = 1.0 and residence time =50ms.	61
Figure 3. 7- Effect of temperature on a) H ₂ :CO Ratio and b) CO:CO ₂ of promoted nickel based catalysts with alumina support under C/O ratio of 0.5 and C/S ratio of 1.0. (▲) Ni, (●) Pt-Ni, (▼) Ru-Ni, (■) Re-Ni, (◆) Rh-Ni.	62
Figure 3. 8- Effect of carbon to oxygen feed ratio (C/O) and catalyst promoters on the selectivity of Char (■), Tar (■) and Gas (■) based upon carbon balance. The numbers on the top of each bar represent gasification efficiency which is the percentage of carbon in the gas and tar combined. Reaction conditions: cellulose flow rate = 15 g/h, Temperature = 750°C, C/S = 1.0 and residence time =50ms. Here Tar is defined as water soluble organics.	64
Figure 3. 9- Effect of carbon to oxygen feed ratio (C/O) and catalyst promoters on product gas composition. C ₂ compounds include ethane, ethylene and acetylene. Reaction conditions:	

cellulose flow rate = 15 g/h, Temperature = 750°C, C/S = 1.0 and residence time =50ms.	65
Figure 3. 10- Effect of Carbon to Oxygen Ratio on a) H ₂ :CO Ratio and b) CO:CO ₂ Ratio of promoted nickel based catalysts with alumina support at temperature of 750°C and C/S ratio of 1.0. (●) Pt-Ni, (▼) Ru-Ni, (◆)Rh-Ni, (■)Re-Ni.....	66
Figure 3. 11- Effect of carbon to steam feed ratio (C/S) and catalyst promoters on the selectivity of Char (■), Tar (■) and Gas (■) based upon carbon balance. The numbers on the top of each bar represent gasification efficiency which is the percentage of carbon in the gas and tar combined. Reaction conditions: cellulose flow rate = 15 g/h, Temperature = 750°C, C/O = 0.6 and residence time =50ms. Here Tar is defined as water soluble organics.....	68
Figure 3. 12- Effect of carbon to steam feed ratio (C/S) and catalyst promoters on product gas composition. C ₂ compounds include ethane, ethylene and acetylene. Reaction conditions: cellulose flow rate = 15 g/h, Temperature = 750°C, C/O = 0.6 and residence time =50ms.	69
Figure 3. 13- Effect of Carbon to Steam Ratio on a) H ₂ :CO Ratio and b) CO:CO ₂ Ratio of promoted nickel based catalysts with alumina support at temperature of 750 °C and C/O ratio of 0.6. (●) Pt-Ni, (▼) Ru-Ni, (◆) Rh-Ni, (■) Re-Ni.....	70
Figure 3. 14- TEM images of spent catalysts (a) Ni, (b) Pt-Ni, (c) Ru-Ni, (d) Rh-Ni and (e) Re-Ni. Spent catalyst samples selected for the imaging had char selectivity of 2 – 12%.....	73
Figure 3. 15- TEM images of Rh-Ni catalyst in its spent (a) and fresh (b) condition, and Re-Ni catalyst in its spent (c) and fresh (d) condition.....	74
Figure 3. 16- Powder X-ray diffraction curves of γ -alumina support: (a) as received; calcined at (b) 750°C; (c) 800°C; and treated in air + steam atmosphere at (d) 750°C, and (e) 800°C	76

Chapter 4

Figure 4. 1- Schematic diagram of custom built wire-mesh isothermal thermogravimetric reactor. In each experiment the furnace was preheated to the desired temperature under constant N ₂ flow following by switching to gasification agent and then lowering the sample into the reactor.	88
Figure 4. 2- Effect of gasifying agent on the pyrolysis and gasification of cellulose: (a) Pyrolysis under pure N ₂ flow; (b) Gasification under pure CO ₂ ; (c) Gasification under 50 mole% steam in N ₂ ; and (d) Comparison of pseudo first order kinetics under different atmospheres ((■) N ₂ , (●) CO ₂ , and (▼) 50/50 N ₂ /steam). For graphs (a) to (c) the bullet points are experiment data from several repeat runs and the broken line is the fitted curve. For graph (d) the bullet points are fitted data of several repeat runs. All the experiments were carried out at isothermal reactor temperature of 750°C.....	91

Figure 4. 3- Comparison of pyrolytic decomposition and gasification mass loss of (a) Xylan and (b) Lignin. The bullet points are experiment data from several repeat runs and the broken line is the fitted curve. (c) Comparison of pseudo first order kinetics of different components under 50/50 N ₂ /Steam atmosphere ((●) Cellulose, (▲) Xylan and (■) Lignin). All the experiments were carried out at isothermal reactor temperature of 750°C.	96
Figure 4. 4- Comparison of pyrolytic decomposition and gasification mass loss of (a) Synthetic biomass mixture; and pinewood sawdust with particle size range: (b) 63-112 μm and (c) 250-300 μm. (d) Comparison of flash volatilisation first order kinetics of various feedstocks ((●) Synthetic biomass mixture, (▼) pinewood sawdust 63-112 μm and (■) 250-300 μm). The bullet points are experiment data from several repeat runs and the broken line is the fitted curve. All the experiments were carried out in an isothermal reactor at 750°C.	97
Figure 4. 5- Comparison of reactive flash volatilisation first order kinetics of microcrystalline cellulose at (a) 700°C, (b) 750°C and (c) 800°C; and pinewood sawdust at (d) 700°C, (e) 750°C, and (f) 800°C with and without catalysts. The bullet points are fitted values of experiment data from several repeat runs: (×) without Catalyst, (▲) Ni, (●) Pt-Ni, (▼) Ru-Ni, (◆) Rh-Ni, (■) Re-Ni. The kinetic regimes are labelled as (I) pyrolytic decomposition, (II) reforming, and (III) char gasification.	99
Figure 4. 6- (a) Composition of gas produced with and without catalyst in the wire-mesh isothermal thermogravimetric reactor during reactive flash volatilisation of cellulose. (b) Constable-Cremer plot of various catalysts used in reactive flash volatilisation of cellulose.	101
Figure 4. 7- (a) Composition of gas produced with and without catalyst in the wire-mesh isothermal thermogravimetric reactor during reactive flash volatilisation of pinewood sawdust. (b) Constable-Cremer plot of various catalysts used in reactive flash volatilisation of pinewood sawdust.	103
Chapter 5	
Figure 5. 1- Effect of C/O feed and catalyst promoters on the selectivity of gas (■), char (■) and tar (■) based on carbon balance. The numbers on the top of each bar represent gasification efficiency, which is the percentage of carbon in gas and tar combined. Reaction conditions: Pinewood sawdust flow rate= 15 g h ⁻¹ , 750 °C, C/S=1.17. Here tar is defined as water-soluble organics.	117
Figure 5. 2- Effect of C/O feed ratio and catalyst promoters on product gas composition. C ₂ compounds include ethane, ethylene and acetylene. Reaction conditions: Pinewood sawdust flow rate= 15 g h ⁻¹ , 750 °C, C/S=1.17. Here tar is defined as water-soluble organics.	118

Figure 5. 3- Effect of carbon to oxygen ratio on a) H ₂ :CO ratio and b) CO:CO ₂ ratio of promoted nickel based catalysts with alumina support at temperature of 750°C and C/S ratio of 1.17. (●) Re-Ni, (▼) Ru-Ni (▲) Rh-Ni.	121
Figure 5. 4- Effect of C/S feed and catalyst promoters on the selectivity of gas (■), char (■) and tar (■) based on carbon balance. The numbers on the top of each bar represent gasification efficiency, which is the percentage of carbon in gas and tar combined. Reaction conditions: Pinewood sawdust flow rate= 15 g h ⁻¹ , 750 °C, C/O=0.74. Here tar is defined as water-soluble organics.	123
Figure 5. 5- Effect of C/S feed ratio and catalyst promoters on product gas composition. C ₂ compounds include ethane, ethylene and acetylene. Reaction conditions: Pinewood sawdust flow rate= 15 g h ⁻¹ , 750 °C, C/O=0.74. Here tar is defined as water-soluble organics.	123
Figure 5. 6- Effect of carbon to steam ratio on a) H ₂ :CO ratio and b) CO:CO ₂ ratio of promoted nickel based catalysts with alumina support at temperature of 750°C and C/O ratio of 0.74. (●) Re-Ni and (▲) Rh-Ni.	124
Figure 5. 7- Effect of C/O ratio in RFV of eucalyptus sawdust on the selectivity of gas (■), char (■) and tar (■) based on carbon balance. The numbers on the top of each bar represent gasification efficiency, which is the percentage of carbon in gas and tar combined. Reaction conditions: Eucalyptus sawdust flow rate= 15 g h ⁻¹ , 750 °C, C/S=1.11. Here tar is defined as water-soluble organics.	126
Figure 5. 8- Effect of C/O ratio in RFV of eucalyptus sawdust on product gas composition. C ₂ compounds include ethane, ethylene and acetylene. Reaction conditions: Eucalyptus sawdust flow rate= 15 g h ⁻¹ , 750 °C, C/S=1.11. Here tar is defined as water-soluble organics.	127
Figure 5. 9- Compare char yield of different biomass feedstock.	127
Figure 5. 10- Compare product gas composition of RFV with different biomass feedstocks at 750 °C. (a) Re-Ni (■ Cellulose, C/O-0.6, C/S-1.0, ■ Pinewood, C/O-0.68, C/S-1.17 and ■ Eucalyptus, C/O-0.64, C/S-1.11) (b) Rh-Ni (■ Cellulose, C/O-0.7, C/S-1.0, ■ Pinewood, C/O-0.68, C/S-1.17 and ■ Eucalyptus, C/O-0.7, C/S-1.11)	130
Figure 5. 11- Gas product evolutions over time on stream (a) Re-Ni C/O=0.74 (b) Re-Ni C/O=0.82.	132
Figure 5. 12- TEM images of (a) Fresh Re-Ni catalyst. (b) Spent Re-Ni Catalyst from Pinewood RFV (750 °C, C/O- 0.68, C/S-1.17, Runtime- 255 min) (c) Fresh Rh-Ni (d) Spent Rh-Ni from Pinewood RFV (750 °C, C/O- 0.68, C/S-1.17, Runtime- 260 min). Scale bar = 100 nm.	134

Figure 5. 13- Powder XRD patterns of Fresh and Spent Catalysts of Pinewood RFV- I) Re-Ni, II) Rh-Ni, III) Ru-Ni at different C/O ratios- a) Fresh Catalyst b) C/O-0.68 c) C/O-0.74 d) C/O-0.82. (Δ) γ -alumina (\square) δ -alumina (\circ) NiO.	135
Figure 5. 14- (a) Bright field image, (b) dark field high angle annular dark field (HAADF) image and EDS elemental mapping of (c) Ni and (d) noble metal promoter on freshly reduced promoted nickel catalysts.....	137
Figure 5. 15- Bright field, high angle annular dark field (HAADF) TEM images and TEM-EDS elemental distribution for Ni, noble metal promoter Re, K and Mg on spent Re-Ni catalyst from pinewood RFV. Reaction conditions: Pinewood flow rate= 15 g/h, Temperature= 750 °C, C/O= 0.68, C/S = 1.17 and Runtime= 255 min.	138
Figure 5. 16- Bright field, high angle annular dark field (HAADF) TEM images and TEM-EDS elemental distribution for Ni, noble metal promoter Rh, K and Mg on spent Rh-Ni catalyst from pinewood RFV. Reaction conditions: Pinewood flow rate= 15 g/h, Temperature= 750 °C, C/O= 0.68, C/S = 1.17 and Runtime= 260 min.....	139
Figure 5. 17- TEM-EDS spectra of: (a) freshly reduced Re-Ni catalyst (b) Spent Re-Ni catalyst from pinewood RFV (Temp= 750 °C, C/O= 0.68, C/S = 1.17, TOS= 255 min) (c) freshly reduced Rh-Ni catalyst (d) Spent Rh-Ni catalyst from pinewood RFV (Temp= 750 °C, C/O= 0.68, C/S = 1.17, TOS= 260 min).	140

List of Tables

Chapter 2

Table 2. 1- Comparison of tar content in product gas of different gasification technologies.	17
Table 2. 2- Performance comparison of commercial nickel catalysts used as primary catalyst in biomass gasification and pyrolysis.	20
Table 2. 3- Comparison of the properties of commercially available nickel based catalyst.	21
Table 2. 4- Comparison of nickel catalysts with different support materials used in pyrolysis and steam reforming of bio-oil.	26
Table 2. 5- Comparison of promoted nickel catalysts used in pyrolysis and steam reforming of biomass.	29
Table 2. 6- Comparison of chemisorption results of various research based nickel catalysts.	30

Chapter 3

Table 3. 1- Gasification reactions and their enthalpies for C ₆ compound.	47
Table 3. 2- Comparison of the specific surface area, total pore volume, amount of active metal, metal dispersion, NiO, Al ₂ O ₃ and promoter contents of various promoted nickel based catalysts with alumina support.	55
Table 3. 3- Comparison of the amount of H ₂ consumed and amount of CO and CO ₂ adsorbed on each catalyst.	55
Table 3. 4- Comparison of the specific surface area of fresh (calcined) and hydrothermally treated mono-metallic and promoted nickel catalysts supported on γ -alumina.	75

Chapter 4

Table 4. 1- Comparison of the pyrolytic decomposition rate constant and reforming rate constant in flash volatilisation of cellulose with various gasifying agents at 750°C.	90
Table 4. 2- Comparison of the pyrolytic decomposition regime rate constant (k), apparent pre-exponential factor ($A_{apparent}$) and apparent activation energy ($E_a - apparent$) in reactive flash volatilisation of various biomass feedstock.	94
Table 4. 3- Comparison of the reforming regime rate constant (k), apparent pre-exponential factor ($A_{apparent}$) and apparent activation energy ($E_a - apparent$) in reactive flash volatilisation of various biomass feedstock.	95
Table 4. 4- Comparison of the reforming rate constant (k), apparent pre-exponential factor ($A_{apparent}$) and apparent activation energy ($E_a - apparent$) in reactive flash volatilisation of cellulose using various catalysts.	101
Table 4. 5- Comparison of the reforming rate constant (k), apparent pre-exponential factor ($A_{apparent}$) and apparent activation energy ($E_a - apparent$) in reactive flash volatilisation of pinewood sawdust using various catalysts.	103

Chapter 5

Table 5. 1- Physical and Chemical properties of Pinewood and Eucalyptus Sawdust 115

Abstract

Biomass gasification is a promising technology for delivering renewable energy. However, tar formation remains one of the main challenges. This research aims to develop *in-situ* nickel based catalysts for reactive flash volatilization (RFV) of biomass. RFV is a catalytic gasification process which uses high carbon space velocity and mass flow rate, with oxygen and steam as gasification agents, to produce tar free synthesis gas from non-volatile feedstock in a milliseconds residence time reactor. Ni, Pt-Ni, Ru-Ni, Re-Ni and Rh-Ni supported catalysts were investigated in this study.

Effects of various operating parameters on the product selectivity (gas, tar and char) and syngas composition were evaluated. The operating parameters studied here include catalyst promoter, reaction temperature, carbon to oxygen feed ratio (C/O), carbon to steam feed ratio (C/S) and biomass ash content. Products were analysed using gas chromatography, total organic carbon (TOC) and CHNS/O analyses. Catalysts were characterised using Temperature Programmed Reduction, Temperature Programmed CO-Desorption, Transmission Electron Microscopy, nitrogen physisorption, X-ray Fluorescence and Powder X-ray Diffraction.

Re-Ni, Rh-Ni and Ru-Ni, in that order, exhibited higher gasification efficiency in RFV of cellulose. This can be attributed to these catalysts' higher reducibility and active metal surface area, and better coke resistance. Highest gasification efficiency was achieved at 750°C with C/O of 0.6 and C/S of 1.0, without any oxygen breakthrough.

Kinetics study using a wire-mesh isothermal thermogravimetric analyser was conducted to investigate the role of catalyst in RFV. Result was modelled using a pseudo first order reaction model. Three distinct regimes of rate of mass loss were identified: pyrolytic decomposition, reforming and char gasification. Catalysts increased the rate of mass loss in reforming regime and improved the quality of synthesis gas. Rate of pyrolytic decomposition of lignocellulose was found to be limited by devolatilisation of crystalline cellulose.

Gasification efficiencies of pinewood and eucalyptus sawdust were found to be higher than cellulose under similar reaction conditions. Higher gas selectivity and lower char selectivity during pinewood and eucalyptus sawdust RFV was a result of more amorphous structure of lignocellulose compared to microcrystalline cellulose, and the catalytic effects of alkali and alkaline earth metals (AAEM) found in the lignocellulose ash. The catalytic effects of AAEM further reduced the coke deposition on the Ni catalysts, making the effect of noble metal promoter on the Ni catalysts less significant. Future studies may reduce the loading of noble metal to make RFV more economical.

Monash University

Declaration for thesis based or partially based on conjointly published or unpublished work

General Declaration

In accordance with Monash University Doctorate Regulation 17.2 Doctor of Philosophy and Research Master's regulations the following declarations are made:

I hereby declare that this thesis contains no material which has been accepted for the award of any other degree or diploma at any university or equivalent institution and that, to the best of my knowledge and belief, this thesis contains no material previously published or written by another person, except where due reference is made in the text of the thesis.

This thesis includes three original papers published in peer reviewed journals and one unpublished publications. The core theme of the thesis is to develop a stable promoted nickel based catalyst for lignocellulose reactive flash volatilization. The ideas, development and writing up of all the papers in the thesis were the principal responsibility of myself, the candidate, working within the Faculty of Engineering, Department of Chemical Engineering under the supervision of Dr. Akshat Tanksale.

The inclusion of co-authors reflects the fact that the work came from active collaboration between researchers and acknowledges input into team-based research.

In the case of chapter 2, 3, 4 and 5 my contribution to the work involved the following:

Thesis chapter	Publication title	Publication status*	Nature and extent of candidate's contribution
2	Review of recent developments in Ni-based catalysts for biomass gasification	Published	Initiation, key ideas, experimental and analysis works, development and writing up of the paper.
3	Catalytic Steam Gasification of Cellulose Using Reactive Flash Volatilisation	Published	
4	Kinetic study of Catalytic Steam Gasification of Biomass by Using Reactive Flash Volatilisation	Published	
5	Catalytic Steam Gasification of Pinewood and Eucalyptus Sawdust Using Reactive Flash Volatilisation	Manuscript in Preparation	

I have not renumbered sections of submitted or published papers in order to generate a consistent presentation within the thesis.

Signed: 

Date: 15/05/2015

Acknowledgement

I would like to express my sincere gratitude to all of those who help me to complete this thesis. First and foremost, I would like to thank my thesis advisor, Dr. Akshat Tanksale for his guidance and supervision throughout this research project. It was a great pleasure for me to conduct this thesis under his supervision. Second, I would like to acknowledge my thesis committee members: Prof. Wei Shen, Prof. Andrew Hoadley and Prof. Sankar Bhattacharya. Their valuable feedback helped me to improve the thesis in many ways.

In addition, I am grateful for the financial support from the following funding agencies: Monash Institute of Graduate Research (MIGR), Rural Industries Research and Development Corporation (RIRDC) and The Swedish Foundation for International Cooperation in Research and Higher Education (STINT).

Also, I would also like to give my sincere thanks to my fellow Catalysis for Green Chemicals group members. Special thanks to Alimohammad Bahmanpour and Sheryl Moh for helping me in the lab.

I would like to acknowledge Ms Lilyanne Price, Jill Crisfied, Chloe Priebee, Rebecca Bulmer, Kim Phu, Ronald Graham, Gamini Ganegoda, Harry Bouwmeester, Ross Ellingham and Martin Watkins for their invaluable assistance and support during my Phd tenure. Also, sincere appreciation is extended to all the academic staff and postgraduate students in the department for their help. Thanks to Prof Sankar Bhattacharya, Prof Huanting Wang and Dr Lian Zhang for allowing me to use their instruments for my research.

I am also grateful for all the assistance I received from MCEM. Thanks Dr Tim Wiliam for his time and expertise in helping me in TEM-EDS analysis. Also, special thanks to Prof. Kentaro Umeki for his generous hospitality and assistants during my visit to Luleå University of Technology, Sweden.

Last but not least, I would like to thank my family for supporting me through all these years. I would like to thank my wife Yah Nan Chia, and my parent for all the love, support and encouragements given to me.

List of Publications

Journal Publications

Chan, F.L. and Tanksale, A. (2014). "Review of recent developments in Ni-based catalysts for biomass gasification." Renewable and Sustainable Energy Reviews 38(0):428-438.

Chan, F.L. and Tanksale, A. (2014). "Catalytic Steam Gasification of Cellulose Using Reactive Flash Volatilization." ChemCatChem 6(9):2727-2739.

Chan, F.L., Umeki, K., Tanksale, A. (2015). "Kinetic Study of Catalytic Steam Gasification of Biomass by Reactive Flash Volatilisation." ChemCatChem 7(8):1329-1337.

Referred Conference Paper

Chan, F.L. and Tanksale, A. (2013). "Promoted nickel supported catalyst for reactive flash volatilisation of cellulose to produce tar free synthesis gas." CHEMECA 2013: Challenging Tomorrow, Brisbane, Australia.

Conference Proceedings

Chan, F.L. and Tanksale, A. (2014). "Conversion of Cellulose to Tar Free Synthesis Gas over Nickel Based Catalysts." 22nd European Biomass Conference and Exhibition, Hamburg, Germany.

Abbreviations

AAEM	Alkali and Alkaline Earth Metal
AS	Australian Standards
BET	Brunauer- Emmett- Teller
BJH	Barrett- Joyner- Halenda
C/O	Carbon to Oxygen
C/S	Carbon to Steam
CHNS/O	Carbon Hydrogen Nitrogen Sulphur/ Oxygen
CO-TPD	Carbon Monoxide Temperature Programmed Desorption
DME	Dimethyl Ether
EDS	Energy Dispersive X-Ray Spectroscopy
EN	European Standards
FEG	Field Emission Gun
GC	Gas Chromatography
H ₂ -TPR	Hydrogen Temperature Programmed Reduction
HAADF	High Angle Annular Dark Field
HPLC	High Performance Liquid Chromatography
IWI	Incipient Wetness Impregnation
JCPDS	Joint Committee on Powder Diffraction Standards
MTO	Methyl-Rhenium Trioxide
PAH	Polynuclear aromatic hydrocarbons
PD	Precipitation-Deposition
RFV	Reactive Flash Volatilisation
RGA	Residual Gas Analyser
SG	Sol-Gel
STEM	Scanning Transmission Electron Microscopy
TEM	Transmission Electron Microscope
TGA	Thermogravimetric Analysis

TOC	Total Organic Carbon
TPD	Temperature Programmed Desorption
TPO	Temperature Programmed Oxidation
TPR	Temperature Programmed Reduction
XRD	X-Ray Diffraction
XRF	X-Ray Fluorescence

Nomenclature

wt%	weight percentage
g_{cat}	Catalyst weight in gram
L_{reactor}	Reactor length
r	Reaction rate
X	Fractional conversion
m_0	Initial sample weight
m	Sample weight at time t
k	Rate constant
T	Absolute temperature in K
$E_{a\text{-apparent}}$	Apparent activation energy
A_{apparent}	Apparent pre-exponential factor
R	Universal gas constant

This page intentionally left blank.

Chapter 1: Introduction

This page intentionally left blank.

1.1 Background

Global energy demand is expected to increase greatly in the near future. In the recently released Energy White Paper 2015, the International Energy Agency projected that the world global energy demand will increase by over one-third by year 2040 (Australian Government Department of Industry and Science 2015). Relying heavily on non-renewable fossil fuel such as coals, petroleum and natural gas, to meet our ever-increasing energy need is unattainable. To achieve sustainable future growth, a global transition from fossil fuel to renewable energy is needed. The switch to renewable energy not only reduces our dependence on fossil fuel energy carriers but also contributes to the reduction of greenhouse gas emissions.

Lignocellulose biomass is a renewable energy resource that is derived from plant resources such as energy crops, annual and perennial grasses, agricultural residues and forestry residues. It is recognized as one of the most promising solutions for our current energy crisis and environmental problems. It is considered as a reliable energy source in terms of security of supply in comparison to other renewable energies such as solar energy and wind power, which often suffer from intermittent power generation issue (Kirkels et al. 2010). Also, biomass is the only renewable energy source that can be converted into liquid fuel and utilized as feedstock in chemicals production (Huber et al. 2006).

Biomass can be converted into bio-energy and bio-fuels through thermochemical conversion such as direct combustion, pyrolysis and gasification. Among these processes, biomass gasification is of most interest both industrially and academically due to its high conversion efficiency. In gasification, feedstock is converted into combustible gaseous products, e.g. hydrogen, carbon monoxide and methane under a limited oxygen supply environment. However, it has been mentioned in numerous literature that tar formation in biomass gasification is one of the hurdles that hinders commercialisation of this process. Tar is a complex mixture of heavy hydrocarbons rich in aromatics, mainly comprises of benzene, toluene, phenol, cresols and naphthalene (Łamacz et al. 2011). Accumulation of tar in the reactor leads to severe operational problem such as plugging of the reactor. Tar can be removed via additional downstream processes like filtering, steam reforming followed by preferential oxidation or water gas shift reactor. However, the downstream processes are capital and operationally expensive, making them economically unfavourable.

A novel approach called as reactive flash volatilisation (RFV) was recently proposed for catalytic gasification of non-volatile feedstock in a fixed bed reactor (Salge et al. 2006). RFV combines fast pyrolysis, partial oxidation, steam reforming and water gas shift reactions in a single short

Chapter 1

residence time reactor. Tar free synthesis gas was produced by this approach in an autothermal reactor over Rh-Ce catalyst where bio-oil feedstock was decomposed into hydrogen and carbon monoxide in less than 50 ms without the production of char. The hypothesis presented by the authors was that the formation of char and tar were avoided by rapidly oxidizing the decomposition products into gases. The heat generated from oxidation prevented the quenching of the process that would lead to rapid carbon formation. One of the most important advantages of this reactor is that the amount of catalyst used per unit mass of carbon source is significantly less than the amount of catalyst used in conventional biomass gasifier. Therefore, small scale gasification plants (an order of magnitude smaller than the conventional systems) could be economically viable. A large scale centralised plant may not be required for the biomass gasification process to become economical, which is an advantage due to the sparsely cultivated lignocellulose feedstock. Therefore the small scale RFV plants can be placed closer to the feedstock source to minimise the transportation cost.

1.2 Research Aims

Several research gaps have been identified in the existing literature on this topic. First, although RFV over Rh based catalyst is a promising method for high quality syngas synthesis, it is impractical for larger than bench scale application due to the high cost of the catalysts. Therefore, it is necessary to develop a cost effective catalyst with equal or better performance which can be used in this process. Second, early RFV research was conducted using liquefied organic model compounds as feedstock (Salge et al. 2006; Rennard et al. 2009). Further research is required to study the effectiveness of this process with lignocellulose biomass feedstock. Third, although it has been widely reported in literature that nickel based catalysts are highly effective in eliminating tar and improving the quality of the product gas, these catalysts are also subjected to rapid deactivation when used in a primary gasifier, resulted from carbon fouling, sintering and morphological changes. Therefore, a cost effective nickel based catalyst that can be used in the primary reactor and inhibit the carbon formation is needed.

Overall, the aim of this research is to develop a stable promoted nickel based catalyst for reactive flash volatilisation of lignocellulose biomass. Specific aims of this research include:

- Understand the effects of catalyst promoters and operating conditions (temperature, C/O and C/S ratios) on the product yield and syngas quality. Understand the effect of composition of lignocellulose biomass in its gasification behaviour and kinetics.
- Model the kinetic parameters that affect the reactions during reactive flash volatilisation.

- Investigate the deactivation mechanism of the catalyst in reactive flash volatilisation.

Results and conclusions from this thesis will contribute to the knowledge base which will help in the development and commercialisation of the reactive flash volatilisation process.

1.3 Thesis Structure and Chapter Outline

This thesis is organised into seven chapters.

Chapter 1- Introduction

This chapter contains the background of this research, research aims and an overview of the thesis structure.

Chapter 2- Literature Review

This chapter covers the critical literature review on the use of nickel based catalyst in biomass gasification to eliminate tar. In this chapter some recent developments in nickel based catalysts used in biomass gasification, including commercial and novel catalysts, are reviewed. Detailed discussions on the effects of different supports, promoters and particle sizes on the catalytic performance of the catalysts are also included. In addition, future direction of biomass gasification, including reactive flash volatilisation and steam gasification, is also discussed. This chapter has been published as a journal article in *Renewable and Sustainable Energy Reviews*.

Chapter 3- Catalytic Steam Gasification of Cellulose Using Reactive Flash Volatilisation

In this chapter, production of synthesis gas from Reactive Flash Volatilisation of microcrystalline cellulose over promoted nickel based catalyst is investigated. Effects of temperature, C/O feed ratio and C/S feed ratio on products yield and syngas composition were studied. Fresh and spent catalysts were characterised in detail to understand the effects of catalyst properties on the reaction activity, and to study the mechanism of catalyst deactivation. This chapter has been published as a journal article in *ChemCatChem*.

Chapter 4- Kinetic Study of Catalytic Steam Gasification of Biomass Using Reactive Flash Volatilisation

This chapter investigates the kinetics of reactive flash volatilisation of lignocellulose biomass under steam rich condition using a custom built wire-mesh isothermal thermogravimetric analyser. A pseudo first order kinetic model was used to study the effects of various promoters on the nickel catalysts, composition of the feedstock and gasification agents, on the rate of reaction. Results from this investigation provide direct evidence of the effects of in-situ catalysts in

Chapter 1

removing tar forming compounds during volatilisation of biomass in reactive flash volatilisation. This chapter has been published as a journal article in *ChemCatChem*.

Chapter 5- Catalytic Steam Gasification of Pinewood and Eucalyptus Sawdust Using Reactive Flash Volatilisation

This chapter investigates the production of syngas using reactive flash volatilisation of pinewood and eucalyptus sawdust over promoted nickel based catalysts. This study focussed on evaluating the effects of catalyst promoters, C/O feed ratio, C/S feed ratio and ash, on product yields and product gas composition. A manuscript based on this study is currently under preparation for submission in *Bioresource Technology* journal.

Chapter 6- Conclusions

All the major findings in this thesis are presented in this chapter.

Chapter 7- Recommendations and Future works

Several key recommendations and future research topics in reactive flash volatilisation are presented in this chapter.

1.4 References

Australian Government Department of Industry and Science (2015). Energy white paper 2015. Department of Industry and Science (Australia).

Huber, G. W., S. Iborra, et al. (2006). "Synthesis of Transportation Fuels from Biomass: Chemistry, Catalysts, and Engineering." Chem. Rev. (Washington, DC, U. S.) **106**: 4044-4098.

Kirkels, A. F. and G. P. J. Verbong (2010). "Biomass gasification: Still promising? A 30-year global overview." Renewable Sustainable Energy Rev. **15**: 471-481.

Łamacz, A., M. Pawlyta, et al. (2011). "Characterization of the structure features of CeZrO₂ and Ni/CeZrO₂ catalysts for tar gasification with steam." Archives of Materials Science and Engineering **48**: 89-96.

Rennard, D. C., J. S. Kruger, et al. (2009). "Autothermal catalytic partial oxidation of glycerol to syngas and to non-equilibrium products." ChemSusChem **2**: 89-98.

Salge, J. R., B. J. Dreyer, et al. (2006). "Renewable hydrogen from nonvolatile fuels by reactive flash volatilization." Science **314**: 801-804.

This page intentionally left blank.

Monash University

Declaration for Thesis Chapter 2

Declaration by candidate

In the case of Chapter 2, the nature and extent of my contribution to the work was the following:

Nature of contribution	Extent of contribution (%)
Initiation, key ideas and writing up of the paper	80

The following co-authors contributed to the work. If co-authors are students at Monash University, the extent of their contribution in percentage terms must be stated:

Name	Nature of contribution	Extent of contribution (%) for student co-authors only
Akshat Tanksale	Initiation, key ideas, reviewing and editing of the paper.	

The undersigned hereby certify that the above declaration correctly reflects the nature and extent of the candidate's and co-authors' contributions to this work*.

Candidate's
Signature

	Date 15/05/2015
---	--------------------

Main
Supervisor's
Signature

	Date 15/05/2015
---	--------------------

This page intentionally left blank.

Chapter 2: Literature Review- Review of recent developments in Ni-based catalysts for biomass gasification

Abstract

Biomass gasification is recognized as one of the most promising solutions for renewable energy and environmental sustainability. However, tar formation in gasifier remains one of the main hurdles that hinder commercialization. Nickel based catalyst is widely used in chemical industries and is proven as one of the most effective transition metal catalysts in biomass gasification for tar cracking and reforming. This chapter presents a review of various commercial nickel catalysts that have been evaluated for tar elimination in biomass gasification. This review also looks at recent advancements in nickel based catalyst used in biomass gasification, including discussion on the effects of different support, promoter and particle size on the catalytic performance. Future direction of biomass gasification, including reactive flash volatilization and steam gasification, are also discussed in this review.

This page intentionally left blank.

2.1 Introduction

According to the 2011 Energy White Paper by the Australian Department of Resource, Energy and Tourism, the world global energy demand in year 2035 will be 40 percent higher than current level (Department of Resources 2012). However, with the growing concerns about climate change and greenhouse gas emissions, non-renewable fossil fuels such as coal, petroleum and natural gas can no longer be considered as the only energy sources for the meeting of our future energy needs. In the short to medium term, a versatile and diverse energy plan, comprising both renewable and non-renewable energy sources is required. In the long term, there is a need for global transition to 100% renewable energy and chemical feedstock to achieve sustainable growth.

Biomass is a renewable energy resource derived from biological sources such as energy crops, agricultural residues, forestry residues and municipal wastes (Kechagiopoulos et al. 2006). Biomass utilisation is recognized as one of the most promising solutions for our current energy and environmental problems. Alternative renewable energy technologies such as solar energy and wind power, which often suffer from intermittent power generation issue, are less reliable in term of security of supply (Kirkels et al. 2010). Also, biomass is the only renewable energy source that can be converted into liquid fuel and utilised as feedstock in chemicals production (Huber et al. 2006).

Thermochemical processes for biomass conversion, such as combustion, gasification and pyrolysis, can be used for power generation and biofuels production (Kumar et al. 2009). Among these processes, biomass gasification has attracted the most attention from both industrial and academic researchers due to its high conversion efficiency (Devi et al. 2003). Biomass gasification is a process to convert biomass feedstock into combustible gaseous products like hydrogen, carbon monoxide and methane; however, undesirable products like tar and char are also produced under high temperature and limited oxygen supply environment.

Chemistry of biomass gasification is complex and yet to be fully understood by researchers (Pfeifer 2008). It is generally acceptable to say that the major reactions include pyrolysis, oxidation, partial oxidation, reduction, steam reforming and water gas shift reactions (Wang et al. 1993; Sutton et al. 2001; Huber et al. 2006). Pyrolysis is an endothermic decomposition process which takes place at high temperature in the absence of air or steam. In biomass pyrolysis, the feedstock is converted into gas, liquid tar and solid char products as shown in Figure 2.1 (Shafizadeh 1982).

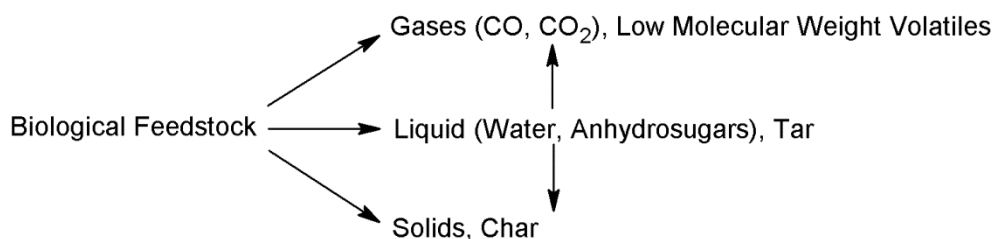
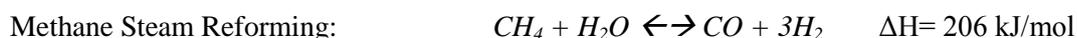
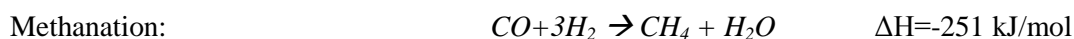
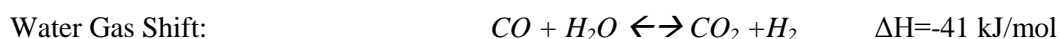
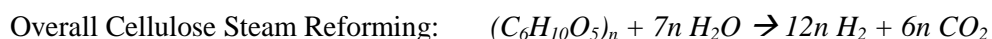


Figure 2. 1- Pathways for biomass pyrolysis.

In oxidation or partial oxidation reactions, carbonaceous products from pyrolysis reaction may react further with oxygen to generate more gas and release heat. In the final step of gasification, product gases are upgraded through steam reforming, which converts low molecular weight hydrocarbons such as CH_4 into CO and H_2 . Water gas shift reaction further converts CO and steam into H_2 and CO_2 . Side reactions such as methanation also occur in gasification but to a lesser extent (Kumar et al. 2009; Haryanto et al. 2009). Using cellulose as a model, the main chemical reactions of biomass gasification can be expressed in the equations below.



Biomass gasification produces condensable heavy hydrocarbons, generally referred to as tar. Tar removal is a major hurdle that hinders the commercialization of the biomass gasification (Huber et al. 2006). Accumulation of tar in the gasifier may lead to severe operational problems such as corrosion, clogging and low gasification efficiency. Recently, significant progress has been made in the gasifier designs coupled with the use of catalysts to overcome these operational problems. The key focus of this chapter is to review some of the recent developments in nickel based catalyst used in biomass gasification and tar removal.

2.2 Tar

Tar consists of more than 100 different compounds and is produced in a series of complex thermochemical reactions. The amount of tar produced in biomass gasification is greatly affected by factors such as type of biomass feedstock, particle size, type of gasifier, type of gasifying agent and operating conditions such as temperature and pressure. Table 2.1 shows an overview of different types of biomass gasification setups. Majority of the gasifiers are operated in a temperature range of 700 –

1000 °C (Hos et al. 1980; Van den Aarsen et al. 1983; Kurkela et al. 1992; Czernik et al. 1993; Pedersen 1993; Narváez et al. 1996; Delgado et al. 1997; Gil et al. 1999; Rapagnà et al. 2000; Dogru et al. 2002; Lv et al. 2007; Hernández et al. 2010; Zhao et al. 2010; Nagel et al. 2011; Ueki et al. 2011; Wang et al. 2011; Qin et al. 2012; Senapati et al. 2012). Generally, higher operating temperatures lead to lower tar content in the product gas. Among the three designs listed in Table 2.1, gas product generated from entrained flow gasifier normally has the lowest tar content because they operate at the higher end of the gasification temperature range (1000 – 1400°C) (Bridgwater 1995). Increasing the pressure of gasifiers also has a positive effect in reducing or eliminating the tar formation (Devi et al. 2003). However, it has been observed that increasing the pressure results in greater reduction of light hydrocarbons compared to the heavy hydrocarbons, therefore the fraction of polynuclear aromatic hydrocarbons (PAH) in the tar increases with pressure (Knight 2000).

In addition to the quantity of tar produced, the composition of tar also depends on the type of biomass feedstock, particle size and gasification conditions used. Fraga et al. (Fraga et al. 1991) showed that the distribution of the furan derivatives in sugarcane bagasse tar was different from the distribution found in silver birch wood tar under the same pyrolysis conditions. Ku et al. demonstrated that the content of PAH found in bamboo pyrolysis tar was higher than the PAH content found in oak and pine wood tar (Ku et al. 2006). Furthermore, Qin et al. reported that PAH concentration in tar from sawdust gasification decreased as the gasification temperature increased from 700°C to 900°C (Qin et al. 2007). Therefore, it is important to understand the composition of tar and the conditions under which different types of tar compounds are formed.

Definition of tar varies widely by study, but it is generally accepted as aromatic hydrocarbons with molecular weight higher than benzene (Li et al. 2009). In order to better understand the characteristics of tar, various ways to classify tar have been suggested. The first approach proposed by Milne et al. (Milne et al. 1998) divides tar into four groups: primary, secondary, alkyl tertiary and condensed tertiary, based on their experimental results obtained from gas phase thermal cracking reactions. Primary tar, which is defined as low molecular weight oxygenated hydrocarbons, is composed of compounds derived from cellulose, analogous hemicellulose and lignin. Examples of primary tar include levoglucosan and furfurals. Secondary tar is composed of phenolic and olefin compound, including cresol and xylene. Alkyl tertiary tar is composed of methyl derivatives of aromatics such as toluene and the condensed tertiary tar is composed of polynuclear aromatics hydrocarbons (PAH) without the branched molecular groups such as benzene and naphthalene. Alkyl tertiary and condensed tertiary tars are products of condensation reaction of the primary tars at high temperature.

Chapter 2

Tar can also be classified based on its components solubility and condensability, as suggested by Kiel et al. (Kiel 2004). It is crucial to understand the condensability and the solubility of tar compounds because condensation of tar in the reactor may lead to severe operating issues and solubility of tar components may increase the processing cost of the wastewater produced from the process. Based on these two properties, Kiel et al. categorized tar into five classes:

- Class 1- GC undetectable heaviest tars which condense at high temperature and very low concentration
- Class 2- Heterocyclic aromatic compounds with high water solubility, including phenol and cresol.
- Class 3- Light hydrocarbons aromatic compound (1 ring), a nonissue regarding condensability and solubility, such as toluene and xylene
- Class 4- Light polyaromatic hydrocarbons (2-3 rings) which condense at relatively high concentrations and intermediate temperatures, including indene and naphthalene
- Class 5- Heavy polyaromatic hydrocarbons (4-7 rings) which condense at relatively high temperature and low concentration, such as pyrene and coronene

A comparison of Milne's and Kiel's tar classification approaches is sketched out in Figure 2.2. It is clear that definition of tar proposed by Milne et al. covers a broader range of products than definition provided by Kiel et al. All the tar components, from class 1 to class 5, discussed in Kiel et al.'s study fall under secondary and tertiary tar categories according to Milne et al.'s definition. Primary tar compounds lighter than heterocyclic aromatics are not included in Kiel et al.'s classification.

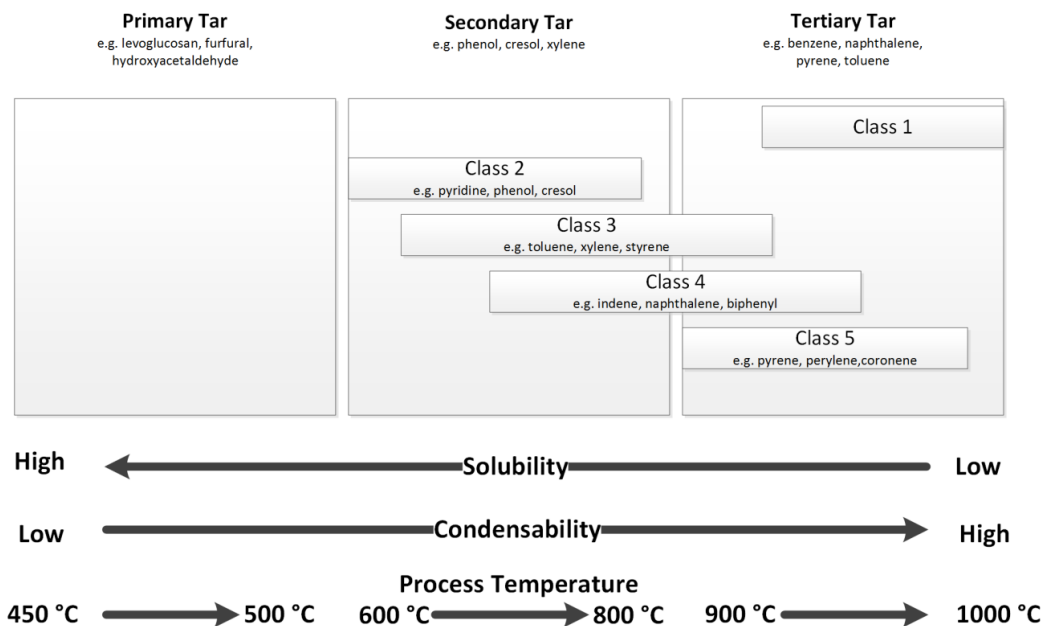


Figure 2. 2- Comparison of the tar classification methods

Table 2. 1 - Comparison of tar content in product gas of different gasification technologies.

Gasifier	Feedstock	Gasifying Agent	Operating Conditions		Tar Content (g/Nm ³ dry gas)	Reference
			Temp (°C)	Pressure (kPa)		
Fixed Bed						
Updraft	Straw	Air	400- 500	-	~ 50.0	(Pedersen 1993)
Updraft	Sawdust	Air	-	-	8.6	(Wang et al. 2011)
Updraft	Wood Pellet	Air and Steam	650	-	90.3	(Najel et al. 2011)
Updraft	Black Pine Wood Pellet	Air	1000	-	132.4	(Ueki et al. 2011)
Downdraft	Wood Chip, Municipal solid waste	-	-	-	0.5	(Hos et al. 1980)
Downdraft	Black Pine Wood Pellet	Air	900	-	32.3	(Ueki et al. 2011)
Downdraft	Hazelnut Shell	O ₂ and Steam	821-1206	-	2.6-4.0	(Dogru et al. 2002)
Downdraft	Pine Wood Block	Air	774-934	-	1.7-4.0	(Lv et al. 2007)
		O ₂ and Steam	870-1108	-	7.7- 21.1	
		Air	910-1090	-	1.2- 2.5	
		O ₂ and Steam	798-910	-		
		Air				
Fluidized Bed						
Bubbling	Almond Shell	Steam	700	-	6.0- 7.0	(Rapagnà et al. 2000)
Bubbling	Pine Sawdust	Steam	820	-	1.0- 1.5	
Bubbling	Pine Sawdust	Air	790-810	-	2.0- 18.0	(Narváez et al. 1996)
Bubbling	Pine Sawdust	Steam	750	~ 101	180.0	(Delgado et al. 1997)
		Steam	780	~ 101	40.0	
Bubbling	Pine Wood	Steam	750 - 780	~ 101	30.0- 80.0	(Gil et al. 1999)
		O ₂ and Steam	750 - 780	~ 101	4.0-30.0	
		Air	750- 780	~ 101	2.0-20.0	
Bubbling	Wood Shaving/ Saw dust	Air	780	-	~ 2.0	(Czernik et al. 1993)
		Air	857	-	~ 0.3	
Bubbling	Rice Husk	Air	750	-	6.0	(Van den Aarsen et al. 1983)
		Air	940	-	0.8	
Circulating	Mixed Sawdust	Air and Steam	701	~ 105	15.1	(Li et al. 2004)
		Air and Steam	815	~ 105	0.4	
Pressurized	Pine Wood Sawdust	Air and Steam	700-850	300-1000	5.6	(Kurkela et al. 1992)
Entrained Flow						
	Grapevine pruning, Pine Sawdust, De-Alcoholised marc of grape Sawdust	Air	750 - 1050	~ 101	negligible	(Herrández et al. 2010)
	Coconut Coir dust	Air	700 - 1000	-	negligible	(Zhao et al. 2010)
		Air	976	~ 101	23.6	(Senapati et al. 2012)
		Air	1100	~ 101	4.8	
Pressurized	Sawdust from soft stem wood	Oxygen	1000 - 1200	~ 195	negligible	(Qin et al. 2012)

2.3 Biomass Gasification with Commercial Nickel Based Catalyst

Significant efforts have been put into developing a cost effective method to eliminate tar in gasification. Among all the proposed solutions, the use of catalysts in gasification *in-situ* is the most promising approach (Sutton et al. 2001; Devi et al. 2003). Catalyst used in biomass gasification can be categorized into three types, they are: natural mineral catalyst, alkali metal catalyst and transition metal catalyst (Sutton et al. 2001; Abu et al. 2004). Dolomite and olivine are two of the most commonly used natural mineral catalysts in biomass gasification. Although the quality of the gaseous product can be improved substantially with these catalysts, additional gas clean-up step is still needed as the quality of the end product is inadequate for direct use in other end user applications, such as fuel cell (Wang et al. 2005). Alkali metals, such as lithium, sodium, potassium, and rubidium, have been widely used as catalysts in biomass gasification (Abu et al. 2004). Despite the fact that these catalysts provide a considerable increase in initial reaction activity, they are susceptible to loss of activity at high temperature due to particle agglomeration. Alternatively, transition metal-based catalysts, particularly nickel, are excellent for biomass gasification due to their high activities in tar elimination and ability to improve producer gas quality.

A large number of studies have been conducted and reported in the literature using commercial nickel based catalysts in biomass gasification to promote steam-reforming, water gas shift reactions and to eliminate tar. These studies can be categorized into two groups. The first group focuses on using nickel catalyst as the primary catalyst in the gasifiers and the second group concentrates on using it as the secondary catalyst in post gasification or post pyrolysis reactor.

2.3.1 Commercial Nickel Catalyst as Primary Catalyst

There are several benefits of using nickel catalyst as the primary catalyst. First, nickel is one of the most effective transition metals for tar cracking and reforming (Baker et al. 1987). In addition to reducing the tar content, nickel catalyst improves the quality of the gaseous product in biomass gasification. Second, it is economically attractive. Because both gasification and gas clean-up processes occur *in-situ*, no downstream reactor or extra heating is required, which results in lower plant capital and operating cost (Devi et al. 2003; Colby et al. 2008).

Nonetheless, little work has been reported on using commercial nickel catalyst as primary catalyst in biomass gasification. One study by Baker et al. (Baker et al. 1987) examined the performance of G-90C catalyst used as primary and secondary catalysts in biomass steam gasification (Table

2.2). In a fluidized bed experiment with G-90C as primary catalyst, synthesis gas yield of 1.8 m³/kg was obtained in the first 5 h of run. However, gas yield started to decline after 5 h and the catalyst was completely deactivated after 7 h. For comparison, the maximum theoretical gas yield with a H₂/CO ratio of 2.0 is 2.4 m³/kg. Similar behaviour was observed in the experiments with G-90C used as a secondary catalyst. The initial activity was high but gradually reduced thereafter. After 16 h of on stream testing, synthesis gas yields of the secondary fixed bed reactor and the secondary fluidized bed reactor stabilized at 1.25 - 1.30 m³/kg and 1.50 m³/kg respectively. The G-90C catalyst performed better as secondary catalyst over longer time period because of lower carbon fouling (1/3rd) compared to the primary catalyst.

Li et al. (Li et al. 2004) also conducted a study using commercial nickel catalyst as primary catalyst in biomass gasification (Table 2.2). The main focus of their studies was to investigate the impact of operating parameters on the final gaseous product composition in a circulating fluidized bed gasifier and to develop a model for the air-blown circulating fluidized bed biomass gasification. They reported that tar yields in two of the runs with Sud-Chemie catalyst C11-9 LDP were substantially lower when compared with the runs with no catalyst added under the same operating temperature. The tar yield reduced from 10.26 g/Nm³ to 2.35 g/Nm³ and 0.04 g/Nm³ respectively. However, no further investigation and characterization was conducted on the spent catalyst and deactivation of the catalyst was not reported.

Both Baker and Li's studies demonstrated the advantages and limitations of commercial nickel catalyst used as primary catalyst in biomass gasification. The catalysts were effective in increasing the gaseous product yield and reducing tar yield. However, the catalysts suffered from rapid deactivation. The deactivation of nickel catalyst in *in-situ* gasification is commonly caused by carbon formation on the catalyst surface and nickel sintering (Sehested 2006). The deactivation of catalysts in gasification may be minimized through the use of additives and promoters, which is discussed in section 2.4 of this chapter.

2.3.2 Commercial Nickel Catalyst as Secondary Catalyst

Secondary catalysts are used in post gasification or post pyrolysis reactor to improve the quality of the product gas or to reform the bio-oil produced in the primary reactor. Secondary catalysts are active for longer duration because coke formation on the catalyst surface is minimized in a downstream reactor. In this review, studies using nickel catalysts as secondary catalyst will be discussed for upgrading synthesis gas and bio-oil in separate sections. Comparison of the results from literature is listed in Table 2.3.

Table 2. 2- Performance comparison of commercial nickel catalysts used as primary catalyst in biomass gasification and pyrolysis.

Catalyst	NiO (wt %)	Support	BET Surface Area (m ² /g)	Reactor Conditions		Carbon Conversion			Reference
				Temp (°C)	Pressure (kPa)	to gas, %	to solid, %	to liquid, %	
No Catalyst	-	-	-	750	101	80.0	13.0	7.0	(Baker et al. 1987)
with G-90C	15	70-76% Alumina, 5-8%	3 – 15	750	101	90.0	10.0	0.0	
No Catalyst	-	-	-	728	119	89.8	6.9	3.3	(Li et al. 2004)
With C11-9 LDP	N/A	Alumina	N/A	739 – 805	119	95.0 - 98.3	1.7 – 4.2	0.0 - 0.9	

Table 2. 3- Comparison of the properties of commercially available nickel based catalyst.

Catalyst	NiO Content (wt %)	Support	Surface Area (m ² /g)	Reactor Temp (°C)	Initial Tar Conversion (%)	Reference
Heavy Hydrocarbons Reforming						
BASF						
GI-25/1	25	CaO-Al ₂ O ₃ -SiO ₂ -K ₂ O	16.4	785- 850	98 – 99	(Corella et al. 1998; Pfeifer 2008)
GI-50	20	MgO-CaO-Al ₂ O ₃ -SiO ₂ -K ₂ O	19.9	660- 800	89 – 99	(Corella et al. 1998; Corella et al. 1999)
Haldor Topsoe						
R-67	15	MgAl ₂ O ₄ -SiO ₂ -K ₂ O	17	780- 840	95 – 100	(Corella et al. 1998; Corella et al. 1999)
ICI Katalco						
46-1	22	MgO-CaO-Al ₂ O ₃ -SiO ₂ -K ₂ O	16.2	700- 875	73 – 100	(Baker et al. 1987; Corella et al. 1998; Wang et al. 1998; Corella et al. 1999; Garcia et al. 2000)
Sud Chemie						
CI1-NK	20-25	MgO-CaO-SiO ₂ -Al ₂ O ₃	8.8	600- 900	-	(Garcia et al. 2000; Kechagiopoulos et al. 2006; Pfeifer 2008)
Light Hydrocarbons Reforming						
BASF						
GI-25S	12-15		2.5	785	88 – 97	(Caballero et al. 1997; Aznar et al. 1998)
VI693	10.2		-	850- 900	-	(Pfeifer 2008)
Haldor Topsoe						
RKS-1	15	MgAl ₂ O ₄ -SiO ₂ -K ₂ O	6.8	785- 800	92	(Caballero et al. 1997; Aznar et al. 1998; Corella et al. 1998; Corella et al. 1999)
R-67-7H	16-18	MgAl ₂ O ₄	12 - 20	690- 780	99	(Aznar et al. 1993)
ICI Katalco						
57-3	12	CaO-Al ₂ O ₃ -SiO ₂	2.9	-	69	(Caballero et al. 1997; Aznar et al. 1998; Corella et al. 1998; Corella et al. 1999)
Sud Chemie						
G-90LDP	14	CaO-Al ₂ O ₃	-	850- 900	99	(Pfeifer 2008)
G-90EW	14	CaO-Al ₂ O ₃	-	850- 900	99	(Pfeifer 2008)
G-90B	14	CaO-Al ₂ O ₃	5-7	650- 900	99	(Kinoshita et al. 1995; Pfeifer 2008)
United Catalyst						
CI1-9-061	10 – 15	Al ₂ O ₃	2.9	725- 800	-	(Caballero et al. 1997; Aznar et al. 1998; Corella et al. 1998; Corella et al. 1999)

2.3.2.1 Synthesis Gas Upgrading

Studies conducted by Caballero et al. (Caballero et al. 1997) and Aznar et al. (Aznar et al. 1993; Aznar et al. 1998) looked into the feasibility of using commercial nickel catalyst as secondary catalyst in biomass gasification. Four out of eight catalysts used in their studies were made for heavy hydrocarbons steam reforming, while the remaining were made for light hydrocarbons steam reforming. Catalysts were tested in a reactor set up shown in Figure 2.3 for pine wood chips gasification. It was found that catalysts made for heavy hydrocarbons steam reforming were more effective in eliminating tar, promoting hydrogen and carbon monoxide productions and suppressing the formations of the undesired methane and carbon dioxide (Corella et al. 1998; Corella et al. 1999; Caballero et al. 2000). No catalyst deactivation was reported after 45 h of on-stream testing in a temperature range of 780°C-830°C. These findings agree with the result reported by Pfeifer et al. (Pfeifer 2008).

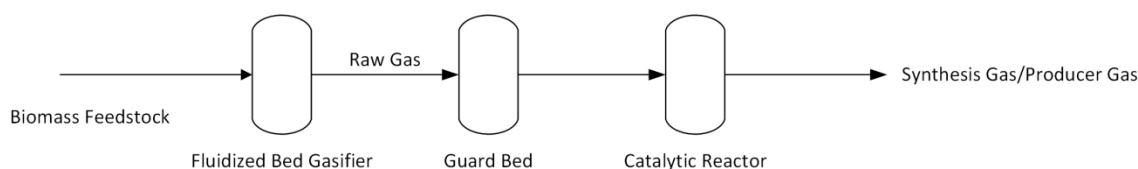


Figure 2. 3- Simplified reactor setup used in Caballero et al. and Aznar et al.

Pfeifer et al. tested six commercial nickel catalysts, also made for heavy and light hydrocarbons reforming, in toluene steam reforming reaction with a fixed bed quartz reactor (Pfeifer 2008). They found that heavy hydrocarbons steam reforming catalysts were more effective in converting tars and ammonia into gaseous product than light hydrocarbons reforming catalysts. High conversion of tar (98%) and ammonia (40%) was achieved at a space velocity of 1200 h⁻¹ and operating temperature of 850°C to 900°C. Selectivity toward CO formation was higher with heavy hydrocarbons reforming catalysts. No deactivation of catalyst was reported from the 12 h test which implies that these catalysts were able to suppress coke deposition.

One of the catalysts, G-90B, studied by Pfeifer was also used in Kinoshita et al. sawdust gasification investigation (Kinoshita et al. 1995). Using in an indirectly heated fluidized bed catalytic reformer, they noticed that carbon conversion, tar conversion and gas yield, particularly carbon monoxide and hydrogen yield, increased as the temperature and space time increased. Complete conversion of tar was achieved at 700 – 800°C at space velocity >1.2 s. Hydrogen to carbon monoxide ratio also improved by increasing steam to biomass ratio. However, increasing the steam to biomass ratio lowers the heating value of the product gas due to high vapour content in the product gas.

In summary, commercial catalysts used in heavy hydrocarbons reforming performed better in converting tar and suppressing coke formation. The nickel loading of the heavy hydrocarbons reforming catalysts is typically 5-10wt % higher than light hydrocarbons reforming catalysts. The catalyst BET surface area of the heavy hydrocarbons reforming catalyst was on average 3 times the surface area of the light hydrocarbons reforming catalysts. High BET surface area along with higher metal loading would provide large metal surface area which is one of the reasons for better activity of heavy hydrocarbon catalysts. Another reason is the presence of magnesium compounds in the heavy hydrocarbons reforming catalysts. Oxides of magnesium play a key role in suppressing coke formation in gasification (Garcia et al. 2000; Vizcaíno et al. 2008).

2.3.2.2 Bio-Oil Steam Reforming

Steam reforming of bio-oil with commercial nickel catalyst is a well-studied approach for synthesis gas production (Wang et al. 1998; Garcia et al. 2000; Kechagiopoulos et al. 2006). Bio-oil is produced by fast pyrolysis of biomass and steam reforming of bio-oil produces synthesis gas rich in hydrogen. The commercial catalysts are used in the secondary reactor to facilitate bio-oil steam reforming reaction. All the published work reviewed in this chapter conclude that the nickel catalysts suffers from rapid deactivation (Wang et al. 1998; Garcia et al. 2000; Kechagiopoulos et al. 2006).

Three commercial catalysts were investigated by Wang et al. (Wang et al. 1998), including G-90C, G-91 from United Catalyst and a dual catalyst 46-1/46-4 from ICI Katalco. By using rapid catalyst screening method, they found that all catalysts were efficient in converting model compounds like methanol, acetic acid, an aqueous solution of hydroxyl-acetaldehyde, a methanol solution of 4-allyl-2,6-dimethoxyphenol and a mixture model compounds of 67% acetic acid, 16% *m*-cresol, and 16% syringol into hydrogen rich gaseous products (>99%). The dual catalyst 46-1/46-4 was more effective in inhibiting carbonaceous deposition than G-90C and G-91 because the former catalysts contained MgO additive in the support. Further investigation carried out by Garcia et al. (Garcia et al. 2000) demonstrated that similar performance was achieved with commercial catalysts G-91, C11-NK and 46-1/46-4 in steam reforming of poplar wood pyrolysis bio-oil into gaseous product. Carbon conversion into CO and CO₂ started at 85 - 90% and gradually decreased to 75 - 85% in 25 min. Decrease in hydrogen and carbon dioxide yields accompanied by increase of carbon monoxide, methane, benzene and other aromatics yields during the run which indicated catalyst deactivation.

Deactivation of C11-NK catalyst, used in a bio-oil steam reforming, was also reported by Kechagiopoulos et al. (Kechagiopoulos et al. 2006). They reported complete conversion of model

compounds including acetone, ethylene, glycol, and acetic acid at temperatures higher than 600°C, gas hourly space velocity of 1500 h⁻¹ and steam to carbon ratio higher than 3. Hydrogen yield in product gas was as high as 90%. However, steam reforming of aqueous-phase beech wood pyrolysis bio-oil produced lower hydrogen yield at around 60%. The real bio-oil led to substantially higher coke formation compared to the model compounds which led to rapid deactivation and lower hydrogen yield.

The catalysts reviewed in this chapter suffered significantly faster deactivation due to coke formation in bio-oil steam reforming compared to synthesis gas upgrading. Hydrogen yield from bio-oil steam reforming using ICI-46 series catalyst and UCI G-91 decreased from 80% to 60% in 300 min and from 75% to 70% in 150 min of run, respectively (Wang et al. 1998). Garcia et al. also reported an average drop of 20% in hydrogen yield in 25 min (Garcia et al. 2000), while the C11-NK catalyst used by Kechagiopoulos et al. deactivated completely after 17 h of run (Kechagiopoulos et al. 2006). Coke formation was identified as the primary cause of deactivation. Section 2.4 reviews the advancements in gasification using nickel catalysts to overcome the coke deposition. A comparison of catalysts reviewed in this section can also be found in Table 2.3.

2.4 Recent Advancements in Nickel Based Catalyst for Biomass Gasification

Various catalyst supports, metal additives and synthesis methods have been developed by researchers to improve stability and activity of nickel catalysts. These studies can be divided into the effect of support material, the effect of promoter and the effect of particle size. Some of the most commonly used support materials include olivine, dolomite (Srinakruang et al. 2005), alumina (Srinakruang et al. 2005; Kong et al. 2011; Efika et al. 2012), silica (Srinakruang et al. 2005; Kong et al. 2011; Efika et al. 2012) and magnesium oxide (Kong et al. 2011). Promoter such as platinum (Nishikawa et al. 2008; Chaiprasert et al. 2009), palladium (Nishikawa et al. 2008), rhodium (Nishikawa et al. 2008), ruthenium (Nishikawa et al. 2008), cobalt (Chaiprasert et al. 2009; Wang et al. 2012), iron (Chaiprasert et al. 2009) and copper (Bimbela et al. 2012) are widely used in catalyst synthesis to improve catalyst performance.

2.4.1 Effect of Support on Nickel Based Catalysts

One of the prominent issues with using nickel catalyst in biomass gasification is rapid loss of catalytic activity due to carbon deposition. Varying degree of success has been achieved in suppressing coke formation by changing the type of support material. Srinakruang et al. studied the effectiveness of three catalyst supports, alumina, silica-alumina mixed oxide and dolomite, in suppressing carbon deposition in gasification (Srinakruang et al. 2005). Ni/Al₂O₃ and Ni/SiO₂-Al₂O₃ catalysts were synthesized using impregnation method while Ni/dolomite catalyst was prepared by precipitation-deposition method with aqueous solution of nickel nitrate hexahydrate. Detailed catalyst preparation parameters are listed in Table 2.4. Catalytic activity of toluene conversion in a fixed bed reactor decreased in the following order Ni/Al₂O₃ > Ni/SiO₂-Al₂O₃ > Ni/dolomite. However, Ni/dolomite catalyst was stable for the longest duration (7 h). Results from thermogravimetric analysis (TGA) showed that the amount of coke formation was in the following order Ni/dolomite < Ni/Al₂O₃ < Ni/SiO₂-Al₂O₃, measured at 0.0 wt%, 1.7wt% and 7.2wt% respectively. Srinakruang et al. attributed the better performance of Ni/dolomite catalyst to the basicity of the dolomite support. Basic oxides, such as MgO and CaO found in dolomite, help to promote forming of surface oxide ions which assist in gasifying of deposited carbon.

Kong et al. (Kong et al. 2011) conducted a study on carbon dioxide reforming of toluene in a fluidized bed reactor with nickel catalyst on various support materials, including alumina, silica, zirconium oxide and magnesium oxide. All the catalysts were prepared by impregnation method. From their studies, they found that Ni/MgO and Ni/ α -Al₂O₃ were more stable than other supported catalysts for up to 400 min on stream. Nickel catalyst supported on acidic supports were least coke resistant and the synthesis method play a big role in catalyst stability. Ni/SiO₂ catalyst made by sol-gel method had the highest surface area (765 m²/g), gas yield (54wt%) and coke deposition (19.4 wt%) compared to Ni/SiO₂ made by incipient wetness method (136 m²/g, 49.8 wt% and 3.7 wt%, respectively) (Efika et al. 2012).

Support material plays an important role in defining the activity and service life of the catalyst. Studies reviewed here have concluded that catalyst with high surface area support generally exhibits higher catalytic activity. However, the catalyst support acidity is important for stability. Basic supports such as dolomite and MgO are better at inhibiting carbon fouling (Caballero et al. 1997; Aznar et al. 1998; Srinakruang et al. 2005; Kong et al. 2011).

Table 2. 4- Comparison of nickel catalysts with different support materials used in pyrolysis and steam reforming of bio-oil.

Catalyst	Ni, wt %	BET Surface Area, m ² /g	Synthesis Method [§]	Precursor	Drying		Calcination		Reduction		Reaction Temp °C	Conversion of Toluene, %	Gas Yield (wt %)	Coke Deposition (wt %)	Ref
					Temp, °C (time, h)										
Ni/dolomite	15	10.8	PD	Ni(NO ₃) ₂ ·6H ₂ O, dolomite, (NH ₄) ₂ CO ₃	120 (~12)	750 (2)	700 (2)	700 (2)	92.0*	-	0.0 ^a	(Srinakruang et al. 2005)			
Ni/Al ₂ O ₃	15	322	IWI	Ni(NO ₃) ₂ ·6H ₂ O, Al ₂ O ₃	120 (~12)	750 (2)	700 (2)	770 (0.25)	99.0*	-	1.7 ^a				
Ni/SiO ₂ -Al ₂ O ₃	15	362	IWI	Ni(NO ₃) ₂ ·6H ₂ O, SiO ₂ -Al ₂ O ₃	120 (~12)	750 (2)	700 (2)	700 (2)	90.0*	-	7.2 ^a				
Ni/MgO	5	31.8	IWI	Ni(NO ₃) ₂ , MgO	120 (6)	700 (6)	600 (6)	600 (6)	91.0	-	0.3 ^a				
Ni/α-Al ₂ O ₃	5	27.1	IWI	Ni(NO ₃) ₂ , α-Al ₂ O ₃	120 (6)	700 (6)	600 (6)	600 (6)	67.2	-	1.2 ^a	(Kong et al. 2011)			
Ni/γ-Al ₂ O ₃	5	152.7	IWI	Ni(NO ₃) ₂ , γ-Al ₂ O ₃	120 (6)	700 (6)	700 (1)	700 (1)	74.2	-	4.1 ^a				
Ni/ZrO ₂	5	8.1	IWI	Ni(NO ₃) ₂ , ZrO ₂	120 (6)	700 (6)	600 (6)	600 (6)	32.8	-	3.4 ^a				
Ni/SiO ₂	5	319.4	IWI	Ni(NO ₃) ₂ , SiO ₂	120 (6)	700 (6)	600 (6)	600 (6)	11.1	-	3.8 ^a				
Ni/Al ₂ O ₃	20	147	IWI	Ni(NO ₃) ₂ ·6H ₂ O, Al ₂ O ₃	105 (~12)	450 (3)	760	450 (3)	-	49.5	-				
Ni/CeO ₂ -Al ₂ O ₃	20	111	IWI	Ni(NO ₃) ₂ ·6H ₂ O, Ce(NO ₃) ₃ ·6H ₂ O, Al ₂ O ₃	105 (~12)	450 (3)	760	No	-	47.6	-				
Ni/SiO ₂	20	136	IWI	Ni(NO ₃) ₂ ·6H ₂ O, SiO ₂	105 (~12)	450 (3)	760	Reduction	-	49.8	3.7 ^b	(Efika et al. 2012)			
Ni/SiO ₂	20	765	SG	Ni(NO ₃) ₂ ·6H ₂ O, Citric Acid, Ethanol, SiC ₈ H ₂₀ O ₄	80 (~12)	450 (3)	760	Reduction	-	54.0	19.4 ^b				

§ PD = Precipitation-Deposition, IWI = Incipient Wetness Impregnation, SG = Sol-Gel

^a Measured by Thermogravimetric analyser after reaction for 7 h

^b Measured by X-ray photoelectron spectroscopy after reaction

* Data extracted from the figures.

2.4.2 Promoted Nickel Based Catalyst

Another method to improve the activity and coke resistance of nickel supported catalysts is to dope it with noble metals (Nishikawa et al. 2008; Chaiprasert et al. 2009), alkali metals (Bimbela et al. 2012), rare earth metals (Nishikawa et al. 2008) or transition metals (Chaiprasert et al. 2009; Bimbela et al. 2012; Wang et al. 2012). Table 2.5 compares the experimental parameters and catalyst synthesis methods and Table 2.6 compares catalysts properties based on chemisorption measurements.

Nishikawa et al. examined the effect of noble metals, including Pt, Pd, Rh and Ru, on the performance of Ni/CeO₂-Al₂O₃ catalyst in cedar wood biomass steam gasification with a laboratory scale continuous feeding dual bed reactor (Nishikawa et al. 2008). The Ni/CeO₂-Al₂O₃ was prepared by co-impregnation method, whereas, the noble metal promoter was impregnated later. Although the addition of noble metals, especially Pt, was effective in promoting steam gasification, these additives had minimal effect in inhibiting coke formation. Nonetheless, high catalytic activity of Pt promoted catalyst was the result of the strong interaction between the platinum and nickel metals. They also noted that unreduced platinum catalyst had the same catalytic performance as the reduced catalyst, which suggested that hydrogen pre-treatment may not be required.

Chaiprasert et al. studies Pt, Fe and Co as promoter for Ni catalysts in a fluidized bed coconut shell gasification (Chaiprasert et al. 2009). Catalysts were prepared by impregnation and co-precipitation methods with 1wt% promoter and 10wt% Ni loading on dolomite supported catalysts. XRD analysis suggested that catalysts synthesized by these two methods had similar crystalline structure. Gasification results indicated that the addition of Pt promoter enhanced steam reforming and water-gas shift reactions. Product gas generated had higher concentration of hydrogen, carbon monoxide and carbon dioxide. Fe promoted catalyst was only effective in promoting water gas shift reaction, which increased the production of hydrogen and carbon dioxide. Cobalt promoted catalyst was more effective in promoting methanation and reforming of methane. While all the three promoters reduced coke deposition, Pt promoted catalyst exhibited the highest coke resistance. The amount of coke deposited onto the Pt, Fe, Co promoted catalysts, and non-promoted catalysts were 6.5, 8.3, 9.3 and 16.5 wt% respectively.

The effect of cobalt concentration on the performance of nickel catalyst in steam reforming of toluene was investigated by Wang et al. (Wang et al. 2012). Catalysts were prepared by co-impregnating Co up to 12 wt% onto 12 wt% Ni/Al₂O₃ catalyst. The catalytic activity initially improved with the increase of Co loading up to 3 wt% but later dropped with higher Co loadings.

Chapter 2

Similar trend was observed in the study of Cu promoted catalytic steam reforming of acetic acid (Bimbela et al. 2012). This behaviour can be explained by lowering of nickel surface area at high promoter loading. Nevertheless, Co and Cu promoted nickel catalysts were more effective than non-promoted Ni/Al₂O₃ catalysts in reforming oxygenates and inhibiting coke formation.

In summary, bimetallic catalysts, especially with the noble metal additive such as Pt, performs significantly improves catalytic activity and suppresses coke deposition during gasification.

Table 2. 5- Comparison of promoted nickel catalysts used in pyrolysis and steam reforming of biomass.

Catalyst	Ni wt %	Promoter wt %	Synthesis Method ^s	Precursor	Drying temp, °C (time, h)	Calcination Temp, °C (time, h)	Reaction Temp, °C	C Based Gas Yield, %	Coke Deposit- tion, wt % per min of run	Ref
Ni/CeO ₂ -Al ₂ O ₃	4	0	Incipient Wetness	Ni(NO ₃) ₂ ·6H ₂ O, Ce(NH ₄) ₂ (NO ₃) ₆ , Al ₂ O ₃	110 (12)	500 (3)	550 - 650	65 - 82	0.33	
Pt-Ni/CeO ₂ -Al ₂ O ₃	4	0.1	Incipient Wetness	Ni(NO ₃) ₂ ·6H ₂ O, Ce(NH ₄) ₂ (NO ₃) ₆ , Al ₂ O ₃ Pt(NO ₂) ₂ (NH ₃) ₂	110 (12)	500 (3)	550 - 650	70 - 82	>0.33	
Pd-Ni/CeO ₂ -Al ₂ O ₃	4	0.1	Incipient Wetness	Ni(NO ₃) ₂ ·6H ₂ O, Ce(NH ₄) ₂ (NO ₃) ₆ , Al ₂ O ₃ , Pd(NO ₃) ₂	110 (12)	500 (3)	550 - 650		>0.33	(Nishikawa et al. 2008)
Rh-Ni/CeO ₂ -Al ₂ O ₃	4	0.1	Incipient Wetness	Ni(NO ₃) ₂ ·6H ₂ O, Ce(NH ₄) ₂ (NO ₃) ₆ , Al ₂ O ₃ , Rh(NO ₃) ₃	110 (12)	500 (3)	550 - 650	67 - 83	>0.33	
Ru-Ni/CeO ₂ -Al ₂ O ₃	4	0.5	Incipient Wetness	Ni(NO ₃) ₂ ·6H ₂ O, Ce(NH ₄) ₂ (NO ₃) ₆ , Al ₂ O ₃ , Ru(NO)(NO) ₃	110 (12)	500 (3)	550 - 650	70 - 82	>0.33	
Pt-Ni/Dolomite	15	1		Ni(NO ₃) ₂ ·6H ₂ O, dolomite, (NH ₄) ₂ CO ₃ , H ₂ PtCl ₆	120 (~12)	600	800	79.19	0.05	
Fe-Ni/Dolomite	15	1	Precipitation & Impregnation	Ni(NO ₃) ₂ ·6H ₂ O, dolomite, (NH ₄) ₂ CO ₃ , FeCl ₃	120 (~12)	600	800	78.12	0.07	
Co-Ni/Dolomite	15	1		Ni(NO ₃) ₂ ·6H ₂ O, dolomite, (NH ₄) ₂ CO ₃ , Co(NO ₃) ₂	120 (~12)	600	800	49.53	0.08	(Chaiprasert et al. 2009)
Pt-Ni/Dolomite	15	1		Ni(NO ₃) ₂ ·6H ₂ O, dolomite, (NH ₄) ₂ CO ₃ , H ₂ PtCl ₆	120 (~12)	600	800	50.51		
Fe-Ni/Dolomite	15	1	Co-precipitation	Ni(NO ₃) ₂ ·6H ₂ O, dolomite, (NH ₄) ₂ CO ₃ , FeCl ₃	120 (~12)	600	800	57.46		
Co-Ni/Dolomite	15	1		Ni(NO ₃) ₂ ·6H ₂ O, dolomite, (NH ₄) ₂ CO ₃ , Co(NO ₃) ₂	120 (~12)	600	800	41.82		
Co-Ni/Al ₂ O ₃	12	0.72 - 12	Co-Impregnation	Ni(NO ₃) ₂ ·6H ₂ O, Co(NO ₃) ₂ ·6H ₂ O, Al ₂ O ₃	110 (12)	500 (3)	550	54 - 68	0.01	(Wang et al. 2012)

Table 2. 6- Comparison of chemisorption results of various research based nickel catalysts.

Catalyst	Ni Content, wt %	Promoter Content, wt %	BET Surface Area, m ² /g	Reduction degree (TPR), %	Particle Size of Ni, nm	H ₂ adsorption @298 K, 10 ⁵ mol/g _{cat}	Dispersion	H ₂ consumption in TPR, 10 ⁻³ mol/g _{cat}	Metal surface area, m ² /g	Ref
Ni/MgO	5	0	31.8	8	Not determine					
Ni/ α -Al ₂ O ₃	5	0	27.1	76	9.9					(Kong et al. 2011)
Ni/ γ -Al ₂ O ₃	5	0	152.7	11	7.9					
Ni/ZrO ₂	5	0	8.1	97	20.7					
Ni/SiO ₂	5	0	319.4	101	22.1					
Ni/CeO ₂ -Al ₂ O ₃	4	0	15	149		40	5.8	1.02		
Pt-Ni/CeO ₂ -Al ₂ O ₃	4	0.1	14-15	142		57	8.4	0.97		
Pd-Ni/CeO ₂ -Al ₂ O ₃	4	0.1	18	138		55	8.0	0.95		(Nishikawa et al. 2008)
Rh-Ni/CeO ₂ -Al ₂ O ₃	4	0.1	16	144		61	9.0	1.0		
Ru-Ni/CeO ₂ -Al ₂ O ₃	4	0.5	15	146		62	9.0	1.1		
Pt-Ni/Dolomite	15	1	6.74		77				0.97	
Fe-Ni/Dolomite	15	1	5.76		364				0.20	
Co-Ni/Dolomite	15	1	11.18		2671				0.03	(Chairasert et al. 2009)
Pt-Ni/Dolomite	15	1	5.33		166				0.06	
Fe-Ni/Dolomite	15	1	4.77		1532				0.05	
Co-Ni/Dolomite	15	1	8.76		2715				0.02	
Co-Ni/Al ₂ O ₃	12	0.72 - 12	N/A		25 - 34	47 - 57	2.7 - 4.7	2.1 - 4.9		(Wang et al. 2012)

2.4.3 Nickel Nanoparticle Catalyst

A nanoparticle catalyst is defined as a catalyst with a particle size in the range of 1 – 100 nm (Astruc 2008). Nanoparticle catalysts can be either unsupported or supported on alumina (Li et al. 2008; Li 2009), carbon nanotubes (Azadi et al. 2009) and other types of support material. Li et al. conducted several studies supported and unsupported nickel nanoparticle catalyst for biomass pyrolysis (Li et al. 2007). The catalyst used in this study was synthesized using homogenous-precipitation method and had a specific surface area of 187.98 m²/g and cubic crystals size of 7.5nm. Performance of this nanoparticle catalyst and a commercial nickel based microparticle catalyst was evaluated in a TGA, measured from ambient temperature to 900°C. The results showed that the cellulose pyrolysis onset temperature with the nanoparticle catalyst was slightly lower than the onset temperature with the microparticle catalyst, measured at 294°C and 303°C respectively. Lower onset temperatures were also observed in hemicellulose and lignin pyrolysis with nanoparticle catalyst, which indicated that the nanoparticle catalyst help to lower the activation energy required for pyrolysis reaction.

Supported nanoparticle catalysts, Ni/Al₂O₃ and Ni-La-Fe/Al₂O₃, were developed by Li et al. using the deposition-precipitation method and tested for sawdust pyrolysis reaction (Li et al. 2008; Li 2009; Liu et al. 2010). Both the catalysts demonstrated excellent tar conversion (>99%) at a temperature of 800°C, significantly improving in the quality of the product gas, especially CO, CO₂, CH₄ and C₂ yields. Similar results were reported by Liu et al. (Liu et al. 2010) and Feng et al. (Feng 2011) who studied the nano-NiO/γ-Al₂O₃ in municipal solid waste and sawdust steam gasification. Li et al. reported that the nanoparticle Ni/Al₂O₃ and the Ni-La-Fe/Al₂O₃ catalysts negligible to no deactivation, respectively, in the 10 h sawdust pyrolysis life test studies.

It is known from literature that nickel based catalyst with smaller active metal particle size and high degree of dispersion exhibits higher catalytic activity (Nishikawa et al. 2008). Since nanoparticle catalysts have higher number of active sites per gram, these catalysts should have better performance than micro-particle catalysts on the mass basis in gasification as stated by Li et al. However, more study is also needed to validate if there is any size effect per unit active site of the catalyst.

2.5 Future Directions of Biomass Gasification

Conventional biomass gasification is commonly performed by using one of the following reactor setups:

- Fluidized bed gasifier with downstream catalytic tar cleaning reactor
- Fast pyrolysis reactor with downstream catalytic steam reformer
- Catalytic fluidized bed gasifier

Fluidised bed reactors are capital intensive and hence large scale reactors are required to make it economical. According to a study conducted by Leung et al., cost of the gasifier and gas cleaning system can account for 66.7 % to 85.5% of the total capital cost (Leung et al. 2004). This is particularly true for fluidized bed gasifier due to the high cost of blower, continuous feed systems and control systems. In comparison, capital cost of fixed bed reactors for biomass gasification is significantly lower. Therefore, a novel approach called as reactive flash volatilisation, was recently proposed for cellulose gasification (Colby et al. 2008). Reactive flash volatilisation uses a fixed bed gasifier with carbon space velocity and carbon mass flow rate significantly higher than fluidised bed reactors.

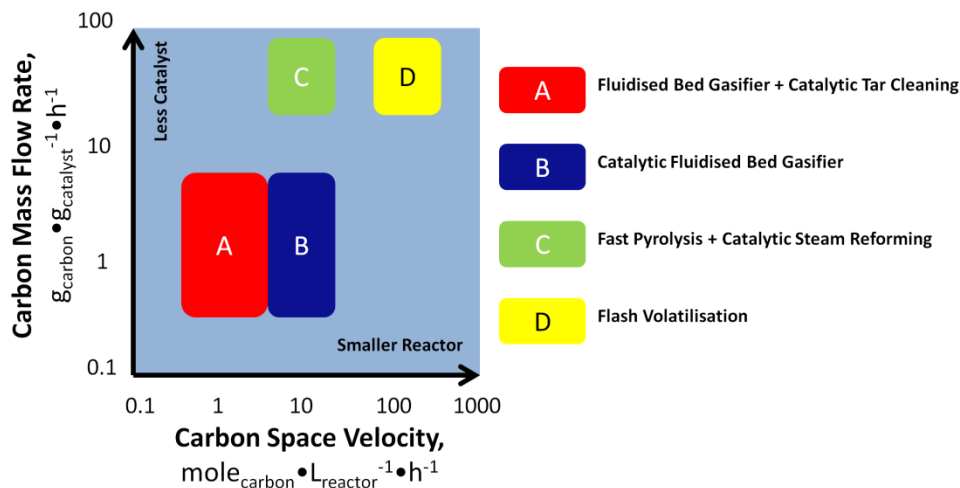


Figure 2. 4- Comparison of the space velocity, mass flow rate, amount of catalyst required and reactor size of various reactor setups. (Adapted from Colby et al.)

Reactive flash volatilization, which combines pyrolysis and partial oxidation, was first introduced by Salge et al. for synthesis gas production from non-volatile fuels such as refined soy oil, biodiesel and aqueous sugar solution (Salge et al. 2006). As illustrated in Figure 2.4, one of the biggest advantages of this reactor is lower amount of catalyst used per unit mass of carbon

feedstock compared to the fluidised bed gasifiers. According to Colby et al., conventional biomass gasification setup-up, such as fluidized bed gasifier with downstream catalytic tar cleaning reactor or catalytic fluidized bed gasifier, has carbon mass velocity of $0.8 - 9.0 \text{ h}^{-1}$ (Colby et al. 2008). In comparison, reactive flash volatilization has carbon mass velocity of $50.0 - 80.0 \text{ h}^{-1}$. Although similar carbon mass velocity can be achieved with fast pyrolysis reactor with downstream catalytic steam reformer, size of the reactive flash volatilization reactor is at least an order of magnitude smaller than other reactors (Figure 2.4). Carbon space velocity of $100 - 300 \text{ mol L}^{-1} \text{ h}^{-1}$ can be easily attained with reactive flash volatilization. Because of its high carbon space velocity ($\text{mol C/L}_{\text{reactor}} \cdot \text{h}$) and high carbon mass flow rate ($\text{g C/g}_{\text{cat}} \cdot \text{h}$), reactive flash volatilization reactors can be economical at a small scale, which is important for decentralised biomass gasification (Dauenhauer et al. 2007). Small scale gasification plants can be placed closer to the feedstock source which minimizes transportation cost of low energy density biomass.

In Salge et al.'s study, synthesis gas was produced with Rh-Ce catalyst where non-volatile feed are decomposed into hydrogen and carbon monoxide in less than 50ms without the production of carbon (Salge et al. 2006). The formation of carbon was avoided by rapidly oxidizing the decomposition products into gases. The heat generated from oxidation reaction prevented condensation reactions that might lead to rapid carbon formation. 99% conversion of the feed at ~70% hydrogen selectivity was achieved without catalyst deactivation of at the end of 20 h run. Lower C/O ratio led to higher catalyst bed temperature, feed conversion, and hydrogen and carbon monoxide selectivities.

Cellulose gasification using reactive flash volatilization was conducted by Colby et al. (Colby et al. 2008). This is a more complex process compared to the liquid feeds because it involves pyrolysis, partial oxidation, steam reforming, and water gas shift reactions. 2 wt% Rh-2 wt% Ce/ Al_2O_3 catalyst was used for microcrystalline cellulose gasification which produced C_1 products within 24 – 33 ms residence time temperature of $600 - 825 \text{ }^\circ\text{C}$. Increasing the C/O ratio increased the hydrogen and CO yield. Whereas, increasing the S/C (steam to carbon) ratio increased the hydrogen yield and decreased the CO yield, which is attributed to forward water gas shift reaction. Selectivity of hydrogen was 14% to 47% and selectivity of carbon monoxide was 21% to 38%.

Reactive flash volatilization with Rh based catalyst is a promising method for high quality syngas production but it is impractical for larger than bench scale application due to the high cost of the Rh-Ce catalyst. Moreover, lignocellulose feedstock must be used instead of purified microcrystalline cellulose to make this process commercially viable. Gasification of lignocellulose feedstock will be a greater challenge for the catalysts. Therefore, it is necessary to

Chapter 2

develop a cost effective and robust catalyst for reactive flash volatilization of lignocellulose. Further research is required to study the effectiveness of this process in raw biomass gasification. In this regard, nickel catalysts discussed in this chapter (supported, unsupported, promoted, nanoparticles etc) may play a vital role.

2.6 Conclusions

Nickel catalyst has been widely employed in various chemical processes for decades. It has been proven as one of the most cost effective transition metal catalyst, especially in eliminating tar and improving the quality of the product gas of biomass gasification. However, various reports have pointed out that these catalysts suffer rapid deactivation as a primary catalyst in the gasification due to carbon fouling, sintering and morphological changes. Nonetheless, nickel based catalyst is still very effective in tar steam reforming and adjusting the CO-H₂ ratio when used as secondary catalyst in a downstream reactor.

Key factors that define the catalytic activity of the nickel based catalyst are the metal particle size and its dispersion. Small crystallite size and high degree of dispersion of nickel on the supports lead to high catalytic activity. Catalytic activity can also be improved by the addition of metal promoter, such as Pt, Co and Cu. These metal promoters improve the reaction activity through enhancing the nickel metal reducibility by forming strong interaction with nickel metal. Metal promoters also enhance dispersion of the nickel metal on the support and provide higher resistance to coke formation.

Coke deposition on catalyst, which results in deactivation, is the primary concern in catalytic biomass gasification and pyrolysis. The amount of coke deposition is associated with the types of supports used. Basic supports are more coke resistant than acidic supports. Carbon deposition can be reduced by addition of alkaline earth metals and effective use of catalyst supports such as dolomite and MgO.

2.7 Acknowledgement

The authors are grateful for the financial support from the Rural Industries Research and Development Corporation (RIRDC) project grant PRJ-004758.

2.8 References

Abu, E. Z., E. A. Bramer, et al. (2004). "Review of Catalysts for Tar Elimination in Biomass Gasification Processes." Ind. Eng. Chem. Res. **43**: 6911-6919.

Astruc, D. (2008). Transition-metal Nanoparticles in Catalysis: From Historical Background to the State-of-the Art. Nanoparticles and Catalysis, Wiley-VCH Verlag GmbH & Co. KGaA: 1-48.

Azadi, P., R. Farnood, et al. (2009). "Preparation of Multiwalled Carbon Nanotube-Supported Nickel Catalysts Using Incipient Wetness Method." The Journal of Physical Chemistry A **114**: 3962-3968.

Aznar, M. P., M. A. Caballero, et al. (1998). "Commercial Steam Reforming Catalysts To Improve Biomass Gasification with Steam-Oxygen Mixtures. 2. Catalytic Tar Removal." Ind. Eng. Chem. Res. **37**: 2668-2680.

Aznar, M. P., J. Corella, et al. (1993). "Improved steam gasification of lignocellulosic residues in a fluidized bed with commercial steam reforming catalysts." Ind. Eng. Chem. Res. **32**: 1-10.

Baker, E. G., L. K. Mudge, et al. (1987). "Steam gasification of biomass with nickel secondary catalysts." Ind. Eng. Chem. Res. **26**: 1335-1339.

Bimbela, F., D. Chen, et al. (2012). "Ni/Al coprecipitated catalysts modified with magnesium and copper for the catalytic steam reforming of model compounds from biomass pyrolysis liquids." Applied Catalysis B: Environmental **119-120**: 1-12.

Bridgwater, A. V. (1995). "The technical and economic feasibility of biomass gasification for power generation." Fuel **74**: 631-653.

Caballero, M. A., M. P. Aznar, et al. (1997). "Commercial Steam Reforming Catalysts To Improve Biomass Gasification with Steam-Oxygen Mixtures. 1. Hot Gas Upgrading by the Catalytic Reactor." Ind. Eng. Chem. Res. **36**: 5227-5239.

Caballero, M. A., J. Corella, et al. (2000). "Biomass Gasification with Air in Fluidized Bed. Hot Gas Cleanup with Selected Commercial and Full-Size Nickel-Based Catalysts." Ind. Eng. Chem. Res. **39**: 1143-1154.

Chaiprasert, P. and T. Vitidsant (2009). "Effects of promoters on biomass gasification using nickel/dolomite catalyst." Korean Journal of Chemical Engineering **26**: 1545-1549.

Colby, J. L., P. J. Dauenhauer, et al. (2008). "Millisecond autothermal steam reforming of cellulose for synthetic biofuels by reactive flash volatilization." Green Chemistry **10**: 773-783.

Corella, J., A. Orio, et al. (1998). "Biomass Gasification with Air in Fluidized Bed: Reforming of the Gas Composition with Commercial Steam Reforming Catalysts." Ind. Eng. Chem. Res. **37**: 4617-4624.

Corella, J., A. Orio, et al. (1999). "Biomass Gasification with Air in a Fluidized Bed: Exhaustive Tar Elimination with Commercial Steam Reforming Catalysts." Energy Fuels **13**: 702-709.

Czernik, S., P. G. Koeberle, et al. (1993). Gasification of Residual Biomass via the Biosyn Fluidized Bed Technology. Advances in Thermochemical Biomass Conversion. A. V. Bridgwater, Springer Netherlands: 423-437.

Chapter 2

Dauenhauer, P. J., J. Colby, et al. (2007). Reactive flash volatilization of nonvolatile carbohydrates for synthesis gas, Salt Lake City, UT.

Delgado, J., M. P. Aznar, et al. (1997). "Biomass Gasification with Steam in Fluidized Bed: Effectiveness of CaO, MgO, and CaO–MgO for Hot Raw Gas Cleaning." Industrial & engineering chemistry research **36**: 1535-1543.

Department of Resources, E. a. T. (2012). Energy White Paper 2012- Australia's energy transformation. E. a. T. Department of Resources.

Devi, L., K. J. Ptasiniski, et al. (2003). "A review of the primary measures for tar elimination in biomass gasification processes." Biomass Bioenergy **24**: 125-140.

Dogru, M., C. R. Howarth, et al. (2002). "Gasification of hazelnut shells in a downdraft gasifier." Energy **27**: 415-427.

Efika, C. E., C. Wu, et al. (2012). "Syngas production from pyrolysis–catalytic steam reforming of waste biomass in a continuous screw kiln reactor." Journal of Analytical and Applied Pyrolysis **95**: 87-94.

Feng, Y. (2011). "Influence of catalyst and temperature on gasification performance by externally heated gasifier." Smart grid and renewable energy **2**: 177.

Fraga, A. R., A. F. Gaines, et al. (1991). "Characterization of biomass pyrolysis tars produced in the relative absence of extraparticle secondary reactions." Fuel **70**: 803-809.

Garcia, L., R. French, et al. (2000). "Catalytic steam reforming of bio-oils for the production of hydrogen: effects of catalyst composition." Appl. Catal., A **201**: 225-239.

Gil, J., J. Corella, et al. (1999). "Biomass gasification in atmospheric and bubbling fluidized bed: Effect of the type of gasifying agent on the product distribution." Biomass and Bioenergy **17**: 389-403.

Haryanto, A., S. D. Fernando, et al. (2009). "Upgrading of syngas derived from biomass gasification: A thermodynamic analysis." Biomass and Bioenergy **33**: 882-889.

Hernández, J. J., G. Aranda-Almansa, et al. (2010). "Gasification of biomass wastes in an entrained flow gasifier: Effect of the particle size and the residence time." Fuel processing technology **91**: 681-692.

Hos, J. J., M. J. Groeneveld, et al. (1980). "Gasification of organic solid wastes in cocurrent moving bed reactors " AIAA Paper: 333-349.

Huber, G. W., S. Iborra, et al. (2006). "Synthesis of Transportation Fuels from Biomass: Chemistry, Catalysts, and Engineering." Chem. Rev. (Washington, DC, U. S.) **106**: 4044-4098.

Kechagiopoulos, P. N., S. S. Voutetakis, et al. (2006). "Hydrogen Production via Steam Reforming of the Aqueous Phase of Bio-Oil in a Fixed Bed Reactor." Energy Fuels **20**: 2155-2163.

Kiel, J. H. A. (2004). Primary Measures to Reduce Tar Formation in Fluidised-bed Biomass Gasifiers: Final Report SDE Project P1999-012, Netherlands Energy Research Foundation.

Kinoshita, C. M., Y. Wang, et al. (1995). "Effect of Reformer Conditions on Catalytic Reforming of Biomass-Gasification Tars." Ind. Eng. Chem. Res. **34**: 2949-2954.

- Kirkels, A. F. and G. P. J. Verbong (2010). "Biomass gasification: Still promising? A 30-year global overview." Renewable Sustainable Energy Rev. **15**: 471-481.
- Knight, R. A. (2000). "Experience with raw gas analysis from pressurized gasification of biomass." Biomass and Bioenergy **18**: 67-77.
- Kong, M., J. Fei, et al. (2011). "Influence of supports on catalytic behavior of nickel catalysts in carbon dioxide reforming of toluene as a model compound of tar from biomass gasification." Bioresource Technology **102**: 2004-2008.
- Ku, C. S. and S. P. Mun (2006). "Characterization of pyrolysis tar derived from lignocellulosic biomass." Journal of Industrial and Engineering Chemistry **12**: 853-861.
- Kumar, A., K. Eskridge, et al. (2009). "Steam–air fluidized bed gasification of distillers grains: Effects of steam to biomass ratio, equivalence ratio and gasification temperature." Bioresource Technology **100**: 2062-2068.
- Kumar, A., D. D. Jones, et al. (2009). "Thermochemical biomass gasification: a review of the current status of the technology." Energies (Basel, Switz.) **2**: 556-581.
- Kurkela, E. and P. Ståhlberg (1992). "Air gasification of peat, wood and brown coal in a pressurized fluidized-bed reactor. I. Carbon conversion, gas yields and tar formation." Fuel processing technology **31**: 1-21.
- Leung, D. Y. C., X. L. Yin, et al. (2004). "A review on the development and commercialization of biomass gasification technologies in China." Renewable and Sustainable Energy Reviews **8**: 565-580.
- Li, C. and K. Suzuki (2009). "Tar property, analysis, reforming mechanism and model for biomass gasification-An overview." Renewable and Sustainable Energy Reviews **13**: 594-604.
- Li, J. (2009). "Development of a nano-Ni-La-Fe/Al₂O₃ catalyst to be used for syn-gas production and tar removal after biomass gasification." BioResources **4**: 1520.
- Li, J., R. Yan, et al. (2008). "Development of Nano-NiO/Al₂O₃ Catalyst to be Used for Tar Removal in Biomass Gasification." Environ. Sci. Technol. **42**: 6224-6229.
- Li, J., R. Yan, et al. (2007). "Preparation of Nano-NiO Particles and Evaluation of Their Catalytic Activity in Pyrolyzing Biomass Components†." Energy & Fuels **22**: 16-23.
- Li, X. T., J. R. Grace, et al. (2004). "Biomass gasification in a circulating fluidized bed." Biomass Bioenergy **26**: 171-193.
- Liu, J., J. Li, et al. (2010). Fuel gas production from catalytic steam gasification of municipal solid wastes, Wuhan.
- Lv, P., Z. Yuan, et al. (2007). "Hydrogen-rich gas production from biomass air and oxygen/steam gasification in a downdraft gasifier." Renewable Energy **32**: 2173-2185.
- Milne, T. A., R. J. Evans, et al. (1998). Biomass Gasifier "Tars": Their Nature, Formation, and Conversion. Other Information: PBD: 1 Nov 1998.
- Nagel, F. P., S. Ghosh, et al. (2011). "Biomass integrated gasification fuel cell systems–Concept development and experimental results." Biomass and Bioenergy **35**: 354-362.

Chapter 2

Narváez, I., A. Orío, et al. (1996). "Biomass Gasification with Air in an Atmospheric Bubbling Fluidized Bed. Effect of Six Operational Variables on the Quality of the Produced Raw Gas." Industrial & engineering chemistry research **35**: 2110-2120.

Nishikawa, J., K. Nakamura, et al. (2008). "Catalytic performance of Ni/CeO₂/Al₂O₃ modified with noble metals in steam gasification of biomass." Catalysis Today **131**: 146-155.

Pedersen, K. (1993). Catalytic Hydrocracking of Tar from Gasification of Straw. Advances in Thermochemical Biomass Conversion. A. V. Bridgwater, Springer Netherlands: 246-264.

Pfeifer, C. (2008). "Development of catalytic tar decomposition downstream from a dual fluidized bed biomass steam gasifier." Powder technology **180**: 9.

Qin, K., P. A. Jensen, et al. (2012). "Biomass Gasification Behavior in an Entrained Flow Reactor: Gas Product Distribution and Soot Formation." Energy & Fuels **26**: 5992-6002.

Qin, Y., H. Huang, et al. (2007). "Characterization of tar from sawdust gasified in the pressurized fluidized bed." Biomass and Bioenergy **31**: 243-249.

Rapagnà, S., N. Jand, et al. (2000). "Steam-gasification of biomass in a fluidised-bed of olivine particles." Biomass and Bioenergy **19**: 187-197.

Salge, J. R., B. J. Dreyer, et al. (2006). "Renewable hydrogen from nonvolatile fuels by reactive flash volatilization." Science **314**: 801-804.

Sehested, J. (2006). "Four challenges for nickel steam-reforming catalysts." Catalysis Today **111**: 103-110.

Senapati, P. K. and S. Behera (2012). "Experimental investigation on an entrained flow type biomass gasification system using coconut coir dust as powdery biomass feedstock." Bioresource Technology **117**: 99-106.

Shafizadeh, F. (1982). "Introduction to pyrolysis of biomass." Journal of Analytical and Applied Pyrolysis **3**: 283-305.

Srinakruang, J., K. Sato, et al. (2005). "A highly efficient catalyst for tar gasification with steam." Catalysis communications **6**: 437-440.

Sutton, D., B. Kelleher, et al. (2001). "Review of literature on catalysts for biomass gasification." Fuel Process. Technol. **73**: 155-173.

Ueki, Y., T. Torigoe, et al. (2011). "Gasification characteristics of woody biomass in the packed bed reactor." Proceedings of the Combustion Institute **33**: 1795-1800.

Van den Aarsen, F. G., A. A. C. M. Beenackers, et al. (1983). Performance of a rice husk fueled fluidized bed pilot plant gasifier. First International Producer Gas Conference, Colombo, Sri Lanka.

Vizcaíno, A. J., P. Arena, et al. (2008). "Ethanol steam reforming on Ni/Al₂O₃ catalysts: Effect of Mg addition." International journal of hydrogen energy **33**: 3489-3492.

Wang, D., S. Czernik, et al. (1998). "Production of Hydrogen from Biomass by Catalytic Steam Reforming of Fast Pyrolysis Oils." Energy Fuels **12**: 19-24.

Wang, D., W. Yuan, et al. (2011). "Char and char-supported nickel catalysts for secondary syngas cleanup and conditioning." Applied Energy **88**: 1656-1663.

Wang, L., D. Li, et al. (2012). "Catalytic performance and characterization of Ni–Co catalysts for the steam reforming of biomass tar to synthesis gas." Fuel **112**: 654-661.

Wang, T. J., J. Chang, et al. (2005). "The steam reforming of naphthalene over a nickel-dolomite cracking catalyst." Biomass Bioenergy **28**: 508-514.

Wang, Y. and C. M. Kinoshita (1993). "Kinetic model of biomass gasification." Sol. Energy **51**: 19-25.

Zhao, Y., S. Sun, et al. (2010). "Experimental study on sawdust air gasification in an entrained-flow reactor." Fuel processing technology **91**: 910-914.

This page intentionally left blank.

Monash University

Declaration for Thesis Chapter 3

Declaration by candidate

In the case of Chapter 3, the nature and extent of my contribution to the work was the following:

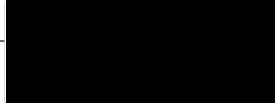
Nature of contribution	Extent of contribution (%)
Initiation, key ideas, experimental and analysis works, development and writing up of the paper.	85

The following co-authors contributed to the work. If co-authors are students at Monash University, the extent of their contribution in percentage terms must be stated:

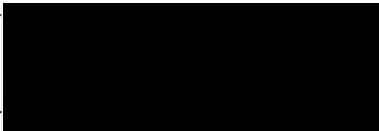
Name	Nature of contribution	Extent of contribution (%) for student co-authors only
Akshat Tanksale	Initiation, key ideas, reviewing and editing of the paper.	

The undersigned hereby certify that the above declaration correctly reflects the nature and extent of the candidate's and co-authors' contributions to this work*.

Candidate's
Signature

	Date 15/05/2015
---	--------------------

Main
Supervisor's
Signature

	Date 15/05/2015
---	--------------------

This page intentionally left blank.

Chapter 3: Catalytic Steam Gasification of Cellulose Using Reactive Flash Volatilization

Abstract

Biomass gasification is considered one of the most promising technologies for delivering renewable energy. However, tar formation in the gasifiers is one of the main challenges. Ni based catalysts are proven as an effective transition metal catalysts in biomass gasification for tar cracking and reforming. Alumina supported Ni, Pt-Ni, Ru-Ni, Re-Ni and Rh-Ni catalysts were tested for their activity in Reactive Flash Volatilisation (RFV) of cellulose to produce synthesis gas in 50 ms reaction time. RFV is a catalytic gasification process which utilises high carbon space velocity and mass flow rate, with oxygen and steam as gasification agents. Re-Ni, Rh-Ni and Ru-Ni supported catalysts showed higher gasification efficiency than the other catalysts, which was due to their higher metal surface area and high reducibility. Highest gasification efficiency was achieved at 750°C with carbon to oxygen ratio of 0.6 and carbon to steam ratio of 1.0, without any oxygen breakthrough.

This page intentionally left blank.

3.1 Introduction

Lignocellulosic biomass is a renewable energy resource that can be derived from organic sources such as energy crops, agricultural residues, forestry residues and recycled cardboard and paper (Ni et al. 2006). Biomass utilisation for fuels and energy production is recognised as one of the most promising solutions for the energy crisis and anthropological carbon dioxide emission problems (Kumar et al. 2009). Thermochemical processes for biomass conversion, such as combustion, gasification and pyrolysis, can be used for power generation and biofuels production (Kumar et al. 2009). Among the biomass conversion technologies, gasification is one of the most interesting technology from both industrial and academic research point of view due to its high conversion efficiency (Devi et al. 2003). Biomass gasification can be achieved at temperatures in excess of 700°C in the presence of oxygen or air, with or without additional steam. However, at this temperature significant amount of condensable oxygenated hydrocarbons, commonly referred to as tar is produced. In the absence of catalysts, tar free gasification requires higher temperatures ($\geq 1000^\circ\text{C}$) (Hernández et al. 2010; Qin et al. 2012).

Tar removal is a major hurdle that hinders the commercialisation of biomass gasification (Huber et al. 2006). Many factors can affect the amount and type of tar formed during gasification. These factors include gasifier type and design, operating parameters (temperature, pressure, heating rate and residence time), type of feedstock, and type of catalysts used. Optimising these factors may maximise the efficiency of gasification with minimum tar formation. Dolomite and $\text{CeO}_2/\text{SiO}_2$ supported Ni, Pt, Pd, Ru and alkali metal-oxides have been used in the past to catalyse gasification reactions, reduce tar formation, improve conversion efficiency and also improve the product gas purity (Baker et al. 1987; Rapagnà et al. 2000; Tomishige et al. 2004). Since Ni based catalysts are industrially used for steam reforming of methane and naphtha (Rostrup-Nielsen 1975; Farrauto et al. 1997), they are expected to catalyse the steam reforming of tars and subsequent water gas shift reaction to produce H_2 . However, monometallic nickel catalysts suffer rapid deactivation due to coke formation when used as primary catalysts in fluidised bed gasifiers (Baker et al. 1987; Li et al. 2004). Doping Ni catalysts with small amount of noble metal increases its reforming activity, reducibility and coke resistance (Tanksale et al. 2007; Tanksale et al. 2008; Tanksale et al. 2009).

Chapter 3

Biomass gasification is conventionally performed in one of the following reactor setups:

- Fluidized bed gasifier with downstream catalytic tar cleaning reactor
- Fast pyrolysis reactor with downstream catalytic steam reformer
- Catalytic fluidised bed gasifier
- Entrained flow gasifier

Fluidised bed reactors are capital intensive and hence large scale reactors are required to make it economical. Capital cost of the gasifier and gas cleaning system can account for 66.7 % to 85.5% of the total capital cost (Leung et al. 2004). Entrained flow gasifiers are more expensive due to higher flow velocities and temperatures in excess of 1000°C, requiring nickel based alloys (e.g. hastelloy) which provide oxidation resistance, and high-temperature strength. In comparison, capital cost of fixed bed reactors for biomass gasification is significantly lower. Therefore, a novel approach called as reactive flash volatilisation (RFV) was recently proposed for cellulose gasification (Salge et al. 2006; Colby et al. 2008).

RFV uses a fixed bed gasifier with carbon space velocity and carbon mass flow rate 10 to 100 times higher than fluidised bed reactors (Colby et al. 2008). As a result, RFV reactors require significantly less catalyst and smaller reactor volume to process a unit mass of carbon feedstock compared to the fluidised bed gasifiers. Therefore, RFV reactors can be economically viable at small scale operation which is useful for distributed or decentralised biomass processing facilities. The advantage of decentralised facilities is that the cost of transporting large volumes of low energy density biomass is minimised by placing these facilities closer to the source of biomass (Dauenhauer et al. 2007; Shastri et al. 2012).

Similar to conventional gasification, chemistry of reactive flash volatilization is complex and yet to be fully understood by researchers. However, it is generally accepted that the major reactions include pyrolysis, oxidation, partial oxidation, reduction, steam reforming and water gas shift reactions (Wang et al. 1993; Sutton et al. 2001; Huber et al. 2006). Methanation may also occur, but to a lesser extent (Haryanto et al. 2009; Kumar et al. 2009). These reactions have been summarised in Table 3.1.

In RFV, the formation of char is avoided by rapidly oxidising the cellulose pyrolytic products into gases via steam reforming and partial oxidation reactions. The heat generated from oxidation reaction is used in steam reforming reaction, making the RFV process autothermal. 99% conversion of the feed at ~70% hydrogen selectivity can be achieved without catalyst deactivation

(Salge et al. 2006). However, so far the RFV studies have been carried out at temperatures $>800^{\circ}\text{C}$ and by using Rh-Ce supported catalysts (Salge et al. 2006; Colby et al. 2008). There is a need to develop low cost catalyst which is active and selective at lower temperatures to make this process economically attractive. In this regard, promoted nickel catalysts may play a vital role.

Table 3. 1- Gasification reactions and their enthalpies for C_6 compound

Reaction Name	Stoichiometric equation	$\Delta\hat{H}_r^{\circ}$ at $T = 27^{\circ}\text{C}$ and $x = 6$
Pyrolysis	$\text{C}_x\text{H}_y\text{O}_z \rightarrow (1-x)\text{CO} + \frac{y}{2}\text{H}_2 + \text{C}$ (3.1)	180
	$\text{C}_x\text{H}_y\text{O}_z \rightarrow (1-x)\text{CO} + \frac{(y-4)}{2}\text{H}_2 + \text{CH}_4$ (3.2)	300
Partial oxidation	$\text{C}_x\text{H}_y\text{O}_z + \frac{1}{2}\text{O}_2 \rightarrow x\text{CO} + \frac{y}{2}\text{H}_2$ (3.3)	71
	$\text{C}_x\text{H}_y\text{O}_z + \text{O}_2 \rightarrow (1-x)\text{CO} + \text{CO}_2 + \frac{y}{2}\text{H}_2$ (3.4)	-213
	$\text{C}_x\text{H}_y\text{O}_z + 2\text{O}_2 \rightarrow \frac{y}{2}\text{CO} + \frac{y}{2}\text{CO}_2 + \frac{y}{2}\text{H}_2$ (3.5)	-778
Steam reforming	$\text{C}_x\text{H}_y\text{O}_z + \text{H}_2\text{O} \rightarrow x\text{CO} + y\text{H}_2$ (3.6)	310
	$\text{C}_x\text{H}_y\text{O}_z + n\text{H}_2\text{O} \rightarrow a\text{CO} + (x-a)\text{CO}_2 + y\text{H}_2$ (3.7)	230
Water gas shift	$\text{C}_x\text{H}_y\text{O}_z + (2x-z)\text{H}_2\text{O} \rightarrow x\text{CO}_2 + (2n + \frac{y}{2} - z)\text{H}_2$ (3.8)	64
	$\text{CO} + \text{H}_2\text{O} \rightarrow \text{CO}_2 + \text{H}_2$ (3.9)	-41
Methanation	$\text{CO} + 3\text{H}_2 \rightarrow \text{CH}_4 + \text{H}_2\text{O}$ (3.10)	-206

3.2 Experimental Section

3.2.1 Catalyst Preparation

Five nickel based catalysts were developed using the impregnation method. They were Ni/ Al_2O_3 , Pt-Ni/ Al_2O_3 , Ru-Ni/ Al_2O_3 , Rh-Ni/ Al_2O_3 and Re-Ni/ Al_2O_3 . Nickel nitrate ($\text{Ni}(\text{NO}_3)_2 \cdot 6\text{H}_2\text{O}$), alumina (Al_2O_3) and chemicals such as H_2PtCl_6 , RuCl_3 , RhCl_3 and NH_4ReO_4 obtained from Sigma Aldrich were used as the precursors for the catalyst synthesis. First, the required amount of nickel nitrate was measured and dissolved in distilled water. Then, corresponding amount of alumina and metal promoter precursor were added into the solution. Monometallic Ni/ Al_2O_3 catalyst had a Ni content of 11wt% and all bimetallic catalysts had Ni content of 10wt% and metal promoter content of 1wt%. To ensure a homogeneous mix of all precursors with alumina, the solution was heated up to 65°C and maintained for 5 h under constant stirring. The solutions were then dried overnight in a 100°C oven. Dry solid were recovered and calcined in a muffle furnace at 600°C for 6 h under air atmosphere. Only the Re-Ni/ Al_2O_3 catalyst was not calcined at high temperature due to the high volatility of rhenium (VI) and (VII) oxides. The resultant calcined catalysts were reduced *in-situ* before the reaction studies under 60 ml/min of H_2/N_2 flow at 400°C for at least 4 h.

3.2.2 Catalyst Characterization

Catalysts were characterized using techniques including nitrogen Physisorption, carbon monoxide chemisorption, X-ray Fluorescence Spectroscopy (XRF), Transmission Electron Microscopy (TEM), hydrogen Temperature Programmed Reduction (H₂-TPR) and carbon monoxide Temperature Programmed Desorption (CO-TPD).

3.2.2.1 Nitrogen Physisorption

Catalyst specific surface area, pore size distribution and pore volume were measured using N₂ physisorption with a Belsorp mini-II instrument. Surface area was characterized using Brunauer, Emmett and Teller (BET) method, whereas, pore size distribution and pore volume were measured by BJH method on the adsorption-desorption isotherm curve. 200 mg of catalyst was degassed at high vacuum at 120°C for at least 5 h prior to the measurement.

3.2.2.2 X-Ray Florescence (XRF) Spectroscopy

Elemental composition of nickel and alumina of prepared catalysts were determined using an Ametek Spectro iQ II XRF and the promoter content was calculated based on mass balance.

3.2.2.3 CO Chemisorption

Amount of active metal sites and dispersion of catalyst were measured using CO chemisorption with a Micromeritics ASAP 2020. 200 mg of catalyst was loaded into a flowthrough quartz tube reactor where *in-situ* reduction was performed. Sample was reduced with 5.22% H₂/N₂ gas mixture at temperature of 400 °C for 5 h and then cooled to room temperature under N₂ flow. Chemisorption measurement was started once the sample reached 30 °C.

3.2.2.4 Temperature Programmed Reduction

Temperature programmed reduction measurement was carried out to investigate the reducibility of the fresh catalyst and examine the interaction between nickel, metal promoters and support. Measurements were performed in a custom build instrument consisting of a vacuum compartment fitted with an Agilent Technologies TPS Compact vacuum pump and a Stanford Research Systems Residual Gas Analyser (RGA) 300. A simplified schematic diagram of the setup is presented in Figure 3.1. 500 mg catalyst was loaded into a custom made quartz reactor which was placed in a vertical tube furnace (Labec) and heated from room temperature to 800°C at the heating rate of 10°C/min. During the heating process, a 5.22% H₂/N₂ gas mixture was continuously fed into the reactor at the flow rate of 50 ml/min to reduce the metal oxide to its pure metal state. The resultant gas was introduced into the vacuum chamber via a capillary tube and a leak valve. The RGA, which is a quadrupole mass spectrometer, analysed the gases in the vacuum chamber and reported partial pressure of gases with respect to time on stream. To report the

results, the partial pressures were converted into molar flows, based on the volumetric flow rate used and the time on stream was converted to temperatures, based on the ramp rate of furnace.

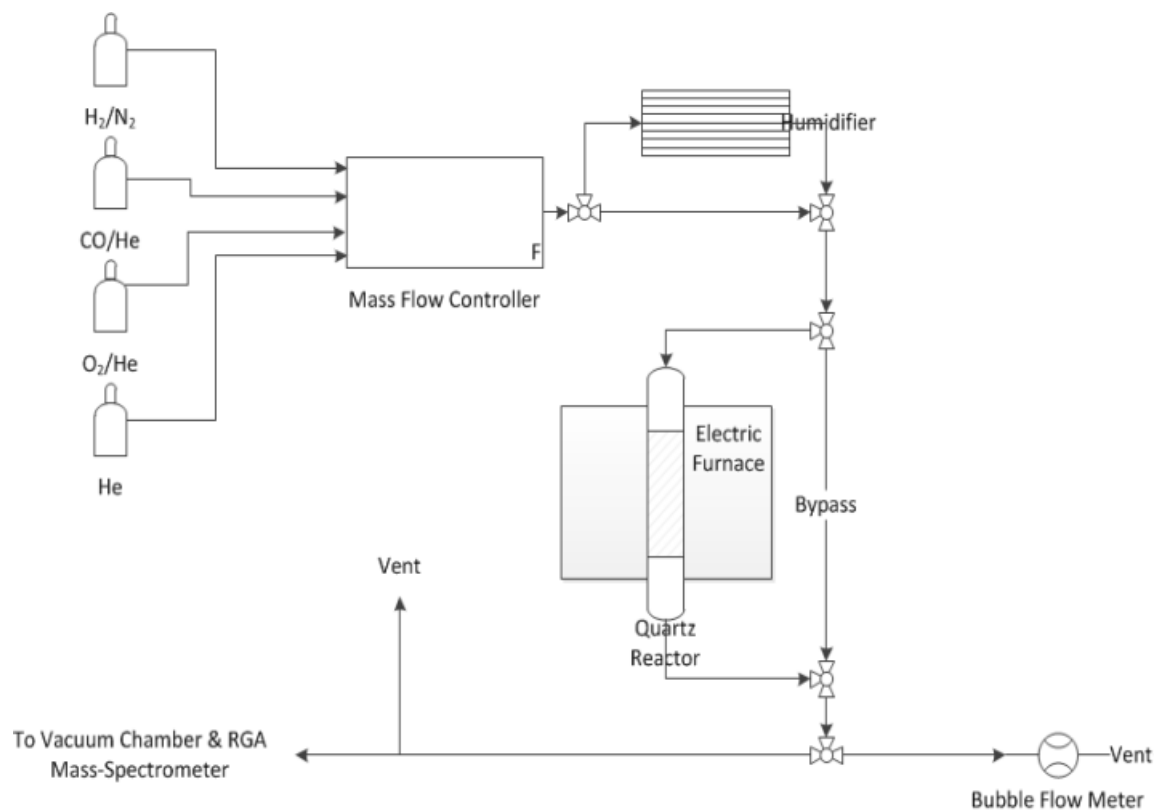
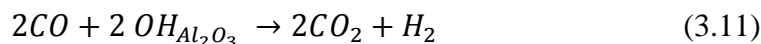


Figure 3. 1- Schematic diagram of the custom made TPR-TPD-TPO Instrument

3.2.2.5 CO Temperature Programmed Desorption

CO-TPD was carried out to examine the interaction between nickel and metal promoter, and to measure the strength and number of metal active sites available on the catalyst surface. The same custom build instrument described in H₂-TPR study was also used in this investigation. In this study, fresh catalyst sample was loaded into the quartz reactor and reduced it *in-situ* under 60 ml/min of 5.22% H₂/N₂ gas mixture at temperature of 400°C for 5 h, followed by purging with 100 ml/min of He gas at 400°C for 1 h. The catalyst was then cooled to room temperature under He gas. To dope the catalyst surface with CO, 10% CO/He gas mixture was fed into the reactor for 15 min at a flow rate of 100 ml/min, followed by purging with He gas at 100 ml/min for 2 h to remove any excess CO such that only a monolayer CO adsorbed was left on the surface of the catalyst. Once the CO partial pressure, monitored using the RGA, was stable, He flow was subsequently reduced to 50 ml/min and the TPD data was recorded while the sample was heated from room temperature to 800°C at 10°C/min. Typical CO-TPD products include CO and CO₂. It is believed that the formation of carbon dioxide is largely due to the water gas shift (3.11) and Boudouard (3.12) reactions occurred when the adsorption layer becomes mobile at high temperature (Tanksale et al. 2008). However CO₂ formation is largely dominated by reaction

(3.11). As a result, both CO and CO₂ partial pressures were monitored and reported in CO-TPD analysis.



3.2.2.6 Powder X-Ray Diffraction

Powder X-ray diffraction measurement was carried out in a Rigaku Miniflex powder diffractometer with mono-chromatized Cu K α radiation ($\lambda = 0.154$ nm) at 40 kV and 15 mA.

3.2.3 Catalytic Activity Evaluation

3.2.3.1 Reactor Setup

The catalytic activity was evaluated in a bench-scale reactor setup consisting of a 25 mm OD and 700 mm long quartz tube reactor, a K-Tron twin screw powder feeder (K-MV-KT20), an Alltech HPLC pump (model 426), three Teledyne Hasting mass flow controllers for nitrogen and oxygen, a Labec vertical split tube furnace, a Brooks Instrument DLI Series evaporator and a custom built gas-liquid separator. Schematic diagram of the reactor setup is shown in Figure 3.2.

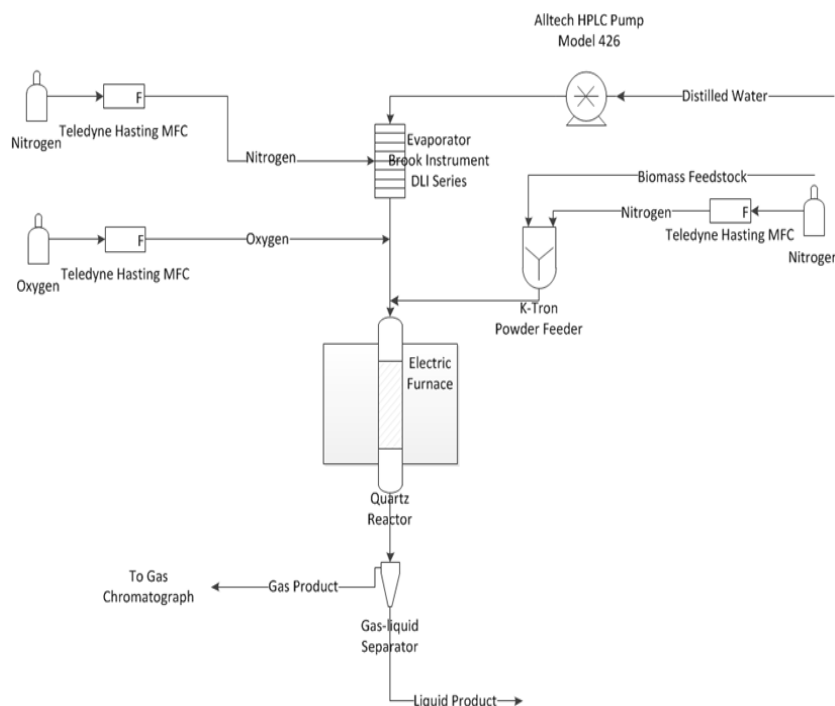


Figure 3. 2- Schematic diagram of Reactive Flash Volatilization Reactor Setup

1g catalyst was loaded into the quartz reactor prior to assembling it in the furnace. Catalyst was held in the centre by a porous quartz disk. Before the catalytic tests, *in-situ* reduction was carried out with H₂/N₂ gas mixture at 400 °C for at least 4h. Reactive flash volatilisation was performed at the temperatures of 700, 750 and 775 °C with various C/O and C/S ratios. During these

experiments, 15g/h of cellulose was gravity fed by the twin screw powder feeder and a mixture of O₂, N₂ and steam was flown into the reactor. The amounts of steam and O₂ fed into the reactor were controlled by the HPLC pump and the mass flow controller, respectively. N₂ was used as a control parameter for varying the reactor space velocity. Product gases from the reactor were fed into a custom built gas-liquid separator where the gaseous products were periodically sampled for composition analysis. Gases were analysed by a Shimadzu gas chromatograph GC-2014 equipped with a molecular sieve 5A column (60/80 mesh, 1/8 inch diameter with 6 feet in length), using a Thermal Conductivity detector and a Flame Ionisation Detector. Volumetric flow rate of the gaseous product was determined after each GC analysis using a 50 ml bubble flow meter. Detailed operating parameters are listed below –

Temperature	700°C, 750°C, 775 °C
Cellulose Type	Cellets 200
Cellulose Feed Rate, g/h	15
N ₂ Flow Rate, sccm	235
Residence time	50 ms
C/O Ratio	0.5, 0.6, 0.7
C/S Ratio	1.0, 1.5, 2.0

Gas yield and composition results are computed by using trapezoid rule, which integrate the molar flow rate of each gas species over total run time. Carbon balance was performed by calculating the moles of carbon atoms in the gas, liquid and solid products collected from the reactor. Carbon in the gas phase was calculated by measuring the amount of carbonaceous molecules in the gas phase using the gas chromatographer (as described above). Carbon atoms in the liquid phase (tar) were calculated by measuring the Total Organic Carbon using Shimadzu TOC-L series analyser. 0.5 ml of liquid sample was diluted with 200 ml of deionized water prior to the analysis. Moles of carbon atoms in the solid products (char) were calculated by measuring elementary carbon using Perkin Elmer 2400 Series II CHNS /O system. Based on the carbon balance selectivity for gas, tar and char are reported according to the following equations –

$$\text{Gas Selectivity} = \frac{\text{Moles of Carbon atoms in the gas phase}}{\text{Moles of Carbon atoms in the products}} \times 100\%$$

$$\text{Tar Selectivity} = \frac{\text{Moles of Carbon atoms in the liquid phase}}{\text{Moles of Carbon atoms in the products}} \times 100\%$$

$$\text{Char Selectivity} = \frac{\text{Moles of Carbon atoms in the solid phase}}{\text{Moles of Carbon atoms in the products}} \times 100\%$$

3.2.3.2 Biomass Feedstock

High purity microcrystalline cellulose, Cellets 200 (Pharmatrans Sanaq AG) was used in our studies. The particle size of Cellets 200 was 200 – 355 μm .

3.3 Results and Discussion

3.3.1 Catalyst Characterisation

3.3.1.1 Nitrogen Physisorption

The specific surface area, total pore volume and pore size of the catalysts prepared in this project are summarised in Table 3.2. The BET surface area of commercial alumina support used in this study was 101.62 m^2/g , but it dropped by varying amounts for the impregnated catalysts. This is expected due to the pore blockage caused by impregnated metals. Among the impregnated catalysts, Ru-Ni catalyst had the highest specific surface area of 95.74 m^2/g and Re-Ni catalyst had the lowest surface area of 43.62 m^2/g . This is because the Re-Ni catalyst was not calcined before doing the BET measurement, therefore, the metal precursors are expected to remain on the alumina surface and block large proportion of the pores. After reduction the BET surface area of Re-Ni catalyst increased to 74.16 m^2/g .

3.3.1.2 X-Ray Fluorescence Spectroscopy

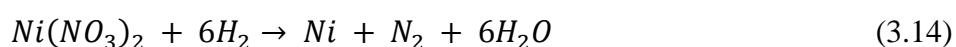
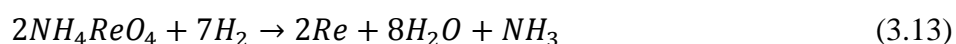
The results of XRF elemental analyses of the catalysts are presented in Table 3.2. NiO and Al_2O_3 contents were directly measured in the analyses and the promoter metals content was calculated based on mass balance. The XRF results and calculated promoter contents for Ni, Pt-Ni, Ru-Ni and Rh-Ni are in agreement with the nominal values, indicating the effectiveness of the catalyst preparation procedure.

3.3.1.3 Hydrogen Temperature Programmed Reduction

Reducibility of Ni catalysts is an important factor in determining the activity of the catalyst. It is known that Ni^0 is active for steam reforming and water gas shift reaction, whereas, Ni^{2+} or NiO is not active. H_2 -TPR was conducted to test the reducibility of prepared catalysts as shown in Figure 3.3. The monometallic Ni catalyst had the highest onset reduction temperature of $\sim 420^\circ\text{C}$ and the reduction was not complete 800°C . The low reducibility of Ni catalyst is attributed to nickel aluminate (NiAl_2O_4) spinel (Wang 1998) formation when Ni supported on alumina is calcined at or above 500°C (Rynkowski et al. 1993). All the promoted catalyst showed lower onset reduction temperature. The onset reduction temperature increased in the following order: Ru-Ni (165°C) < Pt-Ni (240°C) \sim Re-Ni (240°C) < Rh-Ni (362°C) < Ni (420°C). It is known from the literature that noble metals promote the reduction of NiO through surface migration of a

chemisorbed hydrogen atom, a phenomenon known as the hydrogen spill-over effect (Hou et al. 2006; Tanksale et al. 2010; El Doukkali et al. 2012). The most promising catalyst was Re-Ni, which was almost fully reduced at 800 °C.

Total hydrogen consumed by each catalyst in H₂-TPR was calculated by integrating the area under the curve using trapezoidal method (Table 3.3). Since Re-Ni catalyst was not calcined prior to the H₂-TPR measurement, the precursors of Re and Ni present on the surface of the catalyst react with hydrogen through reactions (3.13) and (3.14) and lead to high hydrogen consumption (Profeti et al. 2009).



3.3.1.4 Carbon Monoxide Chemisorption

Results obtained from CO-chemisorption are listed in Table 3.2. Re-Ni catalyst had the highest amount of irreversible CO uptake, and therefore, largest metal surface area and dispersion. Overall, all the promoted nickel catalysts exhibited higher metal surface area, than the monometallic nickel catalyst. This is because of higher reducibility of the promoted catalyst and higher dispersion of larger atomic weight noble metals.

3.3.1.5 CO-Temperature Programmed Desorption

Figures 3.4 shows the CO-TPD profiles of all the catalysts used in this study. CO chemisorption is not activated on Ni and noble metals active sites (Hayward et al. 1964), therefore at room temperature (~21°C) full coverage can be easily achieved. CO desorption at elevated temperatures is a complex process and not well understood (Profeti et al. 2009). Nonetheless, it is well known that the rate of desorption is a function of heat and activation energy of adsorption, and low activation energy sites exhibit higher rate of CO desorption at lower temperatures. Figure 3.4(a) shows profiles for CO desorption, while Figure 3.4(b) shows profiles for CO₂ evolution, which is formed due to dehydroxilation of alumina and subsequent reaction with desorbed CO (Jackson et al. 1993; Tanksale et al. 2008).

Low temperature CO and CO₂ desorption peaks that appear at 120°C for Ni, Ru-Ni and Re-Ni catalysts were attributed to weak multilayer chemisorption of CO over the catalyst. Low temperature CO₂ peak was also observed for Rh-Ni catalyst but the corresponding CO peak was not observed, suggesting that Rh-Ni promotes rapid conversion of CO into CO₂ at ~120°C.

Chapter 3

Second CO desorption peak observed at higher temperature of 275 – 300°C can be attributed to strong monolayer adsorption of CO on the metal surface that requires higher temperature and energy to desorb. Broad CO and CO₂ desorption peaks were observed for Ni, Pt-Ni and Rh-Ni catalysts in this temperature range (275 – 320°C), while a shoulder peak was observed for Re-Ni catalyst in this temperature range. CO uptake of each catalyst was quantified by integrating the area under the curves for CO and CO₂ desorption curves, using trapezoidal method. Re-Ni and Rh-Ni showed the highest amount of CO+CO₂ desorption, in that order (Table 3.3).

In summary, from the results of characterisation of the catalysts used in this project it can be observed that compared to the mono-metallic Ni catalysts, the promoted Ni catalysts had significantly lower reduction temperature, higher dispersion and higher amount of active metal sites. This is extremely important, because only a small amount of noble metal was used in this study, which resulted in significant improvement in the catalyst properties. Therefore, it is expected that the promoted Ni catalysts will be more active for the reactive flash volatilisation run. Overall, Re-Ni catalyst showed the highest metal surface area, as seen from H₂-TPR, CO-TPD and CO-chemisorption.

Table 3. 2- Comparison of the specific surface area, total pore volume, amount of active metal, metal dispersion, NiO, Al₂O₃ and promoter contents of various promoted nickel based catalysts with alumina support.

Catalyst	Nitrogen Physisorption		CO Chemisorption		X-ray Fluorescence Spectroscopy					
	BET Surface Area (m ² g ⁻¹)	BJH Pore Volume (p/p ₀) (cm ³ g ⁻¹)	Irreversible CO uptake (μmol g ⁻¹)	Metal Dispersion (%)	NiO (Wt %)		Al ₂ O ₃ (Wt %)		Promoter (Wt %)	
					Theoretical	Measured	Theoretical	Measured	Calculated ^(a)	
Al ₂ O ₃	101.62	0.18	N.D.	N.D.	-	-	-	-	-	-
Ni	91.99	0.21	12.32	0.66	13.59	15.13 ± 0.02	86.41	84.09 ± 0.07	-	-
Pt-Ni	77.18	0.14	67.88	3.87	12.37	13.25 ± 0.02	86.53	84.30 ± 0.05	1.37	1.37
Ru-Ni	95.74	0.23	41.96	2.33	12.36	11.96 ± 0.07	86.44	86.95 ± 0.05	1.09	1.09
Re-Ni ^(b)	43.62	0.07	78.92	4.49	12.36	10.25 ± 0.08	86.43	50.42 ± 0.18	N.D.	N.D.
Rh-Ni	77.92	0.15	37.67	2.09	12.36	14.99 ± 0.08	86.41	83.72 ± 0.10	1.29	1.29

^(a) Calculated based on mass balance

^(b) Uncalcined catalyst

Table 3. 3- Comparison of the amount of H₂ consumed and amount of CO and CO₂ adsorbed on each catalyst.

Catalyst	H ₂ Consumed in TPR	CO Desorbed in TPD			CO ₂ Desorbed in TPD	
		CO Desorbed in TPD	CO ₂ Desorbed in TPD	CO+CO ₂ Desorbed in TPD		
Ni	124	31.98	1637	1669		
Pt-Ni	163	33.45	1025	1058		
Ru-Ni	306	29.01	1789	1818		
Re-Ni	344	22.41	2124	2146		
Rh-Ni	107	31.49	2501	2533		

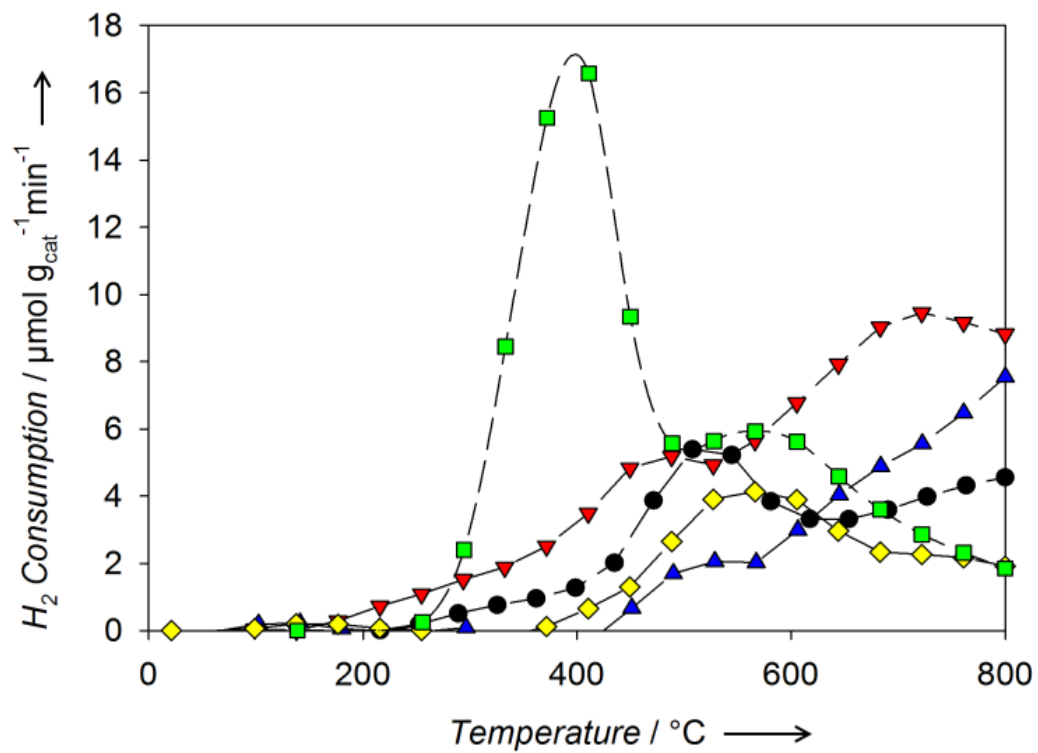


Figure 3-3- Comparison of the TPR profile of promoted nickel supported on alumina catalysts: (▲) Ni, (●) Pt-Ni, (▼) Ru-Ni, (■) Re-Ni, (◆) Rh-Ni.

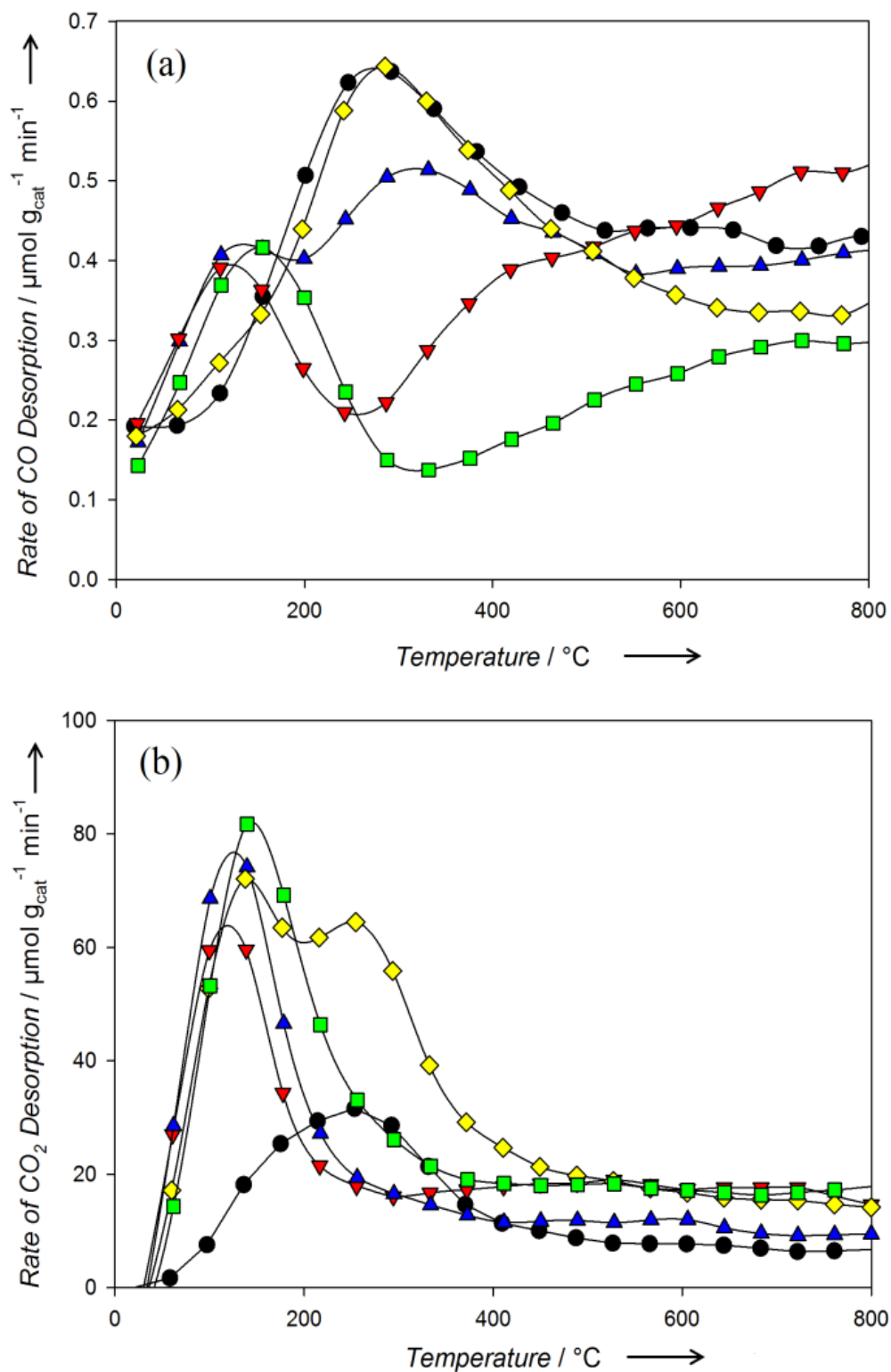


Figure 3. 4- (a) CO TPD profiles and (b) CO₂ TPD profiles of promoted nickel based catalysts with alumina support. (▲) Ni, (●) Pt-Ni, (▼) Ru-Ni, (■) Re-Ni, (◆) Rh-Ni.

3.3.2 Reactive Flash Volatilisation of Cellulose

3.3.2.1 Effect of Gasification Temperature

Catalysts were tested for their activity and stability in the reactive flash volatilisation at three operating temperatures (700, 750 and 775°C) by keeping carbon to oxygen (C/O) and carbon to steam (C/S) ratios constant at 0.5 and 1.0, respectively. The temperature range for gasification was selected based on the thermodynamic analysis of Colby *et al.* who used HSC chemistry software to demonstrate that CO selectivity increased with increasing temperature, while H₂ selectivity peaked around 700°C (Colby *et al.* 2008). As it can be seen from Figure 3.5, significant amount of char was produced at 700°C with all the catalysts, except Re-Ni, which lead to eventual clogging of the reactor (reduction in product gas flow rate). Re-Ni catalyst showed char selectivity of only 1%, while all other catalysts showed char selectivity of 19 – 35%. Gasification efficiency increased with increasing temperature, whereas the gas selectivity was highest at 750°C. Re-Ni, Ru-Ni and Rh-Ni catalysts performed the best at this temperature in terms of high gas yield (in that order) and no char. Figure 3.6 shows the composition of synthesis gas, on dry basis, produced in these runs. In general, all the catalysts showed high selectivity of CO over methane and C₂ compounds as results of high activity for steam reforming reactions.

Lower char selectivity and higher gasification efficiency at 750 and 775°C were observed because steam reforming and partial oxidation reactions are favourable at higher temperatures (Shiraga *et al.* 2007). These reactions convert the char and tar into gaseous products. It is known from literature that the cellulose particles undergo oxidative pyrolysis reaction on the hot surface of catalysts, forming a film of bio-oils which undergo catalytic steam reforming and partial oxidation (Colby *et al.* 2008). Therefore, higher temperatures led to complete conversion of cellulose into gases with small amount of unconverted volatile organics. However, for Ni and Ru-Ni catalysts, temperatures higher than 750°C were not favourable because of sintering of metal particles at this temperature (Sehested *et al.* 2006). Sintering of active metal reduces the metal surface available for reactions and therefore reduces the gasification efficiency. Ni catalysts supported on alumina also suffered from the transformation of NiO/Al₂O₃ to NiAl₂O₄ spinel at temperatures above 750 °C (Shrotri *et al.* 2013). Noble metal promoter is able to suppress this phase transformation of Ni catalyst into spinel by keeping the Ni in a reduced state via hydrogen spillover mechanism (Tanksale *et al.* 2008; Tanksale *et al.* 2009).

Figure 3.7 shows the ratio of hydrogen to carbon monoxide (Figure 3.7 (a)) and the ratio of carbon monoxide to carbon dioxide (Figure 3.7 (b)). These ratios are important for the downstream application in biofuels production. For example, for DME synthesis, H₂:CO ratio of

close to 1 is desirable due to the overall stoichiometry of DME synthesis from CO and H₂ (reaction 3.18). Whereas, for methanol synthesis, H₂:CO ratio of 2.0 is desirable (reaction 3.15). Therefore, the ability to tune the H₂:CO ratio by changing reaction parameters is an advantage in this process.



As seen in Figure 3.7(a), the H₂:CO ratio of close to 1.0 is achieved at 750°C with most the catalysts, while a wider distribution of this ratio is achieved at lower and higher temperatures. Results obtained ranged from a minimum of 0.66 with Re-Ni catalyst at 700 °C to a maximum of 1.57 with Rh-Ni catalyst at 750°C. In general the CO:CO₂ ratio showed an inverse relationship with temperature. The ratio of CO:CO₂ decreased at higher temperature due to complete oxidation of carbon and higher water gas shift activity on promoted catalysts (Asadullah et al. 2004; Omata et al. 2008). Low CO:CO₂ is not desirable as it reduces the calorific value of the synthesis gas. Therefore, further tests were carried out at 750°C and the effect of feed ratios of C/O and C/S on the product H₂:CO and CO:CO₂ ratios were tested to achieve the desired target.

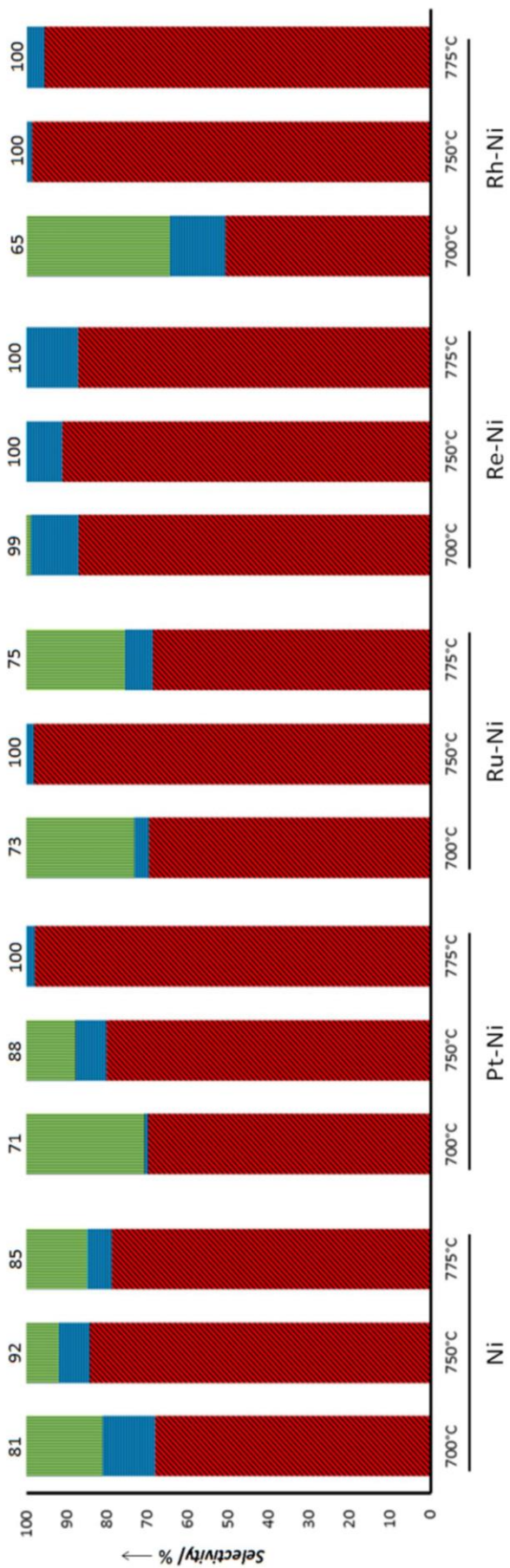


Figure 3. 5- Effect of reactive flash volatilisation temperature and catalyst promoters on the selectivity of Char (█), Tar (█) and Gas (█) based upon carbon balance. The numbers on the top of each bar represent gasification efficiency which is the percentage of carbon in the gas and tar combined. Reaction conditions: cellulose flow rate = 15 g/h, C/O = 0.5, C/S = 1.0 and residence time = 50ms. Here Tar is defined as water soluble organics.

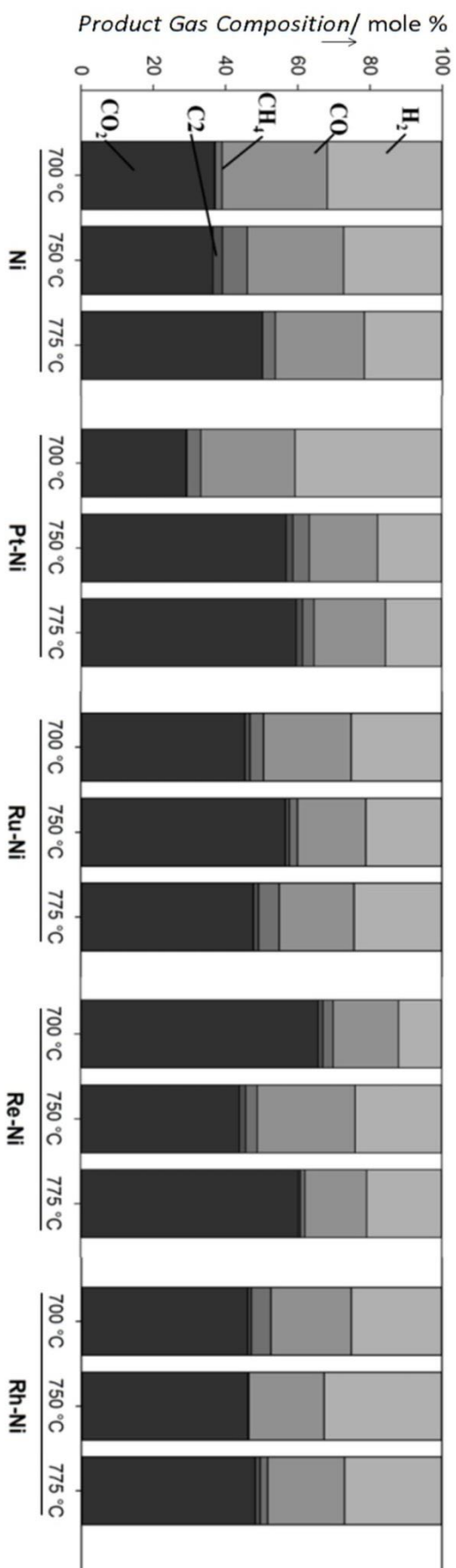


Figure 3. 6- Effect of reactive flash volatilisation temperature and catalyst promoters on product gas composition. C₂ compounds include ethane, ethylene and acetylene. Reaction conditions: cellulose flow rate = 15 g/h, C/O = 0.5, C/S = 1.0 and residence time = 50ms.

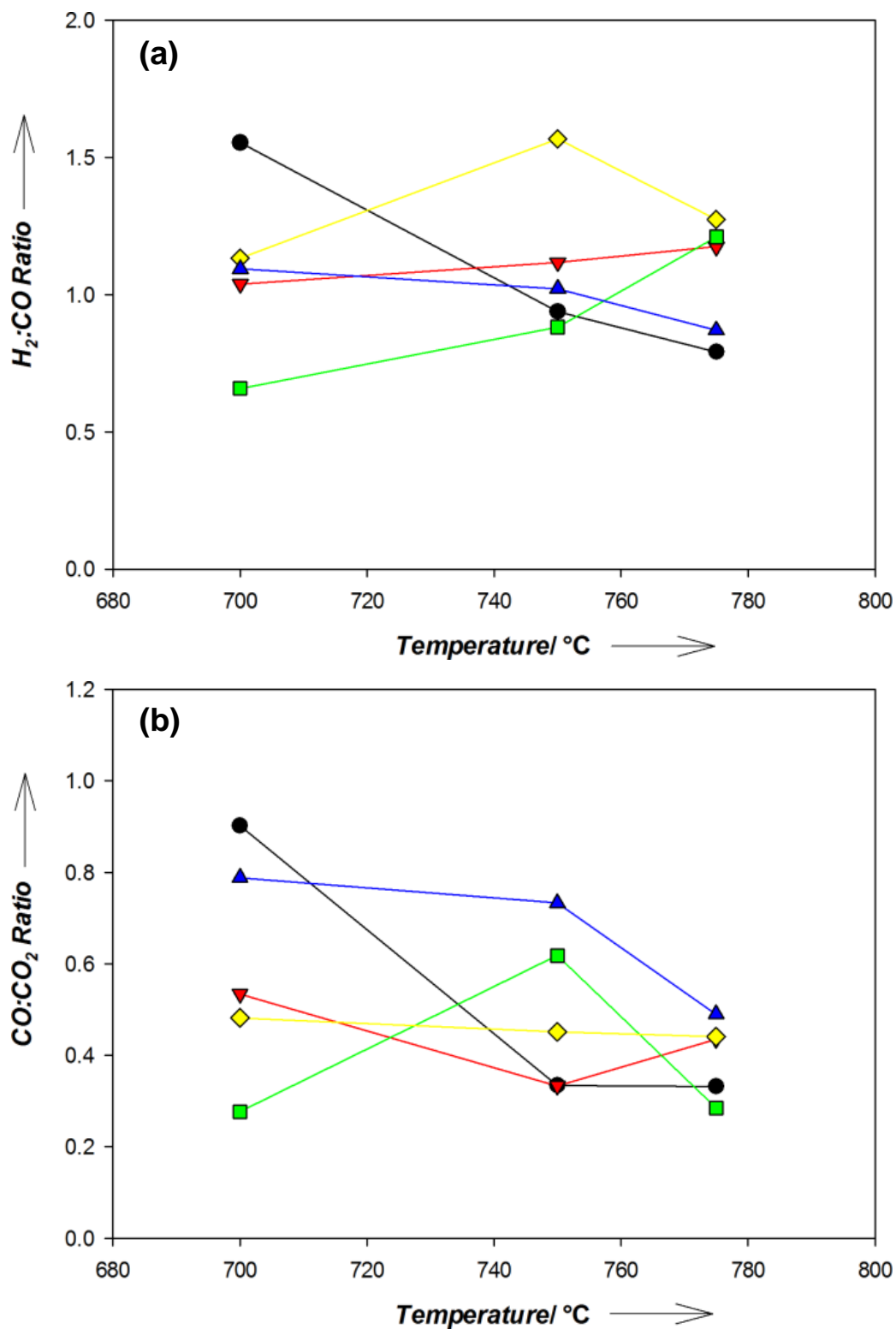


Figure 3. 7- Effect of temperature on a) H₂:CO Ratio and b) CO:CO₂ of promoted nickel based catalysts with alumina support under C/O ratio of 0.5 and C/S ratio of 1.0. (▲) Ni, (●) Pt-Ni, (▼) Ru-Ni, (■) Re-Ni, (◆) Rh-Ni.

3.3.2.2 Effect of Carbon to Oxygen Ratio in the Feed

The effect of carbon to oxygen feed ratio (C/O) was tested on all the promoted catalysts. Monometallic Ni catalyst was not considered for these tests because of the high char selectivity observed with this catalyst at all the temperatures tested above. The cellulose feed rate was kept constant at 15 g/h, similar to the tests above, while the oxygen flow rate in these tests were controlled such that C/O ratio were 0.5, 0.6 and 0.7. Reactor temperature and C/S ratio for these runs were kept constant at 750°C and 1.0, respectively. The results, illustrated in Figure 3.8, show that all the promoted Ni catalysts showed high gasification efficiency of 88 – 100% at all the C/O ratios tested. In general the gasification efficiency decreased with increasing C/O ratio which was expected, because higher C/O ratio means lower oxygen flow rate and therefore, lower partial oxidation. This result is consistent with previous observations where higher C/O in air-steam gasification led to lower carbon conversion (Lv et al. 2004; Wei et al. 2007). While lower C/O ratio may lead to high gasification temperatures (hot spots in catalyst bed), which is favourable for steam reforming, the higher rate of oxidation reactions may also result in oxidation of CO to CO₂ and H₂ to H₂O. Therefore, low C/O ratios may degrade the quality of synthesis by increasing CO₂ and H₂O mole fraction. This is precisely what was observed in our experiments (Figure 3.9). C/O ratio of 0.5 resulted in CO₂ mole fraction in the dry synthesis gas in excess of 50 %. Increasing the C/O ratio to 0.6 decreased the CO₂ mole fraction to approximately 40 %. However, further increasing the C/O ratio resulted in incomplete gasification in most cases, i.e. formation of char. Ru-Ni catalyst performed the best amongst all the promoted catalysts. The char selectivity with Ru-Ni catalyst was zero at all the C/O ratios. Ru is known to exhibit higher activity for C-C bond cleavage than Re, Rh and Pt, in that order (Sinfelt 1973). Ru also shows higher water gas shift reaction activity than Pt and Rh, while it is nearly equal to Re (Grenoble et al. 1981). Therefore, it is expected that Ru will perform well under gasification conditions which requires a combination of C-C bond cleavage and water gas shift reaction. Figure 3.10 confirms that the water gas shift activity was high because of the high H₂:CO ratio and low CO:CO₂ ratio observed for the promoted Ni catalysts.

In summary, higher C/O ratio, especially C/O = 0.6, was favourable as it improved gasification efficiency, synthesis gas quality and the mole fractions of H₂ and CO in the product gas. In addition, catalysts are less likely to be re-oxidized under oxygen deficit environment (high C/O), which can significantly improve the catalyst service life.

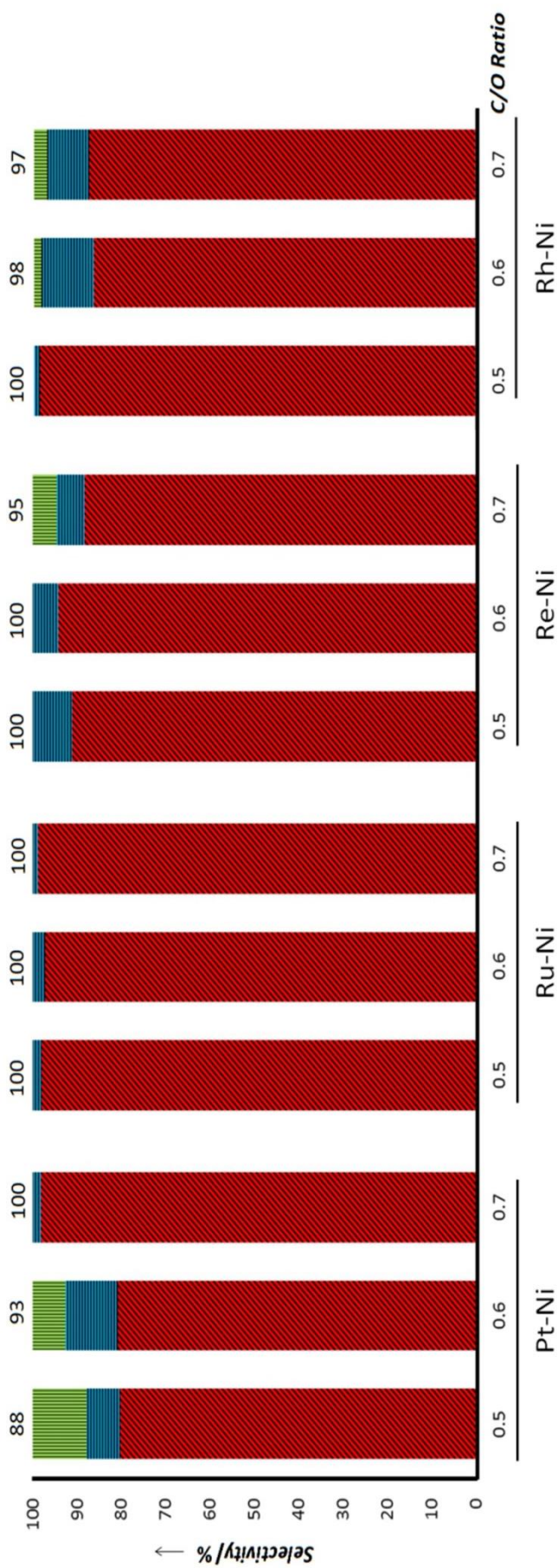


Figure 3. 8- Effect of carbon to oxygen feed ratio (C/O) and catalyst promoters on the selectivity of Char (), Tar () and Gas () based upon carbon balance. The numbers on the top of each bar represent gasification efficiency which is the percentage of carbon in the gas and tar combined. Reaction conditions: cellulose flow rate = 15 g/h, Temperature = 750°C, C/S = 1.0 and residence time = 50ms. Here Tar is defined as water soluble organics.

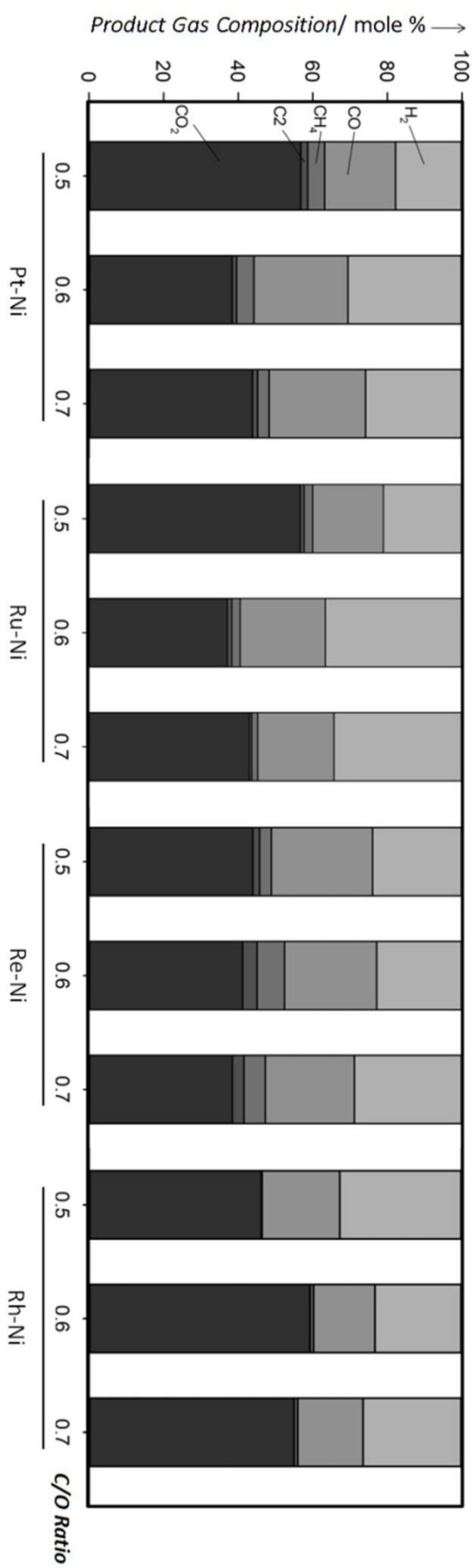


Figure 3. 9- Effect of carbon to oxygen feed ratio (C/O) and catalyst promoters on product gas composition. C₂ compounds include ethane, ethylene and acetylene. Reaction conditions: cellulose flow rate = 15 g/h, Temperature = 750°C, C/S = 1.0 and residence time = 50ms.

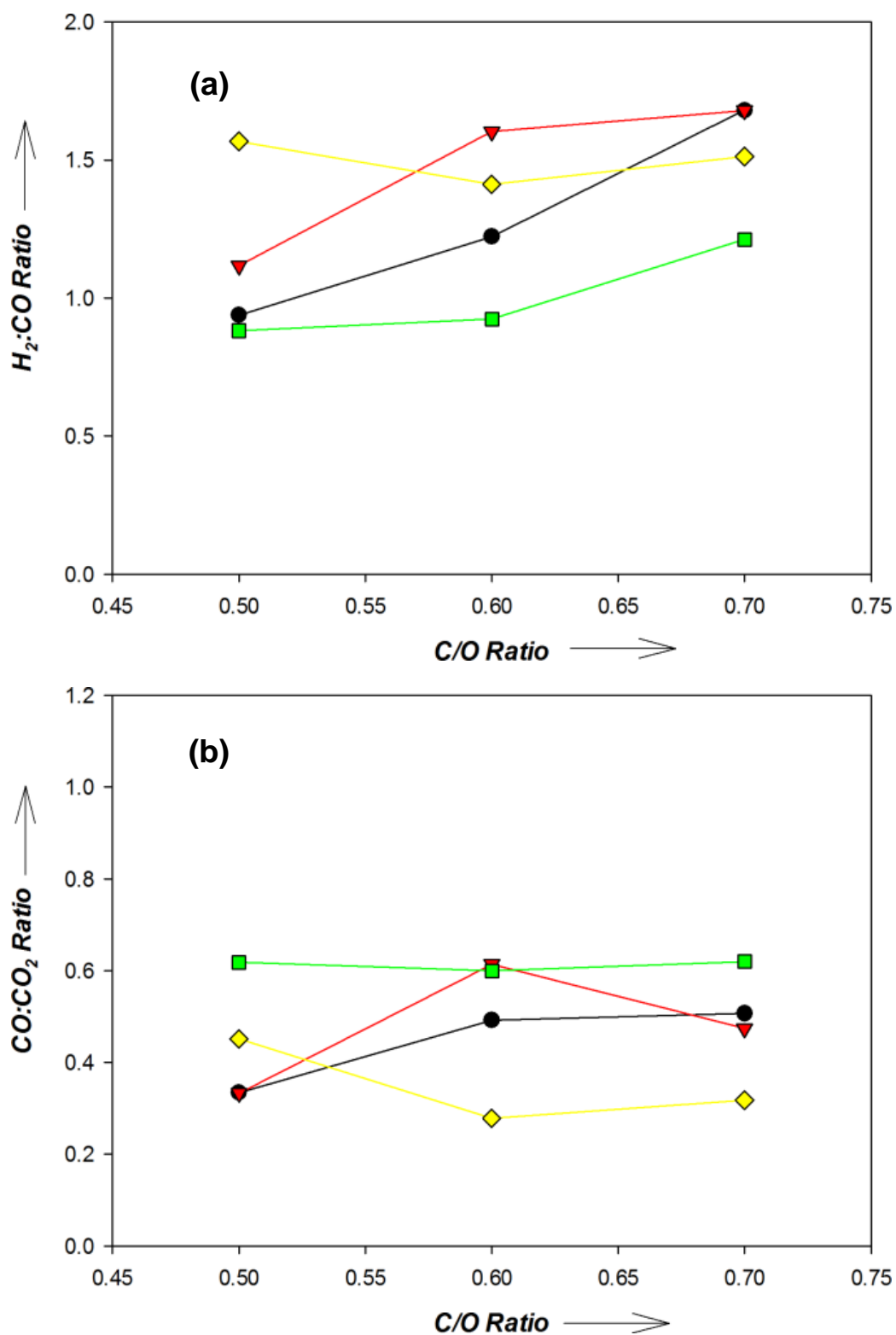


Figure 3. 10- Effect of Carbon to Oxygen Ratio on a) H₂:CO Ratio and b) CO:CO₂ Ratio of promoted nickel based catalysts with alumina support at temperature of 750°C and C/S ratio of 1.0. (●) Pt-Ni, (▼) Ru-Ni, (◆)Rh-Ni, (■)Re-Ni.

3.3.2.3 Effect of Carbon to Steam Ratio in the Feed

The effect of carbon to steam ratio was tested on all the promoted catalysts. Monometallic Ni catalyst was not considered for these tests because of the high char selectivity observed with this catalyst at all the temperatures tested in previous section. The cellulose feed rate was kept constant at 15 g/h, similar to the tests above, while the steam flow rate in these tests were controlled such that C/S ratio were 1.0, 1.5 and 2.0. Reactor temperature and C/O ratio for these runs were kept constant at 750°C and 0.6, respectively. The results, illustrated in Figure 3.11, show that all the promoted Ni catalysts showed high gasification efficiency of 82 – 100% at all the C/S ratios tested. In general the gasification efficiency reduced with increasing C/S ratio (i.e. lower steam flow rate), which is expected because of the reduction in steam reforming and water gas shift activity at high C/S ratios. This result is consistent with catalytic steam gasification (Moghtaderi 2007) and air-steam gasification (Campoy et al. 2009) of biomass observations in the previous studies. While lower C/S ratios increase the rate of steam reforming reaction, it can reduce the temperature of catalyst bed because steam reforming is highly endothermic. The required heat for steam reforming reaction is provided by partial oxidation and water gas shift reactions. In this section a high C/O ratio was used, therefore, high C/S ratios were not favourable because the amounts of both the gasifying agents (O_2 and steam) were low, resulting in incomplete gasification. Figure 3.12 shows the molar composition of the product gases and it is clear from this figure that higher C/S ratios led to higher fraction of CO_2 in the product gas because the oxidation reactions dominated the gasification reaction when steam flow rate was reduced (higher C/S ratios). The fraction of CO_2 went up from approximately 40% to over 50% when the C/S ratio was increased from 1.0 to 1.5. Figure 3.13 shows the $H_2:CO$ and $CO:CO_2$ ratios against the changes in C/S ratio. The $H_2:CO$ ratio recorded in this part of the study was the highest among all the previous tests reported in previous two sections. On average the $H_2:CO$ ratio ranged from 1.0 to 1.5, which is believed to be because of high C/S ratio leading to oxidation dominated gasification and conversion of CO into CO_2 . This led to reduction in the $CO:CO_2$ ratio as seen in Figure 3.13(b).

Among the catalysts tested in this study, Re-Ni and Ru-Ni catalysts performed the best in terms of gasification efficiency and hydrogen yield. As seen in catalyst characterization section, Re-Ni and Ru-Ni catalysts had higher metal surface area, low reduction temperature and high CO uptake in the CO-TPD which combined together explains the superior performance of these two catalysts in the gasification experiments.

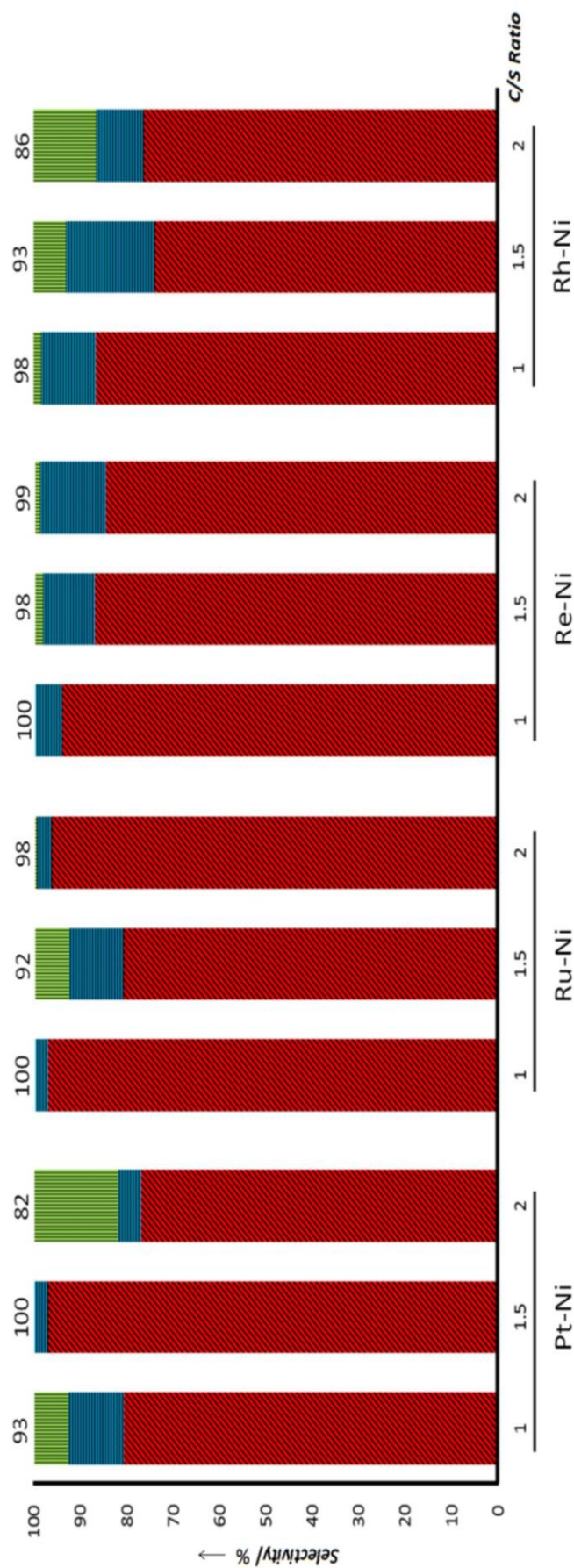


Figure 3. 11- Effect of carbon to steam feed ratio (C/S) and catalyst promoters on the selectivity of Char (█), Tar (█) and Gas (█) based upon carbon balance. The numbers on the top of each bar represent gasification efficiency which is the percentage of carbon in the gas and tar combined. Reaction conditions: cellulose flow rate = 15 g/h, Temperature = 750°C, C/O = 0.6 and residence time = 50ms. Here Tar is defined as water soluble organics.

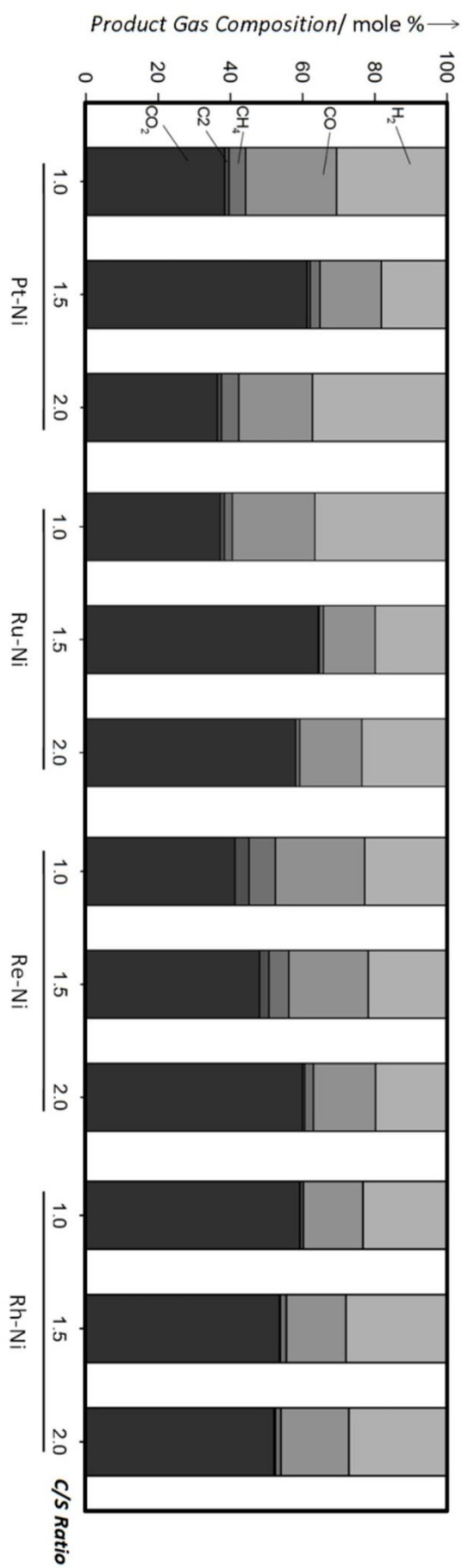


Figure 3. 12- Effect of carbon to steam feed ratio (C/S) and catalyst promoters on product gas composition. C₂ compounds include ethane, ethylene and acetylene. Reaction conditions: cellulose flow rate = 15 g/h, Temperature = 750°C, C/O = 0.6 and residence time = 50ms.

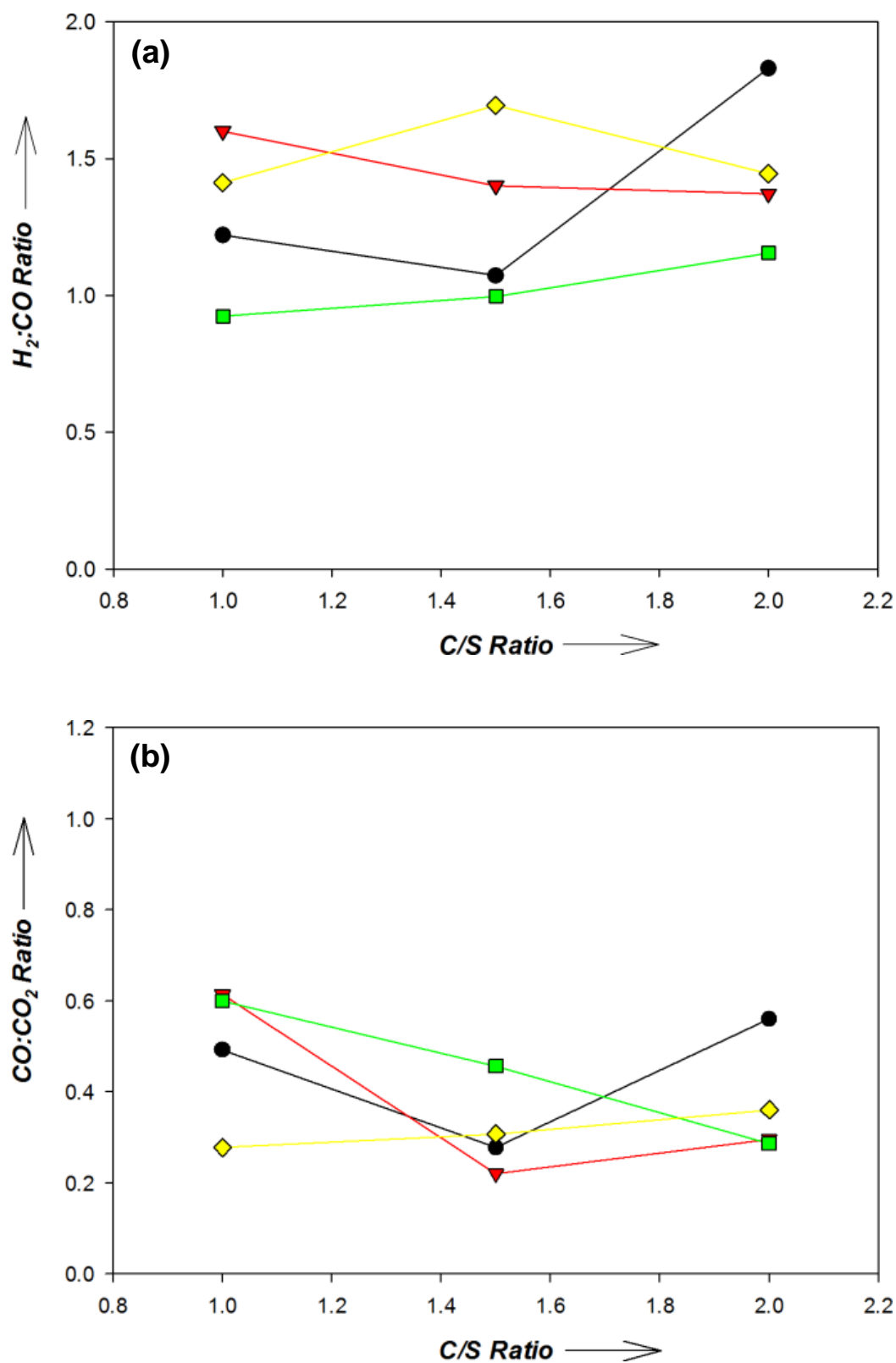


Figure 3. 13- Effect of Carbon to Steam Ratio on a) H₂:CO Ratio and b) CO:CO₂ Ratio of promoted nickel based catalysts with alumina support at temperature of 750 °C and C/O ratio of 0.6. (●) Pt-Ni, (▼) Ru-Ni, (◊) Rh-Ni, (■) Re-Ni.

Overall, results from the catalyst characterisation section and reactive flash volatilization section combined show that the Re-Ni, Rh-Ni and Ru-Ni catalysts were the best catalysts among all the catalysts tested in this project. Among the conditions tested in this study, the best condition was determined to be reaction temperature of 750°C, C/O = 0.6 and C/S = 1.0. This conclusion is based upon the overall gasification efficiency, in particular low char selectivity and the product gas composition, in particular low CO₂ mole fraction in the gas phase. These conditions resulted in sustained performance of the catalysts for a long period of time (>300 min) without noticeable deactivation of the catalyst. Extended duration of the gasification study could not be performed due to health and safety aspect. The gasification rig had to be manually operated and monitored at all times and it was considered a potential hazard to leave the rig unattended overnight, given the toxic and highly flammable nature of the product gases.

3.3.2.4 Stability of the catalysts

Rapid deactivation of Ni catalysts due to coke formation is a well-known problem in gasification and hydrocarbon reforming reactions (Baker et al. 1972; Baker et al. 1987; Li et al. 2004; Tanksale et al. 2007; Tanksale et al. 2008). Commercial Ni catalysts used as a primary catalysts in biomass gasification is especially prone to deactivation due to fouling, sintering and coke deposition (Baker et al. 1987; Li et al. 2004; Tanksale et al. 2006). Methods to improve the activity and coke resistance of nickel supported catalysts including doping it with noble metals (Hou et al. 2006; El Doukkali et al. 2012), alkali metals (Shiraga et al. 2007), rare earth metals (El Doukkali et al. 2012) or transition metals (Hou et al. 2006; Shiraga et al. 2007; Omata et al. 2008). In this project, the first strategy of promoting the Ni catalyst with noble metals was adopted. Coke deposition over the spent catalysts used in these investigations were studied by using Transmission Electron Microscopy (TEM) and the resulting images are shown in Figure 3.14. The spent catalyst samples selected for the imaging had char selectivity of 2 – 12%, which is believed to be in the range where the catalysts started to deactivate. Coke deposition of varying degrees was found on all five catalysts. Highest coke deposition was found on monometallic nickel catalyst which explains its rapid deactivation that led to high char selectivity. Modification of Ni catalyst with addition of noble metal reduced the extent of coke deposition to a great extent. Re-Ni and Rh-Ni showed highest coke resistance among the catalysts tested. This result concurs with previous reports where noble metal promoted Ni was used in biofuel steam reforming (Profeti et al. 2009) and partial oxidation of propane (Shiraga et al. 2007). Interestingly, the monometallic catalysts, which showed the highest coke deposition was used for the shortest time in the gasification run (180 min), whereas, Re-Ni and Rh-Ni catalysts which showed negligible coke deposition were used in the gasification run for over (300 min). Therefore, the rate of coke deposition on Ni catalyst was several times higher than the Re and Rh promoted catalysts. Carbon

deposited on the catalysts can be categorised into three types: amorphous, filamentous and graphitic (Asadullah et al. 2004). Amorphous carbon is formed at the lowest temperature range of $T \leq 570^\circ\text{C}$, followed by filamentous carbon at $570^\circ\text{C} < T < 1000^\circ\text{C}$ and finally graphitic carbon at highest temperature range of $\geq 1000^\circ\text{C}$. In our study, only filamentous carbon deposit was found on the spent catalyst. This is because the reaction temperatures used in our experiments ($700 - 775^\circ\text{C}$) were favourable for the formation of filamentous carbon.

Deactivation of catalyst may also be caused by sintering of metal crystallites leading to loss of active metal surface area (Sinfelt 1973; Lv et al. 2004; Sehested et al. 2006; Wei et al. 2007). High temperature and presence of steam, jointly referred to as hydrothermal condition, may lead to sintering of Ni nanoparticles (Grenoble et al. 1981). To test the hydrothermal stability of the catalysts, TEM images of the spent catalysts were taken. The spent catalyst samples selected for the imaging had char selectivity of 2 – 12%. Figure 3.15 shows the fresh (calcined) Re-Ni and Rh-Ni catalysts compared to the spent catalysts, which had been used in gasification run for over 300 min. Although it was difficult to quantify the sintering effect, it can be said qualitatively that the metal particle size of spent catalysts were slightly larger than the fresh catalyst. However the effect of sintering on gasification is unclear because for the duration of the study the catalyst was stable. We could not perform longer gasification runs to determine the maximum duration for which the catalyst can remain active.

In addition to testing the coke deposition and metal sintering during the gasification runs, the stability of alumina support under the hydrothermal condition was also studied. Phase transformation from γ -alumina into δ -alumina or θ -alumina phases may take place at high temperatures leading to loss of support surface area (Moghtaderi 2007; Campoy et al. 2009). Loss of support surface area may lead to lower catalytic activity by increasing the diffusional and film mass transport resistances. Support surface area of fresh (calcined) catalyst was compared against spent catalysts in the gasification runs. Results from the BET measurement of the fresh and spent catalysts are listed in Table 3.4. The results clearly indicate that the surface area of the spent catalyst had reduced, which was an indication of possible phase change.

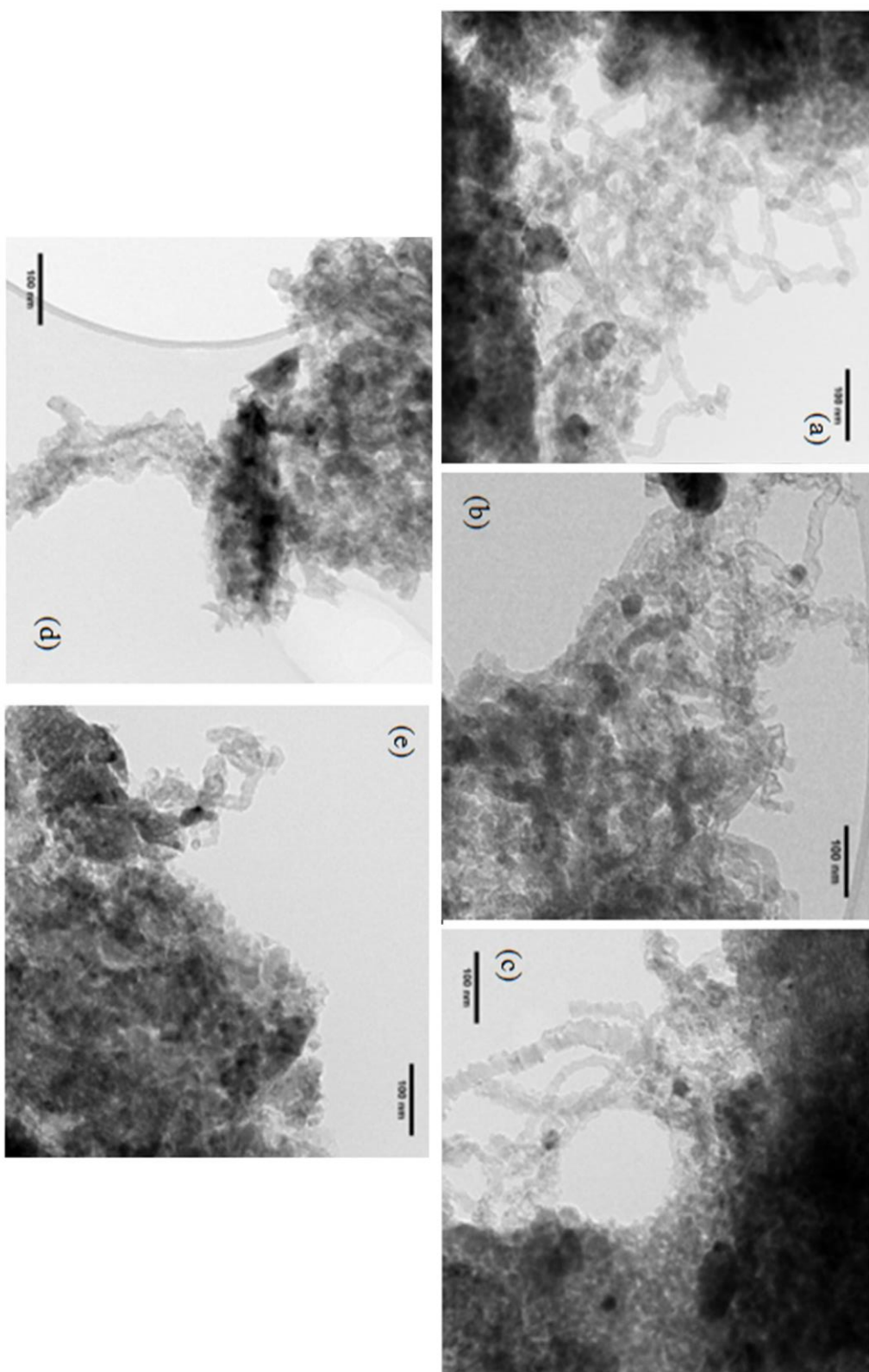


Figure 3. 14- TEM images of spent catalysts (a) Ni, (b) Pt-Ni, (c) Ru-Ni, (d) Rh-Ni and (e) Re-Ni. Spent catalyst samples selected for the imaging had char selectivity of 2 – 12%.

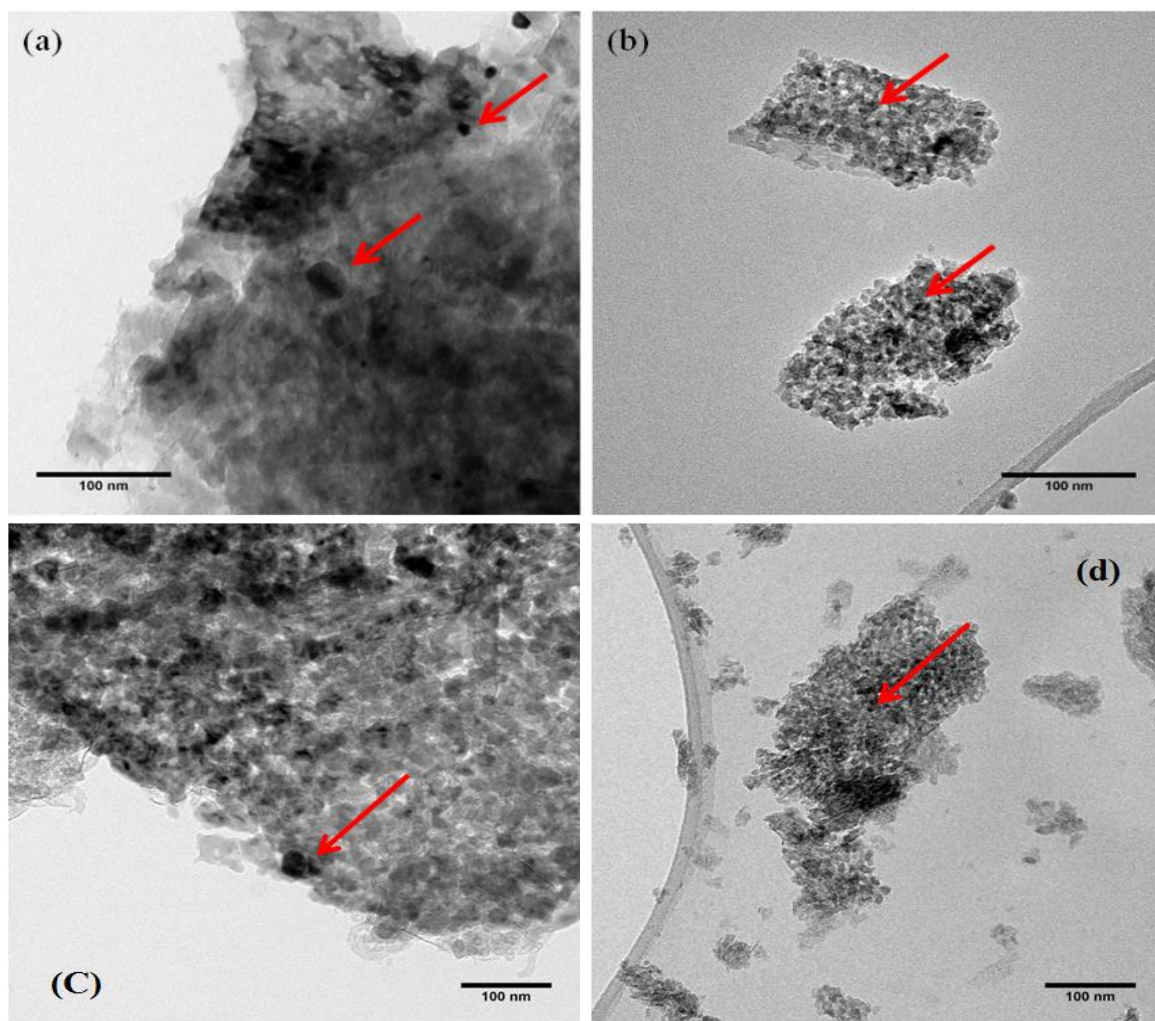


Figure 3. 15- TEM images of Rh-Ni catalyst in its spent (a) and fresh (b) condition, and Re-Ni catalyst in its spent (c) and fresh (d) condition.

Table 3. 4- Comparison of the specific surface area of fresh (calcined) and hydrothermally treated mono-metallic and promoted nickel catalysts supported on γ -alumina.

Catalysts	Fresh Catalyst BET Surface Area, m ² g ⁻¹	Experimental Conditions			Spent Catalyst BET Surface Area, m ² g ⁻¹	Change in BET Surface Area, %
		Temperature, °C	C/O	C/S		
Ni	91.99	750	0.5	1.0	25.42	-72.36
Pt-Ni	77.18	750	0.5	1.0	31.25	-59.51
Ru-Ni	95.74	775	0.5	1.0	34.78	-63.67
Rh-Ni	77.92	750	0.6	1.5	40.64	-47.84
Re-Ni	74.16 ^[a]	750	0.6	1.5	31.83	-57.08
Re-Ni	74.16 ^[a]	750	0.7	1.0	28.56	-61.49

^[a] Re-Ni catalyst was reduced. All other catalysts were calcined only.

TEM images (Figures 3.14 and 3.15) of the spent catalysts also suggest that all five catalysts had gone through some phase transformation. The TEM images of spent catalysts showed that alumina particles had agglomerated, whereas the particles in the fresh catalyst were much smaller in size and had a more porous texture. Phase transformation of γ -alumina to δ -alumina may occur at temperatures as low as 780°C, and may further transform into θ -alumina at around 950°C (Moghtaderi 2007; Campoy et al. 2009). To test the hydrothermal stability of the commercial γ -alumina support used in this study, we heated the alumina samples to 750 and 800°C under air (calcination) and air + steam atmospheres and then analysed their morphology using powder X-ray diffraction. Figure 3.16 shows the resultant XRD curves. Curve (a) corresponds to as received commercial γ -alumina sample. Curves (b) and (c) correspond to the γ -alumina support calcined at 750°C and 800°C, respectively, whereas, curves (d) and (e) correspond to the γ -alumina support treated under air + steam atmosphere at 750°C and 800°C, respectively. XRD curves (a) and (b) are nearly identical, which indicates that calcination at 750°C does not change the alumina phase. However, increasing the temperature and addition of steam has an effect on alumina phase change. The peaks at 21.3° and 23.7°, which corresponds to δ -alumina, increase in intensity from the curve (b) to (e). Increasing the treatment temperature under air from 750°C to 800°C has a small but measurable impact in phase transformation of γ -alumina to δ -alumina. It is, however, under air + steam atmosphere that the phase transform is more pronounced.

Therefore, from Table 3.4 and Figure 3.16, it can be concluded that the alumina support used in this study was not completely stable during the reactive flash volatilisation. Although all the catalysts used in this project were calcined at 600°C in air, except Re-Ni catalyst, the reaction temperatures of 700 - 775°C in presence of steam caused alumina pores to collapse leading to loss

of BET surface area and phase transformation of γ -alumina to δ -alumina. Although the phase transformation of γ -alumina to δ -alumina begins at $\sim 780^\circ\text{C}$, which is higher than all the reactive flash volatilisation experiments, the presence of steam in the reactor lowered the phase transition temperature.

In summary, coke deposition, active metal sintering and alumina phase transformation all contributed, in the descending order, towards deactivation of the catalysts used in this study. Monometallic Ni catalyst was the worst performing catalysts due to high coke deposition and Ni sintering. Addition of small amount of noble metal prevented coke deposition to a great extent and reduced Ni sintering as well. Combining the results presented in catalyst characterisation section and reactive flash volatilization section, it can be said that the noble metal promoted Ni catalysts were effective for reactive flash volatilisation because of their superior metal surface area, higher steam reforming and water gas shift activity and better coke resistance. In particular, Re-Ni, Rh-Ni and Ru-Ni, in that order, provided much improved performance over monometallic Ni catalyst.

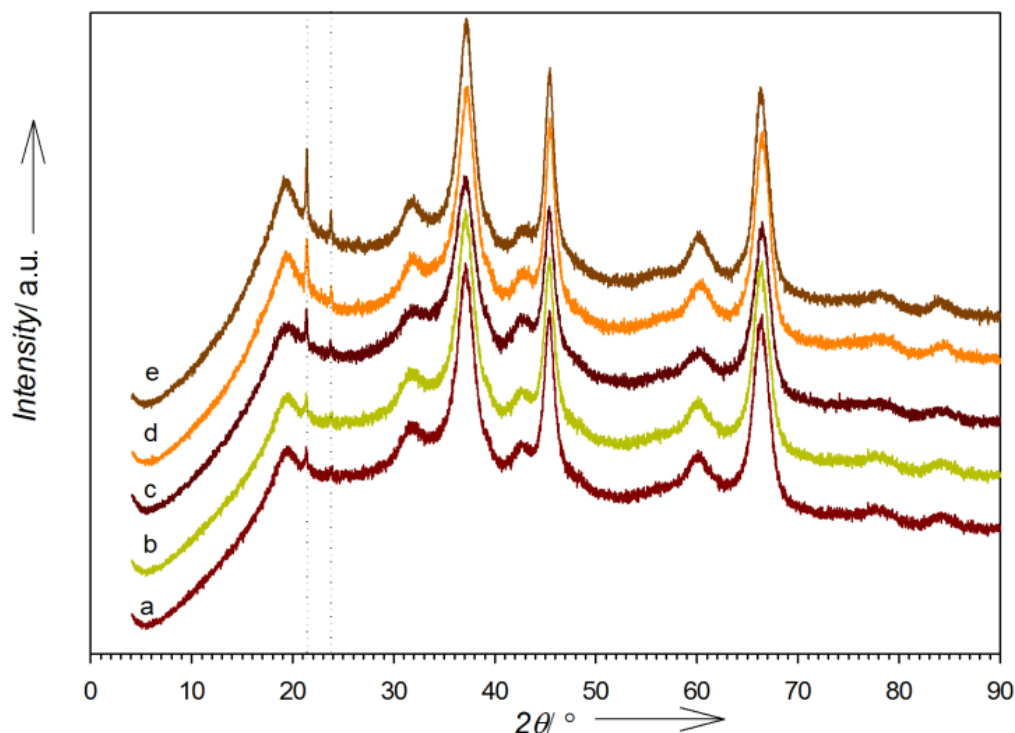


Figure 3. 16- Powder X-ray diffraction curves of γ -alumina support: (a) as received; calcined at (b) 750°C ; (c) 800°C ; and treated in air + steam atmosphere at (d) 750°C , and (e) 800°C

3.4 Conclusions

Various reaction conditions were tested for reactive flash volatilisation, including the effects of temperature, C/O feed ratio, C/S feed ratio, and catalyst promoter. It was found that the highest gasification efficiency was achieved at 750°C, using C/O = 0.6 and C/S = 1.0. It was also observed that Re, Rh and Ru promoted Ni catalysts performed the best in that order. This conclusion is based on the catalysts properties, gasification efficiency and catalyst stability. Monometallic Ni was found to be active for the reactive flash volatilization; however, the catalyst suffered rapid deactivation due to coke deposition, metal active site sintering, and alumina support pore collapse due to phase change. Coke deposition and sintering were reduced significantly by using noble metal promoters. The noble metal promoters increased the activity of Ni catalysts by increasing the metal surface area, reducibility and reducing the CO desorption temperature. The noble metal promoters also increased coke resistance, and reduced sintering. Therefore, the promoted Ni catalysts were active for longer duration with little to no deactivation.

3.5 Acknowledgements

The authors are grateful for the financial support from the Rural Industries Research and Development Corporation (RIRDC) project grant PRJ-004758 and the Department of Chemical Engineering, Monash University.

3.6 References

- Asadullah, M., T. Miyazawa, et al. (2004). "A comparison of Rh/CeO₂/SiO₂ catalysts with steam reforming catalysts, dolomite and inert materials as bed materials in low throughput fluidized bed gasification systems." *Biomass and Bioenergy* **26**: 269-279.
- Baker, E. G., L. K. Mudge, et al. (1987). "Steam gasification of biomass with nickel secondary catalysts." *Industrial & Engineering Chemistry Research* **26**: 1335-1339.
- Baker, R. T. K., M. A. Barber, et al. (1972). "Nucleation and growth of carbon deposits from the nickel catalyzed decomposition of acetylene." *Journal of Catalysis* **26**: 51-62.
- Campoy, M., A. Gómez-Barea, et al. (2009). "Air–steam gasification of biomass in a fluidised bed: Process optimisation by enriched air." *Fuel Processing Technology* **90**: 677-685.
- Colby, J. L., P. J. Dauenhauer, et al. (2008). "Millisecond autothermal steam reforming of cellulose for synthetic biofuels by reactive flash volatilization." *Green Chemistry* **10**: 773-783.
- Dauenhauer, P. J., J. Colby, et al. (2007). *Reactive flash volatilization of nonvolatile carbohydrates for synthesis gas*, Salt Lake City, UT.
- Devi, L., K. J. Ptasinski, et al. (2003). "A review of the primary measures for tar elimination in biomass gasification processes." *Biomass Bioenergy* **24**: 125-140.

Chapter 3

El Doukkali, M., A. Iriondo, et al. (2012). "A comparison of sol-gel and impregnated Pt or/and Ni based γ -alumina catalysts for bioglycerol aqueous phase reforming." Applied Catalysis B: Environmental **125**: 516-529.

Farrauto, R. J. and C. Bartholomew (1997). Introduction to Industrial Catalytic Processes. London, Chapman and Hall.

Grenoble, D. C., M. M. Estadt, et al. (1981). "The Chemistry and Catalysis of the Water Gas Shift Reaction: 1. The Kinetics over Supported Metal Catalysts." J. Catal. **67**: 90-102.

Haryanto, A., S. D. Fernando, et al. (2009). "Upgrading of syngas derived from biomass gasification: A thermodynamic analysis." Biomass and Bioenergy **33**: 882-889.

Hayward, D. O. and B. M. W. Trapnell (1964). Chemisorption. London, Butterworths.

Hernández, J. J., G. Aranda-Almansa, et al. (2010). "Gasification of biomass wastes in an entrained flow gasifier: Effect of the particle size and the residence time." Fuel Processing Technology **91**: 681-692.

Hou, Z., P. Chen, et al. (2006). "Production of synthesis gas via methane reforming with CO₂ on noble metals and small amount of noble-(Rh-) promoted Ni catalysts." International journal of hydrogen energy **31**: 555-561.

Huber, G. W., S. Iborra, et al. (2006). "Synthesis of Transportation Fuels from Biomass: Chemistry, Catalysts, and Engineering." Chem. Rev. (Washington, DC, U. S.) **106**: 4044-4098.

Jackson, S. D., B. M. Glanville, et al. (1993). "Supported Metal-Catalysts - Preparation, Characterization, and Function .2. Carbon-Monoxide and Dioxygen Adsorption on Platinum Catalysts." Journal of Catalysis **139**: 207-220.

Kumar, A., K. Eskridge, et al. (2009). "Steam-air fluidized bed gasification of distillers grains: Effects of steam to biomass ratio, equivalence ratio and gasification temperature." Bioresource Technology **100**: 2062-2068.

Kumar, A., D. D. Jones, et al. (2009). "Thermochemical biomass gasification: a review of the current status of the technology." Energies (Basel, Switz.) **2**: 556-581.

Leung, D. Y. C., X. L. Yin, et al. (2004). "A review on the development and commercialization of biomass gasification technologies in China." Renewable and Sustainable Energy Reviews **8**: 565-580.

Li, X. T., J. R. Grace, et al. (2004). "Biomass gasification in a circulating fluidized bed." Biomass Bioenergy **26**: 171-193.

Lv, P. M., Z. H. Xiong, et al. (2004). "An experimental study on biomass air-steam gasification in a fluidized bed." Bioresource Technology **95**: 95-101.

Moghtaderi, B. (2007). "Effects of controlling parameters on production of hydrogen by catalytic steam gasification of biomass at low temperatures." Fuel **86**: 2422-2430.

Ni, M., D. Y. C. Leung, et al. (2006). "An overview of hydrogen production from biomass." Fuel Processing Technology **87**: 461-472.

- Omata, K., Y. Endo, et al. (2008). "Effective additives of Ni/ α -Al₂O₃ catalyst at low methane conversion of oxidative reforming for syngas formation." Applied Catalysis A: General **351**: 54-58.
- Profeti, L. P. R., E. A. Ticianelli, et al. (2009). "Production of hydrogen via steam reforming of biofuels on Ni/CeO₂-Al₂O₃ catalysts promoted by noble metals." International journal of hydrogen energy **34**: 5049-5060.
- Qin, K., P. A. Jensen, et al. (2012). "Biomass Gasification Behavior in an Entrained Flow Reactor: Gas Product Distribution and Soot Formation." Energy & Fuels **26**: 5992-6002.
- Rapagnà, S., N. Jand, et al. (2000). "Steam-gasification of biomass in a fluidised-bed of olivine particles." Biomass and Bioenergy **19**: 187-197.
- Rostrup-Nielsen, J. R. (1975). Steam Reforming Catalysts: An Investigation of Catalysts for Tubular Steam Reforming of Hydrocarbons. Copenhagen, Taknisk Forlag.
- Rynkowski, J. M., T. Paryjczak, et al. (1993). "On the nature of oxidic nickel phases in NiO/ γ -Al₂O₃ catalysts." Applied Catalysis A: General **106**: 73-82.
- Salge, J. R., B. J. Dreyer, et al. (2006). "Renewable hydrogen from nonvolatile fuels by reactive flash volatilization." Science **314**: 801-804.
- Sehested, J., J. A. P. Gelten, et al. (2006). "Sintering of nickel catalysts: Effects of time, atmosphere, temperature, nickel-carrier interactions, and dopants." Applied Catalysis A: General **309**: 237-246.
- Shastri, Y. N., L. F. Rodriguez, et al. (2012). "Impact of distributed storage and pre-processing on Miscanthus production and provision systems." Biofuels, Bioproducts and Biorefining **6**: 21-31.
- Shiraga, M., D. Li, et al. (2007). "Partial oxidation of propane to synthesis gas over noble metals-promoted Ni/Mg(Al)O catalysts—High activity of Ru–Ni/Mg(Al)O catalyst." Applied Catalysis A: General **318**: 143-154.
- Shrotri, A., L. K. Lambert, et al. (2013). "Mechanical depolymerisation of acidulated cellulose: Understanding the solubility of high molecular weight oligomers." Green Chemistry **15**: 2761-2768.
- Sinfelt, J. H. (1973). Specificity in Catalytic Hydrogenolysis by Metals. **23**: 91-119.
- Sutton, D., B. Kelleher, et al. (2001). "Review of literature on catalysts for biomass gasification." Fuel Process. Technol. **73**: 155-173.
- Tanksale, A., J. N. Beltramini, et al. (2008). "Effect of Pt and Pd promoter on Ni supported catalysts-A TPR/TPO/TPD and microcalorimetry study." Journal of Catalysis **258**: 366-377.
- Tanksale, A., J. N. Beltramini, et al. (2010). "A review of catalytic hydrogen production processes from biomass." Renewable and Sustainable Energy Reviews **14**: 166-182.
- Tanksale, A., J. N. Beltramini, et al. (2006). "Reaction mechanisms for renewable hydrogen from liquid phase reforming of sugar compounds." Developments in Chemical Engineering and Mineral Processing **14**: 9-18.

Chapter 3

Tanksale, A., Y. Wong, et al. (2007). "Hydrogen generation from liquid phase catalytic reforming of sugar solutions using metal-supported catalysts." International journal of hydrogen energy **32**: 717-724.

Tanksale, A., C. H. Zhou, et al. (2009). "Hydrogen production by aqueous phase reforming of sorbitol using bimetallic Ni-Pt catalysts: Metal support interaction." Journal of Inclusion Phenomena and Macrocyclic Chemistry **65**: 83-88.

Tomishige, K., M. Asadullah, et al. (2004). "Syngas production by biomass gasification using Rh/CeO₂/SiO₂ catalysts and fluidized bed reactor." Catalysis Today **89**: 389-403.

Wang, S. (1998). "CO₂ reforming of methane on Ni catalysts: Effects of the support phase and preparation technique." Applied catalysis. B. Environmental **16**: 269-277.

Wang, Y. and C. M. Kinoshita (1993). "Kinetic model of biomass gasification." Solar Energy **51**: 19-25.

Wei, L., S. Xu, et al. (2007). "Steam gasification of biomass for hydrogen-rich gas in a free-fall reactor." International journal of hydrogen energy **32**: 24-31.

Monash University

Declaration for Thesis Chapter 4

Declaration by candidate

In the case of Chapter 4, the nature and extent of my contribution to the work was the following:

Nature of contribution	Extent of contribution (%)
Initiation, key ideas, experimental and analysis works, development and writing up of the paper.	80

The following co-authors contributed to the work. If co-authors are students at Monash University, the extent of their contribution in percentage terms must be stated:

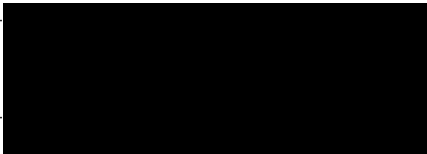
Name	Nature of contribution	Extent of contribution (%) for student co-authors only
Akshat Tanksale	Initiation, key ideas, reviewing and editing of the paper.	
Kentaro Umeki	Key ideas, reviewing and editing of the paper.	

The undersigned hereby certify that the above declaration correctly reflects the nature and extent of the candidate's and co-authors' contributions to this work*.

Candidate's
Signature

	Date 15/05/2015
---	--------------------

Main
Supervisor's
Signature

	Date 15/05/2015
---	--------------------

This page intentionally left blank.

Chapter 4: Kinetic Study of Catalytic Steam Gasification of Biomass by Reactive Flash Volatilisation

Abstract

Reactive flash volatilisation (RFV) is an autothermal process to convert biomass into tar free syngas under steam rich condition. This chapter studies the kinetics of RFV using Ni, Pt-Ni, Ru-Ni, Re-Ni and Rh-Ni catalysts supported on alumina. Rates of mass loss of cellulose, xylan and lignin were measured and compared with synthetic biomass mixture and pinewood sawdust. Kinetic parameters were calculated with and without catalysts using a wire-mesh isothermal thermogravimetric analyzer under equimolar steam/N₂ atmosphere and high heating rates of 8.6×10^3 , 1.1×10^5 , and 1.3×10^4 °C/min at 700, 750 and 800°C, respectively. The results showed three distinct regimes of rate of mass loss: pyrolytic decomposition, reforming and char gasification. Catalysts improved the rate of mass loss in the reforming regime. Rh-Ni and Ru-Ni supported catalysts showed higher reforming rates than other catalysts. This study provides direct evidence of in-situ catalytic tar removal during gasification of biomass.

This page intentionally left blank.

4.1 Introduction

Utilization of lignocellulose for transportation fuels and stationary power production is recognized as one of the most promising solutions for the energy crisis and environmental problems (Kumar et al. 2009). Lignocellulose conversion into biofuels generally follows a two-step process in which dried and milled lignocellulose is first converted into an intermediate product like synthesis gas (via gasification), bio-oils (via fast pyrolysis) or aqueous sugars (via hydrolysis) followed by conversion of intermediates into biofuels (Tanksale et al. 2010). Among the lignocellulosic biomass conversion technologies, synthesis gas produced via gasification is among the most interesting, both industrially and academically, due to its high conversion efficiency (Devi et al. 2003). Biomass gasification can be achieved at temperatures in excess of 700°C in the presence of oxygen or air, with or without additional steam. However, at this temperature significant amount of condensable oxygenated hydrocarbons, commonly referred to as tar is produced. In conventional gasifiers, tar free gasification requires higher temperatures ($\geq 1000^\circ\text{C}$) (Hernández et al. 2010; Qin et al. 2012). Schmidt group developed a catalytic steam gasification process called as Reactive Flash Volatilisation (RFV) which is an one-step autothermal process of converting non-volatile oxygenated hydrocarbons into tar free synthesis gas using a down-draft fixed bed catalytic reactor operating at $\sim 900^\circ\text{C}$ (Salge et al. 2006). This is a complex reaction process in which pyrolysis, oxidation, partial oxidation, reduction, steam reforming and water gas shift reactions takes place in the catalyst bed (Sutton et al. 2001; Colby et al. 2008). Previous chapter has demonstrated that synthesis gas can be produced from cellulose in a RFV reactor over promoted nickel catalysts at 700 – 775°C in 50 ms residence time with negligible amount of char or tar produced (Chan et al. 2014). It has been proposed that the biomass feedstock initially goes through pyrolytic decomposition and the resulting bio-oils go through reforming reactions in the catalyst bed to produce synthesis gas (Colby et al. 2008).

However, chemistry of RFV of cellulose and lignocellulose is complex and yet to be fully understood. There is also a lack of kinetic data of catalytic gasification under steam rich conditions and high heat fluxes. Previous studies have investigated lignocellulose fast pyrolysis, which is only the first step of the RFV (Milosavljevic et al. 1995). Majority of the previous reports on lignocellulose fast pyrolysis were conducted with low heating rate, typically from 1 – 100°C/min (Antal et al. 1995; Milosavljevic et al. 1995; Caballero et al. 1997; Várhegyi et al. 1997; Orfão et al. 1999; Yang et al. 2007; Biagini et al. 2009; Shen et al. 2009). A comprehensive review by Antal et al. summarized that there are two major pathways during cellulose fast pyrolysis: one leads to the selective formation of glycoaldehyde and the other leads to the formation of levoglucosan and higher heating rates favor glycoaldehyde forming pathway, which

has a lower boiling point than levoglucosan (Antal et al. 1995). This results in higher volatiles fraction compared to the lower heating rates (Shuangning et al. 2006). It is also known from literature that higher heating rate lead to lower activation energy (Milosavljevic et al. 1995).

Therefore, to understand the kinetics of RFV of lignocellulose, there is a need to conduct a study at significantly higher heating rates than fast pyrolysis conditions. Various models have been proposed to analyze pyrolysis, reforming and gasification kinetics (Koufopoulos et al. 1989; Várhegyi et al. 1997; Orfão et al. 1999; Fisher et al. 2002). The reported activation energies and pre-exponential factors from these studies vary widely from 40 to 250 kJ/mol and 10^4 to 10^{20} s⁻¹, respectively (Koufopoulos et al. 1989). However, due to the substantial differences in the experimental methods, operating conditions, chemical composition of raw materials and the models used, these kinetics data are only consistent within a particular study but cannot be compared against one another. Nevertheless, what is acceptable is that the irreversible mass loss of biomass or its derivatives in pyrolysis and gasification are mainly governed by first order or pseudo first order models (Lee et al. 2002; Lin et al. 2009). As a result, in this work, a pseudo first order reaction model is proposed to model RFV of cellulose and pinewood sawdust as it is considered as the most realistic approach in the case of irreversible mass loss of lignocellulosic materials (Antal et al. 1995; Vamvuka et al. 2003). This chapter shows the effects of gasifying agents, feedstock, and catalysts on the apparent reaction rate constant, activation energy and pre-exponential factor.

4.2 Experimental Section

4.2.1 Materials

Biomass Feedstocks: High purity microcrystalline cellulose (200 – 350 µm from Vivapur®) was used as cellulose feedstock. Xylan (Meyer ltd.) was used as hemicellulose model compound and lignin, alkali (Sigma-Aldrich) was used as lignin model compound. Pinewood Sawdust (63 – 112 µm and 250 – 300 µm from Stenvalls Trä AB) was used as real biomass feedstock.

Catalyst: Five nickel based catalysts: Ni, Pt-Ni, Ru-Ni, Rh-Ni and Re-Ni supported on alumina were developed using impregnation method. The synthesized monometallic Ni catalyst had a nickel content of 11wt% and all bimetallic catalysts had nickel content of 10 wt% and metal promoter content of 1 wt%. Detailed synthesis procedures and characterization of the catalysts can be found in 3.2.1 and 3.3.1 (Chan et al. 2014).

4.2.2 Experimental Methods

Isothermal Thermogravimetric Analysis: A custom built wire-mesh isothermal thermogravimetric analyzer, illustrated in a schematic diagram (Figure 4.1), was used in this study. A vertical tubular reactor was housed in an electric furnace with a PID controller. A molybdenum or stainless steel wire mesh basket was used as a sample holder inside the reactor. Sample holder was connected to a precision scale with a stainless steel wire. Dead weight was added between the sample holder and the balance to increase stability of the sample holder. Four mass flow controllers (H₂, N₂, CO, CO₂) and a syringe pump were used to create desired gasification atmosphere in the reactor. The scale used in this study had precision measurement of ± 1 mg.

Before taking measurements, the furnace was preheated under N₂ flow to the desired experiment temperature. Once the temperature was reached, gasifying agents such as CO₂ and steam were introduced into the reaction vessel through a bottom distribution plate. The experiments were performed at 700, 750 and 800°C under either 6 L/min N₂ or 6 L/min CO₂ or 6 L/min (volume at STP) of equimolar mixture of N₂ and steam. The heating rates were calculated using theoretical energy balances and estimated to be 8.6×10^3 °C/min, 1.1×10^5 °C/min, and 1.3×10^4 °C/min at 700, 750 and 800°C, respectively. (See Appendix A for calculation)

Experiments were started by lowering the sample holder containing 100 – 200 mg of biomass sample, with or without 10 – 20 mg of catalyst, into the pre-heated reactor. The biomass to catalyst mass ratio was maintained at 10:1. Mass loss of the biomass sample was recorded every 2 seconds continuously. Each experiment was repeated 3 – 5 times to minimize random handling errors.

Effluent Gas Analysis: To analyze the effect of catalysts on the composition of the effluent gas from reactive flash volatilization of biomass, 200 mg of biomass and 100 mg of catalyst was used in the procedure described in Isothermal Thermogravimetric Analysis section and the effluent gas was analyzed using a micro-GC (Agilent Micro-GC 490). High catalyst amount used in this part was to ensure sufficient contact between catalyst and feedstock during the reaction. The effluent gases were collected in three 3.8 L gas sampling bags before analysing with the micro-GC.

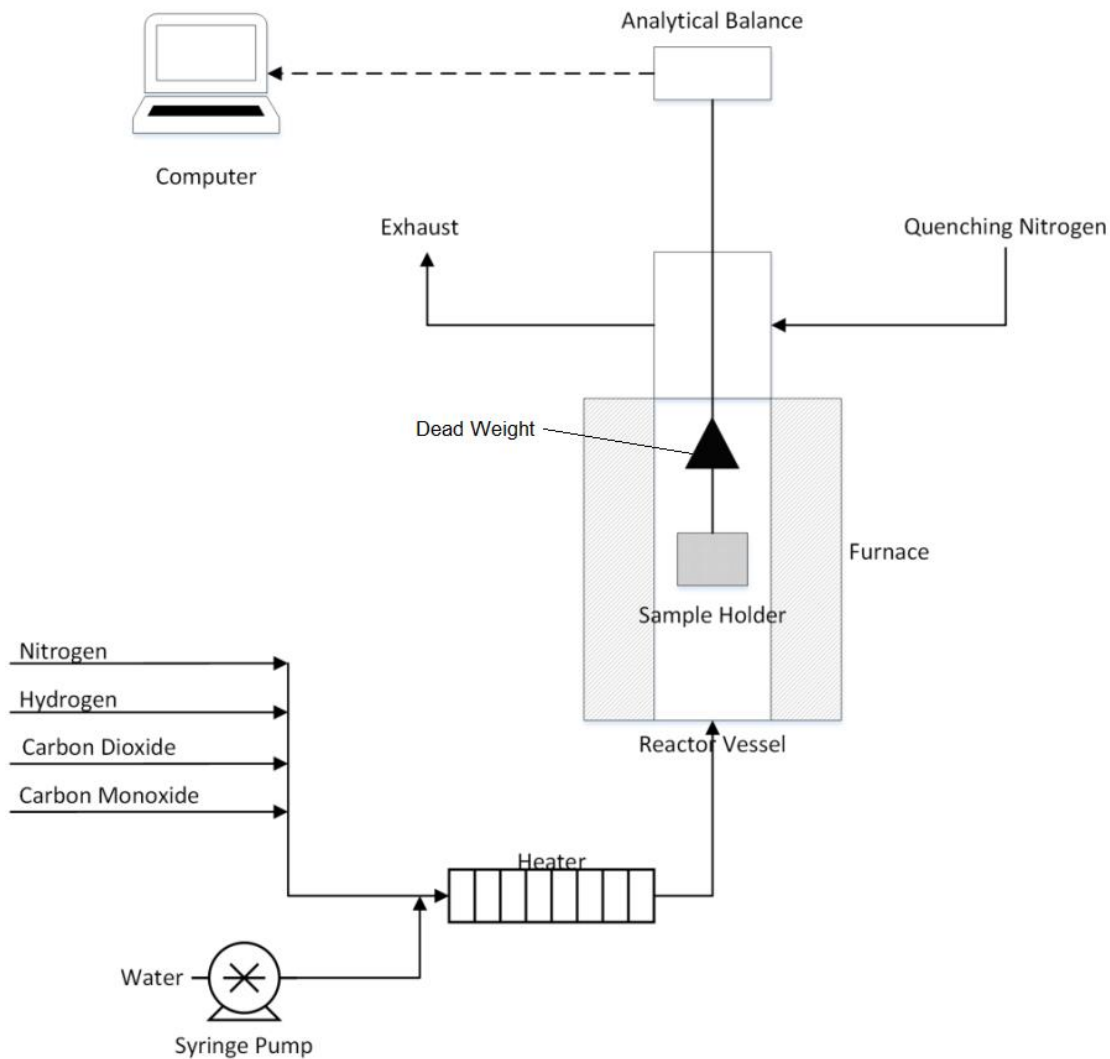


Figure 4. 1- Schematic diagram of custom built wire-mesh isothermal thermogravimetric reactor. In each experiment the furnace was preheated to the desired temperature under constant N₂ flow following by switching to gasification agent and then lowering the sample into the reactor.

4.2.3 Pseudo First Order Kinetic Model

A simplified pseudo first order kinetic model of biomass devolatilisation was adopted to model the conversion process from solid raw feedstock to volatiles and char. By assuming the biomass flash volatilisation as a first order reaction, governing equations of biomass volatilisation can be expressed with the equation below

First order rate equation

$$r = -\frac{d[Biomass]}{dt} = k [Biomass] \quad (4.1)$$

Here biomass concentration at time t can be expressed in terms of residual mass fraction. Residual mass fraction is defined as –

$$\begin{aligned} [Biomass] &= \text{Residual Mass Fraction} \\ &= \frac{\text{mass of biomass at time } t}{\text{mass of biomass at time } t = 0} \end{aligned}$$

Therefore, it follows that fractional conversion $X = 1 - [Biomass]$ or, $X = \frac{m_0 - m}{m_0}$, where m_0 is the initial sample weight and m is the sample weight at time t .

By integrating equation (4.1) and writing in terms of fractional conversion, first order equation for biomass RFV may be written as –

$$\ln[1 - X] = -kt \quad (4.2)$$

Apparent rate constant k at each reaction temperature (700, 750 and 800°C) was determined by plotting $\ln[1 - X]$ against t , and graphically estimating the slope of the line. Once the k was known, the apparent pre-exponential factor and apparent activation energy was also calculated graphically by plotting $\ln k$ against $1/T$ according to the Arrhenius equation –

$$\ln(k) = -\left(\frac{E_{a\text{-apparent}}}{R} \frac{1}{T}\right) + \ln(A_{\text{apparent}}) \quad (4.3)$$

where k is the apparent rate constant of volatilisation (s^{-1}), $E_{a\text{-apparent}}$ is apparent activation energy ($\text{kJ}\cdot\text{mol}^{-1}$), R is the universal gas constant ($8.314 \text{ kJ}\cdot\text{mol}^{-1}\cdot\text{K}^{-1}$), T is the absolute temperature (K) and A_{apparent} is the apparent pre-exponential factor (s^{-1}).

4.3 Results and Discussion

4.3.1 Effect of Gasification Agent on Cellulose Volatilisation Kinetics without a Catalyst

Figure 4.2 (a), (b) and (c) show percentage mass loss of cellulose under N₂, CO₂ and 50 mol% steam/N₂ conditions, respectively, against time *t* at 750°C. Figure 4.2 (d) shows the plot of equation (4.2) for the three gasifying agents. Three kinetic rate regimes were observed which can be broadly classified as (I) pyrolytic decomposition, (II) reforming and (III) char gasification (Dupont et al. 2009). In the pyrolytic decomposition regime, which is dominated by thermal decomposition, the rate constant *k* was between 0.03 – 0.08 s⁻¹ (Table 4.1). In the reforming regime, which is dominated by secondary thermal decomposition and reforming of volatile intermediates by CO₂ and steam, the rate constant *k* increased to 0.12 – 0.15 s⁻¹. In the char gasification regime, which is characterized by slow gasification of char, the rate constant *k* was negligible in comparison and hence not determined. All the cellulose samples showed pyrolysable fraction (volatiles) of ~95 wt% of the initial mass, which is in good agreement with the values reported in literature (Ranzi et al. 2008). Overall the rate of reactive flash volatilisation under N₂ and CO₂ atmospheres was found to be comparable. As shown in Figure 4.2 (a) and (b), the devolatilization of cellulose was completed in 26 s. However, the rate of volatilisation was significantly slower under steam/N₂ atmosphere. As shown in Figure 4.2 (c), the devolatilization of cellulose was completed in 38 s, which may be explained by the hydrogen inhibition effect occurred during steam gasification (Yang et al. 1985; Hüttinger et al. 1992; Lussier et al. 1998). In the absence of air or oxygen, the third regime (char gasification) is kinetically limited; therefore, gasification of char at 750°C was completed only after approximately 200 s.

Table 4. 1- Comparison of the pyrolytic decomposition rate constant and reforming rate constant in flash volatilisation of cellulose with various gasifying agents at 750°C.

Gasifying Agent	Pyrolytic Decomposition Rate, s ⁻¹	Reforming Rate, s ⁻¹
	<i>k</i> · 10 ²	<i>k</i> · 10 ²
Nitrogen	7.66	12.7
Carbon Dioxide	6.25	14.5
50/50 Nitrogen/Steam	3.90	13.1

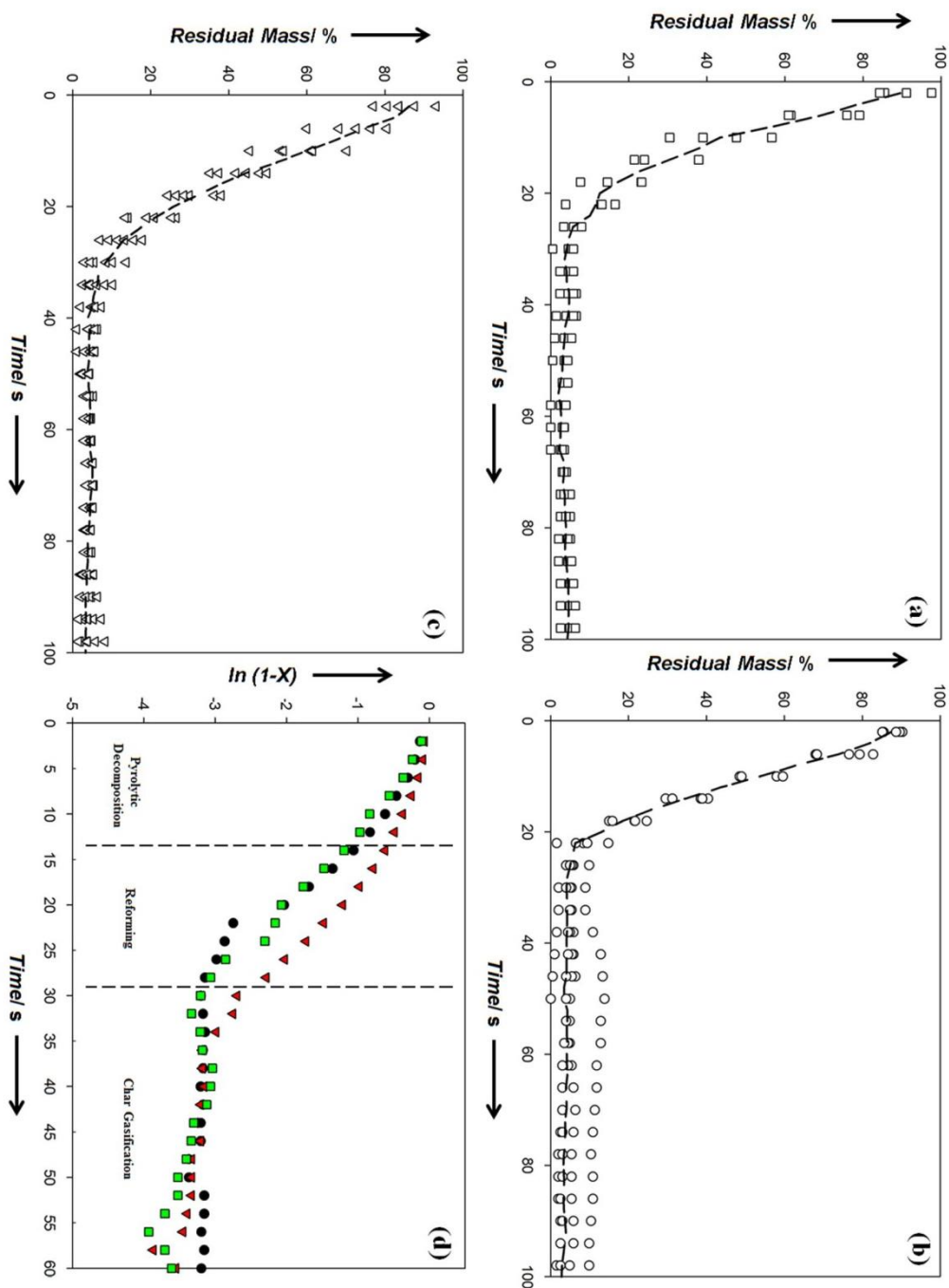


Figure 4. 2- Effect of gasifying agent on the pyrolysis and gasification of cellulose: (a) Pyrolysis under pure N_2 flow; (b) Gasification under pure CO_2 ; (c) Gasification under 50 mole% steam in N_2 ; and (d) Comparison of pseudo first order kinetics under different atmospheres ((\square) N_2 , (\bullet) CO_2 , and (\blacktriangledown) 50/50 N_2 /steam). For graphs (a) to (c) the bullet points are experiment data from several repeat runs and the broken line is the fitted curve. For graph (d) the bullet points are fitted data of several repeat runs. All the experiments were carried out at isothermal reactor temperature of 750°C.

4.3.2 Effect of Biomass Feedstock on Volatilisation Kinetics without a Catalyst

The kinetic rates of RFV were studied by using cellulose, hemicellulose (xylan), lignin, synthetic mixed biomass (45 wt% cellulose, 30 wt% xylan, 25wt% lignin), and pinewood sawdust as feedstock. Chemical composition of pinewood sawdust varies greatly from its species, growth environment and the section of the wood. The composition of cellulose, hemicellulose and lignin in pinewood may range from 37 – 50 wt%, 17 – 38 wt%, 12 – 32 wt%, respectively (Kurjatko et al. 2006; Salge et al. 2006; Liu et al. 2008; Naik et al. 2010). Therefore, the synthetic mixed biomass used in this investigation represented average composition of the constituents of biomass as recommended by Thomas (Thomas 1977). The advantage of testing synthetic mixed biomass was that these components contained negligible inorganic content. Inherent inorganic contents in biomass, such as alkaline earth metals, may act as catalysts during the reactive flash volatilization (Lv et al. 2010). A comparison between synthetic mixed biomass and real biomass may provide insight into the catalytic effects of these inorganic contents.

Steam rich gasifying agent was used in these experiments which was similar to the conditions used in previous chapter (Chan et al. 2014). It is evident from Figure 4.3 that different components of lignocellulosic biomass have different fractional conversion and reaction rates. The apparent rate constants (k), apparent pre-exponential factors ($A_{apparent}$) and apparent activation energies ($E_{a-apparent}$) of different feedstock in the pyrolysis regime and the reforming regime were calculated separately, and are presented in Tables 4.2 and 4.3, respectively. In comparison to cellulose, xylan and lignin showed considerably higher rate of volatilisation in pyrolytic decomposition regime. This is due to the lower pyrolysis onset temperatures of xylan and lignin because of their amorphous structure, which leads to shorter volatilisation time as illustrated in Figure 4.3 (Yang et al. 2007). Xylan, which had the lowest activation energy values in our study, is thermally the least stable component among the three lignocellulose components (Burhenne et al. 2013). Moreover, pyrolysis of cellulose is endothermic, whereas, pyrolysis of xylan and lignin is exothermic, which may be another reason why the rates of pyrolysis of xylan and lignin were faster than cellulose at the temperatures studied in this work (Yang et al. 2007).

Major products of pyrolytic decomposition of cellulose are levoglucosan and glycolaldehyde, which showed higher rate of reaction in the reforming regime than the products of pyrolytic decomposition of xylan and lignin which typically yields acids, furans, polycyclic aromatic hydrocarbons and phenolic compounds (Qu et al. 2011). Moreover, cellulose showed higher fraction of pyrolytic volatiles (95 wt%) than both xylan and lignin (85 wt% and 60 wt% respectively).

As seen in Figure 4.3 (c), the rate of reaction was lowest in the char gasification regime (rate constants not calculated). Complete gasification of xylan and lignin char at 750°C was observed after approximately 200 s and 460 s respectively.

Figure 4.4 (a) shows the mass loss of mixed synthetic biomass at 750°C. The pyrolytic decomposition and steam reforming regimes were found to be approximately 8 s each, and the pyrolytic volatiles fraction of mixed synthetic biomass was found to be 85 wt%. Complete char gasification was attained only after approximately 250 s. The fraction of char observed in the mixed synthetic biomass was consistent with the weighted average fraction of char from cellulose, xylan and lignin combined. In the pyrolytic decomposition regime, the reaction rate of synthetic biomass was consistent with xylan and lignin pyrolysis rates, within the range of error in our measurement. In the reforming regime, the reaction rate of synthetic biomass was lower than cellulose and xylan but higher than lignin. Lignin devolatilisation takes place over a wide range of temperature, therefore the volatile intermediates generated from cellulose and hemicellulose pyrolysis may get re-adsorbed rapidly on lignin and char, resulting in further inhibition of lignin and char decomposition, therefore resulting in the slower rate of reaction in the reforming regime (Mullen et al. 2008; Tanksale et al. 2010).

The rates of pyrolytic decomposition and steam reforming regimes of pinewood sawdust were both observed to be higher than the synthetic mixed biomass (Tables 4.2 and 4.3). The rates increased by 27% and 59% (at 750°C), respectively, which may be attributed to the catalytic effect of the inherent inorganic contents found in pinewood (Lv et al. 2010). However, fraction of pyrolytic volatiles was consistent with synthetic mixed biomass. The rate of pyrolytic decomposition was higher for particle size range of 63 – 112 µm, compared to the larger particle size range of 250 – 300 µm. This suggests that as the particle size increases, this reaction moves away from kinetic control towards heat transfer control (Hernández et al. 2010).

In summary, result of this study reveals that pyrolytic decomposition of cellulose is the rate limiting step in the conversion of lignocellulose into synthesis gas via RFV. This is believed to be due to the highly ordered crystalline structure of cellulose. The intermediates (bio-oils) produced in the pyrolytic decomposition step goes through gas phase reactions such as steam reforming and water gas shift, which has been called as reforming regime in this chapter. In this regime, the rate of reforming of intermediates produced from lignin decomposition is the limiting step. The rates and apparent activation energies of synthetic biomass and pinewood sawdust were found to be comparable in both the regimes.

Table 4. 2- Comparison of the pyrolytic decomposition regime rate constant (k), apparent pre-exponential factor (A_{apparent}) and apparent activation energy ($E_{a-\text{apparent}}$) in reactive flash volatilisation of various biomass feedstock.

Feedstock	Pyrolytic Decomposition				Apparent Pre-exponential Factor A_{apparent} (s^{-1})	Apparent Activation Energy $E_{a-\text{apparent}}$ ($kJ\ mol^{-1}$)
	Rate, (s^{-1}) $k \cdot 10^2$					
	700°C	750°C	800°C			
Cellulose	3.03	3.90	4.92	5.49	42.1	
Xylan	6.38	6.41	8.28	0.96	22.3	
Lignin	4.99	8.57	8.63	21.1	48.3	
Synthetic Biomass ^[a]	6.44	8.96	9.74	5.89	36.2	
Pinewood Sawdust (63-112 μm)	-	13.8	-	-	-	
Pinewood Sawdust (250-300 μm)	8.48	10.6	13.5	12.1	40.2	

^[a] 45wt% cellulose, 30wt% xylan and 25wt% lignin

Table 4. 3- Comparison of the reforming regime rate constant (k), apparent pre-exponential factor ($A_{apparent}$) and apparent activation energy ($E_{a-apparent}$) in reactive flash volatilisation of various biomass feedstock.

Feedstock	Steam Reforming				
	Rate, (s ⁻¹) $k \cdot 10^2$			Apparent Pre-exponential Factor $A_{apparent}$ (s ⁻¹)	Apparent Activation Energy $E_{a-apparent}$ (kJ mol ⁻¹)
	700°C	750°C	800°C		
Cellulose	9.81	13.1	18.6	93.3	55.6
Xylan	9.88	11.9	13.1	2.01	24.3
Lignin	5.33	5.68	8.47	6.82	39.7
Synthetic Biomass ^[a]	8.62	10.9	12.6	5.07	32.9
Pinewood Sawdust (63-112 µm)	-	10.1	-	-	-
Pinewood Sawdust (250-300 µm)	14.4	16.6	21.2	9.03	33.6

^[a] 45wt% cellulose, 30wt% xylan and 25wt% lignin

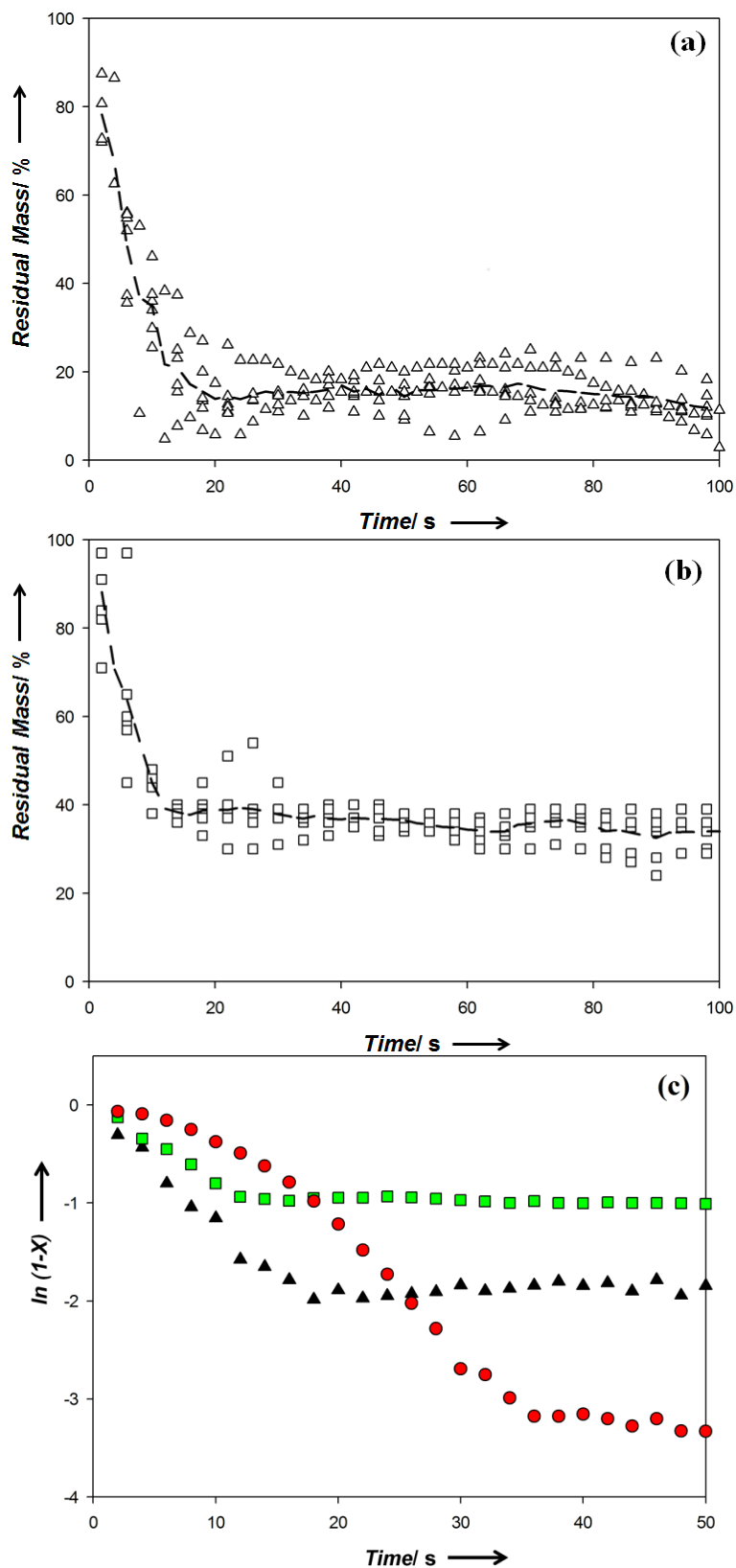


Figure 4.3- Comparison of pyrolytic decomposition and gasification mass loss of (a) Xylan and (b) Lignin. The bullet points are experiment data from several repeat runs and the broken line is the fitted curve. (c) Comparison of pseudo first order kinetics of different components under 50/50 N_2 /Steam atmosphere ((●) Cellulose, (▲) Xylan and (■) Lignin). All the experiments were carried out at isothermal reactor temperature of 750°C.

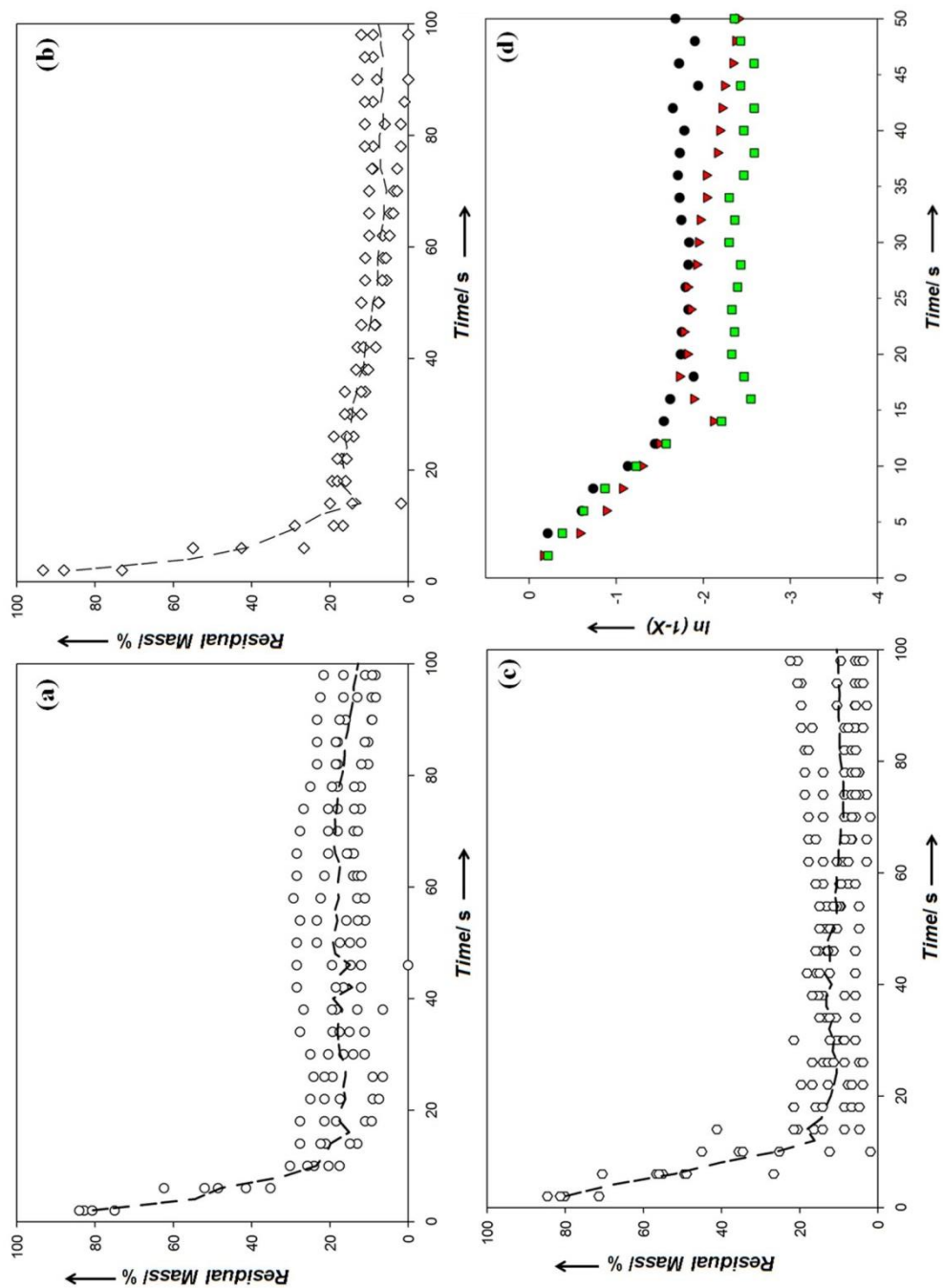


Figure 4. 4- Comparison of pyrolytic decomposition and gasification mass loss of (a) Synthetic biomass mixture; and pinewood sawdust with particle size range: (b) 63-112 μm and (c) 250-300 μm . (d) Comparison of flash volatilisation first order kinetics of various feedstocks ((●) Synthetic biomass mixture, (▼) pinewood sawdust 63-112 μm and (■) 250-300 μm). The bullet points are experiment data from several repeat runs and the broken line is the fitted curve. All the experiments were carried out in an isothermal reactor at 750°C.

4.3.3 Effect of Catalysts on Cellulose Volatilisation Kinetics

Figure 4.5 (a) - (c) shows $\ln(1-X)$ vs residence time plots for reactive flash volatilization of cellulose, with various catalysts, at three temperatures (700, 750 and 800°C). In these figures, the bullet points are average values of experiment data from several repeat runs (not shown here for clarity). The effect of different catalysts is compared against a control, i.e. without any catalyst, which is same as reported in the previous section. With and without the catalysts, the rate of mass loss is observed over three distinct regimes - pyrolytic decomposition, reforming and char gasification. The following discussion is limited to pyrolytic decomposition and reforming regimes only, since the rate of char gasification is very small and is largely independent of reaction conditions in this work.

As seen in Figure 4.5 (a) - (c), the rate of mass loss of cellulose in the pyrolytic decomposition regime is independent of the catalyst used. This is expected since the reactions in this regime are dominated by thermal decomposition of cellulose into gases, condensable vapours and solid residuals (Ranzi et al. 2008). Moreover, the contact between solid catalyst and cellulose particles is negligible. Increasing the reaction temperature reduced the range of pyrolytic decomposition. The pyrolytic decomposition regime reduced from 18 s at 700°C to 14 s and 12 s at 750°C and 800°C, respectively. Since the pyrolytic decomposition of cellulose is an endothermic reaction and is limited by heat transfer, higher radiant heat transfer at higher temperature is favourable and hence resulted in faster pyrolysis rate (Yang et al. 2007). Overall, the pyrolytic decomposition rate constant k was between 0.03 – 0.05 s⁻¹.

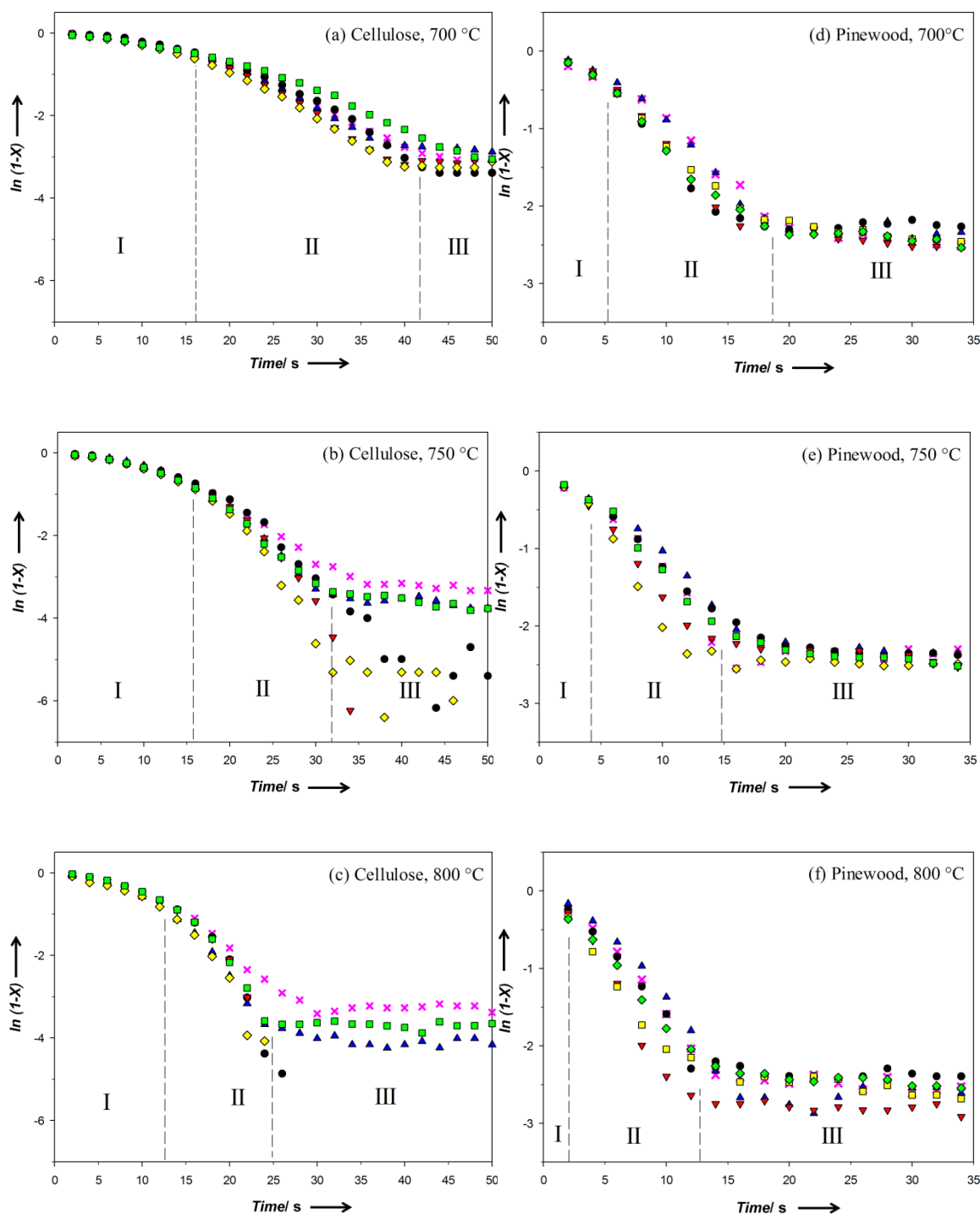


Figure 4. 5- Comparison of reactive flash volatilisation first order kinetics of microcrystalline cellulose at (a) 700°C, (b) 750°C and (c) 800°C; and pinewood sawdust at (d) 700°C, (e) 750°C, and (f) 800°C with and without catalysts. The bullet points are fitted values of experiment data from several repeat runs: (x) without Catalyst, (▲) Ni, (●) Pt-Ni, (▼) Ru-Ni, (◆) Rh-Ni, (■) Re-Ni. The kinetic regimes are labelled as (I) pyrolytic decomposition, (II) reforming, and (III) char gasification.

Chapter 4

The rate of mass loss of cellulose in the reforming regime is greatly improved by the use of catalysts. Ru-Ni and Rh-Ni catalysts showed the highest rate of mass loss rate in this regime. In the control run, volatile components produced in the first regime may undergo homogeneous gas phase reactions to form oxygenated hydrocarbons or re-polymerise on the surface to form heavy tar and char (Di Blasi 1996; Ranzi et al. 2008). In the presence of the catalysts, steam reforming and water gas shift reactions are promoted, converting low molecular weight oxygenated hydrocarbons into H₂, CO and CO₂. Side reactions including methanation may also occur in this regime but to a lesser extent (Haryanto et al. 2009; Kumar et al. 2009). To validate this effect of catalysts, the product gases leaving the wire mesh reactor were analysed using a micro-GC. Figure 4.6(a) shows the gas composition obtained from runs at 750°C under N₂ and steam/N₂ atmospheres. The results confirm that the amount of synthesis gas produced from cellulose N₂ pyrolysis was significantly lower compared to the run under steam/ N₂ atmosphere, both with and without the catalysts. The quality and quantity of synthesis gas (CO + H₂) improved with the use of catalyst in the following order – Re-Ni > Rh-Ni > Ru-Ni > Pt-Ni > Ni > No catalyst. The results confirmed that the extent of steam reforming and water gas shift reaction is higher with promoted Ni catalyst which is well established (Sinfelt 1973; Grenoble et al. 1981; Wheeler et al. 2004).

The rates of mass loss of cellulose in the reforming regime were significantly greater than the rates observed in the pyrolytic decomposition regime. This is because the reactions in the second regime are predominantly gas phase reactions on the surface of the catalysts, whereas, the reactions in first regime are solid decomposition which are limited by heat and mass transfer. Similar to the first regime, the range of the second regime is also reduced by increasing the temperature. The reforming regime reduced from 20 s at 700°C to 16 s and 12 s at 750 and 800°C, respectively. Since steam reforming reaction is endothermic, it is favoured at higher temperature and hence resulted in faster reforming rates (Chan et al. 2014).

The rate constants (k), apparent activation energies ($E_{a\text{-apparent}}$) and pre-exponential factors (A_{apparent}) in the reforming regime are summarised in the Table 4.4. Constable-Cremer plot shown in Figure 4.6(b) illustrates the “compensation effect”, which is a correlation commonly used by researchers to study one reaction with a series of similar catalysts or to study different reactions with one catalyst (Agrawal 1986; Bond 1999; Bond et al. 2000). In such cases $\ln(A_{\text{apparent}})$ varies linearly with apparent activation energy ($E_{a\text{-apparent}}$), which is exactly what we observed. $E_{a\text{-apparent}}$ of Ru-Ni, Rh-Ni and Re-Ni catalysts were significantly higher than Pt-Ni and monometallic nickel catalyst. Large $E_{a\text{-apparent}}$ values indicate that k is more sensitive to increase in temperatures (Cybulski et al. 2001). This can be observed from Table 4.4, where the k values for all the catalysts were nearly equal at 700°C but the k for Rh-Ni, Ru-Ni and Re-Ni increases by much higher value at 800°C. Rh-Ni exhibited the highest $E_{a\text{-apparent}}$ and A_{apparent} values among all the catalysts, which is consistent with the most active catalyst, given that the temperature of the reaction is above the characteristic isokinetic temperature, T_{iso} (Bond et al. 2000). However, the rate constant of Re-Ni catalyst was lower than Rh-Ni because of smaller A_{apparent} , even though the $E_{a\text{-apparent}}$ values were identical.

4.3.4 Effect of Catalysts on Pinewood Sawdust Volatilisation Kinetics

Figure 4.5 (d) – (f) show $\ln(1-X)$ vs residence time plots for reactive flash volatilization of pinewood sawdust, with various catalysts, at three temperatures (700, 750 and 800°C). The results are characterized by considerably shorter pyrolytic decomposition regime when compared to cellulose. The pyrolytic decomposition regime at 700, 750 and 800°C lasted only 6, 4 and 2 s, respectively. This may be attributed to lower pyrolysis onset temperature of hemicellulose and lignin which leads to more volatiles generated at shorter residence time, leading to early onset of the reforming regime. Pyrolysis onset temperatures of cellulose (315°C) is significantly higher than hemicellulose and lignin at 220 and 150°C, respectively (Yang et al. 2007).

Moreover, alkali metals such as Na, K, Mg and Ca, found in the pinewood acts as catalysts to enhance the decomposition process, leading to the formation of low molecular weight volatile species such as formic acid, glycoaldehyde and acetol (Fahmi et al. 2007; Patwardhan et al. 2010). The rate constants in this regime at 700, 750 and 800°C were found to be 0.08 s^{-1} , 0.11 s^{-1} and 0.13 s^{-1} respectively. Similar to the observation in the previous section, the length of pyrolytic decomposition and reforming regimes shorten with increasing temperature.

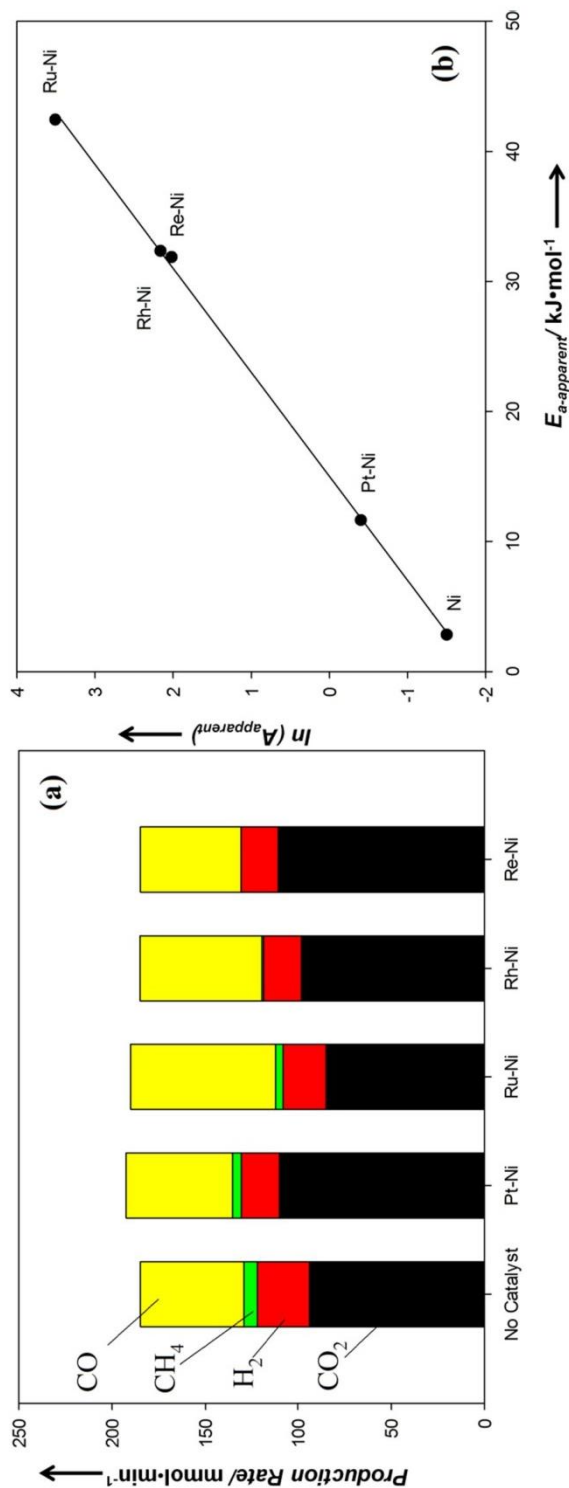


Figure 4. 7- (a) Composition of gas produced with and without catalyst in the wire-mesh isothermal thermogravimetric reactor during reactive flash volatilisation of pinewood sawdust. (b) Constable-Cremer plot of various catalysts used in reactive flash volatilisation of pinewood sawdust.

Table 4. 5- Comparison of the reforming rate constant (k), apparent pre-exponential factor ($A_{apparent}$) and apparent activation energy ($E_{a-apparent}$) in reactive flash volatilisation of pinewood sawdust using various catalysts.

Catalyst	Reforming			
	Rate, (s ⁻¹)		Apparent Activation Energy $E_{a-apparent}$ (kJ mol ⁻¹)	
	$k \cdot 10^2$	$A_{apparent}$ (s ⁻¹)		
	700°C	750°C	800°C	
Without Catalyst	14.4	16.6	21.2	33.6
Ni	17.0	13.3	17.8	2.84
Pt-Ni	16.2	16.2	18.5	11.7
Ru-Ni	18.3	20.8	30.0	42.5
Rh-Ni	14.1	24.9	20.2	32.4
Re-Ni	14.2	18.9	20.5	31.9

Chapter 4

The reforming regime of RFV of pinewood sawdust is also significantly influenced by the type of catalysts used. However, as shown in Table 4.5, the differences in the reaction rate constants between various catalysts were smaller. This may be due to the effect of heavier tars produced by pyrolytic decomposition of lignin which are difficult to reform. The rate constants were, in general, lower for pinewood than for cellulose in the reforming regime. Moreover, the inorganic matter present in the pinewood ash may act as catalyst, which dampens the effect of external catalysts. Overall, the rate constants in the reforming regime of RFV of pinewood sawdust were in the following order: Ru-Ni > Rh-Ni > Re-Ni > Pt-Ni > Ni. The low activity of Ni catalyst supported on alumina may be attributed to the transformation of NiO/Al₂O₃ to NiAl₂O₄ spinel at temperatures above 750°C, which reduces the metal active site (Tanksale et al. 2008; Chan et al. 2014).

Analyses of the effluent gas from the RFV of pinewood sawdust are shown in Figure 4.7(a). The composition of synthesis gas was observed to be nearly the same in all the cases within the range of errors in measurement.

The Constable-Cremer plot (Figure 4.7(b)) shows similar linear trend between the $\ln(A_{\text{apparent}})$ and $E_{a\text{-apparent}}$. Effective catalysts such as Ru-Ni, Rh-Ni and Re-Ni had relatively higher apparent activation energies in comparison to Pt-Ni and Ni catalysts, which is consistent with the finding from previous section.

4.4 Conclusions

Kinetics of the reactive flash volatilisation, an autothermal process of converting non-volatile oxygenated hydrocarbons into tar free synthesis gas under steam rich condition and high heat flux, was measured in a wire-mesh isothermal gravimetric reactor. Pseudo first order reaction model was used to study the volatilisation of different biomass derived feedstock under various gasification conditions. The results showed that there are three distinct regimes of rate of mass loss: (I) pyrolytic decomposition, (II) reforming, and (III) char gasification. Comparison of kinetics under steam rich conditions with the use of promoted nickel catalyst showed that the catalysts increase the rate of mass loss in the reforming regime only. Moreover, the effect of the catalyst in the reforming regime was found to improve the quality of synthesis gas (higher CO and H₂). Comparing the rate of volatilisation of the three lignocellulose components, it was observed that pyrolytic decomposition of cellulose is the rate limiting step. Increasing the reaction temperature increased the rate of mass loss and shortened both the pyrolytic decomposition and

reforming regimes. Ru-Ni and Rh-Ni catalysts supported of alumina were found to be the best in this work because of the high rate of volatilisation both cellulose and pinewood sawdust.

4.5 Acknowledgements

The authors thank the Rural Industries Research and Development Corporation and the Department of Chemical Engineering, Monash University for funding and support. Finally the authors would like to thank Prof Kristiina Oksman and the Swedish Foundation for International Cooperation in Research and Higher Education for providing travel grant support to FLC.

4.6 References

- Agrawal, R. (1986). "On the compensation effect." *Journal of thermal analysis* **31**: 73-86.
- Antal, M. J., Jr. and G. Varhegyi (1995). "Cellulose Pyrolysis Kinetics: The Current State of Knowledge." *Industrial & Engineering Chemistry Research* **34**: 703-717.
- Biagini, E., L. Guerrini, et al. (2009). "Development of a Variable Activation Energy Model for Biomass Devolatilization." *Energy & Fuels* **23**: 3300-3306.
- Bond, G. C. (1999). "Kinetics of alkane reactions on metal catalysts: activation energies and the compensation effect." *Catalysis Today* **49**: 41-48.
- Bond, G. C., M. A. Keane, et al. (2000). "Compensation Phenomena in Heterogeneous Catalysis: General Principles and a Possible Explanation." *Catalysis Reviews* **42**: 323-383.
- Burhenne, L., J. Messmer, et al. (2013). "The effect of the biomass components lignin, cellulose and hemicellulose on TGA and fixed bed pyrolysis." *Journal of Analytical and Applied Pyrolysis* **101**: 177-184.
- Caballero, J. A., J. A. Conesa, et al. (1997). "Pyrolysis kinetics of almond shells and olive stones considering their organic fractions." *Journal of Analytical and Applied Pyrolysis* **42**: 159-175.
- Chan, F. L. and A. Tanksale (2014). "Catalytic Steam Gasification of Cellulose Using Reactive Flash Volatilization." *ChemCatChem* **6**: 2727-2739.
- Colby, J. L., P. J. Dauenhauer, et al. (2008). "Millisecond autothermal steam reforming of cellulose for synthetic biofuels by reactive flash volatilization." *Green Chemistry* **10**: 773-783.
- Cybulski, A., J. A. Moulijn, et al. (2001). 5 - Process Development. *Fine Chemicals Manufacture*. A. C. A. M. M. S. A. Sheldon. Amsterdam, Elsevier Science B.V.: 193-413.
- Devi, L., K. J. Ptasinski, et al. (2003). "A review of the primary measures for tar elimination in biomass gasification processes." *Biomass Bioenergy* **24**: 125-140.
- Di Blasi, C. (1996). "Heat, momentum and mass transport through a shrinking biomass particle exposed to thermal radiation." *Chemical Engineering Science* **51**: 1121-1132.

Chapter 4

Dupont, C., L. Chen, et al. (2009). "Biomass pyrolysis: Kinetic modelling and experimental validation under high temperature and flash heating rate conditions." Journal of Analytical and Applied Pyrolysis **85**: 260-267.

Fahmi, R., A. V. Bridgwater, et al. (2007). "The effect of alkali metals on combustion and pyrolysis of Lolium and Festuca grasses, switchgrass and willow." Fuel **86**: 1560-1569.

Fisher, T., M. Hajaligol, et al. (2002). "Pyrolysis behavior and kinetics of biomass derived materials." Journal of Analytical and Applied Pyrolysis **62**: 331-349.

Grenoble, D. C., M. M. Estadt, et al. (1981). "The chemistry and catalysis of the water gas shift reaction: 1. The kinetics over supported metal catalysts." Journal of Catalysis **67**: 90-102.

Haryanto, A., S. D. Fernando, et al. (2009). "Upgrading of syngas derived from biomass gasification: A thermodynamic analysis." Biomass and Bioenergy **33**: 882-889.

Hernández, J. J., G. Aranda-Almansa, et al. (2010). "Gasification of biomass wastes in an entrained flow gasifier: Effect of the particle size and the residence time." Fuel Processing Technology **91**: 681-692.

Hüttinger, K. J. and W. F. Merdes (1992). "The carbon-steam reaction at elevated pressure: Formations of product gases and hydrogen inhibitions." Carbon **30**: 883-894.

Koufopoulos, C. A., A. Lucchesi, et al. (1989). "Kinetic modelling of the pyrolysis of biomass and biomass components." The Canadian Journal of Chemical Engineering **67**: 75-84.

Kumar, A., K. Eskridge, et al. (2009). "Steam-air fluidized bed gasification of distillers grains: Effects of steam to biomass ratio, equivalence ratio and gasification temperature." Bioresource Technology **100**: 2062-2068.

Kumar, A., D. D. Jones, et al. (2009). "Thermochemical biomass gasification: a review of the current status of the technology." Energies (Basel, Switz.) **2**: 556-581.

Kurjatko, S., J. Kúdela, et al. (2006). Wood Structure and Properties '06, Arbora Publishers.

Lee, I.-G., M.-S. Kim, et al. (2002). "Gasification of Glucose in Supercritical Water." Industrial & Engineering Chemistry Research **41**: 1182-1188.

Lin, Y.-C., J. Cho, et al. (2009). "Kinetics and Mechanism of Cellulose Pyrolysis." The Journal of Physical Chemistry C **113**: 20097-20107.

Liu, Z. and F.-S. Zhang (2008). "Effects of various solvents on the liquefaction of biomass to produce fuels and chemical feedstocks." Energy Conversion and Management **49**: 3498-3504.

Lussier, M. G., Z. Zhang, et al. (1998). "Characterizing rate inhibition in steam/hydrogen gasification via analysis of adsorbed hydrogen." Carbon **36**: 1361-1369.

Lv, D., M. Xu, et al. (2010). "Effect of cellulose, lignin, alkali and alkaline earth metallic species on biomass pyrolysis and gasification." Fuel Processing Technology **91**: 903-909.

Milosavljevic, I. and E. M. Suuberg (1995). "Cellulose Thermal Decomposition Kinetics: Global Mass Loss Kinetics." Industrial & Engineering Chemistry Research **34**: 1081-1091.

- Mullen, C. A. and A. A. Boateng (2008). "Chemical Composition of Bio-oils Produced by Fast Pyrolysis of Two Energy Crops†." Energy & Fuels **22**: 2104-2109.
- Naik, S., V. V. Goud, et al. (2010). "Characterization of Canadian biomass for alternative renewable biofuel." Renewable Energy **35**: 1624-1631.
- Orfão, J. J. M., F. J. A. Antunes, et al. (1999). "Pyrolysis kinetics of lignocellulosic materials—three independent reactions model." Fuel **78**: 349-358.
- Patwardhan, P. R., J. A. Satrio, et al. (2010). "Influence of inorganic salts on the primary pyrolysis products of cellulose." Bioresource Technology **101**: 4646-4655.
- Qin, K., P. A. Jensen, et al. (2012). "Biomass Gasification Behavior in an Entrained Flow Reactor: Gas Product Distribution and Soot Formation." Energy & Fuels **26**: 5992-6002.
- Qu, T., W. Guo, et al. (2011). "Experimental Study of Biomass Pyrolysis Based on Three Major Components: Hemicellulose, Cellulose, and Lignin." Industrial & Engineering Chemistry Research **50**: 10424-10433.
- Ranzi, E., A. Cuoci, et al. (2008). "Chemical Kinetics of Biomass Pyrolysis." Energy & Fuels **22**: 4292-4300.
- Salge, J. R., B. J. Dreyer, et al. (2006). "Renewable hydrogen from nonvolatile fuels by reactive flash volatilization." Science **314**: 801-804.
- Shen, D. K. and S. Gu (2009). "The mechanism for thermal decomposition of cellulose and its main products." Bioresource Technology **100**: 6496-6504.
- Shuangning, X., L. Zhihe, et al. (2006). "Devolatilization characteristics of biomass at flash heating rate." Fuel **85**: 664-670.
- Sinfelt, J. H. (1973). Specificity in Catalytic Hydrogenolysis by Metals. Advances in Catalysis. H. P. D.D. Eley and B. W. Paul, Academic Press. **Volume 23**: 91-119.
- Sutton, D., B. Kelleher, et al. (2001). "Review of literature on catalysts for biomass gasification." Fuel Process. Technol. **73**: 155-173.
- Tanksale, A., J. N. Beltramini, et al. (2008). "Effect of Pt and Pd promoter on Ni supported catalysts—A TPR/TPO/TPD and microcalorimetry study." Journal of Catalysis **258**: 366-377.
- Tanksale, A., J. N. Beltramini, et al. (2010). "A review of catalytic hydrogen production processes from biomass." Renewable and Sustainable Energy Reviews **14**: 166-182.
- Thomas, R. J. (1977). Wood: Structure and Chemical Composition. Wood Technology: Chemical Aspects. United States of America, ACS. **43**: 1-23.
- Vamvuka, D., E. Kakaras, et al. (2003). "Pyrolysis characteristics and kinetics of biomass residuals mixtures with lignite." Fuel **82**: 1949-1960.
- Várhegyi, G., M. J. Antal Jr, et al. (1997). "Kinetic modeling of biomass pyrolysis." Journal of Analytical and Applied Pyrolysis **42**: 73-87.
- Wheeler, C., A. Jhalani, et al. (2004). "The water–gas–shift reaction at short contact times." Journal of Catalysis **223**: 191-199.

Chapter 4

Yang, H. P., R. Yan, et al. (2007). "Characteristics of hemicellulose, cellulose and lignin pyrolysis." Fuel **86**: 1781-1788.

Yang, R. T. and R. Z. Duan (1985). "Kinetics and mechanism of gas-carbon reactions: Conformation of etch pits, hydrogen inhibition and anisotropy in reactivity." Carbon **23**: 325-331.

Chapter 5: Catalytic Steam Gasification of Pinewood and Eucalyptus Sawdust Using Reactive Flash volatilization

Abstract

Catalytic steam gasification of cellulose using reactive flash volatilisation (RFV) has been proven as a promising approach for syngas production. However, using cellulose as feedstock is economically unfavoured because biomass pre-treatment represents one of the most expensive steps in the processing of lignocellulose. This chapter investigates the production of syngas using RFV of pinewood and eucalyptus sawdust as feedstock. Experiments were conducted to evaluate the effects of catalyst promoters, carbon to oxygen ratio, carbon to steam ratio, feedstock and ash contents on product yields (i.e. gas, tar and char) and product gas composition. High gasification efficiency and low char selectivity were observed in the pinewood RFV with Re-Ni and Rh-Ni catalysts, which can be explained by the catalysts high active metal substrate dispersion. Additionally, in compared to cellulose, higher gasification efficiencies were also observed in the pinewood and eucalyptus RFV. This can be attributed to the effects resulted from higher amorphous structure of lignocellulose compared to microcrystalline cellulose, and the catalytic effects of alkali and alkaline earth metals (AAEM) found in the lignocellulose ash. The catalytic effects of AAEM further reduced the coke deposition on the Ni catalysts, making the effect of noble metal promoter on the Ni catalysts less significant. The effects on product yields and gas composition from promoters, carbon to oxygen ratio and carbon to steam ratio were less pronounced.

This page intentionally left blank.

5.1 Introduction

With the growing concerns on climate change and greenhouse gas emissions, there is an urgent need for global transition from fossil based energy source to renewable energy sources to achieve sustainable future growth. Biomass, as a renewable and carbon neutral energy source, is recognized as one of the most promising solutions for this issue due to its wide availability, especially lignocellulose. Lignocellulose is the most abundant renewable biomass which has an estimated annual production of 10 billion MT (Alvira et al. 2010). It is the only sustainable energy resource that can be converted into alternative transportation fuels and utilized for chemicals production (Huber et al. 2006).

There are a number of conversion technologies for utilizing biomass as renewable energy resource, such as thermal conversion, biochemical conversion, agrochemical conversion and thermochemical conversion (Lv et al. 2010). Among all the processing technologies, thermochemical biomass gasification receives the most interests from both industrial and academic researchers because of its high conversion efficiency and feedstock flexibility (Devi et al. 2003; Verma et al. 2012). Synthesis gas can be produced *via* conventional biomass gasification in fluidised bed reactor at moderate temperature, usually $>700^{\circ}\text{C}$. However, the product gas, in most cases, contains high concentration of undesired by-products such as tar and soot, which makes it unsuitable for use in downstream applications such as fuel cell (Chan et al. 2014). Furthermore, accumulation of tar in the reactor may also lead to severe operational issues such as corrosion and clogging. Generally, downstream conversion of char and tar is necessary for the clean-up of synthesis gas.

Chapter 3 demonstrated that clean synthesis gas can be produced *via* reactive flash volatilization (RFV) over nickel based catalysts using cellulose as the feedstock (Chan et al. 2014). RFV is a complex process which involves pyrolysis, partial oxidation, steam reforming and water gas shift reactions. With carbon space velocity and carbon mass flow rate of 10-100 times higher than conventional fluidised bed reactors, tar free synthesis gas can be produced in a single, short residence time fixed bed reactor, in less than 50ms. However, using cellulose as feedstock is economically unfavoured because biomass pre-treatment represents one of the most expensive steps in the processing of lignocellulose (Alvira et al. 2010). In fact, the capital investment cost and operating cost of biomass pre-treatment process for a bioethanol production plant can be as high as 19% of the total capital expenditure and 32 - 38% of the total operating expenditure, respectively (Wooley et al. 1999; Bals et al. 2011). Therefore, it is more cost effective to use

Chapter 5

whole lignocellulose such as wood waste, sugarcane bagasse and wheat straw with minimal pre-treatment.

In addition, it has been widely reported that catalytic effects from the inherent alkali and alkaline earth metals (AAEM) in raw biomass can be beneficial to the gasification process as it accelerates the conversion of biochar and leads to higher gaseous product yield (Kajita et al. 2010; Yip et al. 2010; Mitsuoka et al. 2011; Nzihou et al. 2013; Yildiz et al. 2015).

Therefore, in the present work, RFV of untreated pinewood and eucalyptus sawdust over promoted nickel based catalysts were investigated. The focus of this study was to evaluate the effects of carbon to oxygen (C/O), carbon to steam (C/S) ratio, biomass feedstock and inherent alkali and alkaline earth metal (AAEM) species on product yields and the stability of promoted nickel catalysts.

5.2 Experimental

5.2.1 Biomass

Softwood (*pinus radiata*, referred to as pinewood henceforth, 550 μm) and hardwood (*eucalyptus regnans*, referred to as eucalyptus henceforth, 500 μm), obtained from Pollard's Sawdust Supplies, Victoria, Australia, were used as feedstock in this investigation.

5.2.2 Biomass Characterization

Physical and chemical properties of the biomass were characterized according to the European Standards (EN) or Australian Standards (AS). Moisture content of the biomass was determined according to EN14774. Ash yield was determined according to EN14775. Volatile matter, carbon, hydrogen and nitrogen content were determined according to EN15148:2009. Sulphur was determined according to AS1038.6.3.3.

Elemental analysis of the alkali and alkaline earth metals in biomass was performed using an Ametek Spectro iQ II X-Ray Florescence (XRF) Spectrometer. Biomass ashing was carried out by heating desired amount of the sample in air at 600°C for 6 h to remove all the hydrocarbons. Ash residue was then recovered and subjected to XRF elemental analysis.

5.2.3 Catalyst

Three nickel based catalysts: Ru-Ni, Rh-Ni and Re-Ni supported on γ -alumina were developed using impregnation method. These bimetallic catalysts had nickel content of 10 wt% and noble

metal promoter content of 1wt%. Detailed synthesis procedures and characterizations of these catalysts can be found in 3.2.1.

5.2.4 Reactor Setup

Catalytic activity evaluation was conducted in a bench-scale reactor setup. Detailed description of the setup can be found 3.2.3.1.

Approximately 1 g of the promoted nickel catalyst was loaded onto fritted disc mounted at the centre of a 700 mm quartz reactor before housed in an electric furnace. Prior to each experiment, the catalyst was reduced in H₂/N₂ gas mixture at 400°C for 4 h. The RFV experiment was carried out at the temperature of 750°C, which was found to be optimum in Chapters 3 and 4. During the experiment, 15 g/h of pinewood or eucalyptus sawdust was screw-fed from a K-Tron powder feeder in co-current gas flow into an isothermal reactor. The amounts of steam and oxygen fed into the reactor were determined based on the C/O and C/S ratios of the experiment. Nitrogen was used as make-up gas for maintaining the reactor space velocity. Exiting gas from the reactor was fed into a custom built gas-liquid separator where the gas samples were periodically analysed using a Shimadzu gas chromatograph GC-2014 and liquid product was collected in the separator. Volumetric flow rate of the product gas was also determined using a 50 ml soap bubble flow meter.

Moles of carbon atoms in the gas phase were calculated by measuring the amount of carbonaceous molecules in the gas phase using the gas chromatographer. Moles of carbon atoms in the liquid phase (tar) were calculated by measuring the total organic carbon in the condensate using Shimadzu TOC-L series analyser. Liquid sample was diluted to a ratio of 1:400 before the analysis. Moles of carbon atoms in the solid product (biochar) were calculated based on the amount of carbon dioxide and carbon monoxide produced in the temperature programmed oxidation of biochar in the homemade setup used for the temperature programmed reduction and CO-desorption, as illustrated in 3.2.2.4 and 3.2.2.5. By summing up the cumulative moles of carbon atoms in gas, liquid and solid products collected throughout the experiment, overall carbon balance of the run can be calculated. Based on the carbon balance, selectivity for gas, tar and char are computed according to the following equations –

$$S_{gas} = \frac{\text{Moles of Carbon atoms in the gas phase}}{\text{Moles of Carbon atoms in the products}} \times 100 \%$$

$$S_{Tar} = \frac{\text{Moles of Carbon atoms in the liquid phase}}{\text{Moles of Carbon atoms in the products}} \times 100 \%$$

$$S_{char} = \frac{\text{Moles of Carbon atoms in the solid phase}}{\text{Moles of Carbon atoms in the products}} \times 100 \%$$

5.2.5 Catalyst Characterisation

Powder X-ray diffraction measurements of fresh and spent nickel catalysts were carried out in a Rigaku Miniflex powder diffractometer with mono-chromatized Cu K α radiation ($\lambda = 0.154$ nm) at 40 kV and 15 mA.

TEM specimens were prepared using a solvent method. A small amount of catalyst powder and a few millilitre of solvent (butanol) were placed in an agate mortar. The catalyst powder was then gently ground in the solvent until a sufficient amount of fine material was suspended in the solution. A holey carbon coated copper grid (the TEM sample grid) was then dipped in the solution and the prepared TEM specimen was left to dry at room temperature.

Size and morphology of the fresh and spent catalyst nanoparticles were studied using FEI Tecnai G2 F20 S-TWIN Field Emission Gun (FEG) Scanning Transmission Electron Microscope (TEM). Energy Dispersive X-Ray Spectroscopy (EDS) mapping of nickel, noble metal and various alkali and alkaline metal species on spent catalysts were carried out in the STEM mode using a high angle annular dark field (HAADF) Windowless X-ray detector (Bruker Quantax 400). The STEM was operated at 200 kV at magnifications of between 40,000 ~ 225,000 times with 20° of specimen tilt. Collected EDS maps have a resolution of 512 × 512 pixels.

5.3 Results and Discussion

5.3.1 Biomass Characterisation

Physical and chemical properties of pinewood and eucalyptus sawdust used in this study are presented in Table 5.1. Results from the proximate analysis showed that eucalyptus sawdust had ~9 times higher ash content, lower volatile matter and roughly similar fixed carbon content, in comparison to pinewood sawdust. Carbon, hydrogen and oxygen compositions in the two samples were similar, as reported in the ultimate analysis. XRF analysis of the ashes revealed the composition differences of alkali and alkaline earth metals (AAEM) in the biomass ash. Common compounds found in these two biomass ashes include oxides of magnesium, calcium, potassium, silica, phosphorous, sulphur and chlorine. Both samples contained roughly similar composition of magnesium oxide. However, pinewood ash contained higher level of phosphorous and potassium oxides whereas eucalyptus ash had more silica.

Table 5. 1- Physical and Chemical properties of Pinewood and Eucalyptus Sawdust

	Pinewood Sawdust	Eucalyptus Sawdust
Properties		
Acidity (pH)	3.5 – 4.6	Not Available
Colour	cream to light brown	light to dark brown
Density	12 – 18 pounds/cubic feet	Not Available
Solubility in water	< 0.1%	highly insoluble
Specific Gravity	0.5 – 0.8	Not Available
Particle Size	< 550 micron	< 500 micron
Proximate analysis (% db)		
Moisture Content, % ar (EN14774)	7.70	9.80
Ash Yield (EN14775)	0.80	7.30
Volatile	84.1	76.6
Fixed Carbon	15.1	16.0
Ultimate analysis (% db)		
Carbon	50.1	47.3
Hydrogen	6.20	5.30
Nitrogen	0.12	0.14
Sulphur	0.03	0.04
Oxygen ^a	42.8	39.9
Ash analysis (%)		
MgO	30.95	33.08
Al ₂ O ₃	2.59	6.73
SiO ₂	3.40	26.1
P ₂ O ₅	11.27	3.20
SO ₃	6.51	5.11
Cl	3.30	6.95
K ₂ O	22.35	4.14
CaO	17.55	11.33
TiO ₂	0.12	0.46
V ₂ O ₅	Not Available	0.05
Cr ₂ O ₃	0.04	0.12
MnO	1.19	0.48
Fe ₂ O ₃	0.38	1.97
CoO	0.09	0.10
NiO	0.06	0.01
CuO	0.01	0.02
ZnO	0.09	0.05
Ga	0.01	Not Available

^a Calculated by difference

5.3.2 Effect of carbon-to-oxygen ratio in RFV of Pinewood Sawdust

The effect of carbon to oxygen feed ratio (C/O) was tested on all three promoted catalysts. The pinewood sawdust feed rate was kept constant at 15 g/h, while the oxygen was fed at the rate of 143 (C/O= 0.82), 158 (C/O= 0.74) and 173 SCCM (C/O= 0.68). Reactor temperature and C/S ratio for these runs were kept constant at 750°C and 1.17, respectively.

Chapter 5

Test results are illustrated in Figure 5.1 and 5.2. Products selectivity (i.e. gas, char and tar) are calculated based on the carbon atom balance. The product gas composition is measured on a dry basis, whereas water yield is not reported. As seen in Figure 5.1, Re-Ni catalysts exhibited high gas yield (> 99%) in all three C/O ratios. Combined tar and char yields were less than 1%. However, with Rh-Ni and Ru-Ni catalysts, decrease in gas yield and increase in char yield were observed with the increase of C/O ratio. This result is consistent with the findings in Chapter 3 on reactive flash volatilisation of cellulose (Chan et al. 2014). Higher oxygen feed (low C/O) leads to higher catalyst bed temperature, which favours steam reforming and oxidation reactions, and therefore the higher gas yield. Although gas yields were higher, the quality of the syngas produced was lower. This is because higher oxygen input also causes further oxidation of CO into CO₂ and H₂ into H₂O, leading to decrease in product gas heating value. This can be seen with all three catalysts where CO₂ mole percent were the highest at C/O of 0.68 and decreased as the C/O ratio increased.

Although the non-volatile fraction of the pinewood sawdust is higher than the microcrystalline cellulose studied in Chapter 3, char yields were substantially lower in RFV of pinewood sawdust in comparison to RFV of microcrystalline cellulose under similar reaction conditions. This can be explained by three reasons –

- 1) Higher amount of amorphous structure (hemicellulose and lignin) and lower crystalline structure in pinewood sawdust resulted in faster devolatilisation, therefore, lower char production. Amorphous hemicellulose and lignin are known to have faster devolatilisation due to their lower pyrolysis onset temperatures and the reactions' exothermic properties (Chan et al. 2015). Since 48.6 – 63% by mass of pinewood is hemicellulose and lignin (Dekker 1987; Wong et al. 1988; Ferraz et al. 2000), faster devolatilisation can be expected. Also, lower cellulose content per unit feed reduces the production of secondary char. Levoglucosan (an anhydrosugar derivative from pyrolytic decomposition of cellulose) is known to undergo secondary decomposition reactions to form secondary char (Kawamoto et al. 2009; Shen et al. 2009; Ronsse et al. 2012; Chan et al. 2015). Because only 37.0 – 51.4 % by mass of pinewood sawdust is cellulose, amount of levoglucosan produced from cellulose pyrolysis is substantially lower than in RFV of cellulose, and therefore, reduces the amount of char produced from this secondary reaction.

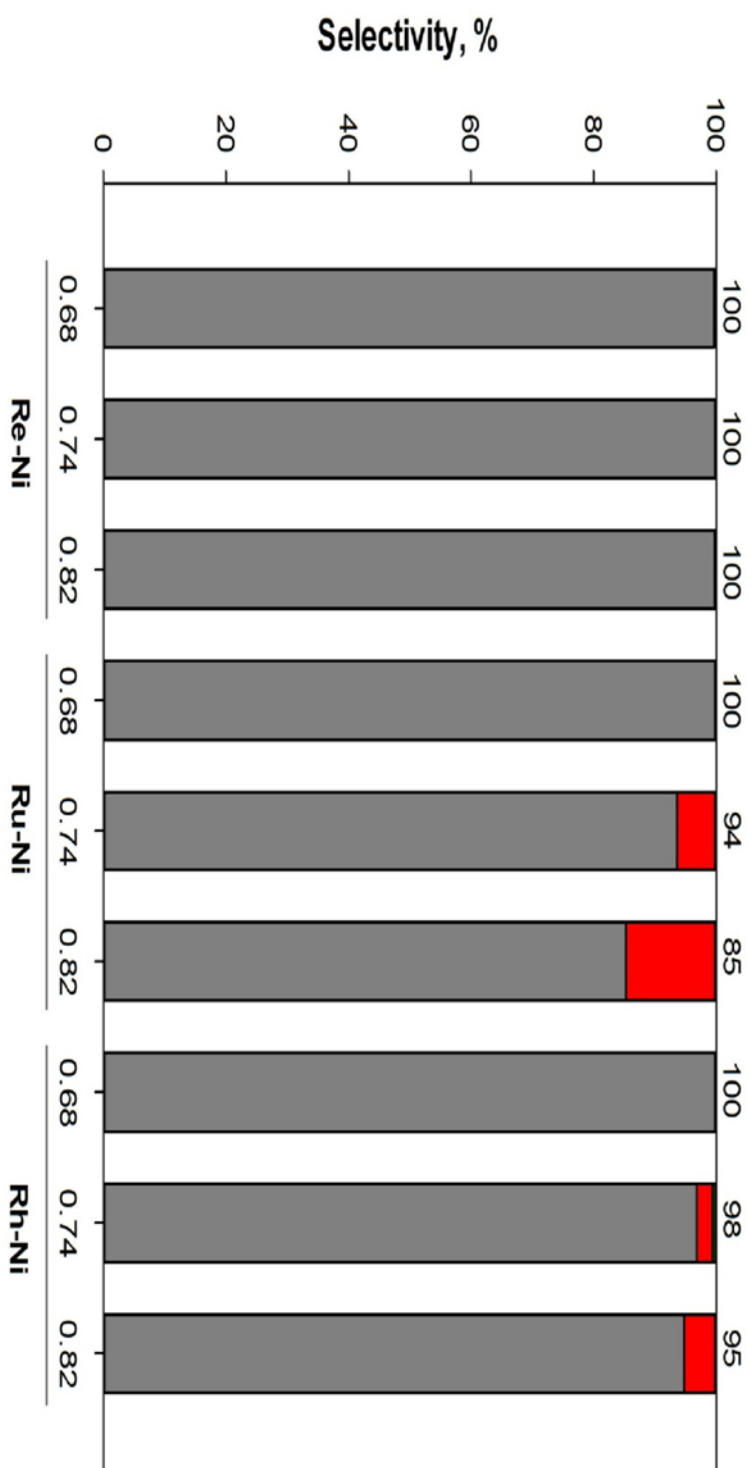


Figure 5. 1- Effect of C/O feed and catalyst promoters on the selectivity of gas (■), char (■) and tar (■) based on carbon balance. The numbers on the top of each bar represent gasification efficiency, which is the percentage of carbon in gas and tar combined. Reaction conditions: Pinewood sawdust flow rate= 15 g h⁻¹, 750 °C, C/S=1.17. Here tar is defined as water-soluble organics.

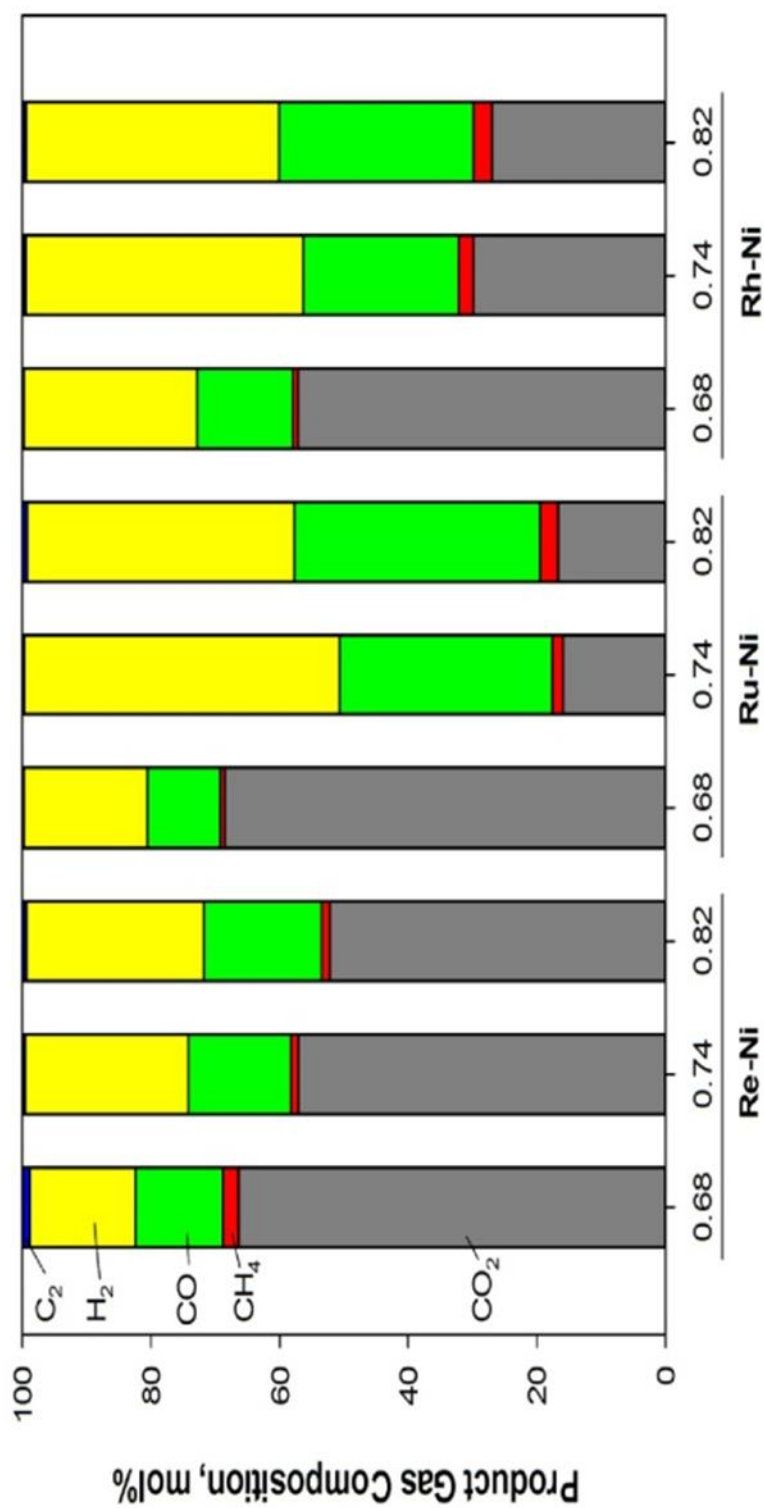


Figure 5. 2- Effect of C/O feed ratio and catalyst promoters on product gas composition. C₂ compounds include ethane, ethylene and acetylene. Reaction conditions: Pinewood sawdust flow rate= 15 g h⁻¹, 750 °C, C/S=1.17. Here tar is defined as water-soluble organics.

2) Synergistic effect between lignocellulosic components (i.e. cellulose, hemicelluloses and lignin) enhances the production of low molecular weight products and leads to lower char production (Hosoya et al. 2007; Giudicianni et al. 2013). The synergy is particularly effective between pyrolytic decomposition products of cellulose and lignin. Lignin-derived products inhibit thermal polymerization of levoglucosan and the formation of 1, 6-anhydro- β -D-glucofuranose while other cellulose derived products inhibit low molecular weight products from carbonisation in vapour phase. In the co-pyrolysis of cellulose and lignin, the presence of lignin derived phenolic products, such as guaiacol (2-Methoxyphenol; *o*-Methoxyphenol), 4-methylguaiacol (Creosol; 2-Methoxy-4-methylphenol) and 4-vinylguaiacol (4-Ethenyl-2 methoxyphenol), help to enhance the production of glycolaldehyde, hydroxyacetone and other low molecular weight products by altering the formation mechanisms of these androsugars and secondary degradation mechanisms of the volatile species (Hosoya et al. 2007). Therefore, char production was lower. Similar findings have been reported elsewhere (Asmadi et al. 2012; Giudicianni et al. 2013). The effectiveness of these phenolic derivatives in inhibiting char formation can be explained with the hydrogen-acceptor/donor theory (Asmadi et al. 2012). It appears that these phenolic derivatives may act as a strong hydrogen donor by providing hydrogen radical to unstable radical compounds formed during the pyrolysis process which otherwise would undergo radical coupling reactions that leads to char formation.

3) Inherent alkali and alkaline earth metals (AAEM) retained in the char catalyse gasification reaction, resulting in faster char decomposition, therefore, lower char yield. It is known in literature that AAEM species, particularly potassium (K), are effective catalysts in promoting C-C bond cleavage reactions and char gasification (Scott et al. 2001; Di Blasi et al. 2009; Wu et al. 2009). The mechanism of how these AAEM catalyses char gasification remains unclear, but some studies have attributed this enhanced catalytic activity to the oxygen transfer cycle occurring during the gasification, either through carbon reduction or oxygenated complexes decomposition promoted under the presence of AAEM (Nzihou et al. 2013).

With Re-Ni catalyst, a linear correlation can be observed between the increase in C/O ratio and the increase in the production of oxygen deficient compounds- H_2 and CO (Figure 5.2). With Rh-Ni and Ru-Ni catalysts, however, H_2 and CO compositions increased with the increase in C/O ratio, the actual production rate per unit gram of pinewood feed were, in fact, lower at higher C/O ratio. The higher H_2 and CO gas percentages in gas stream resulted from significant reduction in the product gas flow rate (not reported), caused by deposition of char in the reactor, which led to clogging and therefore, reduced the output gas flow.

Chapter 5

Re-Ni catalyst had the highest gasifying efficiency in RFV of pinewood sawdust. This can be attributed to the higher dispersion of the active metal substrate on the catalyst (Chapter 3) and higher activity in promoting oxidation. Re can exist in multiple oxidation states, which is effective in promoting oxidation owing to its high oxidation state and cationic charge (Ison et al. 2007). Re oxo-complexes, particularly methyl-rhenium trioxide (MTO), is widely used in oxidation of hydrocarbons because of this property. High CO₂ composition was also observed in RFV of pinewood sawdust over Re-Ni catalyst (Figure 5.2), which confirms that oxidation was the dominating reaction. As oxidation is a much faster and exothermic reaction, higher gasification efficiency can be expected with this catalyst (Pérez-Hernández et al. 2007; Godula-Jopek et al. 2012).

In Figure 5.3(a), a marginal increase in H₂:CO ratio of the product gas can be observed with increase in C/O ratio over Re-Ni catalyst. Higher H₂:CO ratios can be explained by a shift in the dominant reactions from oxidation to steam reforming and water gas shift reactions under low oxygen feed conditions. When using Ru-Ni and Rh-Ni as catalysts, the ratio of H₂:CO in the product gas decreased with the increase in C/O ratio. This implies that under high C/O ratio reaction conditions, Ru-Ni and Rh-Ni catalyst are less effective in promoting steam reforming and water gas shift reactions. Increase in C₂ products and char yields also suggest that the reactions over Ru-Ni and Rh-Ni suffered with slower thermal decomposition reaction.

In Figure 5.3(b) a slight increase in CO:CO₂ ratio was observed with increase in C/O ratio in all Re-Ni runs, which is insignificant. With Rh-Ni and Ru-Ni as catalysts, increase C/O feed ratio led to increase in CO:CO₂ ratio, due to incomplete gasification.

Overall, the gasification efficiency of promoted nickel catalyst in RFV of pinewood sawdust was in the following order: Re-Ni > Rh-Ni > Ru-Ni. Only the Re-Ni catalyst was able to attain sustained operation at all three C/O ratios with negligible amount of char formed for a long period of time (>240 min).

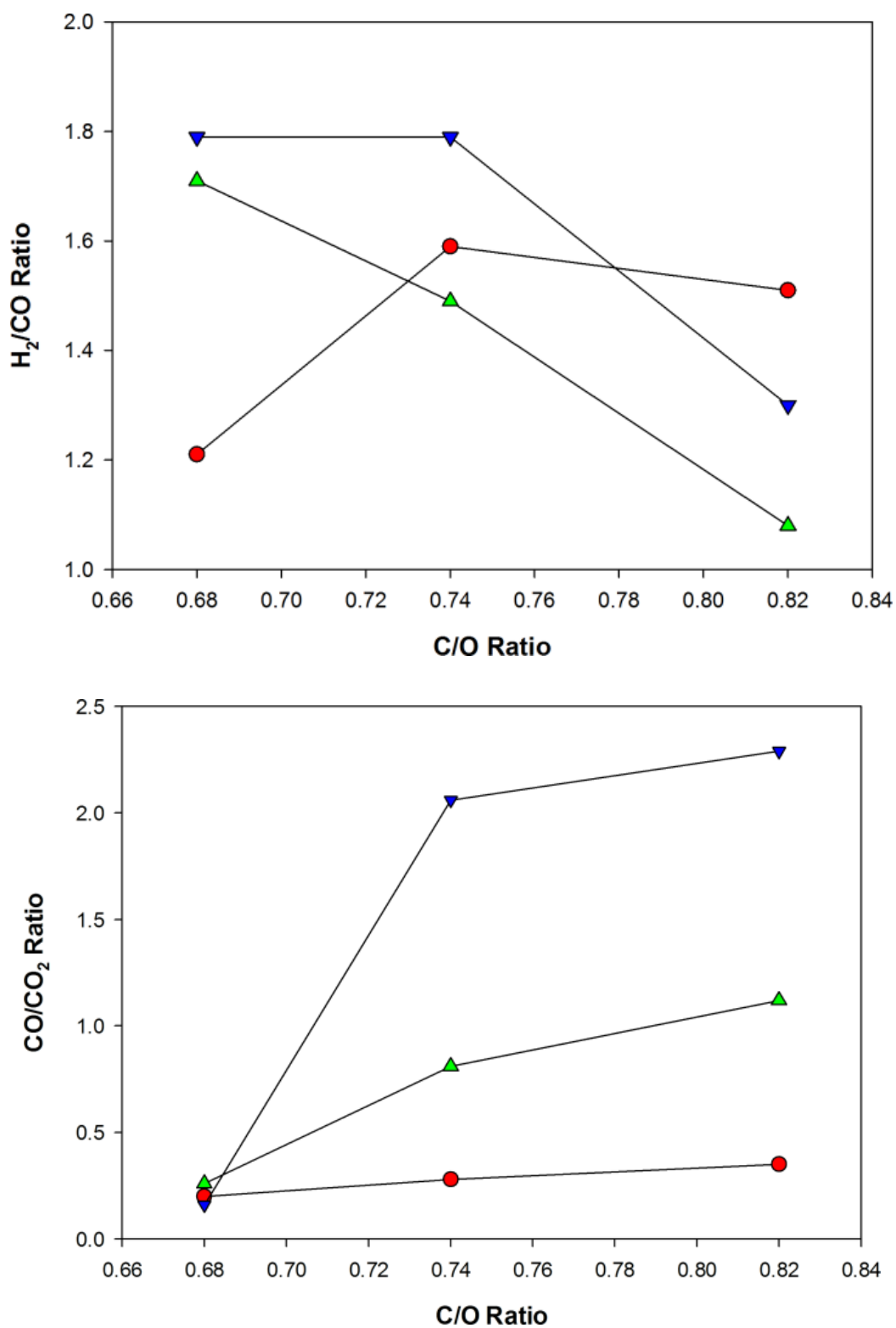


Figure 5. 3- Effect of carbon to oxygen ratio on a) H₂:CO ratio and b) CO:CO₂ ratio of promoted nickel based catalysts with alumina support at temperature of 750°C and C/S ratio of 1.17. (●) Re-Ni, (▼) Ru-Ni (▲) Rh-Ni.

5.3.3 Effect of carbon-to-steam ratio in RFV of Pinewood Sawdust

The effect of carbon to steam feed ratio (C/S) was tested on two promoted catalysts- Re-Ni and Rh-Ni. Ru-Ni catalyst was not considered for this study due to high char selectivity observed in previous section. In this study pinewood sawdust feed rate, reactor temperature and C/O ratio were kept constant at 15 g/h, 750°C and 0.74, respectively, whereas C/S ratio was varied between 0.59 and 2.35.

Results obtained from the various C/S ratio runs are plotted in Figure 5.4 and 5.5. Re-Ni catalyst was able to achieve gas yield of >99% in all C/S ratios. There was no char formed in any of the runs, with <1% of carbonaceous products in tar. The high gas conversion and low char formation can be attributed to the use of Re as promoter, which favours exothermic oxidation under these reaction conditions. Nonetheless, it is expected that the fraction of tar increases with increasing C/S ratio (lower steam) as the steam reforming activity is lower.

The gasification efficiency of Rh-Ni catalyst was lower in all C/S ratios. Product gas yield increased with C/S ratio and was the highest at C/S ratio of 1.17. However, all the runs resulted in sufficient char formation that caused partial clogging of the reactor. The lower catalytic activity can be attributed to the Rh promoter used, which is known to be more effective in promoting partial oxidation than complete oxidation (Eriksson et al. 2007; Horn et al. 2007). Because the energy produced from partial oxidation is at least an order of magnitude lower than complete oxidation, to gasify the same amount of pinewood, higher energy input (and hence higher temperature) would be needed in Rh-Ni catalysed RFV in comparison to Re-Ni. This demand for higher energy input was further compounded by the high amount of steam fed, which led to reduction in temperature due to the endothermic steam reforming reaction, therefore, resulted in incomplete gasification (i.e. char formation). The gasification efficiency increased with lower C/S ratio (i.e. higher steam feed rate) which suggests that lower steam reforming activity is beneficial in case of Rh-Ni catalyst.

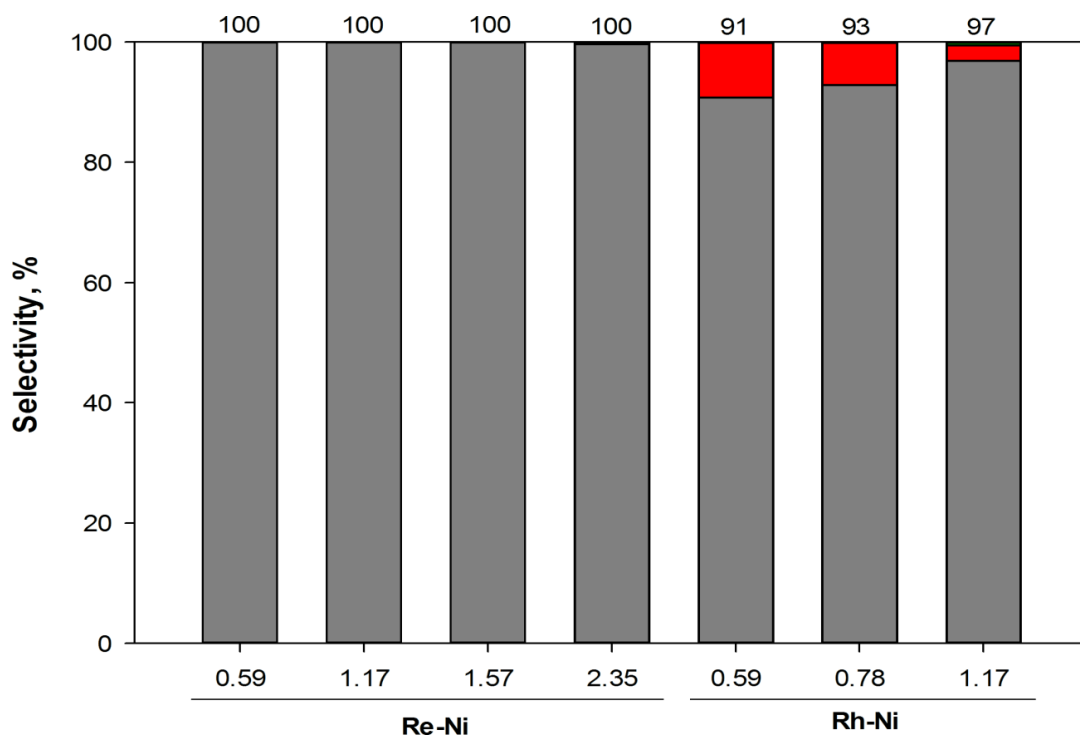


Figure 5. 4- Effect of C/S feed and catalyst promoters on the selectivity of gas (■), char (■) and tar (■) based on carbon balance. The numbers on the top of each bar represent gasification efficiency, which is the percentage of carbon in gas and tar combined. Reaction conditions: Pinewood sawdust flow rate= 15 g h⁻¹, 750 °C, C/O=0.74. Here tar is defined as water-soluble organics.

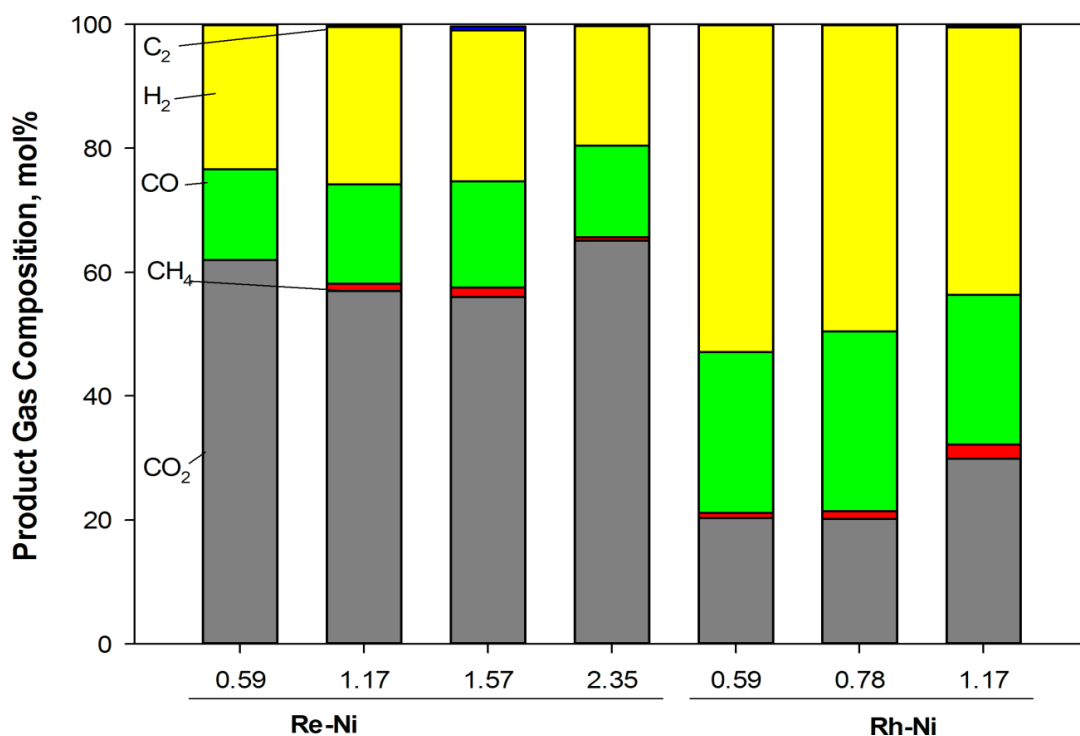


Figure 5. 5- Effect of C/S feed ratio and catalyst promoters on product gas composition. C₂ compounds include ethane, ethylene and acetylene. Reaction conditions: Pinewood sawdust flow rate= 15 g h⁻¹, 750 °C, C/O=0.74. Here tar is defined as water-soluble organics.

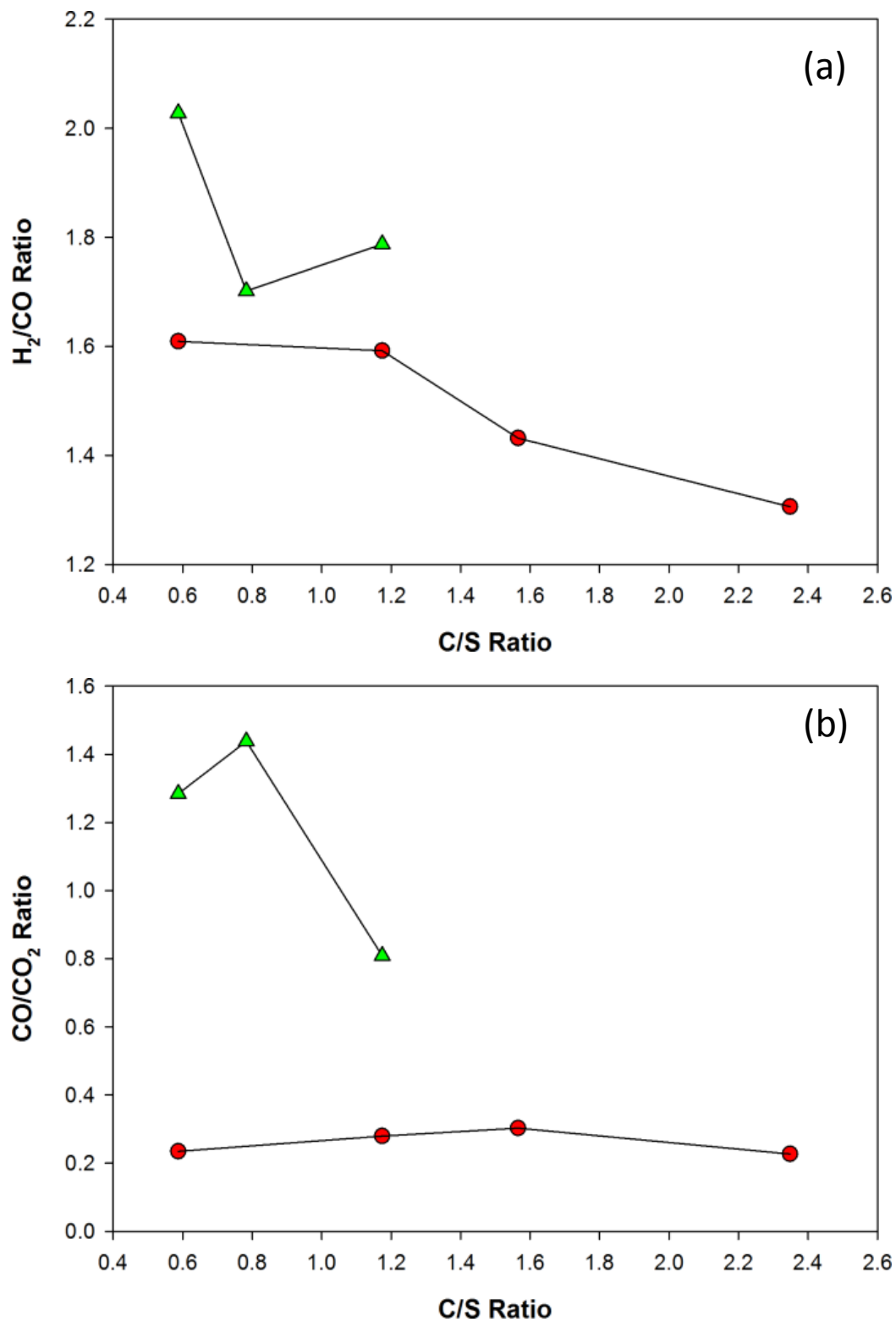


Figure 5. 6- Effect of carbon to steam ratio on a) H₂:CO ratio and b) CO:CO₂ ratio of promoted nickel based catalysts with alumina support at temperature of 750°C and C/O ratio of 0.74. (●) Re-Ni and (▲) Rh-Ni.

Although >99% of gas yield was achieved with Re-Ni catalyst, the quality of the product gas was poor. The product gas was rich in CO₂ (56 – 65%), followed by H₂ and CO (19 – 25% and 14 – 17%, respectively). The high CO₂ yield was resulted from the relatively low C/O ratio used in these experiments and the effectiveness of Re-Ni catalyst in promoting oxidation. Moreover, side reactions such as decarbonylation and decarboxylation, occurred under high steam fraction environment, may also contribute to the production of CO₂ and CO (Kantarelis et al. 2013).

Figure 5.6(a) shows H₂/CO decreases with increase in C/S ratio because of the reduction in water gas shift reaction activity under steam lean atmosphere. The decrease in H₂ yield can be seen with both catalysts as C/S ratio increased.

The effects of C/S ratio on CO/CO₂ ratio in the product gas varied with the type of noble metal promoter used. The CO/CO₂ ratio in the product gas of all Re-Ni runs were unaffected by the change in C/S ratio (Figure 5.6(b)). However, with Rh-Ni catalyst, a clear reduction in CO/CO₂ ratio is observed at high C/S ratio. This difference is believed to be because Re-Ni catalyst is more effective in promoting complete oxidation compared to Rh-Ni. Under the oxygen rich environment (C/O = 0.74), oxidation reaction dominated the complex reaction scheme in the RFV catalysed by Re-Ni catalyst. Whereas, partial oxidation and steam reforming reaction were favoured over Rh-Ni catalyst, which led to the strong correlation between C/S feed ratio and CO/CO₂ product ratio.

In summary, Rh-Ni runs were found to be more affected by the C/S feed ratio compared to Re-Ni runs. Since Re can exhibit multiple oxidation states, working in oxygen rich condition had little impact from the variation in C/S ratio. Overall, these results have showed that change in C/S ratio only has minimal effect in improving the final product gas composition under oxygen rich conditions.

5.3.4 Effect of Feedstock and Alkali and Alkaline Earth Metallic in RFV of Biomass

To study the effect of feedstock, and alkali and alkaline earth metals (AAEM) in RFV, a comparison between pinewood and eucalyptus sawdust gasification is presented, since these two feedstocks had very different ash proportion and composition. As seen in Table 5.1, ash content of the eucalyptus sawdust used in this study was ~9 times higher than the pinewood sawdust. In this experiment, the eucalyptus sawdust feed rate was kept the same as in previous section at 15 g/h, while the oxygen was fed at the rate of 143 (C/O= 0.77), 158 (C/O= 0.70) and 173 SCCM (C/O= 0.64), respectively. Reactor temperature and C/S ratio for these runs were kept constant at 750°C and 1.11, respectively. Because of its high char selectivity reported in previous two sections, Rh-

Ni catalyst was of particular interest in this study. Therefore, three out of the four runs were conducted with Rh-Ni catalyst to find out the effects of ash content on final product distribution, particularly in gas and char yields.

The results (Figure 5.7 and 5.8) showed that all the three runs with Rh-Ni had >97% gas yield using eucalyptus sawdust as feedstock with no char formation. A comparison of char yield from RFV of cellulose, pinewood sawdust and eucalyptus sawdust under similar reaction conditions and Rh-Ni as catalyst is shown in Figure 5.9. The effect of biomass ash content on enhancing char gasification can be clearly seen. RFV of cellulose (no ash) and pinewood sawdust (~1% ash) resulted in significant char formation at high C/O ratios of >0.6. However, no char formation was found in RFV of eucalyptus sawdust (~10% ash) even at C/O of 0.77. This confirms that AAEM in biomass play a critical role in enhancing char gasification as mentioned in 5.3.2. As for Re-Ni catalyst, result was consistent with previous finding that >99% of gas yield was attained.

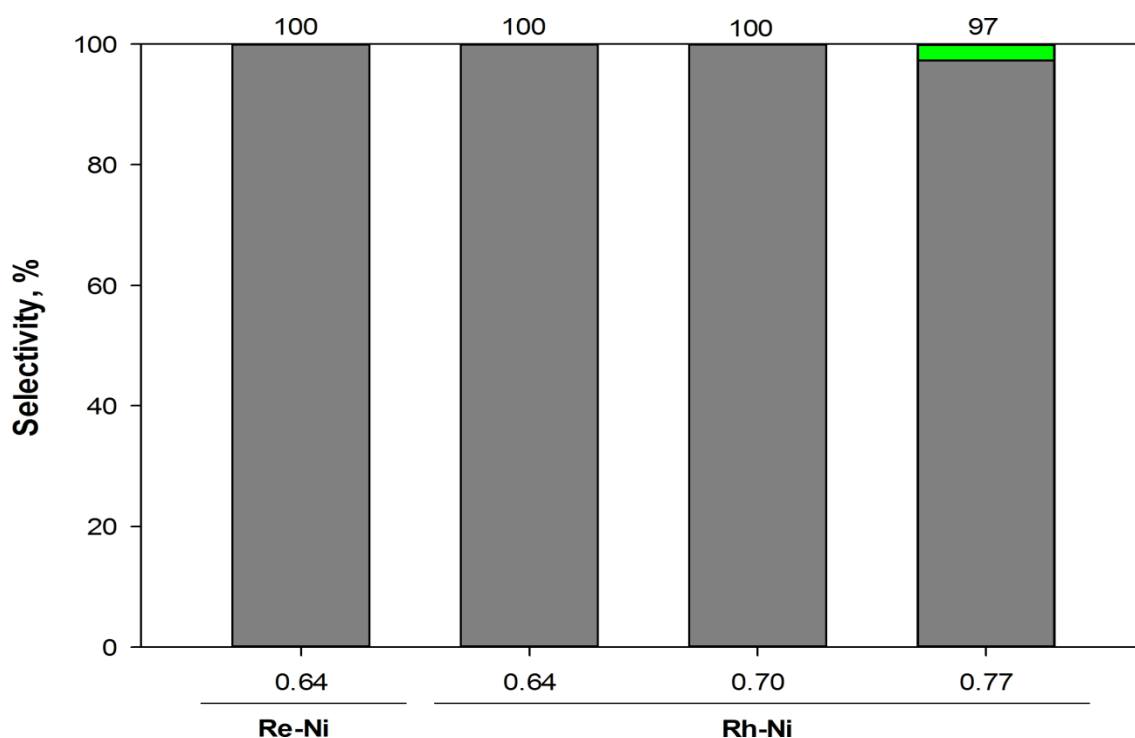


Figure 5. 7- Effect of C/O ratio in RFV of eucalyptus sawdust on the selectivity of gas (■), char (■) and tar (■) based on carbon balance. The numbers on the top of each bar represent gasification efficiency, which is the percentage of carbon in gas and tar combined. Reaction conditions: Eucalyptus sawdust flow rate= 15 g h⁻¹, 750 °C, C/S=1.11. Here tar is defined as water-soluble organics.

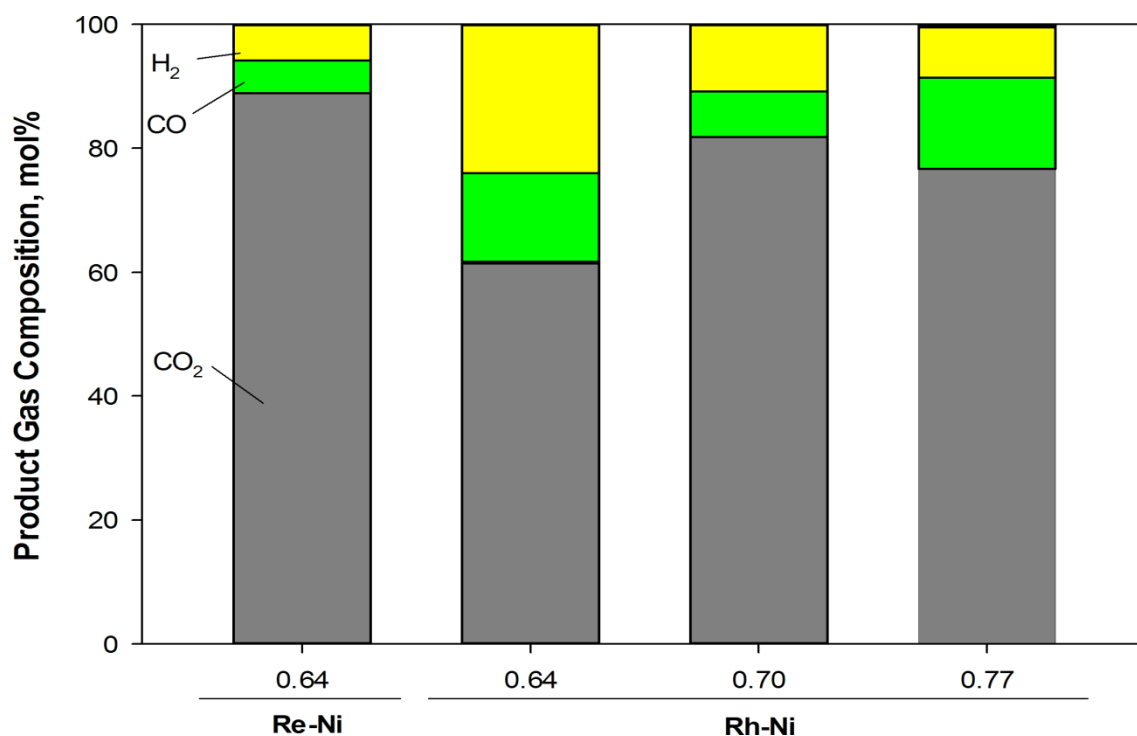


Figure 5. 8- Effect of C/O ratio in RFV of eucalyptus sawdust on product gas composition. C₂ compounds include ethane, ethylene and acetylene. Reaction conditions: Eucalyptus sawdust flow rate= 15 g h⁻¹, 750 °C, C/S=1.11. Here tar is defined as water-soluble organics.

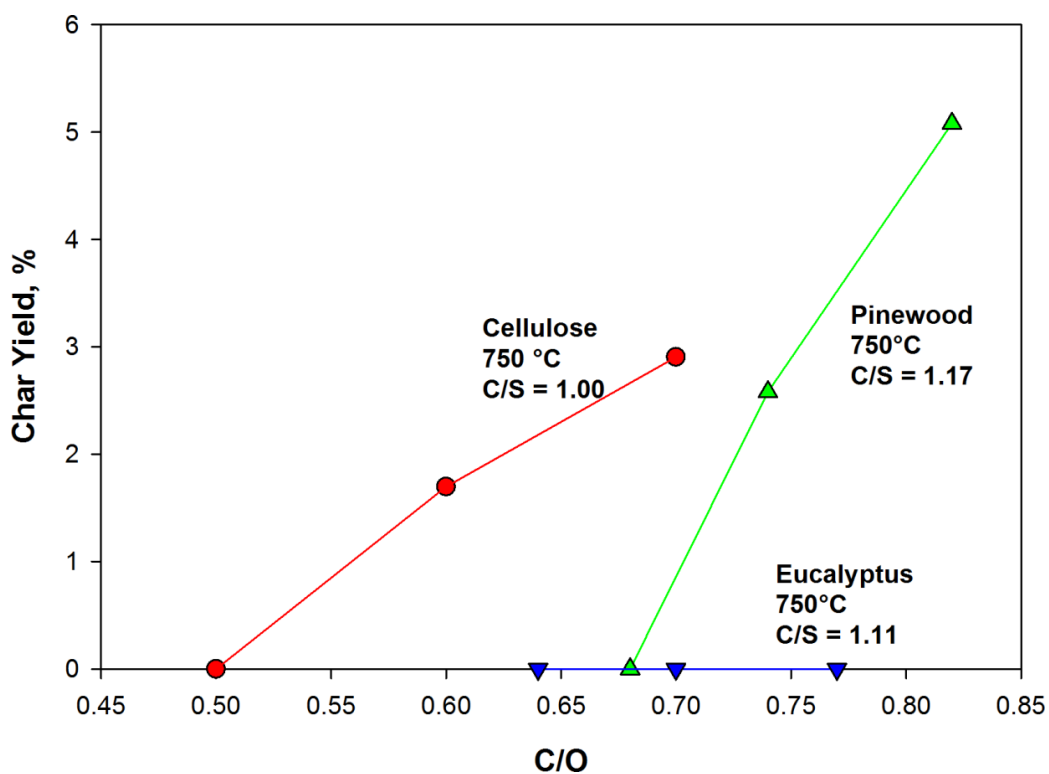


Figure 5. 9- Compare char yield of different biomass feedstock.

The difference in gas and char yields observed in eucalyptus RFV can be explained by several reasons. Firstly, the variation in composition of cellulose, hemicellulose, lignin and ash in eucalyptus and pinewood sawdust lead to different thermal degradation behaviour in RFV. Secondly, differences in AAEM composition of biomass result in different catalytic effects in RFV, which leads to different product distribution. Lastly, higher concentration of AAEM species retained in char further increases the rate of char gasification.

5.3.4.1 Biomass Composition

Typically, eucalyptus contains 15–17 wt% hemicellulose, 38–49 wt% cellulose and 28–31 wt% lignin (Dekker 1987; KibbleWhite et al. 2000; Brink et al. 2012) in comparison to pinewood which contains 16–23 wt% hemicellulose, 37–51 wt% cellulose and 23–31 wt% lignin (Dekker 1987; Wong et al. 1988; Ferraz et al. 2000). Higher hemicellulose and lignin content increases the rate of pyrolytic decomposition as discussed in section 5.3.2 (Chan et al. 2015). Moreover, hemicellulose and lignin in softwood and hardwood contains different types of compounds that can contribute to the different decomposition behaviour. Pinewood hemicellulose contains galactoglucomannans, mannose and galactose units while eucalyptus hemicellulose contains glucuronoxylan, xylan and acetyl groups (Stewart et al. 1953; Timell 1967; Dekker 1987; Grønli et al. 2002; Koch 2008; Reyes et al. 2013). Grønli et al. study has reported faster devolatilisation rate and lower char yield in hardwood hemicellulose pyrolysis.

Woody lignin aromatic nuclei can be generally categorised into two types: guaiacyl (4-hydroxy-3-methoxyphenyl) and syringyl (3,5-dimethoxy-4-hydroxyphenyl). Softwood lignin has only guaiacyl type whereas hardwood lignin has both guaiacyl and syringyl types (Fang et al. 2008; Asmadi et al. 2011). It has been reported in numerous studies that hardwood lignin devolatilise at lower temperature and using less energy in comparison to softwood lignin (Di Blasi et al. 2001; Asmadi et al. 2012). Several theories have been proposed to explain this characteristic. Li et al. study has reported that only the syringyl lignin has positive effect in promoting cell wall degradation, mainly resulting from the physicochemical changes of lignin with more linear structure of syringyl sub-units (Li et al. 2010). Moreover, guaiacyl rich lignin has a higher softening point and much harder to depolymerise in comparison to syringyl rich lignin due to its branched structure and higher degree of polymerization (Stewart et al. 2009).

5.3.4.2 Effect of AAEM on Tar Destruction

Thermal polymerisation of anhydro-monosaccharides (i.e. levoglucosan) into polymers followed by successive dehydration is identified as one of the mechanisms of char production (Kawamoto et al. 2003; Lin et al. 2009). Because eucalyptus sawdust is rich in K, Mg and Cl, metal oxides and salts such as K_2O , KCl, MgO and Mg_2Cl may be formed during RFV. These alkali oxides and salts are known to be effective in promoting the decomposition of tar and levoglucosan into low molecular weight species, such as CO_2 , CO and water (Patwardhan et al. 2010; Yildiz et al. 2015). In fact, MgO and K_2O have been long known for their excellent capabilities in lowering tar formation in biomass gasification (Abu El-Rub et al. 2004).

5.3.4.3 Effect of AAEM on Char Gasification

Eucalyptus sawdust's ash was ~9 times higher than pinewood sawdust. The higher concentration of AAEM species, particularly K and Ca, retained in biochar enhances the char gasification reactivity by reducing the gasification onset temperature (Kajita et al. 2010; Yip et al. 2010; Mitsuoka et al. 2011). Therefore, higher catalytic activity of char gasification can be expected from this eucalyptus biochar.

Although ash helps to lower the char yield, high ash content biomass makes a less desirable fuel due to the lower heating value of its gas product (Demirbas 2005). As shown in Figure 5.8, 61.4 – 81.8% of the product gas generated in Rh-Ni runs was CO_2 . High calorific gas components such as H_2 and CO only accounted for 8.2 – 24.0% and 7.4 – 14.7% respectively. This may be explained by oxidation reaction triggered by AAEM self-ignition at high temperatures under O_2 rich environment. Majority of the AAEM in eucalyptus (Mg, Ca, K, P and S) have relatively low ignition temperatures. Therefore, under the operating condition of RFV, AAEM and its derivatives can self-ignite and propagate combust in the product gas stream, leading to high CO_2 and water vapour production. In comparison to RFV of pinewood, RFV of eucalyptus resulted in increase in CO_2 yield by 51.8% and 92.7% using Re-Ni and Rh-Ni catalysts, respectively under similar reaction conditions.

The effect of biomass ash content on product gas composition during RFV can be seen in Figure 5.10. Using similar reaction conditions, CO_2 yield increased with ash content in biomass feedstock whereas other gas components such as H_2 , CO, CH_4 and C_2 compound yields decreased. Higher condensate yield (i.e, water) was also observed, which suggests that the major reactions in RFV of eucalyptus sawdust were decarboxylation and oxidation, which are partly promoted by ash elements (Sekiguchi et al. 1984; Aho et al. 2013; Yildiz et al. 2015).

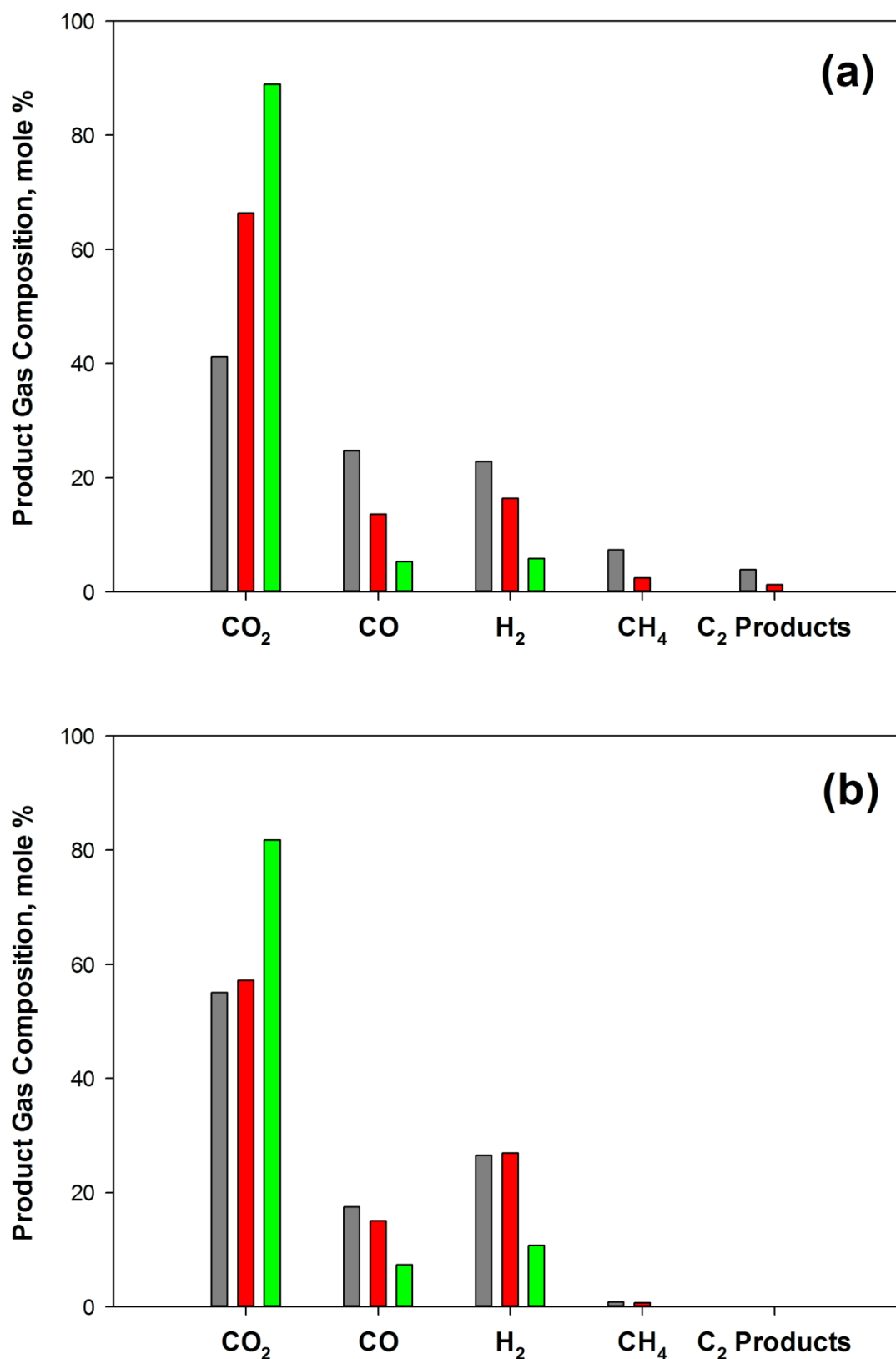


Figure 5. 10- Compare product gas composition of RFV with different biomass feedstocks at 750 °C. (a) Re-Ni (■ Cellulose, C/O-0.6, C/S-1.0, ■ Pinewood, C/O-0.68, C/S-1.17 and ■ Eucalyptus, C/O-0.64, C/S-1.11) (b) Rh-Ni (■ Cellulose, C/O-0.7, C/S-1.0, ■ Pinewood, C/O-0.68, C/S-1.17 and ■ Eucalyptus, C/O-0.7, C/S-1.11)

In comparison to the effect of AAEM, the effect of noble metal catalyst promoter on product distribution is insignificant. The catalytic effect of AAEM species is more dominant due to the high dispersion of AAEM species in the biomass feedstock. Because AAEM is encapsulated within the biomass, gasification reactions are catalysed by these species immediately after pyrolytic decomposition. In contrast, partial oxidation and steam reforming of bio-oil (produced *in-situ*), catalysed by the porous catalyst particles used in the fixed bed, are slower, which may result from the diffusion limitation.

In summary, RFV of ash rich biomass feedstock such as eucalyptus sawdust was dominated by the catalytic effects from the AAEM. However, these catalytic effects reduce the syngas quality by increasing CO₂ yield and lowering the calorific value.

5.3.5 Stability of catalyst

A comparison study of the catalyst stability used in RFV of pinewood and RFV of cellulose is presented in this section. As pointed out in Chapter 3, deactivation of catalyst may happen due to thermal or chemical treatments resulting in structural changes in the catalyst, such as catalyst support phase transformation, active metal agglomeration and/or oxidation, poisoning, and carbon fouling (Chan et al. 2014; Yildiz et al. 2015). Product gas evolution of two pinewood RFV runs with Re-Ni as catalyst, shown in Figure 5.11, suggested that the selectivity of the catalyst was shifting slowly towards methane and C₂ compounds instead of CO and H₂. Composition of methane and C₂ compounds gradually increased from 0% to 1% and 3%, respectively. Similar increase in methane and C₂ products were also observed with Ru-Ni and Rh-Ni catalysts. The increase in minor products production can be attributed to the catalyst deactivation caused by Ni metal sintering at temperatures above 700 °C and partial oxidation of Ni⁰ into NiO (Van Beurden 2004; Nahar et al. 2015). These minor products, particularly methane, are intermediate products produced directly from the decomposition of lignocellulose or hydrocarbons, which later are steam reformed into CO and H₂ on the catalyst (Garcia et al. 2000; Le Valant et al. 2010). However, when Ni metal is sintered/ oxidized, this reduces the active metal surface on the catalyst, and therefore, reduces the catalytic activity and leads to higher production of these minor products. Methane may also be produced from the hydrogenation of CO (methanation reaction), however, given the presence of steam and the high temperature reaction conditions used, this reaction is highly unfavourable. Poisoning by feedstock ash (i.e. sulphur) is another cause which may contribute to the deactivation of catalyst (Engelen et al. 2003; Abild-Pedersen et al. 2005).

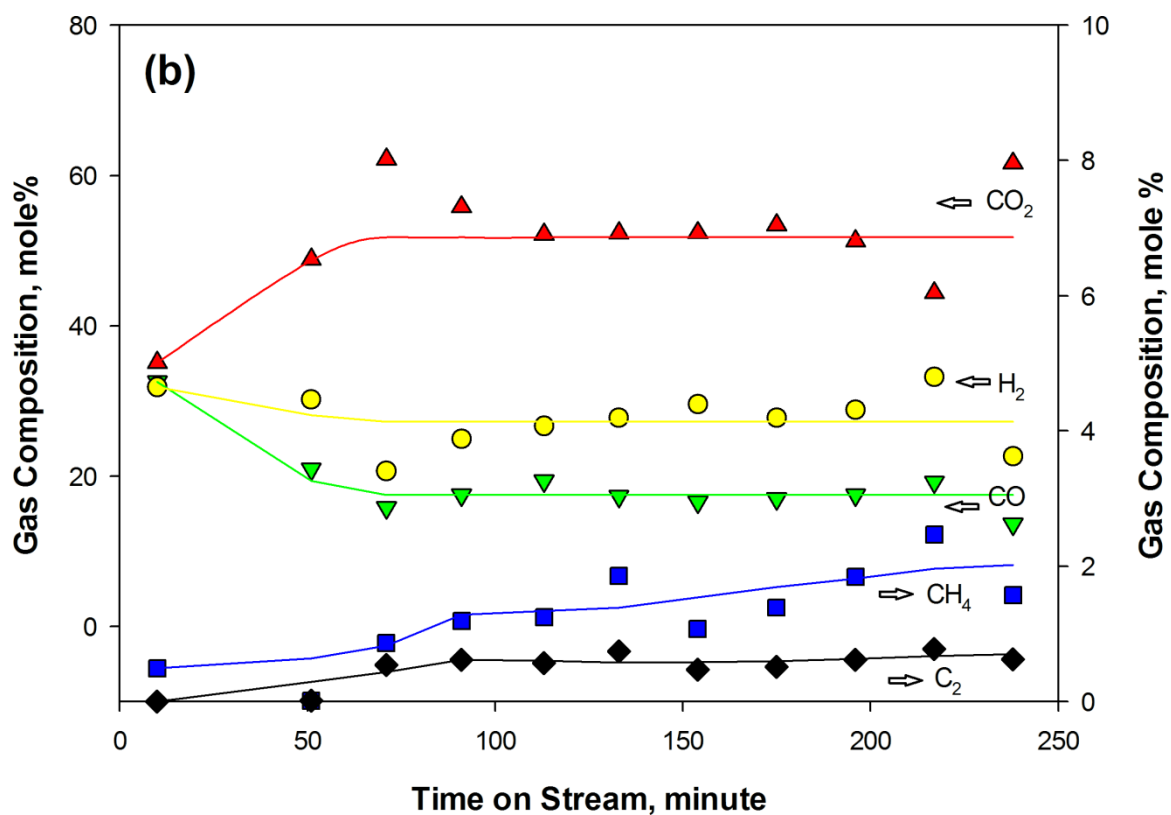
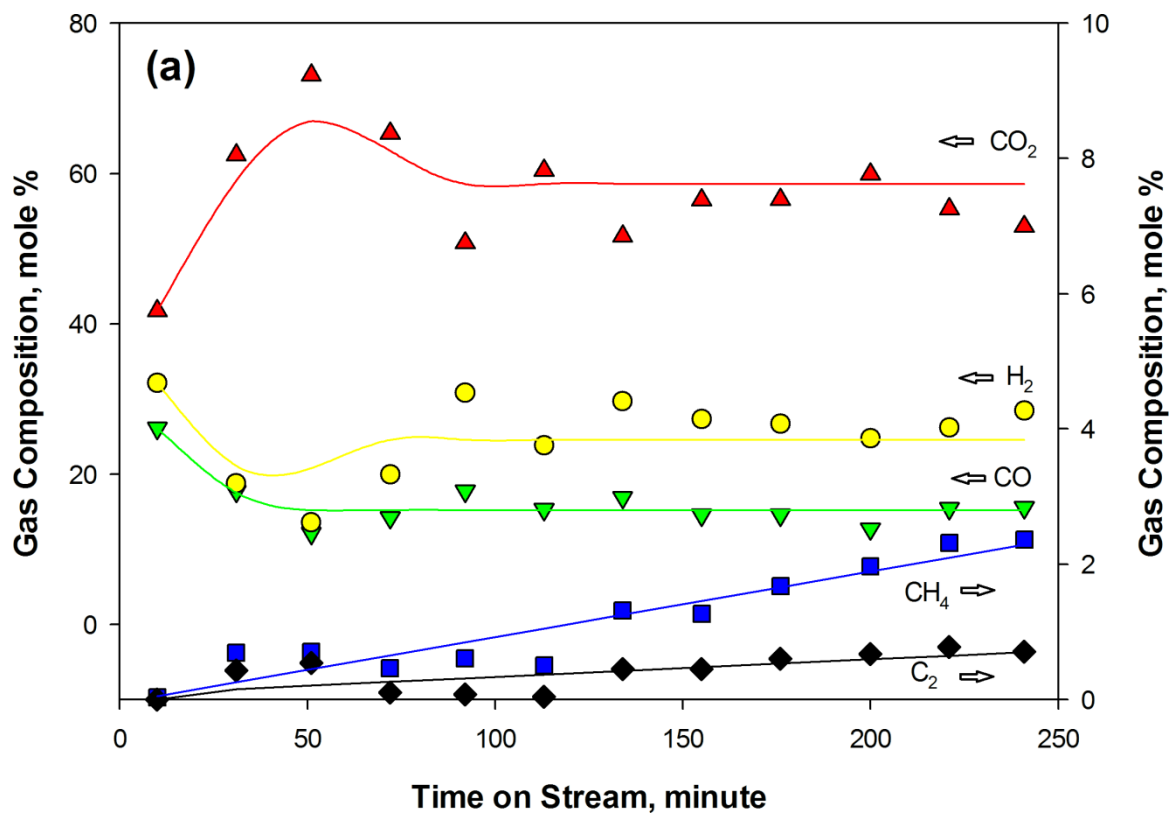


Figure 5. 11- Gas product evolutions over time on stream (a) Re-Ni C/O=0.74 (b) Re-Ni C/O=0.82.

Morphology of the fresh and spent Re-Ni and Rh-Ni catalysts was studied with a TEM and the results are shown in Figure 5.12. Unlike our previous finding in Chapter 3, the spent catalysts did not show significant change in their structure and no visible filamentous carbon deposition was found compared to the catalysts used in RFV of cellulose. However, some agglomeration may be seen in alumina particles of the spent catalyst. Partial phase transformation of γ -alumina into δ -alumina was confirmed in the XRD results (Figure 5.13), which may explain the slight agglomeration. Both fresh and used catalysts exhibit diffraction peaks at 2θ of 45.86° and 67.03° , which is a clear evidence of the existence of γ -alumina phase (JCPDS 10-0425, 29-0063 and 50-0741). However, new peaks appeared in the used catalysts at 2θ of 31.80° and 60.11° corresponding to δ -alumina (JCPDS 16-0394 and 46-1131). The freshly calcined catalysts do not exhibit δ -alumina peaks, suggesting that alumina partial phase transformation occurred during gasification process. As pointed out in Chapter 3, alumina phase transformation is primarily caused by steam rich hydrothermal conditions used in the experiments (Chan et al. 2014).

Diffraction peak corresponding to NiO (2 0 0) (JCPDS 71-1179) at 2θ of 43.28° can be seen in Figure 5.13 for the spent Re-Ni and Rh-Ni catalysts, but not for Ru-Ni catalyst. This suggests that nickel nanoparticles are partially re-oxidized into NiO, which is consistent with the observation of gradual shift in activity towards CH_4 and C_2 compounds during RFV experiments. Unlike Re-Ni and Rh-Ni catalysts, XRD pattern of the fresh and spent Ru-Ni catalyst showed a much weaker peak at 2θ of 43.28° , implies the low presence of NiO on the catalyst. Two theories have been postulated based on this observation. First, the addition of Ru may help to promote the formation of Ru-Ni alloy and resulted in reduction of active Ni substrate. Second, the presence of Ru in bimetallic Ni-Ru systems does not prevent the solid-state diffusion of Ni^{2+} ions into the $\gamma\text{-Al}_2\text{O}_3$ lattice, as suggested by Rynkowski et al. (Rynkowski et al. 1995). Both theories are plausible and may help to explain the poor performance of Ru-Ni catalyst in RFV observed in this study. However, further examinations using X-Ray absorption study (EXAFS) are needed to verify these hypotheses.

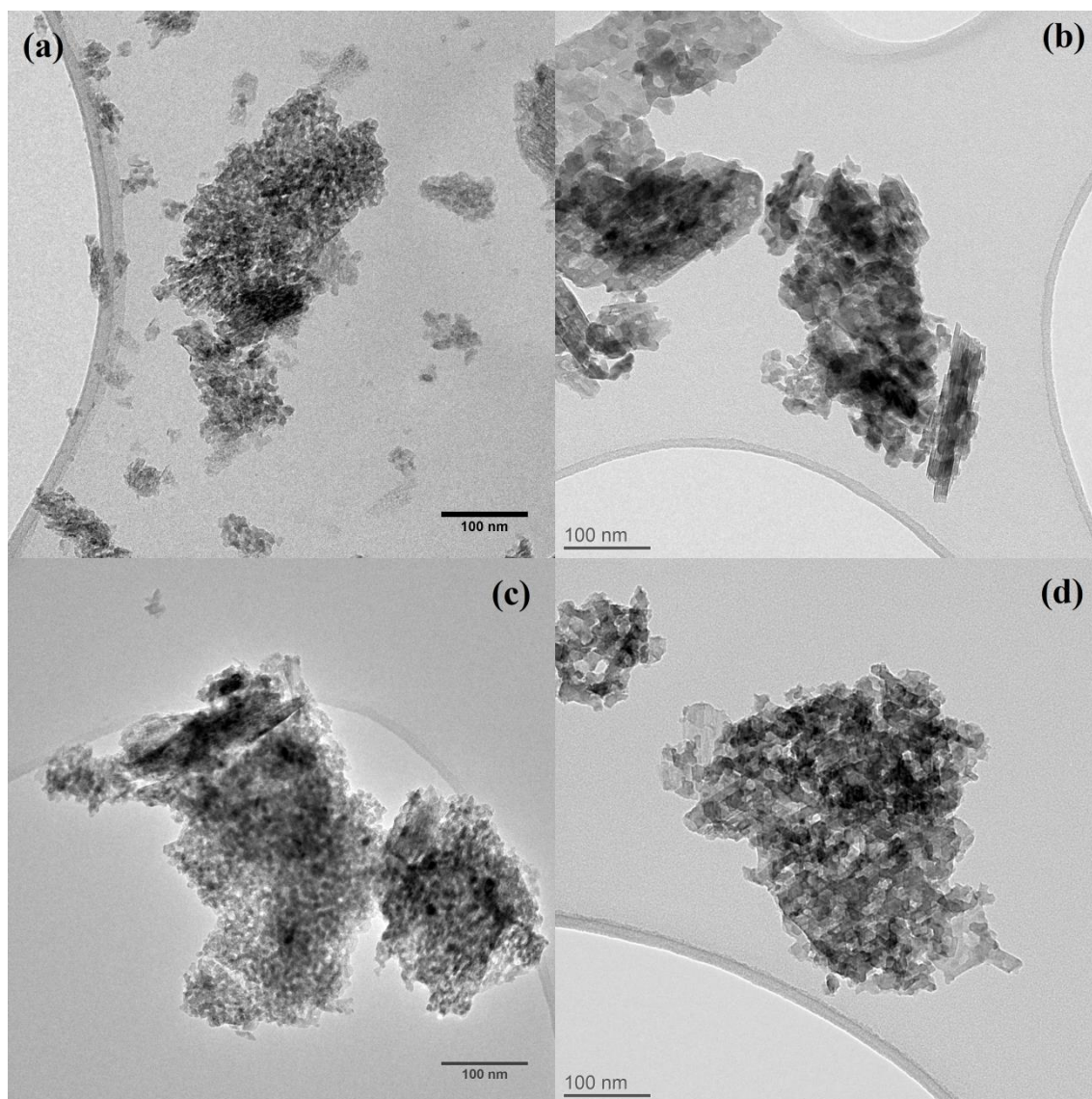


Figure 5. 12- TEM images of (a) Fresh Re-Ni catalyst. (b) Spent Re-Ni Catalyst from Pinewood RFV (750 °C, C/O- 0.68, C/S-1.17, Runtime- 255 min) (c) Fresh Rh-Ni (d) Spent Rh-Ni from Pinewood RFV (750 °C, C/O- 0.68, C/S-1.17, Runtime- 260 min). Scale bar = 100 nm.

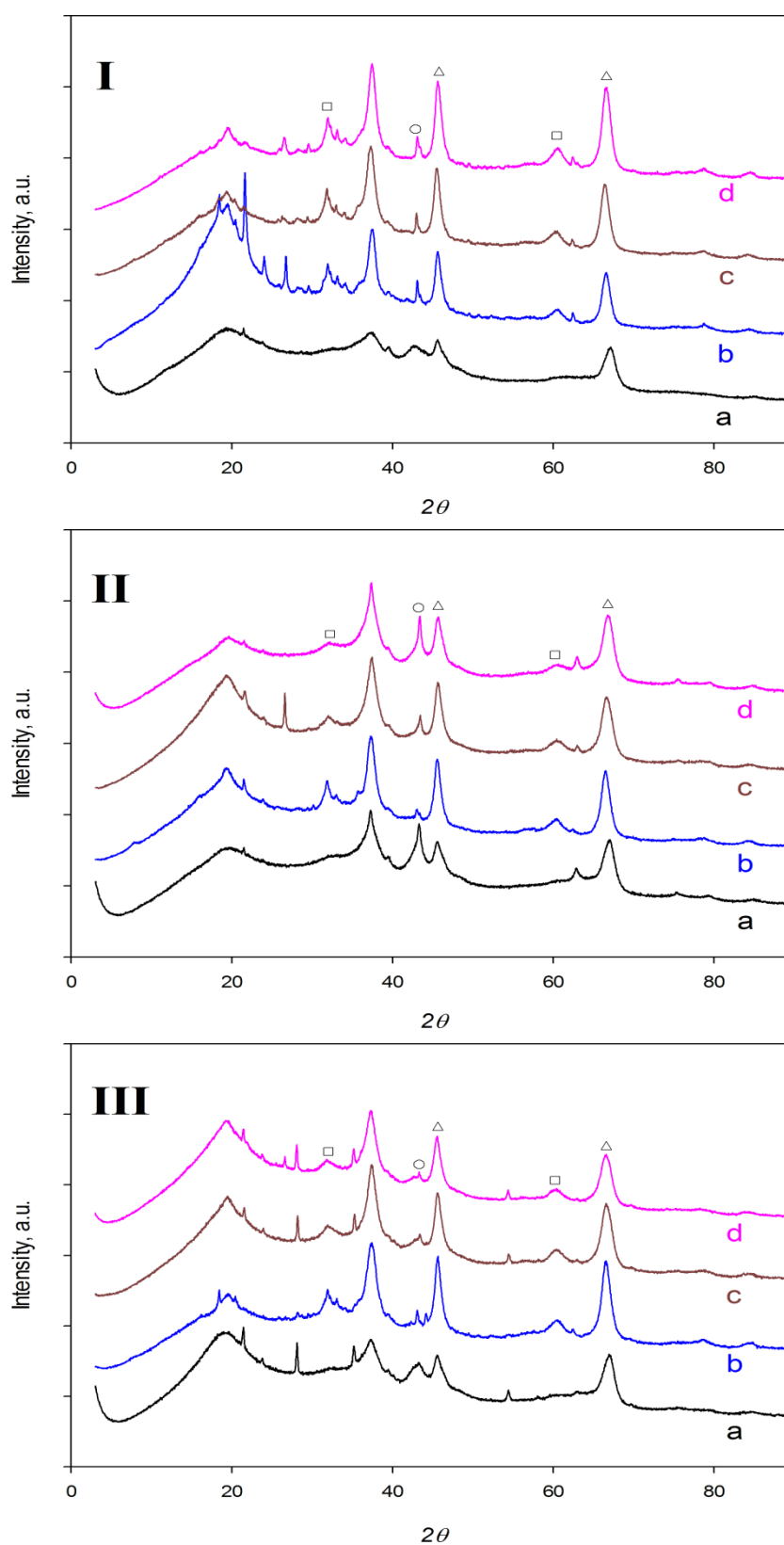


Figure 5. 13- Powder XRD patterns of Fresh and Spent Catalysts of Pinewood RFV- I) Re-Ni, II) Rh-Ni, III) Ru-Ni at different C/O ratios- a) Fresh Catalyst b) C/O-0.68 c) C/O-0.74 d) C/O-0.82. (Δ) γ -alumina (\square) δ -alumina (\circ) NiO.

EDS elemental mapping was carried out in scanning transmission electron microscopy (STEM) mode to study the distribution of metal nanoparticles on the freshly reduced catalysts and the spent catalysts, and to study the distribution of AAEM species on the spent catalysts to understand their interaction. Figure 5.14 illustrates freshly reduced promoted nickel catalysts, which clearly shows finely distributed metal nanoparticles throughout the entire alumina support. This figure confirms that the wet-impregnation technique used in this study was appropriate. EDS spectra of the freshly reduced Re-Ni and Rh-Ni catalysts are showed in Figure 5.17 (a) and (c), respectively. From the images, it can be said that the Ni and noble metal are co-located in the nanoparticles, possibly as solid solutions (alloys), however, Extended X-ray Absorption Fine Structure (EXAFS) study using a synchrotron source is required to confirm this.

Figure 5.15 and 5.16 show the mapping of various metals on the spent catalysts. These figures reveal that the potassium was finely distributed over catalyst surface but magnesium was phase segregated. This suggests that nickel nanoparticles may have strong interaction with K species during the RFV reaction. As a group 1A monovalent alkali metal, K is known to be highly reactive and electropositive (Abu El-Rub et al. 2004). It is particularly effective in promoting cellulose depolymerisation and steam gasification through interacting between carbon (solid) and steam (liquid) during gasification (Lizzio et al. 1991; Padban 2000). However, the high reactivity also poses another problem to the promoted nickel catalyst. Several reports have pointed out that K can react with Ni and causes deactivation in nickel catalyst by faceting the active Ni crystal planes to less active (111) plane (Rostrup-Nielsen et al. 1995; Berger et al. 1996; Cavallaro et al. 2003; Frusteri et al. 2004; Sugiura et al. 2005). In contrast, Mg was phase separated with nickel nanoparticles, which suggests that there was minimal interaction between these two species. Mg is less reactive in gasification compared to K (Kajita et al. 2010), partly due to its bivalent property and partly resulted from the chemical status in the feedstock (Keown et al. 2008). During the gasification/pyrolysis, the bivalent Mg may directly react with the biomass by forming two hydrocarbons–Mg bonds. As a result, to volatilize Mg species during gasification, simultaneous cleavage of these two bonds are required with higher energy intake as compared to only one bond in case of K (Ewsuk et al. 2010). Also, as one of the nutrients needed for plant growth, Mg tends to react with organic counter ions and form complexes which are bound inside the cell wall and organelles, whereas majority of K remains in ionic form (Keown et al. 2008). Because of this “caging effect”, it is much harder for the Mg to “break free” from the feedstock which explains its lower catalytic activity in gasification compared to K.

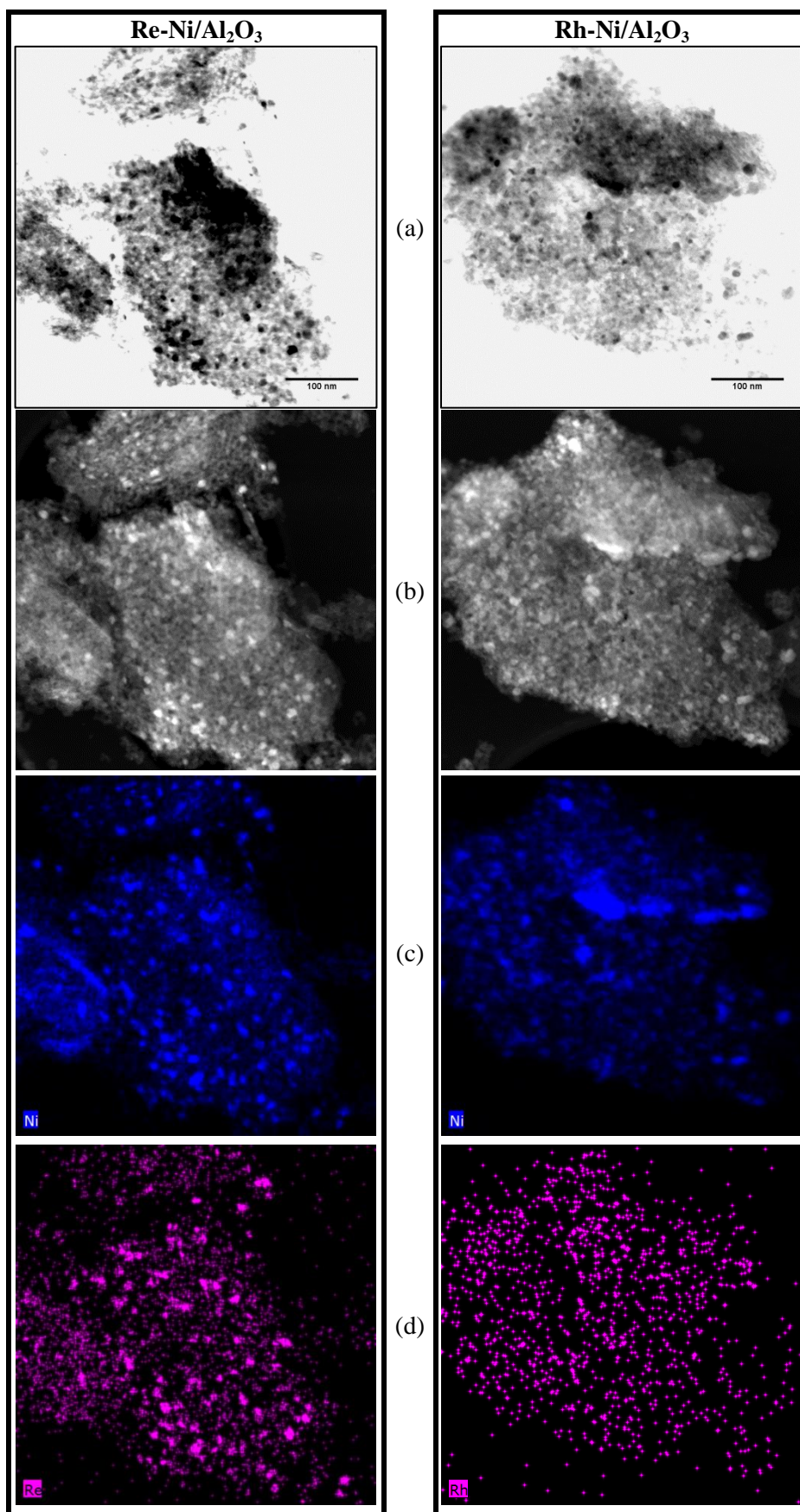


Figure 5. 14- (a) Bright field image, (b) dark field high angle annular dark field (HAADF) image and EDS elemental mapping of (c) Ni and (d) noble metal promoter on freshly reduced promoted nickel catalysts.

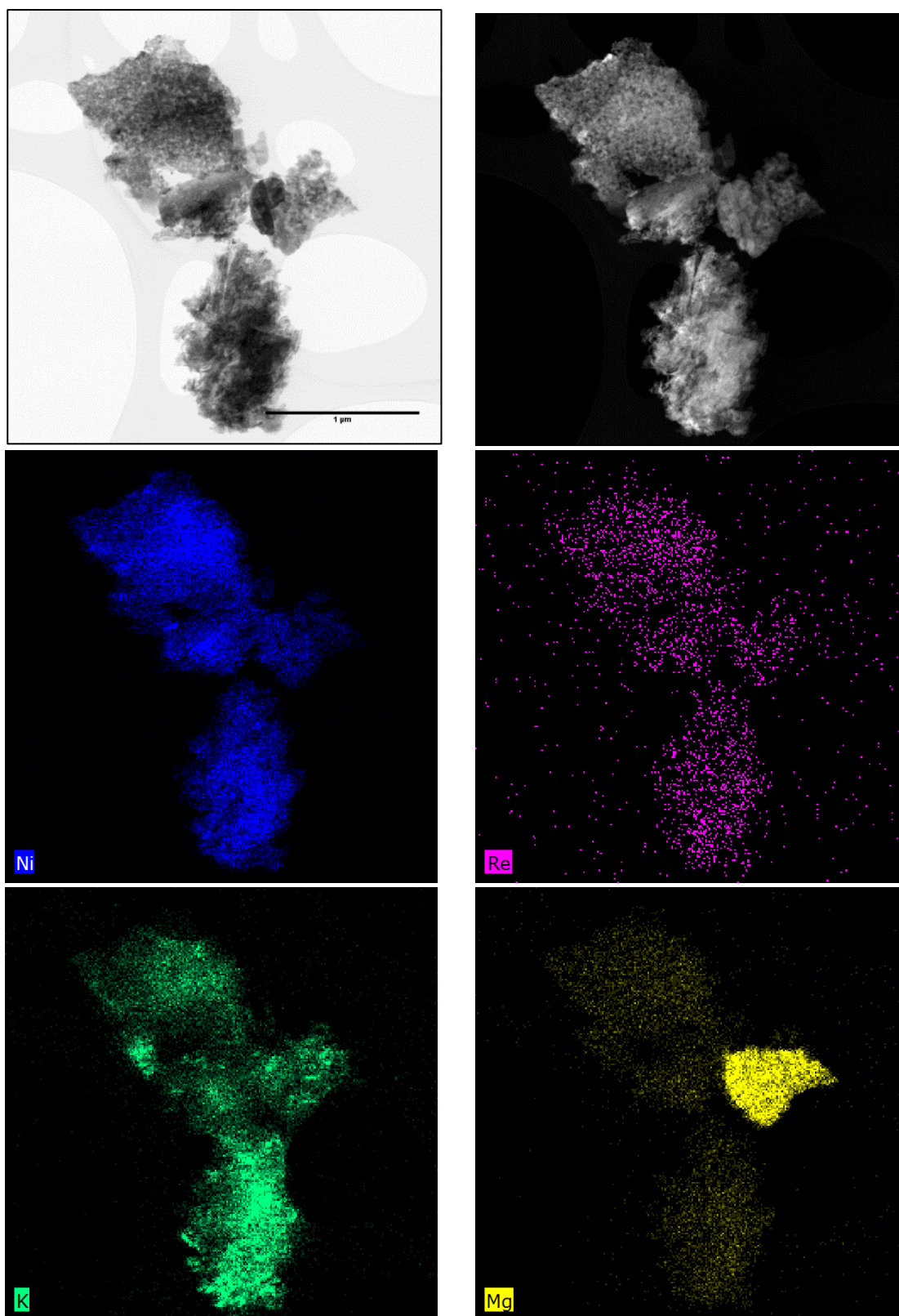


Figure 5. 15- Bright field, high angle annular dark field (HAADF) TEM images and TEM-EDS elemental distribution for Ni, noble metal promoter Re, K and Mg on spent Re-Ni catalyst from pinewood RFV. Reaction conditions: Pinewood flow rate= 15 g/h, Temperature= 750 °C, C/O= 0.68, C/S = 1.17 and Runtime= 255 min.

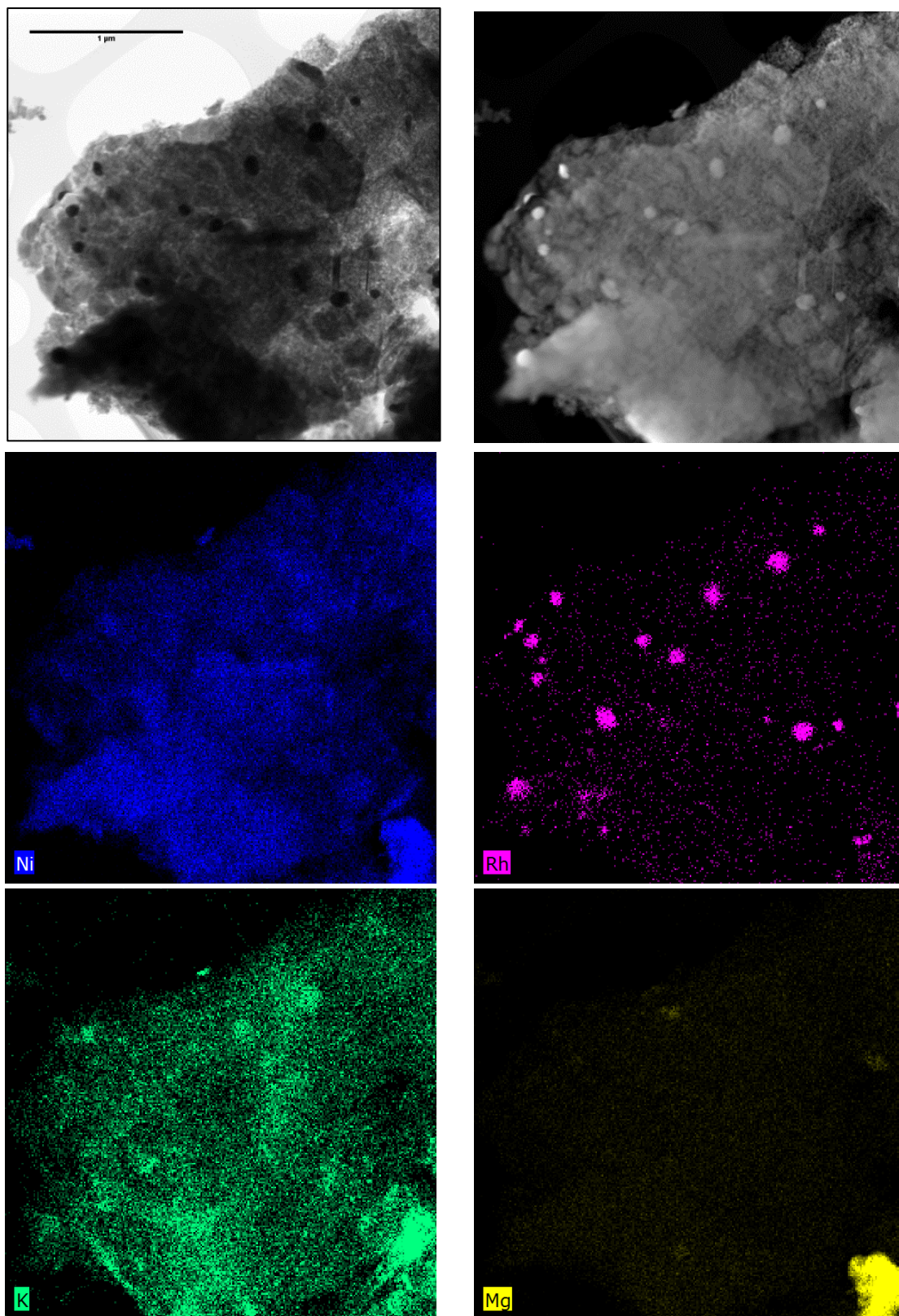


Figure 5. 16- Bright field, high angle annular dark field (HAADF) TEM images and TEM-EDS elemental distribution for Ni, noble metal promoter Rh, K and Mg on spent Rh-Ni catalyst from pinewood RFV. Reaction conditions: Pinewood flow rate= 15 g/h, Temperature= 750 °C, C/O= 0.68, C/S = 1.17 and Runtime= 260 min.

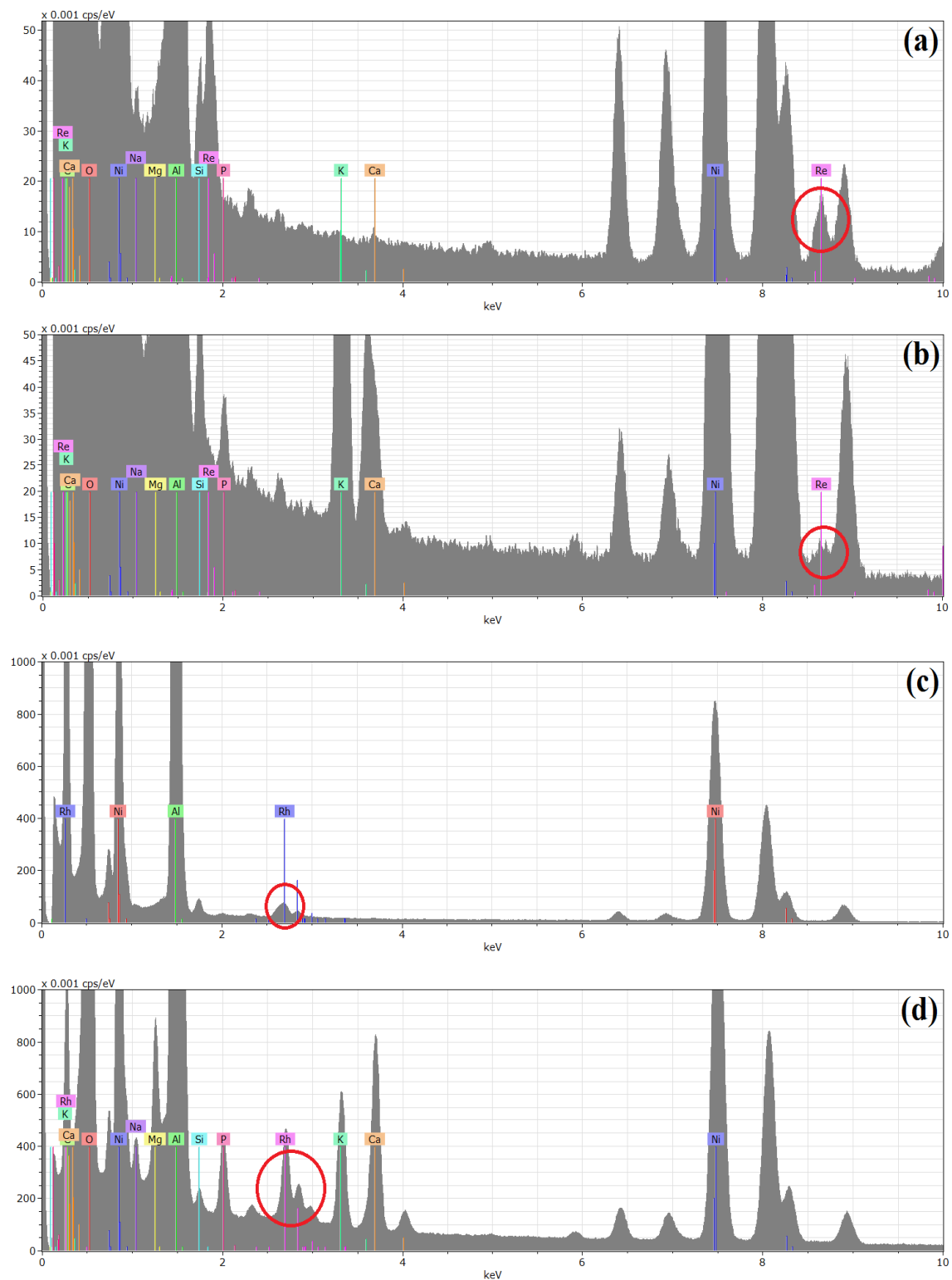


Figure 5.17- TEM-EDS spectra of: (a) freshly reduced Re-Ni catalyst (b) Spent Re-Ni catalyst from pinewood RFV (Temp= 750 °C, C/O= 0.68, C/S = 1.17, TOS= 255 min) (c) freshly reduced Rh-Ni catalyst (d) Spent Rh-Ni catalyst from pinewood RFV (Temp= 750 °C, C/O= 0.68, C/S = 1.17, TOS= 260 min).

From Figure 5.15, it can be seen that the amount of Re detected on the spent Re-Ni catalyst was lower than fresh Re-Ni catalyst, which is also illustrated in the EDS spectra (Figure 5.17 (a) and (b)). Re loss may be observed during high temperature reaction in the presence of excess oxygen due to the conversion of Re^0 into volatile Re heptoxide (Re_2O_7) (Bouchmella et al. 2015). This observation may also explain the gradual shift in product selectivity from CO to CH_4 observed during the RFV experiments. As can be seen in Figure 5.16, the Rh nanoparticles on the spent Rh-Ni catalyst after the RFV reaction were agglomerated, whereas the fresh catalysts had well dispersed Rh nanoparticles. The Rh nanoparticle grew from <10 nm (fresh) to ~ 150 nm clusters after approximately 260 min of run. This Rh^+ nanoparticles agglomeration, known as the reductive agglomeration, is induced by CO thermal desorption. Similar Rh^+ agglomeration has also been observed during steam reforming and hydrogenation reactions (Solymosi et al. 1988; Solymosi et al. 1990; Trautmann et al. 1994; Fonseca et al. 2003; Duarte et al. 2012). The increase in Rh nanoparticles size may reduce Rh-Ni catalytic activity, leading to char formation.

In summary, the extent of alumina phase transformation and carbon fouling of the promoted nickel catalysts were noticeably lower after RFV of pinewood and eucalyptus sawdust in comparison to RFV of cellulose. The deactivation of the catalyst mainly resulted from the partial oxidation of the nickel nanoparticles, sintering of Rh nanoparticles or partial loss of Re due to oxidation into volatile Re_2O_7 and partial loss of the surface area due to alumina phase transformation.

5.4 Conclusions

The gasification efficiency of promoted nickel catalyst in RFV of pinewood sawdust was in the following order: Re-Ni > Rh-Ni > Ru-Ni. Char free gasification was achieved with Re-Ni catalyst only at all the C/O ratios and C/S ratios in the RFV of pinewood and eucalyptus sawdust. Negligible quantity of carbon was detected in the condensate (tar + water) with all the catalysts tested in this part of the research. Higher catalytic activity was attributed to high metal dispersion of the active metals on the catalyst and high activity in promoting partial oxidation and reforming reactions.

Gasification efficiency of high ash content feedstock was found to be significantly higher than that of cellulose. This can be attributed to the effects of higher amorphous structure of lignocellulose compared to microcrystalline cellulose, and the catalytic effects of alkali and alkaline earth metals (AAEM) found in the lignocellulose ash. However, results from RFV of

Chapter 5

pinewood and eucalyptus sawdust showed that the oxygen rich conditions used in this study was not suitable for biomass containing significant ash, since the final product gas contained high CO₂ content with lower calorific value. This is especially true for Re-Ni catalysts since in the oxygen rich conditions, Re was partially lost due to volatilisation as Re₂O₇. Reactive flash volatilisation was catalysed by AAEMs and was found to be dominated by oxidation under these reaction conditions. Therefore, further studies under lower oxygen feed rate must be carried out. The noble metal promoters had lower effect on product yields and gas composition compared to cellulose gasification.

The deactivation of the promoted nickel catalyst used in this study was found to be substantially lower than the RFV of cellulose. Based on the XRD and TEM-EDS results, the main deactivation causes were the re-oxidation of the nickel nanoparticles, loss of surface area of Rh (sintering) and Re (volatilisation) and partially loss of the support surface area due to the alumina phase transformation.

5.5 References

- Abild-Pedersen, F., O. Lytken, et al. (2005). "Methane activation on Ni(111): Effects of poisons and step defects." *Surface Science* **590**: 127-137.
- Abu El-Rub, Z., E. A. Bramer, et al. (2004). "Review of Catalysts for Tar Elimination in Biomass Gasification Processes." *Industrial & Engineering Chemistry Research* **43**: 6911-6919.
- Aho, A., N. DeMartini, et al. (2013). "Pyrolysis of pine and gasification of pine chars – Influence of organically bound metals." *Bioresource Technology* **128**: 22-29.
- Alvira, P., E. Tomás-Pejó, et al. (2010). "Pretreatment technologies for an efficient bioethanol production process based on enzymatic hydrolysis: A review." *Bioresource Technology* **101**: 4851-4861.
- Asmadi, M., H. Kawamoto, et al. (2011). "Thermal reactions of guaiacol and syringol as lignin model aromatic nuclei." *Journal of Analytical and Applied Pyrolysis* **92**: 88-98.
- Asmadi, M., H. Kawamoto, et al. (2012). "The effects of combining guaiacol and syringol on their pyrolysis." *Holzforschung* **66**: 323-330.
- Bals, B., C. Wedding, et al. (2011). "Evaluating the impact of ammonia fiber expansion (AFEX) pretreatment conditions on the cost of ethanol production." *Bioresource Technology* **102**: 1277-1283.
- Berger, R. J., E. B. M. Doesburg, et al. (1996). "Nickel catalysts for internal reforming in molten carbonate fuel cells." *Applied Catalysis A: General* **143**: 343-365.
- Bouchmella, K., M. Stoyanova, et al. (2015). "Avoiding rhenium loss in non-hydrolytic synthesis of highly active Re–Si–Al olefin metathesis catalysts." *Catalysis Communications* **58**: 183-186.
- Brink, M. and E. G. Achigan-Dako (2012). *Fibres*, PROTA Foundation.
- Cavallaro, S., V. Chiodo, et al. (2003). "Performance of Rh/Al₂O₃ catalyst in the steam reforming of ethanol: H₂ production for MCFC." *Applied Catalysis A: General* **249**: 119-128.
- Chan, F. L. and A. Tanksale (2014). "Catalytic Steam Gasification of Cellulose Using Reactive Flash Volatilization." *ChemCatChem* **6**: 2727-2739.
- Chan, F. L. and A. Tanksale (2014). "Review of recent developments in Ni-based catalysts for biomass gasification." *Renewable and Sustainable Energy Reviews* **38**: 428-438.
- Chan, F. L., K. Umeki, et al. (2015). "Kinetic Study of Catalytic Steam Gasification of Biomass by Using Reactive Flash Volatilisation." *ChemCatChem* **7**: 1329-1337.
- Dekker, R. F. H. (1987). "The utilization of autohydrolysis-exploded hardwood (eucalyptus regnans) and softwood (pinus radiata) sawdust for the production of cellulolytic enzymes and fermentable substrates." *Biocatalysis and Biotransformation* **1**: 63-75.
- Demirbas, A. (2005). "Potential applications of renewable energy sources, biomass combustion problems in boiler power systems and combustion related environmental issues." *Progress in Energy and Combustion Science* **31**: 171-192.
- Devi, L., K. J. Ptasinski, et al. (2003). "A review of the primary measures for tar elimination in biomass gasification processes." *Biomass Bioenergy* **24**: 125-140.

Chapter 5

Di Blasi, C., C. Branca, et al. (2001). "Pyrolytic behavior and products of some wood varieties." Combustion and Flame **124**: 165-177.

Di Blasi, C., A. Galgano, et al. (2009). "Influences of the Chemical State of Alkaline Compounds and the Nature of Alkali Metal on Wood Pyrolysis." Industrial & Engineering Chemistry Research **48**: 3359-3369.

Duarte, R. B., M. Nachttegaal, et al. (2012). "Understanding the effect of Sm₂O₃ and CeO₂ promoters on the structure and activity of Rh/Al₂O₃ catalysts in methane steam reforming." Journal of Catalysis **296**: 86-98.

Engelen, K., Y. Zhang, et al. (2003). "A novel catalytic filter for tar removal from biomass gasification gas: Improvement of the catalytic activity in presence of H₂S." Chemical Engineering Science **58**: 665-670.

Eriksson, S., S. Rojas, et al. (2007). "Effect of Ce-doping on Rh/ZrO₂ catalysts for partial oxidation of methane." Applied Catalysis A: General **326**: 8-16.

Ewsuk, K., M. Naito, et al. (2010). Characterization and Control of Interfaces for High Quality Advanced Materials III: Ceramic Transactions, Wiley.

Fang, Z., T. Sato, et al. (2008). "Reaction chemistry and phase behavior of lignin in high-temperature and supercritical water." Bioresource Technology **99**: 3424-3430.

Ferraz, A., J. Baeza, et al. (2000). "Estimating the chemical composition of biodegraded pine and eucalyptus wood by DRIFT spectroscopy and multivariate analysis." Bioresource Technology **74**: 201-212.

Fonseca, G. S., A. P. Umpierre, et al. (2003). "The Use of Imidazolium Ionic Liquids for the Formation and Stabilization of Ir⁰ and Rh⁰ Nanoparticles: Efficient Catalysts for the Hydrogenation of Arenes." Chemistry – A European Journal **9**: 3263-3269.

Frusteri, F., S. Freni, et al. (2004). "Steam reforming of bio-ethanol on alkali-doped Ni/MgO catalysts: hydrogen production for MC fuel cell." Applied Catalysis A: General **270**: 1-7.

Garcia, L. a., R. French, et al. (2000). "Catalytic steam reforming of bio-oils for the production of hydrogen: effects of catalyst composition." Applied Catalysis A: General **201**: 225-239.

Giudicianni, P., G. Cardone, et al. (2013). "Cellulose, hemicellulose and lignin slow steam pyrolysis: Thermal decomposition of biomass components mixtures." Journal of Analytical and Applied Pyrolysis **100**: 213-222.

Godula-Jopek, A., W. Jehle, et al. (2012). Hydrogen Storage Technologies: New Materials, Transport, and Infrastructure, Wiley.

Grønli, M. G., G. Várhegyi, et al. (2002). "Thermogravimetric analysis and devolatilization kinetics of wood." Industrial and Engineering Chemistry Research **41**: 4201-4208.

Horn, R., K. A. Williams, et al. (2007). "Methane catalytic partial oxidation on autothermal Rh and Pt foam catalysts: Oxidation and reforming zones, transport effects, and approach to thermodynamic equilibrium." Journal of Catalysis **249**: 380-393.

- Hosoya, T., H. Kawamoto, et al. (2007). "Cellulose-hemicellulose and cellulose-lignin interactions in wood pyrolysis at gasification temperature." Journal of Analytical and Applied Pyrolysis **80**: 118-125.
- Huber, G. W., S. Iborra, et al. (2006). "Synthesis of Transportation Fuels from Biomass: Chemistry, Catalysts, and Engineering." Chemical Reviews **106**: 4044-4098.
- Ison, E. A., J. E. Cessarich, et al. (2007). "Synthesis of cationic rhenium (VII) oxo imido complexes and their tunability towards oxygen atom transfer." Journal of the American Chemical Society **129**: 1167-1178.
- Kajita, M., T. Kimura, et al. (2010). "Catalytic and Noncatalytic Mechanisms in Steam Gasification of Char from the Pyrolysis of Biomass." Energy & Fuels **24**: 108-116.
- Kawamoto, H., H. Morisaki, et al. (2009). "Secondary decomposition of levoglucosan in pyrolytic production from cellulosic biomass." Journal of Analytical and Applied Pyrolysis **85**: 247-251.
- Kawamoto, H., M. Murayama, et al. (2003). "Pyrolysis behavior of levoglucosan as an intermediate in cellulose pyrolysis: polymerization into polysaccharide as a key reaction to carbonized product formation." Journal of Wood Science **49**: 469-473.
- Keown, D. M., J.-i. Hayashi, et al. (2008). "Effects of volatile-char interactions on the volatilisation of alkali and alkaline earth metallic species during the pyrolysis of biomass." Fuel **87**: 1187-1194.
- Kibblewhite, R. P., M. J. C. Riddell, et al. (2000). "Variation in wood, kraft fibre, and handsheet properties among 29 trees of *Eucalyptus regnans*, and comparison with *e. nitens* and *e. fastigata*." New Zealand Journal of Forestry Science **30**: 458-474.
- Koch, G. (2008). Raw Material for Pulp. Handbook of Pulp, Wiley-VCH Verlag GmbH: 21-68.
- Le Valant, A., N. Bion, et al. (2010). "Preparation and characterization of bimetallic Rh-Ni/Y₂O₃-Al₂O₃ for hydrogen production by raw bioethanol steam reforming: influence of the addition of nickel on the catalyst performances and stability." Applied Catalysis B: Environmental **97**: 72-81.
- Li, X., E. Ximenes, et al. (2010). "Lignin monomer composition affects Arabidopsis cell-wall degradability after liquid hot water pretreatment." Biotechnology for Biofuels **3**: 1-7.
- Lin, Y. C., J. Cho, et al. (2009). "Kinetics and mechanism of cellulose pyrolysis." Journal of Physical Chemistry C **113**: 20097-20107.
- Lizzio, A. A. and L. R. Radovic (1991). "Transient kinetics study of catalytic char gasification in carbon dioxide." Industrial & Engineering Chemistry Research **30**: 1735-1744.
- Lv, G. J., S. B. Wu, et al. (2010). "Kinetic study of the thermal decomposition of hemicellulose isolated from corn stalk." BioResources **5**: 1281-1291.
- Mitsuoka, K., S. Hayashi, et al. (2011). "Gasification of woody biomass char with CO₂: The catalytic effects of K and Ca species on char gasification reactivity." Fuel Processing Technology **92**: 26-31.
- Nahar, G., V. Dupont, et al. (2015). "Feasibility of hydrogen production from steam reforming of biodiesel (FAME) feedstock on Ni-supported catalysts." Applied Catalysis B: Environmental **168-169**: 228-242.

Nzihou, A., B. Stanmore, et al. (2013). "A review of catalysts for the gasification of biomass char, with some reference to coal." Energy **58**: 305-317.

Padban, N. (2000). PFB Air Gasification of Biomass, Investigation of Product Formation and Problematic Issues Related to Ammonia, Tar and Alkali PhD Thesis, Lund University.

Patwardhan, P. R., J. A. Satrio, et al. (2010). "Influence of inorganic salts on the primary pyrolysis products of cellulose." Bioresource Technology **101**: 4646-4655.

Pérez-Hernández, R., A. Gutiérrez-Martínez, et al. (2007). "Effect of Cu loading on for hydrogen production by oxidative steam reforming of methanol." International Journal of Hydrogen Energy **32**: 2888-2894.

Reyes, P., R. T. Mendonça, et al. (2013). "Characterization of the hemicellulosic fraction obtained after pre-hydrolysis of pinus radiata wood chips with hot-water at different initial PH." Journal of the Chilean Chemical Society **58**: 1614-1618.

Ronsse, F., X. Bai, et al. (2012). "Secondary reactions of levoglucosan and char in the fast pyrolysis of cellulose." Environmental Progress & Sustainable Energy **31**: 256-260.

Rostrup-Nielsen, J. R. and L. J. Christiansen (1995). "Internal steam reforming in fuel cells and alkali poisoning." Applied Catalysis A: General **126**: 381-390.

Rynkowski, J. M., T. Paryczak, et al. (1995). "Characterization of alumina supported nickel-ruthenium systems." Applied Catalysis A, General **126**: 257-271.

Scott, D. S., L. Paterson, et al. (2001). "Pretreatment of poplar wood for fast pyrolysis: rate of cation removal." Journal of Analytical and Applied Pyrolysis **57**: 169-176.

Sekiguchi, Y. and F. Shafizadeh (1984). "The effect of inorganic additives on the formation, composition, and combustion of cellulosic char." Journal of Applied Polymer Science **29**: 1267-1286.

Shen, D. K. and S. Gu (2009). "The mechanism for thermal decomposition of cellulose and its main products." Bioresource Technology **100**: 6496-6504.

Solymosi, F., T. Bánsági, et al. (1988). "Effect of NO on the CO-induced disruption of rhodium crystallites." Journal of Catalysis **112**: 183-193.

Solymosi, F. and H. Knozinger (1990). "Infrared study on the interaction of CO with alumina-supported rhodium." Journal of the Chemical Society, Faraday Transactions **86**: 389-395.

Stewart, C. and D. Foster (1953). "The non-resistant components of the Wood of *Eucalyptus regnans* F. Muell. II. Polysaccharide constituents." Australian Journal of Chemistry **6**: 431-438.

Stewart, J. J., T. Akiyama, et al. (2009). "The Effects on Lignin Structure of Overexpression of Ferulate 5-Hydroxylase in Hybrid Poplar." Plant Physiology **150**: 621-635.

Sugiura, K., M. Yamauchi, et al. (2005). "Evaluation of volatile behaviour and the volatilization volume of molten salt in DIR-MCFC by using the image measurement technique." Journal of Power Sources **145**: 199-205.

Timell, T. E. (1967). "Recent progress in the chemistry of wood hemicelluloses." Wood Science and Technology **1**: 45-70.

Trautmann, S. and M. Baerns (1994). "Infrared Spectroscopic Studies of CO Adsorption on Rhodium Supported by SiO₂, Al₂O₃, and TiO₂." Journal of Catalysis **150**: 335-344.

Van Beurden, P. (2004). "On the catalytic aspects of steam-methane reforming." Energy Research Centre of the Netherlands (ECN), Technical Report I-04-003.

Verma, M., S. Godbout, et al. (2012). "Biofuels production from biomass by thermochemical conversion technologies." International Journal of Chemical Engineering.

Wong, K. K. Y., K. F. Deverell, et al. (1988). "Relationship Between Fiber Porosity and Cellulose Digestibility in Steam-Exploded Pinus Radiata." Biotechnology and Bioengineering **31**: 447-456.

Wooley, R., M. Ruth, et al. (1999). "Process Design and Costing of Bioethanol Technology: A Tool for Determining the Status and Direction of Research and Development." Biotechnology Progress **15**: 794-803.

Wu, H., K. Yip, et al. (2009). "Evolution of char structure during the steam gasification of biochars produced from the pyrolysis of various mallee biomass components." Industrial and Engineering Chemistry Research **48**: 10431-10438.

Yildiz, G., F. Ronsse, et al. (2015). "Effect of biomass ash in catalytic fast pyrolysis of pine wood." Applied Catalysis B: Environmental **168-169**: 203-211.

Yip, K., F. Tian, et al. (2010). "Effect of Alkali and Alkaline Earth Metallic Species on Biochar Reactivity and Syngas Compositions during Steam Gasification." Energy & Fuels **24**: 173-181.

This page intentionally left blank.

Chapter 6: Conclusions

This page intentionally left blank.

Re-Ni, Rh-Ni and Ru-Ni catalysts have been identified as the most promising promoted nickel catalysts for the reactive flash volatilisation of lignocellulose in this research. This conclusion is based upon the overall gasification efficiency, in particular low char selectivity and product gas composition. In addition, this research has successfully demonstrated that, the first-ever, tar free synthesis gas can be produced via this technology with promoted nickel catalysts from solid biomass, namely purified microcrystalline cellulose, pinus radiata (pinewood) and eucalyptus regnans sawdust. Key findings on the effects of catalyst promoter, temperature, C/O ratio, C/S ratio, feedstock and ash content on product yield and product gas composition in this research are summarized in this chapter.

6.1 Effects of Catalyst Promoters

In comparison to the monometallic Ni catalyst, the noble metal promoted catalysts were found to have higher catalytic activity, coke resistance and stability in the RFV of microcrystalline cellulose, sawdust of pinus radiata and eucalyptus regnans. Catalyst characterisation studies revealed that noble metal promoters increased the activity of Ni catalysts by increasing the metal dispersion and reducibility. Re, Rh and Ru promoted Ni catalysts (in that order) were found to have the highest gasification efficiency and catalyst stability. Other catalysts such as monometallic Ni and Pt-Ni were active for RFV but suffered rapid deactivation due to coke deposition, metal active site sintering, and alumina support pore collapse due to partial phase change from γ -alumina to δ -alumina. Application of Re, Rh and Ru as promoters greatly reduced the coke deposition and sintering of nickel nanoparticles on the catalyst. Therefore, the promoted Ni catalysts were active for longer duration with little to no deactivation. Amongst the four promoters, Re exhibited the lowest char selectivity in cellulose and lignocellulose RFV. This can be attributed to the property of Re, which can exist in multiple oxidation states, therefore, is more efficient in promoting oxidation and reducing char formation.

6.2 Effects of Temperature

Three temperatures (700, 750 and 775 °C), selected based on literature study, were examined in the RFV of cellulose with promoted nickel catalysts. Gasification efficiency of RFV increased with increasing in reaction temperature, which led to lower char selectivity. Significant improvement in gas production was observed in RFV at temperature $> 750^{\circ}\text{C}$. This is believed to be due to favourable conditions for steam reforming and partial oxidation reactions at higher temperature. However, H_2 and CO compositions in the gaseous product were lower at higher temperature in favour of the production of H_2O and CO_2 , which indicates further oxidation of the product gas. Ni and Ru-Ni had the lowest catalytic activity at temperature higher than 750 °C because of sintering of the metal nanoparticles and

partial oxidation of Ni^0 into Ni^{2+} . Overall, 750 °C is concluded to be the optimum temperature for RFV to achieve high activity while maintaining the stability of the promoted nickel catalyst to achieve high gasification efficiency and high quality syngas production.

6.3 Effects of Carbon to Oxygen Ratio

Carbon to oxygen ratio (C/O) was found to be the most effective parameter to use for maximising the gas yield while minimising the tar and char yields. Generally, the gasification efficiency increased with decrease in C/O ratio. This is expected because lower C/O ratio (higher O_2 input) favours partial oxidation reaction and leads to faster char gasification kinetics, which is known to be the rate limiting step in RFV. However, low C/O ratio may also lead to further oxidation of CO to CO_2 and H_2 to H_2O , degrading the quality of the synthesis gas. Increase in C/O ratio was found to have more impact on the product gas composition of RFV of lignocellulose than RFV of cellulose. Under similar C/O ratio, CO_2 yield was noticeably higher in RFV of lignocellulose than cellulose. This was caused by the catalytic effect of the presence of AAEMs in RFV, which known to be effective in promoting oxidation. In conclusion, the optimum C/O ratio in the range of 0.6 - 0.7 was found to provide the best result in RFV of cellulose and lignocellulose based on high gasification efficiency, better synthesis gas quality and the high mole fractions of H_2 and CO in the product gas.

6.4 Effects of Carbon to Steam Ratio

Carbon to steam ratio (C/S) did not affect the gasification efficiency or the char yield significantly in our study. This is because decomposition of char is dominated by the partial oxidation and kinetic limited steam gasification. However, the C/S ratio was effective in improving the gas composition in RFV of cellulose via steam reforming of volatiles and water gas shift reaction. The same effects were not observed in RFV of pinewood and eucalyptus sawdust. This can be explained by the relatively high oxygen input used in our experiments, which promoted oxidation reactions over steam reforming reaction. In general, increase C/S ratio (low steam flow rate) decreased the gasification efficiency. At high C/S ratio, tar and char yields in the RFV of cellulose were noticeably higher, with lower H_2 and CO composition in the gas phase, which is believed to be lower activity of steam reforming and water gas shift reactions under low steam flow rates. Depending upon the catalysts used, low C/S ratio may lead to higher char yield because of lowering of catalyst bed temperature due to large steam flow rate, resulting in incomplete gasification. The optimum C/S ratio for the RFV of cellulose was 1.0, whereas the optimum C/S ratio for RFV of pinewood and eucalyptus sawdust slightly higher at 1.17 and 1.11 respectively.

6.5 Effects of Biomass Feedstocks and Ash Content

Gasification efficiency in the RFV of pinewood and eucalyptus sawdust was significantly higher than RFV of cellulose. This higher efficiency was the combined result of the higher amorphous structure of lignocellulose compared to microcrystalline cellulose, and the catalytic effects of alkali and alkaline earth metals (AAEM) found in the lignocellulose ash. In this research, it was found that the amorphous hemicellulose and lignin exhibited faster thermal decomposition than cellulose, due to their lower pyrolysis onset temperatures and the reactions exothermic properties. Because hemicellulose and lignin make up 48.6 – 63% of lignocellulose, faster devolatilisation and higher gasification efficiency can be expected in RFV of lignocellulose. In addition, the presence of AAEMs in RFV, particularly K and Mg, further promoted the formation of low molecular weight gaseous products and enhanced the gasification of biochar, led to higher gasification efficiency and faster char gasification. In comparison to catalytic effect from promoted nickel catalyst, catalytic effect from AAEM species was found to be more dominant, which can be attributed to the high dispersion of AAEM species within the biomass feedstock. However, increase in oxidation activity was also observed in the RFV under the presence of AAEM species with the same C/O ratios input condition used for cellulose. This resulted in higher CO₂ yield, and therefore lowered the calorific value of the gaseous products.

6.6 Kinetics of Reactive Flash volatilisation

Kinetics of the RFV of lignocellulosic materials under various gasification conditions, for the very first time, was modelled using a pseudo first order reaction model. Rates of mass loss of cellulose, xylan and lignin were measured and compared with synthetic biomass mixture and pinewood sawdust. Three distinct regimes of rate of mass loss were identified: (I) pyrolytic decomposition, (II) reforming and (III) char gasification. The results showed that promoted nickel catalysts enhanced the rate of mass loss in the reforming regime only. The rate of mass loss in the pyrolytic decomposition was found to be thermodynamically limited, which is evident from the increase in rate of mass loss at higher temperatures. The rate of mass loss in the char gasification regime is kinetically limited, which was improved in the presence of inherent AAEM species in the biomass with high ash content. Among the three regimes, the rate of mass loss was found to be in the following order – reforming > pyrolytic decomposition > char gasification. The catalysts also improved the quality of synthesis gas produced by converting the condensable organic compounds (tar) into CO and H₂. The rate of pyrolytic decomposition of cellulose was found to be the slowest compared to lignin and xylan (hemicellulose). This is believed to be due to the high ordered crystalline structure of cellulose compared to amorphous and porous structure of lignin and xylan. Therefore, in the lignocellulose

Chapter 6

material pyrolytic decomposition is controlled by cellulose decomposition. The Constable-Cremer plot of various catalysts used in the wire-mesh isothermal thermogravimetric reactor confirmed that Rh-Ni, Re-Ni and Ru-Ni catalysts were more effective in catalysing reforming reaction compared to other catalysts used in this study, which is consistent with these catalysts' RFV activity results.

Chapter 7: Recommendations and Future Works

This page intentionally left blank.

Results presented in this thesis have demonstrated the feasibility of using reactive flash volatilisation approach with promoted nickel catalysts to produce tar free synthesis gas from lignocellulosic biomass feedstock. However, there are several key issues that have emerged from this thesis that needs to be addressed prior to commercialisation of this technology. Following recommendations for the future research are presented -

7.1 Catalyst Research

Below is a list of the key research areas for future catalyst development:

7.1.1 Catalyst Support

The γ -alumina support used in the catalysts for this study was found to be unstable over a long period of time. At temperatures above 750°C, and especially in the presence of steam, the γ -alumina phase partially converted into δ -alumina, which has a lower surface area. Reduction in surface area may lead to deactivation of the catalyst due to increase diffusional constraints and pore-blockage, which restricts the access of reactants to the active metal site in the pores. In order to successfully commercialise this technology, it is essential for the researcher to develop an active, high surface area catalyst which is also stable at high temperature for longer on-stream service life.

7.1.2 Active metal nanoparticles

Nickel is known as one of the most cost effective transition metal to use in gasification and tar cleaning. Ni^0 is the active species in all nickel based catalyst, which requires a reduction step before the reaction. However oxygen is one of the feed gas and under the oxidising atmosphere Ni^0 may partially oxidise to Ni^{2+} , which significantly reduces its catalytic activity. This thesis focussed on the use of noble metals as promoters which are able to maintain Ni^0 state by hydrogen transfer mechanism, thereby keeping the catalysts active. However, the cost of noble metals may be prohibitive at large scale. Therefore, future research should focus on exploring the use of other transition metals as promoters for Ni based catalysts. Alternatively, non-Ni catalysts with activity in C-C cleavage and steam reforming may be explored.

7.1.3 Regeneration of the catalyst

In this thesis, noble metal promoters have been shown to be effective in reducing coke formation. However, over a long period of time, it is still possible that sufficient coke deposition may occur as to deactivate the catalyst. Due to the high cost of Ni and noble metals, disposal of spent nickel catalyst is not viable. Coke deposition may be removed from the catalysts by calcining the

catalysts at high temperature followed by reduction. However, future research must be done to establish the activity of the regenerated catalysts.

7.1.4 Fundamental understanding of the effect of promoter on Ni based catalysts

While this thesis demonstrated that the promoters enhanced the activity of Ni based catalysts by increasing the reducibility and coke resistance, it is not clear whether the promoted metal catalysts take active part in the reaction and also whether the noble metals form alloy complexes with Ni nanoparticles. One of the ways to identify the solid solutions of Ni and noble metals is to conduct an X-Ray Absorption Spectroscopy. Therefore, there is a need to conduct a XANES and EXAFS analyses on these noble metals promoted catalyst to understand how these promoters affect the reactivity of the nickel nanoparticles. *In-situ* XANES analysis of reforming reaction can provide insight into the chemistry of the surface reaction on the promoter metals, whereas, EXAFS analysis can provide information about the alloying of promoter metals with Ni nanoparticles by studying the fine structure around Ni and promoter metal atoms. At the time of writing this thesis, this study has been commenced at the Australian Synchrotron.

7.2 Detailed Kinetic Study and Reactor Kinetic Modelling

In this thesis a simple pseudo first order reaction kinetic model was assumed for estimating the rates of reaction in the different regimes of mass loss during gasification. However, in reality there are heat and mass transfer limitations which affect the global rate of reaction. Therefore, for future researchers, it is recommended to study each regime in greater detail. Pyrolytic decomposition can be modelled using coupled radiative and convective heat transfer models followed by kinetics of thermal decomposition. As for the pyrolysis oil generated in the first regime reacts in the catalyst bed, to study this scenario in detail, there is a need to identify appropriate approaches for modelling the two-phase flow and the reaction processes that occur both on the surface and within the catalyst bed. Further kinetic data must be generated for reforming of these bio-oils in kinetically controlled reaction conditions to estimate the intrinsic reaction rate. By studying the reforming of bio-oils, it may be possible to isolate the effects of transport phenomena and thermal decomposition on the global rate of reactions. Finally char gasification models may be developed which may be similar to the coal char gasification models.

7.3 Other Directions for Future Research in RFV

Some other areas worth to be explored have also included-

7.3.1 Alternative Reactor Setup

In this thesis a fixed bed reactor setup was used because of its simplicity and available resources. However, the current setup is susceptible to fouling on the surface of catalyst bed due to char and/or ash deposition. This may eventually lead to clogging on the reactor. Accumulation of ash may cause severe operating problems such as reactor erosion. Therefore, it is vital for the future researchers to look into other potential reactor designs, such as circulating fluidised bed reactor, that can minimize or avoid the accumulation of ash in the reactor.

7.3.2 Alternative Gasifying Agent

Steam and oxygen was used as gasifying agents in this thesis. However, steam caused degradation of alumina support at temperatures lower than the normal phase transformation temperature. Moreover, oxygen is an expensive reagent because air purification is required to produce concentrated oxygen stream. Replacing steam and oxygen with other gasifying agents, such as carbon dioxide, may help to mitigate this problem. Using CO₂ from fossil fuel combustion (such as coal fired power stations) will also reduce the emissions and help mitigate climate change. CO₂ is also a cheaper gasifying agent compared to oxygen and high temperature steam.

7.3.3 Different Feedstock

While pinewood and eucalyptus are among potential resources in Australia, there are other potential feedstock including microalgae, bagasse and wheat straw, that may be studying in reactive flash volatilisation.

This page intentionally left blank.

Appendix

This page intentionally left blank.

Appendix A- Theoretical Estimation of Sample Heating Rate

Taking a control volume at the surface of the sample and starting with the general energy balance equation –

$$\dot{E}_{in} - \dot{E}_{out} + \dot{E}_{gen} = \Delta\dot{E}_{st} \quad (1)$$

We make certain assumptions –

- Constant wall temperature (three cases studied – 700, 750 and 800°C)
- Radiation is the dominating mode of heat transfer from the wall to the sample.
- The sample a small object completely enclosed in a radiating media, which means $\varepsilon = 1$
- No heat generation
- $\dot{E}_{out} = 0$
- Conductivity inside the sample is much faster (a safe assumption since small sample size of 20 μm particles was used)

Therefore Eq. 1 reduces to

$$\Delta\dot{E}_{st} = \dot{E}_{in}$$

$$C_{p\text{-sample}} \times m_{\text{sample}} \frac{dT_{\text{sample}}}{dt} = h_{\text{rad}} \times A_{\text{sample}} \times (T_{\text{wall}} - T_{\text{sample}})$$

Rearranging the above equation –

$$\text{Heating rate} = \frac{dT_{\text{sample}}}{dt} = \frac{h_{\text{rad}} \times A_{\text{sample}} \times (T_{\text{wall}} - T_{\text{sample}})}{C_{p\text{-sample}} \times m_{\text{sample}}} \quad (2)$$

where T_{sample} is the sample temperature, A_{sample} is the surface area of the sample ($1 \times 10^{-4} \text{ m}^2$), T_{wall} is the furnace temperature, $C_{p\text{-sample}}$ is the heat capacity of cellulose ($1400 \text{ J/kg} \cdot \text{K}$), m_{sample} is the mass of the sample ($1 \times 10^{-4} \text{ kg}$) and h_{rad} is the radiant heat transfer coefficient which can be approximated using *Stefan-Boltzmann's law*

$$h_{\text{rad}} = \varepsilon \times \sigma \times (T_{\text{wall}}^2 + T_{\text{sample}}^2) \times (T_{\text{wall}} + T_{\text{sample}})$$

where ε is emissivity and σ is Stefan-Boltzmann constant.

Assuming further that h_{rad} is constant (a safe assumption at $t = 0$ s) and that initial $T_{sample} = 25^{\circ}C$

The initial heating rate can be estimated as follows –

$$\text{At } T_{wall} = 700^{\circ}C, h_{rad} = 74.7 J \cdot K/m^2 \cdot s$$

$$\left[\frac{dT_{sample}}{dt} \right]_{t=0} = 8.6 \times 10^3 K/min \text{ or } ^{\circ}C/min$$

$$\text{At } T_{wall} = 750^{\circ}C, h_{rad} = 85.1 J \cdot K/m^2 \cdot s$$

$$\left[\frac{dT_{sample}}{dt} \right]_{t=0} = 1.1 \times 10^4 K/min \text{ or } ^{\circ}C/min$$

$$\text{At } T_{wall} = 800^{\circ}C, h_{rad} = 96.4 J \cdot K/m^2 \cdot s$$

$$\left[\frac{dT_{sample}}{dt} \right]_{t=0} = 1.3 \times 10^4 K/min \text{ or } ^{\circ}C/min$$

Appendix B- Published Journal Article Front Page

B1- Chapter 2- Literature Review: Review of Recent Developments in Ni-based Catalysts for Biomass Gasification

Renewable and Sustainable Energy Reviews 38 (2014) 428–438



Contents lists available at ScienceDirect

Renewable and Sustainable Energy Reviews

journal homepage: www.elsevier.com/locate/rser



Review of recent developments in Ni-based catalysts for biomass gasification



Fan Liang Chan, Akshat Tanksale*

Department of Chemical Engineering, Monash University, Clayton, Victoria 3800, Australia

ARTICLE INFO

Article history:
Received 6 August 2013
Received in revised form
8 May 2014
Accepted 18 June 2014

Keywords:
Biomass
Gasification
Nickel catalyst
Reactive flash volatilization

ABSTRACT

Biomass gasification is recognized as one of the most promising solutions for renewable energy and environmental sustainability. However, tar formation in gasifier remains as one of the main hurdles that hinder commercialization. Nickel based catalyst is widely used in chemical industries and is proven as one of the most effective transition metal catalysts in biomass gasification for tar cracking and reforming. This paper presents a review of various commercial nickel catalysts that have been evaluated for tar elimination in biomass gasification. This review also looks at recent advancements in nickel based catalyst used in biomass gasification, including discussion on the effects of different support, promoter and particle size on the catalytic performance. Future direction of biomass gasification, including reactive flash volatilization and steam gasification, are also discussed in this review.

© 2014 Elsevier Ltd. All rights reserved.

Contents

1. Introduction	428
2. Tar	429
3. Biomass gasification with commercial nickel based catalyst	431
3.1. Commercial catalyst as primary catalyst	431
3.2. Commercial nickel catalyst as secondary catalyst	432
3.2.1. Synthesis gas upgrading	432
3.2.2. Bio-oil steam reforming	433
4. Recent advancements in nickel based catalyst for biomass gasification	433
4.1. Effect of support on nickel based catalysts	433
4.2. Promoted nickel based catalyst	433
4.3. Nickel nanoparticle catalyst	434
5. Future directions of biomass gasification	436
6. Conclusion	436
Acknowledgment	437
References	437

1. Introduction

According to the 2011 Energy White Paper by the Australian Department of Resource, Energy and Tourism, the world global energy demand in year 2035 will be 40% higher than current level [1]. However, with the growing concerns about climate change

and greenhouse gas emissions, non-renewable fossil fuels such as coal, petroleum and natural gas can no longer be considered as the only energy sources for the meeting of our future energy needs. In the short to medium term, a versatile and diverse energy plan, comprising both renewable and non-renewable energy sources is required. In the long term, there is a need for global transition to 100% renewable energy and chemical feedstock to achieve sustainable growth.

Biomass is a renewable energy resource derived from biological sources such as energy crops, agricultural residues, forestry

<http://dx.doi.org/10.1016/j.rser.2014.06.011>
1364-0321/© 2014 Elsevier Ltd. All rights reserved.

B2- Chapter 3- Catalytic Steam Gasification of Cellulose Using Reactive Flash Volatilization

CHEMCATCHEM
FULL PAPERS



DOI: 10.1002/cctc.201402434

Catalytic Steam Gasification of Cellulose Using Reactive Flash Volatilization

Fan Liang Chan and Akshat Tanksale*^[a]

Biomass gasification is considered to be one of the most promising technologies to deliver renewable energy. However, tar formation in the gasifier is one of the main challenges. Ni-based catalysts are one of the most effective transition-metal catalysts in biomass gasification for tar cracking and reforming. Alumina-supported Ni, Pt-Ni, Ru-Ni, Re-Ni and Rh-Ni catalysts were tested for their activity in the reactive flash volatilisation (RFV) of cellulose to produce synthesis gas in 50 ms reaction time. RFV is a catalytic gasification process that utilises a high

carbon space velocity and mass flow rate with oxygen and steam as gasification agents. Re-Ni, Rh-Ni and Ru-Ni supported catalysts showed a higher gasification efficiency than the other catalysts, which was because of their higher metal surface area, high reducibility and lower CO desorption temperature. The highest gasification efficiency was achieved at 750 °C with a carbon-to-oxygen ratio of 0.6 and a carbon-to-steam ratio of 1.0 without any oxygen breakthrough.

Introduction

Lignocellulosic biomass is a renewable energy resource that can be derived from organic sources such as energy crops, agricultural residues, forestry residues and recycled cardboard and paper.^[1] Biomass utilisation for fuels and energy production is recognised as one of the most promising solutions for the energy crisis and anthropological CO₂ emission problems.^[2] Thermochemical processes for biomass conversion, such as combustion, gasification and pyrolysis, can be used for power generation and biofuels production.^[2] Among the biomass-conversion technologies, gasification is one of the most interesting technologies from both an industrial and academic research point of view because of its high conversion efficiency.^[3] Biomass gasification can be achieved at temperatures in excess of 700 °C in the presence of oxygen or air with or without additional steam. However, at this temperature, a significant amount of condensable oxygenated hydrocarbons, commonly referred to as tar, is produced. In the absence of catalysts, tar-free gasification requires higher temperatures (≥ 1000 °C).^[4]

Tar removal is a major hurdle that hinders the commercialisation of biomass gasification.^[5] Many factors can affect the amount and type of tar formed during gasification. These factors include gasifier type and design, operating parameters (temperature, pressure, heating rate and residence time), type of feedstock and the type of catalyst used. The optimisation of these factors may maximise the efficiency of gasification with minimum tar formation. Dolomite- and CeO₂/SiO₂-supported Ni, Pt, Pd, Ru and alkali metal oxides have been used in the past to catalyse gasification reactions, reduce tar formation, improve conversion efficiency and improve the product gas

purity.^[6] As Ni-based catalysts are used industrially for the steam reforming of methane and naphtha,^[7] they are expected to catalyse the steam reforming of tars and the subsequent water-gas shift reaction to produce H₂. However, monometallic Ni catalysts suffer from rapid deactivation because of coke formation if they are used as primary catalysts in fluidised-bed gasifiers.^[6c,8] The doping of Ni catalysts with a small amount of noble metal increases its reforming activity, reducibility and coke resistance.^[9]

Conventionally, biomass gasification is performed in one of the following reactor setups:

- Fluidised-bed gasifier with a downstream catalytic tar-cleaning reactor
- Fast pyrolysis reactor with a downstream catalytic steam reformer
- Catalytic fluidised-bed gasifier
- Entrained-flow gasifier

Fluidised-bed reactors are capital-intensive and hence large-scale reactors are required to make them economical. The capital cost of the gasifier and gas-cleaning system can account for 66.7 to 85.5% of the total capital cost.^[10] Entrained-flow gasifiers are more expensive because of their higher flow velocities and temperatures in excess of 1000 °C, which require Ni-based alloys (e.g., Hastelloy) to provide oxidation resistance and high-temperature strength. In comparison, the capital cost of fixed-bed reactors for biomass gasification is significantly lower. Therefore, a new approach called reactive flash volatilisation (RFV) was proposed recently for cellulose gasification.^[11]

RFV uses a fixed-bed gasifier with a carbon space velocity and carbon mass flow rate 10–100 times higher than that of fluidised-bed reactors.^[11a] As a result, RFV reactors require significantly less catalyst and a smaller reactor volume to process

[a] F. L. Chan, Dr. A. Tanksale
Department of Chemical Engineering
Monash University
Clayton, VIC 3800 (Australia)

Kinetic Study of Catalytic Steam Gasification of Biomass by Using Reactive Flash Volatilisation

Fan Liang Chan,^[a] Kentaro Umeki,^[b] and Akshat Tanksale^{*[a]}

Reactive flash volatilisation is an autothermal process to convert biomass into tar-free synthesis gas under steam-rich conditions. This article studies the kinetics of reactive flash volatilisation by using Ni, Pt–Ni, Ru–Ni, Re–Ni, and Rh–Ni catalysts supported on alumina. The rates of mass loss of cellulose, xylan, and lignin were measured and compared with those of the synthetic biomass mixture and pinewood sawdust. The kinetic parameters were calculated with and without catalysts by using a wire-mesh isothermal thermogravimetric analyser in

an equimolar steam/N₂ atmosphere and high heating rates of 8.6×10^2 , 1.1×10^3 , and 1.3×10^4 °C min⁻¹ at 700, 750, and 800 °C, respectively. The results revealed three distinct regimes of the rate of mass loss: pyrolytic decomposition, reforming, and char gasification. The catalysts increased the rate of mass loss in the reforming regime. Rh–Ni and Ru–Ni supported catalysts showed higher reforming rates than other catalysts. This study provides direct evidence of the in situ catalytic removal of tar during gasification of biomass.

Introduction

The use of lignocellulose for transportation fuels and stationary power production is recognised as one of the most promising solutions to the energy crisis and environmental problems.^[1] Conversion of lignocellulose into biofuels generally follows a two-step process in which dried and milled lignocellulose is first converted into an intermediate product such as synthesis gas (via gasification), bio-oils (via fast pyrolysis), or aqueous sugars (via hydrolysis) followed by conversion of intermediates into biofuels.^[2] Among the lignocellulosic biomass conversion technologies, the production of synthesis gas via gasification is the most interesting, both industrially and academically, owing to its high conversion efficiency.^[3] Biomass gasification can be achieved at temperatures above 700 °C in the presence of oxygen or air, with or without additional steam. However, at this temperature, a significant amount of condensable oxygenated hydrocarbons, commonly referred to as tar, is produced. In conventional gasifiers, tar-free gasification requires higher temperatures (≥ 1000 °C).^[4] The Schmidt group developed a catalytic steam gasification process known as reactive flash volatilisation (RFV), which is a one-step autothermal process of converting non-volatile oxygenated hydrocarbons into tar-free synthesis gas with a downdraft fixed-bed catalytic reactor operating at approximately 900 °C.^[5] This is a complex reaction process in which pyrolysis, oxidation, partial oxidation, reduc-

tion, steam reforming, and water-gas shift reactions occur in the catalyst bed.^[6] Our previous article has demonstrated that synthesis gas can be produced from cellulose in an RFV reactor over promoted Ni catalysts at 700–775 °C in 50 ms residence time, with a negligible amount of char or tar as the byproduct.^[7] It has been proposed that biomass feedstock goes through pyrolytic decomposition and the resulting bio-oils go through reforming reactions in the catalyst bed to produce synthesis gas.^[6a]

However, kinetics of the RFV of cellulose and lignocellulose is complex and yet to be fully understood. There is also a lack of kinetic data on catalytic gasification under steam-rich conditions and high heat flux. Previous studies have investigated fast pyrolysis of lignocellulose, which is only the first step of RFV.^[8] Most of the previous studies of fast pyrolysis of lignocellulose were conducted at low heating rates, typically from 1 to 100 °C min⁻¹.^[8,9] A comprehensive review by Antal et al. summarised that there are two major pathways in the fast pyrolysis of cellulose: one leads to the selective formation of glycoaldehyde and the other leads to the formation of levoglucosan; higher heating rates favour the formation of glycoaldehyde, which has a lower boiling point than levoglucosan.^[9a] This results in higher volatile fractions compared to the lower heating rates.^[10] It is also known from the literature that higher heating rate lead to lower activation energy.^[8]

Therefore, to understand the kinetics of the RFV of lignocellulose, there is a need to conduct a study at significantly higher heating rates compared to fast pyrolysis conditions. Various models have been proposed to analyse pyrolysis, reforming, and gasification kinetics.^[9d,e,11] The reported activation energies and pre-exponential factors from these studies vary widely from 40 to 250 kJ mol⁻¹ and from 10⁴ to 10²⁰ s⁻¹, respectively.^[11a] However, owing to the substantial differences in the experimental methods, operating conditions, chemical compo-

[a] F. L. Chan, Dr. A. Tanksale
Catalysis for Green Chemicals Group
Department of Chemical Engineering
Monash University, Clayton, VIC 3800 (Australia)

[b] Dr. K. Umeki
Division of Energy Science
Luleå University of Technology
97187 Luleå (Sweden)